Measurements of the derivative of the p wave travel time curve by means of an array network

Derek J. Corbishley

D1

MEASUREMENTS OF THE DERIVATIVE OF THE P WAVE TRAVEL TIME CURVE BY MEANS OF AN ARRAY NETWORK

by

Derek J. Corbishley B.Sc. (London)

University College,

Durham.

November, 1969

I declare that this thesis, submitted for the degree of Ph.D. at the University of Durham, is not substantially the same as any which has previously been submitted to any other University.

Derek J. Corbishley.

Derek J. Corbishley

University of Durham

November 1969

ABSTRACT

Data from the four UKAEA seismic arrays have been combined to measure the slope of the P-wave travel time curve ($dT/d\Delta$, or slowness) of events occurring at distances $\Delta = 30^{\circ}$ to 104°. Slowness is the quantity that enters into any calculation of the compressional velocities to give the main source of direct detailed information regarding the mantle. Multiple regression analysis was used and corrections, which are azimuthally dependent, estimated to correct for the near surface geology under the arrays. By using all available events and removing the bias introduced by the array geology, the slowness-distance curve should represent the best average for the world.

Anomalous features in the slowness curve occur at distances of around $35\text{-}36^{\circ}$, $48\text{-}49^{\circ}$, 60°, $68\text{-}70^{\circ}$ and $84\text{-}85^{\circ}$. These correspond to high velocity gradients within the lower mantle near the depths of 900, 1200, 1550, 1900 and 2500 kms., and support the hypothesis that the mantle is inhomogeneous at depth.

A comparison is made between these features and regions considered to be inhomogeneous found at similar distances by other studies.

The site corrections obtained for each seismometer are attributed to inhomogeneities in the sub-array geology.

The corrections derived for the arrays situated in Canada (YKA) and India (GBA) are small in magnitude and show the crustal layering to be essentially horizontal.

The corrections at the array in Scotland (EKA) are shown to be related to the relative altitudes of the instruments. A velocity of 2.94 km/sec. was derived for the velocity in the top 170 m of crust.

The corrections for the Australian array (WRA) show that to a first approximation, the layering in the crust is dipping at 3.6° in the direction $N195^{\circ}E$. The corrections have a large azimuthal component and show the presence of an anomaly near the cross-over point of the array.

ACKNOWLEDGEMENTS

The opportunity to make this study has only been possible because of the close ties that exist between the United Kingdom Atomic Energy Authority, Blacknest and the Department of Geology, University of Durham. The credit for this cooperation must go to Dr. H. I. S. Thirlaway and Professor M. H. P. Bott. I would like to express my sincere thanks to Professor Bott for allowing me to study in his department and to Dr. Thirlaway and the staff of Blacknest for their help and encouragement. I am grateful to the Director, UKAEA for allowing me leave of absence to study in Durham. I am also indebted to Mr. A. Douglas for his invaluable help throughout this study and for answering the day to day questions as they arose.

I would like to express my thanks to Dr. R.E. Long, who with Dr. Thirlaway supervised me for three years.

I am grateful to Mr. J. Young for providing the solutions to my computing problems.

Also thanks are due to Miss P. Eves who helped with the preparation of the manuscript.

PREFACE

This thesis gives a description of a new method to measure the derivative of the P wave travel time curve and investigates the implication of the results obtained in relation to the physical conditions within the Earth's mantle.

The Introduction describes previous attempts to estimate slowness using travel times and single arrays and discusses the difficulties encountered. The basic data are the observed relative onset times of the wavefront from an event as it crosses a seismic array. The equation for calculating slowness is given in Appendix A, and the method of combining the results from four arrays is described in Section 1.1.

The coordinates and a brief description of each of the four UKAEA arrays used in the study are contained in Appendix E. The data recorded by the network came from the 478 events listed in Appendix G and are discussed in Section 1.2.

The mean values of slowness in the epicentral range $\Delta = 30\text{-}104^{\circ}$ are estimated over two degree distance intervals. By using multiple regression analysis and least squares to invert the data from all the arrays simultaneously, mean values of slowness, corrections for sub-array geology and confidence limits can be obtained directly. The method of obtaining the solution to the matrix equations is given in Appendix B, and Appendix C describes how the values of slowness may be obtained for individual events once the corrections for the sub-array geology have been estimated.

The corrections are discussed in Section 2.2 and listed for each array in Appendix F.

Confidence limits on all unknowns are obtained using the matrix equations given in Appendix D and an analysis of the errors involved given in Section 1.3.

The least squares method depends on the data having a Gaussian distribution if the regression coefficients and confidence limits are to be correctly estimated. The problem of non-normal data is discussed in Section 1.5 which describes a method used to eliminate data associated with large residuals.

The final slowness estimates depend on how accurately the onsets have been obtained from the original records. Section 1.4 describes how the records were read, and an experiment conducted to compare the accuracy of three different methods of obtaining relative onset times.

The slowness results with 95% confidence limits are given in Section 2.1 and compared with the results from other studies in Section 2.3. The body wave results are integrated by the Weichert-Herglotz method in Section 3.1 and used with the results of shearwave studies to calculate the elasticity of the lower mantle in Section 3.2. The conclusions follow in Chapter 4.

The main computer program, used with an IBM 7030, to calculate the velocity structure from the slowness results and to truncate data to a normal distribution are described and listed in Appendix H.

CONTENTS

			Pages
Abstract.			
Acknowledgements.			
Preface.			
Contents.			
Introduction			1
Chapter 1	1.1	Estimation of Slowness	6
	1.2	The Data	11
	1.3	Error analysis	15
	1.4	Reading onset times and random reading errors	18
	1.5	Normal error theory and elimination of extreme values	25
Chapter 2	2.1	Results	30
	2.2	Array Site Corrections	37
	2.3	Discussion	46
Chapter 3	3.1	Inversion: velocity-depth model	54
	3.2	Elasticity of the lower mantle	57
Chapter 4	4.1	Conclusions: the Data	66
	4.2	Conclusions: the site corrections	67
	4.3	Conclusions: Slowness estimates	68
Appendix	A	Equation of slowness for a plane wave	70
	B	Solution of multiple array equations in matrix form	72
	C	Solution of slowness for individual events	77

			Pages
Appendix	D	Confidence Limits	78
	E	The four UKAEA Arrays and coordinates	81
	F	Azimuthal site corrections for the four arrays	83
	G	Events used in the slowness calculations	84
	H	Description of computer programs and listings	85
References			92

The Primary and most
beautiful of Nature's
qualities is motion,
which agitates her at
all times

D. A. F. de Sade

INTRODUCTION

The mantle extends from a depth of between 8 and 70 kms beneath the solid surface of the Earth to the liquid core at a depth of around 2920 kms. Within this region processes are occurring which probably account for the distribution of oceans and continents, the production of volcanoes and earthquakes and the building of mountains. Unfortunately, because of the crust, the mantle at present can only be investigated by indirect methods, and it is the velocity of P and S body waves that provides the most accurate data regarding the structure of the interior of the earth.

From a knowledge of these velocities, and using classical techniques, it is possible to infer the thermal properties, temperature, crustal structure, and orientation and creep rate. Modern methods have been developed to compute the variation of the anelasticity, or Q with depth from the attenuation of body and surface waves, and the study of free oscillations has led to a method of determining density in a direct manner. If densities are estimated from the velocities of P and S waves, then assumptions have to be made concerning the gross structure of the Earth.

The fundamental data of classical seismology are the travel-time tables and these provide the basis for the determination of the velocity distributions in the Earth by the Weichert-Herglotz method. The velocities are in remarkable agreement over the region of the lower mantle, and there can be little doubt that these models do not deviate from the true velocities by more than $\frac{1}{2}$ per cent.

It was on the basis of the available seismic data that Bullen (1940) found it convenient to divide the Earth from the crust to the inner core into the regions A, B,.....G. These regions have since been modified and subdivided as new data has become available.

The regions constituting the mantle are those designated B, C and D. Region D has since been subdivided into D^{1} and D^{11} following evidence

that the velocity gradients below 2700 kms are significantly different.

Region B starts from just below the crust and extends to the transition region (C) at a depth of 413 kms. The most important feature of the B and C regions is the so-called 20^{o} discontinuity. Investigations by Niazi and Anderson (1965) and Anderson (1967) show that the feature probably consists of two distinct discontinuities beginning at depths of 365 and 620 kms. The boundary between C and D^{1} is taken by Bullen to be at a depth of around 950 kms, but neither this nor the 413 km boundary seems to be a sharp discontinuity, and the transition from one region to the other is probably gradual.

Although the study of the B and C regions of the upper mantle has occupied the attention of many writers, (Anderson in "The Earth's Mantle" ed. Gaskell gives an excellent review) velocities in the lower mantle between about 800 and 2800 kms depth have not received a similarly detailed scrutiny until the last two years. The recent increase in interest has undoubtedly been because of the construction of large aperture arrays of seismometers which enable the velocities in the deep mantle to be measured directly. The increased quantity and quality of body wave data from these arrays have produced results which show that although the general trend of velocities with depth are very similar to the models of Gutenberg and Jeffreys, there are significant differences and a revision of velocities is in order. Because these velocities occupy such a fundamental position in our understanding of the lower mantle, any small improvements which can be made in their values are important and worth the effort made in obtaining them.

The standard method of obtaining an average velocity depth curve is by measuring the travel times of earthquake body waves, smoothing the data, measuring the slope $(^{dT}/d\Delta)$ and integrating by the Weichert-Herglotz method.

Scatter is introduced to the travel-time data by errors in the

hypocentre and origin times, two quantities which, with regard to earthquakes propogating over a finite area are necessarily difficult to define. Variations in the crust and upper mantle at the source and near the receiver will also, if large, introduce errors by deflecting the ray from its average path. Calculations of the absolute time of arrival of a phase not only depends on knowing the exact origin time of the event, but also measuring the onset time of the particular phase against a local clock. Further scatter will therefore be introduced if the exact onset of the phase cannot be identified or the clock is in error.

Uncertainty in the hypocentre and origin times can be considerably reduced by using travel times from nuclear explosions, although the data is sparse and tends to be grouped into particular areas. Large computers have made it possible to use data from a great number of source regions covering a large range of azimuths. Regional bias can then be partially eliminated and the effects of crustal variations at the receiver removed, making it meaningful to define an "average" travel time curve. However, such a travel time curve estimated to an accuracy of 0.1 seconds in several hundred (e.g. the Herrin (1968) travel times) will, when numerically differentiated yield a derivative ($^{dT}/d\Delta$) curve accurate to only $\pm$ 0.2 secs/deg. It is clear therefore, that travel times cannot be used to give accurate information concerning the rapidly changing features within the Earth.

The construction of large arrays of seismometers however, has now made it possible to measure the slope ($^{dT}/d\Delta$) of the travel time curve directly. ($^{dT}/d\Delta$) is also known as "slowness", its reciprocal as "phase velocity" or "apparent velocity"). It is $^{dT}/d\Delta$ that enters directly into any calculation of the velocity distribution with depth. The great advantage of this method is that it does not depend upon absolute times, but only on the time difference taken by a seismic phase to cross adjacent seismometers.

As arrays are usually constructed to record the outputs from all the seismometers simultaneously with the time code, the time differences can be easily estimated to a high degree of accuracy. Onsets recorded at an array with an aperture of 200 kms (e.g. LASA, the Large Aperture Seismic Array in Montana) with an accuracy of 0.1 seconds will then yield a slowness curve accurate to 0.05 seconds/degree.

Considerable attention, however has to be given to correcting for the effects of the local crust which separates the mantle from the array. For a large array extending over a geologically inhomogeneous area, these effects may result in erroneous conclusions being drawn about deep mantle variations rather than properly attributing them to features within the crust. Sheppard (1967) has pointed out that errors of up to 0.5 secs/deg. in slowness and 6° in azimuth are observed with LASA if crustal corrections are not made. The size of an array can therefore only be increased by an amount which will be dictated by the geological homogeneity and seismic noise level of the area. The problem may also be worsened when working with events at distances less than 30°, (the angle subtended at the centre of the earth by the source and the receiver) by variations of upper mantle structure with direction. Events within the teleseismic "window" of 30° to 90° emerge from the mantle at a high angle of incidence and are less likely to be affected by lateral inhomogeneities.

Direct measurements of slowness in the teleseismic region have been made using single arrays by Chinnery and Toksöz (1967) and Greenfield and Sheppard (1969) using LASA, and Johnson (1969) who used the extended array at the Tonto Forest Seismological Observatory (TFSO) in Arizona. These papers present curves of slowness as a function of distance for particular regions of the Earth's mantle after independently estimating and correcting for the effects of structure beneath the array. Chinnery and Toksöz derived their corrections from the travel times of the LONGSHOT explosion; Greenfield and Sheppard corrected the observed values of slowness by restricting the events used to only

those from opposite azimuths; and Johnson constructed a model of the crust beneath the TFSO array from seismic refraction and gravity data. All these studies have emphasised the difficulty of determining crustal and upper mantle structure. Because of this, it is better to estimate slowness and the effects of array substructure simultaneously, taking the best site corrections as being those that give the least scatter in results.

Douglas and Corbishley (1968) showed how to do this by combining the data from several arrays, and the method has been used to derive a P wave slowness curve for the distance range 30° - 104° (Corbishley 1969). Within this range the rays are relatively unaffected by the lateral inhomogeneities within the crust and as many event-array ray paths were used regional bias was eliminated. The slowness values should then represent the best average for the world. Another advantage of the method is that confidence limits on the curve can be easily established. The arrays used have sufficiently small apertures to minimise the structure corrections and still produce a stable estimate of slowness, provided special care is taken in reading the records. A section of this thesis has been devoted to the estimation of the minimum random reading errors using the constant event-station paths provided by underground explosions in Kazakh.

The results show anomalously large gradients occur in the slowness curve near the epicentral distance of 35-36, 42-49, 60, 68-70 and 84-85 degrees. The curve has been inverted by the Weichert-Herglotz method and these regions are found to correspond to possible variations in the P-velocity gradient near the depths of 850-900, 1200, 1550, 1800-1900 and 2500 kms. A comparison is made between these features and those found at similar distances by other array studies as well as measurements of travel-time and amplitudes. The hypothesis that there are anomalies in the lower mantle is strongly supported and the implications of these anomalies for variations in the elastic parameters is also investigated.

CHAPTER 1

1.1 ESTIMATION OF SLOWNESS

The slowness $dT/d\Delta$ and azimuth α^o of a plane wave propagated by an event at a distance Δ^o (subtended by the centre of the Earth), and crossing an array of n seismometers is given by:

$$t_i = C - R_i \cos\left(\Theta_i - \alpha\right) \cdot \frac{dT}{d\Delta} + \varepsilon_i \qquad 1.1$$

(Appendix A) where R_i Θ_i are the polar coordinates of seismometer i, t_i is the relative arrival time at seismometer i with respect to an arbitrary origin and will usually be in error ε_i, and C is a constant and defines the position of the arbitrary origin. At each distance Δ, a scatter of points is obtained through which a mean curve must be drawn.

Any systematic trend in the geology beneath the array, including variation in the altitude of the individual seismometers, will produce variations in the observed values of slowness calculated using equation 1.1 which will usually be a function of azimuth.

Chinnery and Toksöz (1967) assumed the geology beneath LASA has such a systematic trend and so restricted their event-to-array paths to only those from a narrow azimuth range. The rays were then effectively travelling up or down dip. The slowness curve was thus displaced by a constant amount and the DC shift corrected for by adding a constant to the observed values.

An obvious disadvantage of this method is that the amount of data available is severely reduced by restricting the azimuth range. Also the exact value of the DC shift has to be obtained from independent data. Chinnery and Toksöz corrected their values of slowness by making the integral under the slowness-distance curve compatable with the observed travel times from the LONGSHOT explosion.

These restrictions can be overcome by assuming the slowness is constant for all events falling within the same (small) distance interval. As all rays from events at the same distance from an array will reach their lowest point at a common depth, this not unreasonable assumption implies

the Earth is radially symmetrical with depth. Events from all azimuths may be included and slowness and the effects of array sub-structure estimated simultaneously.

The equation of condition for the j^{th} event that falls in the k^{th} distance interval is now, for i = 1, 2 ..... n seismometers.

$$t_{ij} = S_i + C_j - R_i \cos\left(\theta_i - \alpha_j\right). {}^{dT}/_{d\Delta_k} + \varepsilon_{ij} \qquad 1.2$$

S_i is the time correction for the effects of geology under the i^{th} seismometer.

The equations can then be solved for S_i, C_j, α_j and ${}^{dT}/_{d\Delta_k}$ by least squares. As only events are used whose epicentres are given on the UDCGS PDE cards, the azimuth α_j is restrained to the value computed from the known epicentre, so reducing the number of unknowns in each equation of condition by one. The S_i and C_j terms are linearly dependent and so any adjustment in one set of parameters can be compensated by an adjustment in the other. To enable equation (1.2) to be solved, the constraint $\sum_1^n S_i = 0$ has to be applied. The unknowns S_i, C_j and ${}^{dT}/_{d\Delta_k}$ can then be evaluated.

Equation 1.2 is difficult to apply because earthquakes are not generally well distributed in azimuth about an array, but occur along narrow belts. The results may then be biased for if many events within the distance range k lie in roughly the same direction, the $R_i \cos\left(\theta_i - \alpha_j\right)$ terms are approximately constant. S_i and ${}^{dT}/_{d\Delta_k}$ will then be linearly dependent and their estimation biased.

The difficulty can be overcome by the simultaneous estimation of site corrections and slowness using several arrays as described by Douglas and Corbishley (1968). The overall distribution of events in azimuth will then be greater. The equation of condition for array h is now:

$$t_{hij} = S_{hi} + C_{hj} - R_{hi} \cos\left(\theta_{hi} - \alpha_{hj}\right) \frac{dT}{d\Delta_k} + \varepsilon_{hij} \qquad 1.3$$

FIG. 1 EXAMPLES OF TWO-TERM FIT TO RESIDUALS.

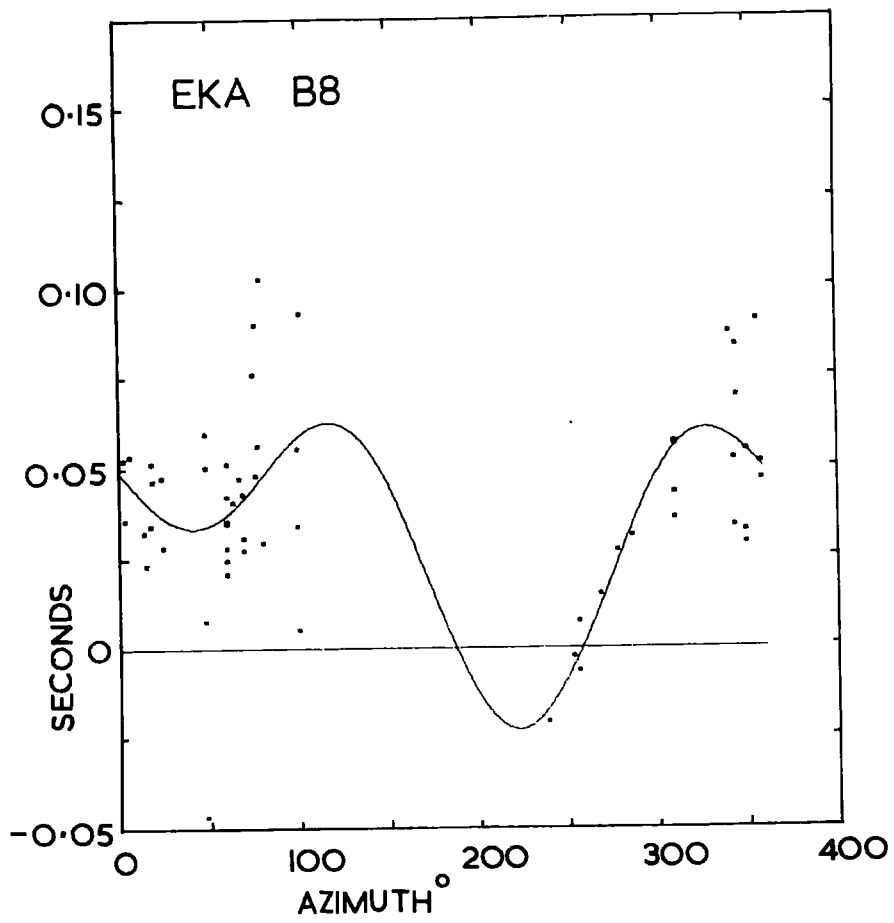

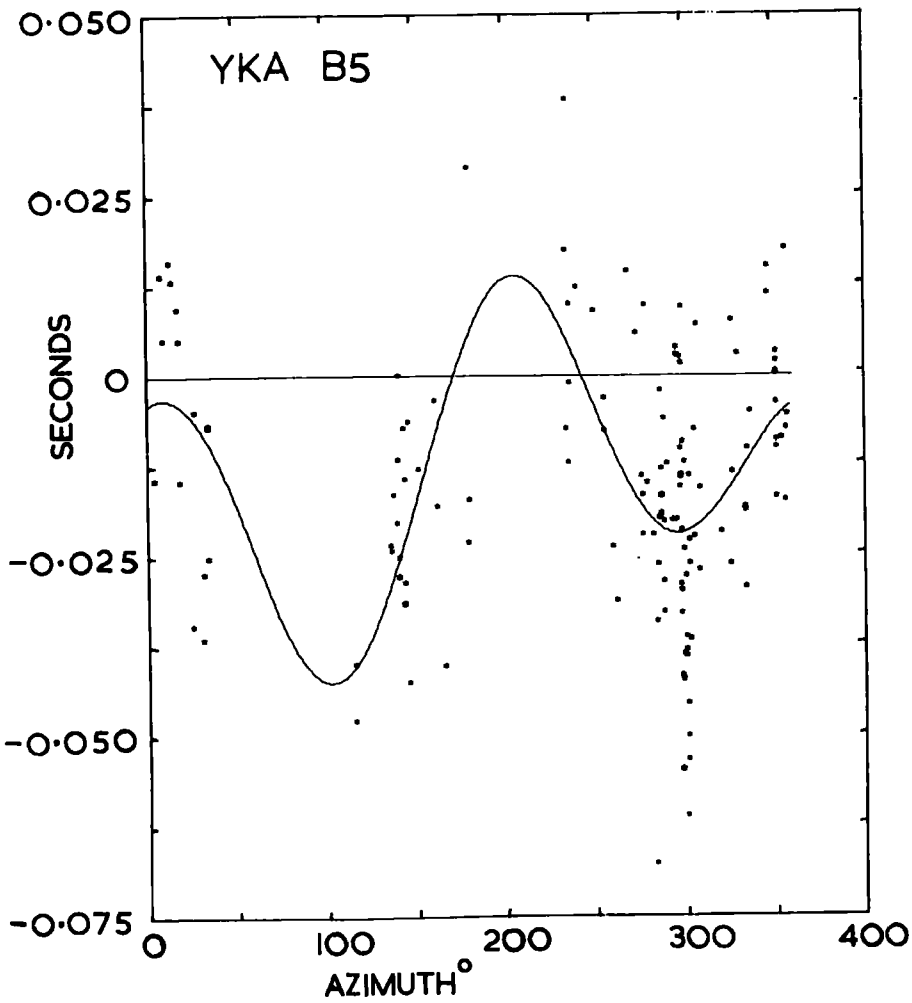

FIG. 2 EXAMPLES OF TWO-TERM FIT TO RESIDUALS.

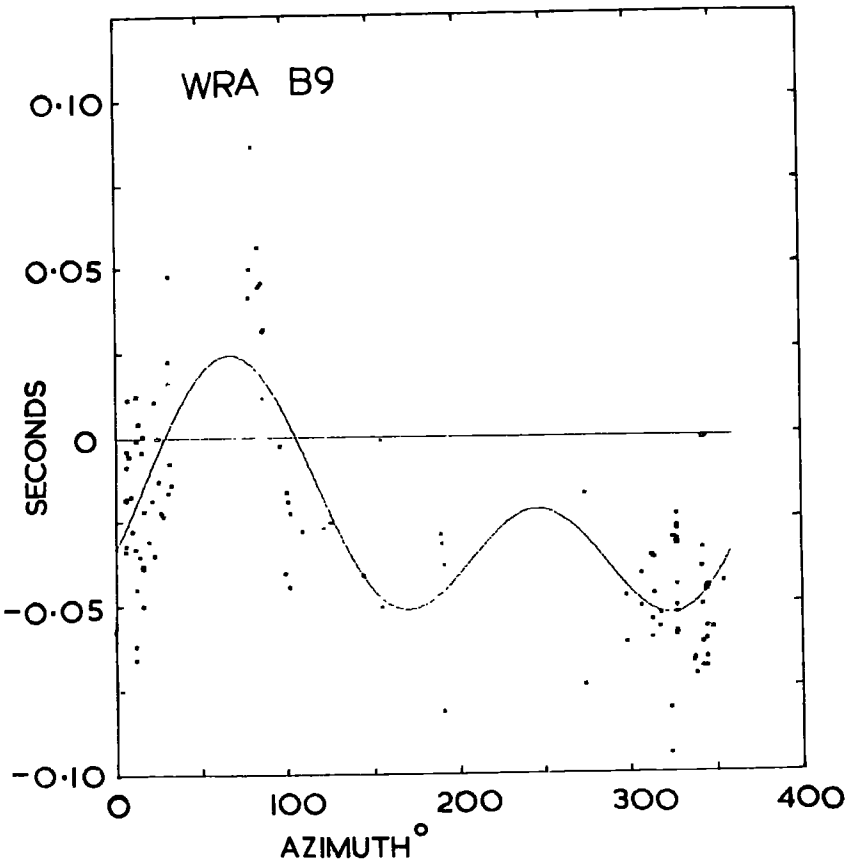

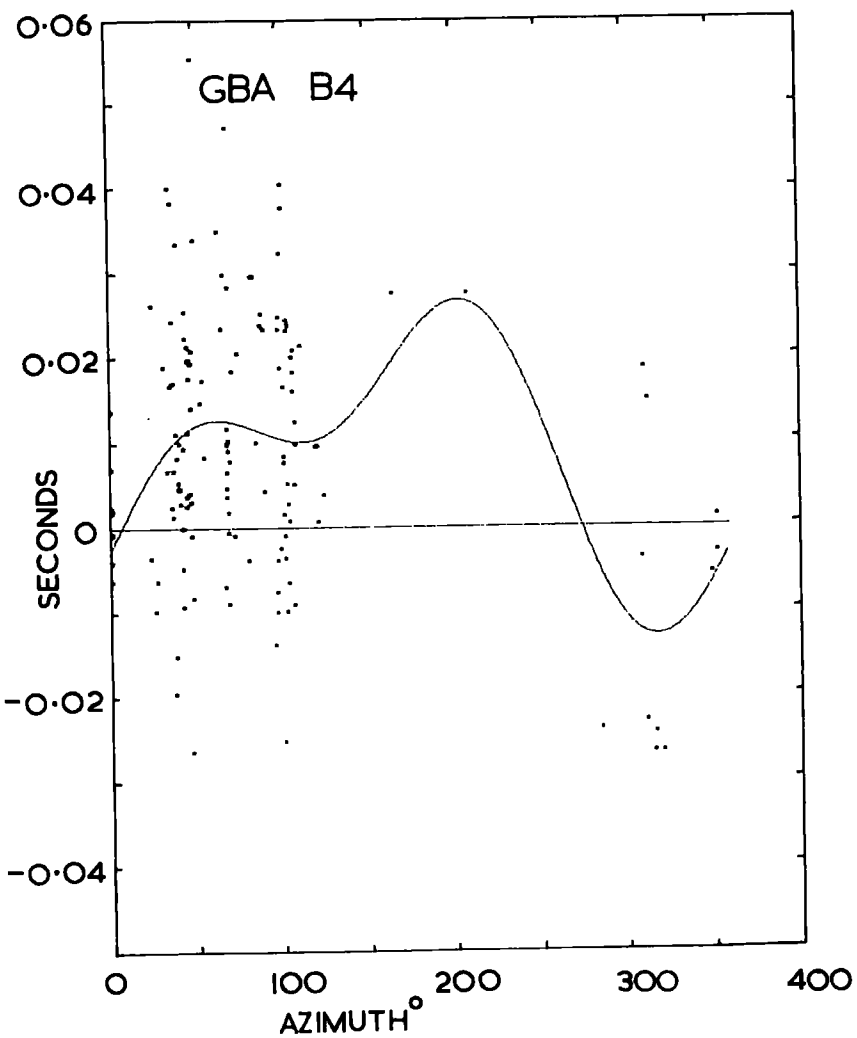

and $\sum_{}^{n} S_{hi}$ for all h.

These equations can thus be solved for the sub-array correction term S_{hi}, the slowness $dT/d\Delta_k$ and the constant C_{hj} (Appendix B). Substitution of these values into equation (1.3) gives the errors ε_{hij} on the onset times t_{hij}. If ε_{hij} are normally distributed about a zero mean, then the variance and 95% confidence limits can be found on all unknowns (Appendix D).

The equations of condition are not set up explicitly but to reduce the computer store needed, the normal equations are formed directly.

By replacing t_i by $t_{hij} - S_{hi} - C_{hj}$ in equation (1.1), values of slowness can be calculated for each event corrected for the effect of structure under the array (Appendix C).

The residuals ε_{hij} are used to define site corrections for each corrections for each seismometer, incorporating both a constant and azimuthally varying term. In the method described here the azimuthal dependence was initially approximated by fitting the following sine curve to the residuals using least squares (the program to do this was written by Mr. R.C. Lilwall):

$$S_{hi} + \varepsilon_{hij} = A_{hi} + B_{hi} \left(\sin \alpha_{hj} + E_{hi} \right) \qquad 1.4$$

where α_{hj} is the azimuth of the j^{th} event at the array h. The site corrections S_{hi} are included with the residuals so that the constant A_{hi} is a better estimate of the DC component of the site correction. It was later found that a better approximation to the residuals was a least square fit of a two term Fourier series:

$$S_{hi} + \varepsilon_{hij} = A_{hi} + B_{hi} \sin \left(\alpha_{hj} + \varepsilon_{hi} \right) + F_{hi} \sin \left(2\alpha_{hj} + G_{hi} \right) \quad 1.$$

The residuals for typical sites at the four arrays and the least squares solution of equation 1.5 are shown in Figures 1 and 2. The least squares solution of equation 1.4 for each seismometer of the WRA array is shown in Figures 24 and 25. A complete list of the five parameters A_{hi}, B_{hi}, E_{hi}, F_{hi} and G_{hi} derived from equations 1.4 and 1.5 is given in Appendix F, and they are discussed more fully in Section 2.2.

With a sufficiently large computer, equations 1.4 or 1.5 could be incorporated into the right-hand side of equation 1.3 and the azimuthal site correction parameters estimated at the same time as the equations are solved for $^{dT}/_{d\Delta}$. Instead, the appropriate time correction for each seismometer, as defined by the five parameters in equation 1.5, are subtracted from the left-hand side of equation 1.3 and the equations of condition again solved for S_{hi}, C_{hj} and $^{dT}/_{d\Delta_k}$.

If the azimuthal corrections have correctly estimated the effects of geology beneath each seismometer, then the residual corrections S_{hi} should now only contain a distance dependent effect and be free of azimuthal bias. The corrections C_{hj} will have the same value as previously and the slowness estimates $^{dT}/_{d\Delta_k}$ will also be corrected for the effects of array sub-structure. Re-substituting $(t_{hij} - S_{hi} - C_{hj})$ back into equation 1.1 gives estimates of the individual values of slowness for each event, corrected for the azimuthally and distance dependent effects of the structure under the array.

By using several arrays with differing, but relatively uncomplicated sub-array structure, an unbiassed estimate of $^{dT}/_{d\Delta_k}$ should be obtained. As the integral beneath the slowness curve is simply the travel time, an independent check on the estimates of $^{dT}/_{d\Delta_k}$, can be made by comparing the travel time obtained by integrating the $^{dT}/_{d\Delta_k}$ curve with known values. Any bias may be corrected for by constraining the area under the $^{dT}/_{d\Delta}$ curve to the observed values. This is done by including the equation of condition:

$$D_1\left(\frac{dT}{d\Delta}\right)_1 + D_2\left(\frac{dT}{d\Delta}\right)_2 \ldots\ldots\ldots\ldots D_k\left(\frac{dT}{d\Delta}\right)_k \ldots\ldots\ldots D_m\left(\frac{dT}{d\Delta}\right)_m = T_m$$

D_k is the integral in degrees over which the slowness is $^{dT}/_{d\Delta_k}$ and T_m is the observed travel times across the range from D_1 to D_m. As will be seen later, the application of this constraint was not necessary.

Even if there are no errors in reading onset times and punching computer cards, real variations in seismic travel times result in the residuals ε_{hij}. In order that an unbiased estimate of the variance is made and the confidence limits give the true 95% coverage, the residuals ε_{hij} from the least squares analysis (after removal of the azimuthal terms) must be normally distributed. A computer program (TRUNCATE) to estimate the residuals showed that after truncation by three standard deviations, the distributions were nearly normal. A full description of TRUNCATE is given in Section 1.5.

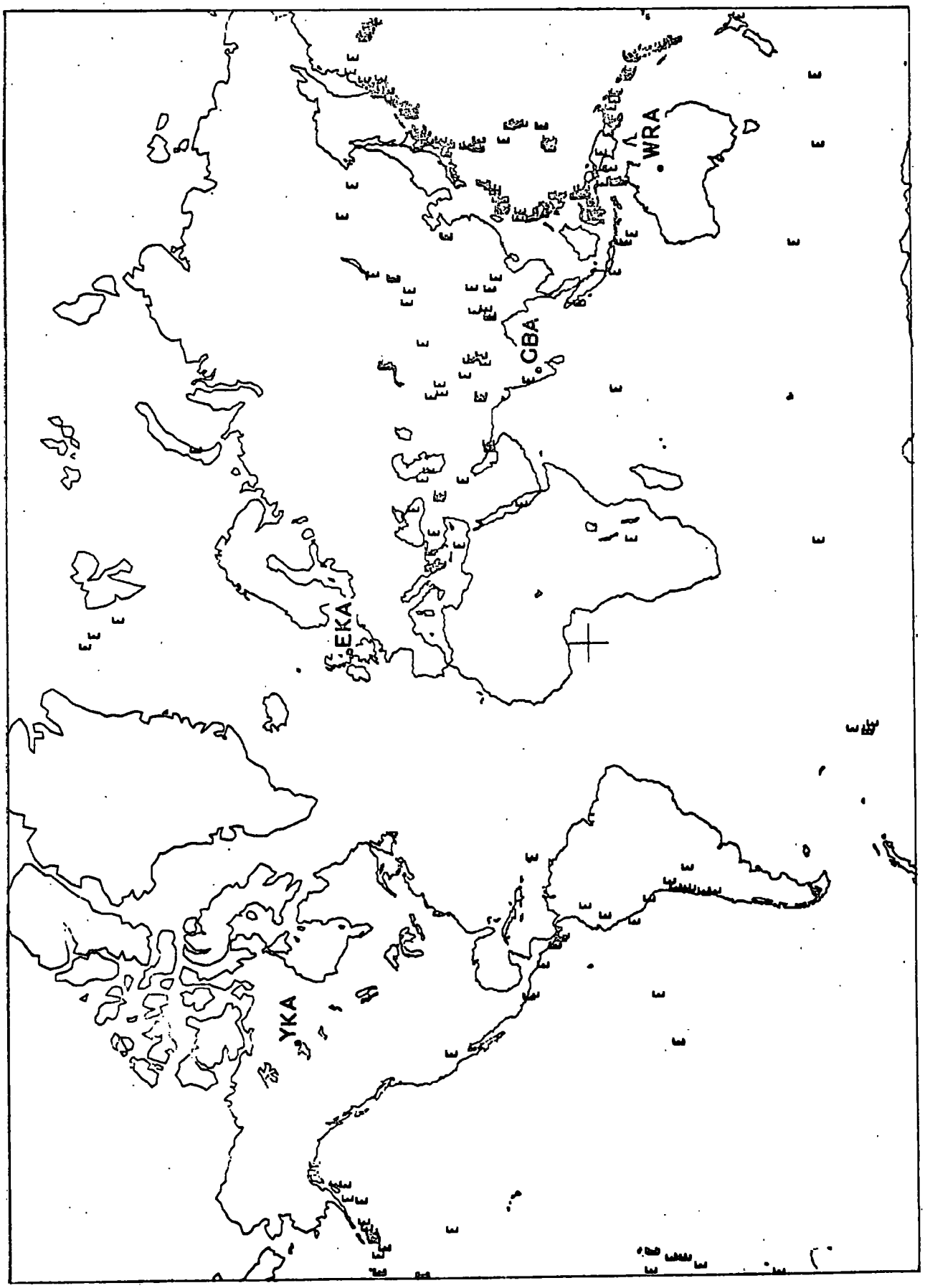

FIG. 3

1.2 THE DATA

Arrival time data for events from a large range of azimuths recorded at four arrays was used to compute slowness. The arrays are located at Eskdalemuir, Scotland (EKA); Yellowknife, Canada (YKA); Gauribidanur, India (GBA); and Tennant Creek, Australia (WRA). They have been described by Truscott (1964) and in an AWRE publication (1967). The configuration of each array and a brief description is given in Appendix E.

All 478 recordings of events, which occurred between October 1965 and January 1968, having magnitudes greater than 4.9, focal depths less than 100 kms, epicentres between 30° and 104° from the arrays and which gave sharp P onsets with a high signal to noise ratio were used in the analysis. The epicentres, depths and magnitudes are assumed to be those given by the USCGS PDE cards. A copy of these cards is held at UKAEA, Blacknest, stored in the program GEDESS (Young & Gibbs 1968). This program sorts and lists the events in accordance with the above criteria and also calculates the azimuth, distance and arrival time for each event with respect to each array. The events and the positions of the four arrays are plotted in Fig 3 and the events are listed in Appendix G.

The relative arrival times for each event were measured from paper records played out so that 60 mm was equivalent to 1 second of recording. The playout speed was accurately determined by measuring the distance between second markers, and the relative onset times measured by matching waveforms as described in Section 1.4. Equation 1.3 was solved with the slowness curve divided into two degree distance intervals, except where the curve appears to be rapidly varying when the interval was decreased to one degree, and except where the data is sparse (between $\Delta = 39^{\circ} - 42^{\circ}$ and $98^{\circ} - 104^{\circ}$) where the interval was increased. The large number of recordings made it impracticable to solve the equations of condition for all the data simultaneously and the curve was estimated in five distance ranges: $30^{\circ} - 44^{\circ}$, $43^{\circ} - 58^{\circ}$, $57^{\circ} - 71^{\circ}$, $70^{\circ} - 84^{\circ}$ and $83^{\circ} - 104^{\circ}$. Any difference

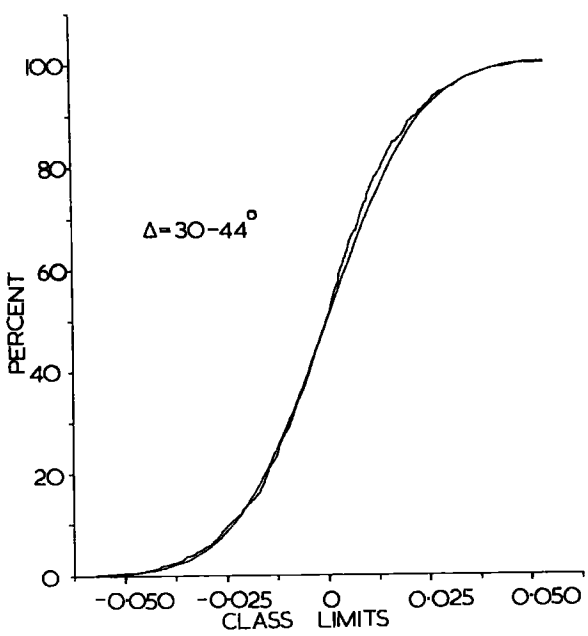

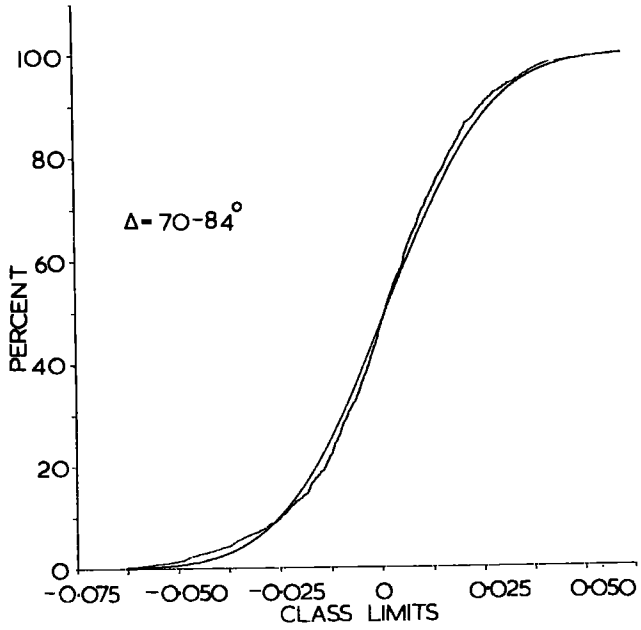

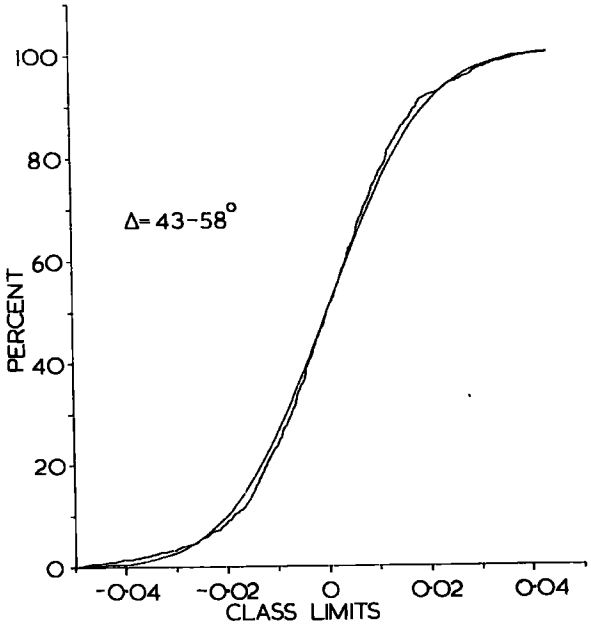

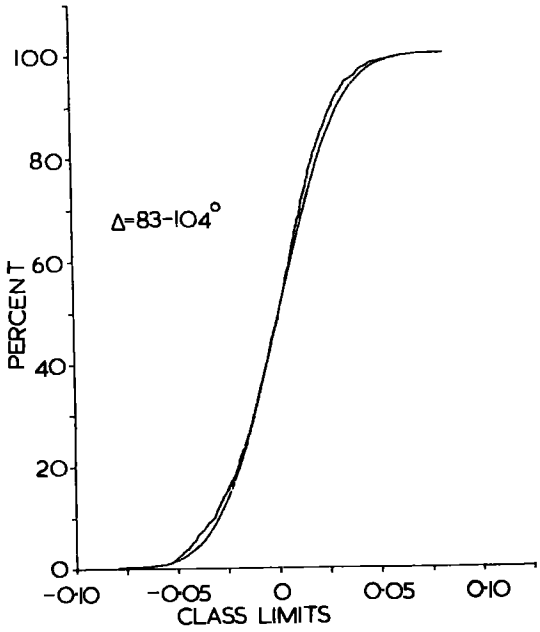

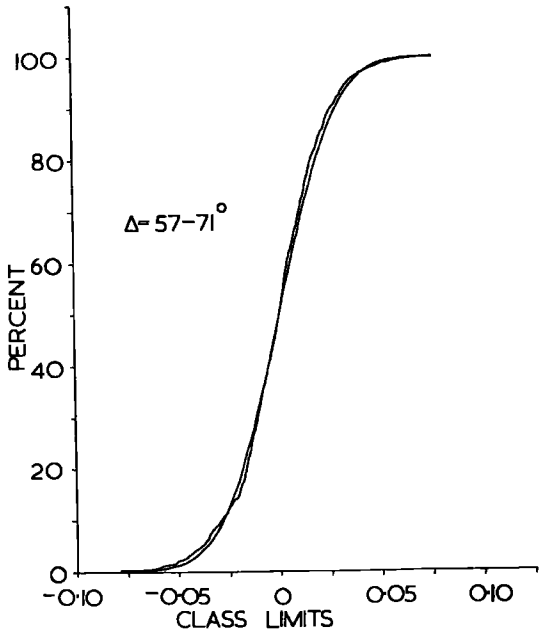

FIG. 4

ALL RESIDUALS (SECONDS) AFTER TRUNCATION BY 3σ.

in $^{dT}/_{d\Delta_k}$ at the one degree overlaps between adjacent distance ranges was always well within the 95% confidence limits, but to obtain a single value at those overlaps, $^{dT}/_{d\Delta_k}$ was restrained to the mean of the two estimates, and the adjacent sections of the curve re-estimated. The mean slowness curve, estimated using two-term azimuthal corrections to remove any bias caused by the geology at the array sites, yielded five sets of onset time residuals ε_{hij}, one set for each distance range.

An accurate estimate of the regression coefficients of the equation of condition relies on these residuals being normally distributed with a zero mean. The residuals for each distance range were tested for normality and gross values (greater than three standard deviations from the meadian) were removed using the program TRUNCATE, described in Section 1.5. This left five approximately normal samples. The number of residuals eliminated after truncation by three standard deviations was as follows (expressed as a percentage):

Range	% Rejected	Total Number, n
$30 - 44^{\circ}$	0.5	1223
$43 - 58^{\circ}$	1.2	1175
$57 - 71^{\circ}$	0	1481
$70 - 84^{\circ}$	0.7	1604
$83 - 104^{\circ}$	0	1482

The very low number of rejected residuals was because misreadings and mispunchings had been eliminated at an earlier stage after recourse to the original records. The normalised, cumulative distribution plots for each distance range after elimination of the gross residuals are shown in Fig 4 along with the theoretical normal distribution.

The population parameters calculated as deviations from the mean, for the five samples are given in the following table:

Range	Mean $\bar{x}$	Variance	Skewness, g_1	Kurtosis, g_2
30 - 44°	-0.00021	.00034	- .040	0.161
43 - 58°	0.00020	.00025	- .113	0.477
57 - 71°	0.00004	.00050	- .080	0.643
70 - 84°	0.00101	.00042	- .226	0.435
83 - 104°	-0.00030	.00057	- .120	0.273

The Kolmogorov-Smirnov distance for each sample showed they are all drawn from normal populations at the 5% level of significance.

The higher moments of skewness and kurtosis are used to infer the effects on the confidence limits of the slight departures from normality that are encountered here.

For a population with mean $\bar{x}$ and variance σ^2, these statistics are defined in terms of expectation as:

$$\text{Skewness, } g_1 = \sigma^{-3} \; E\left[(x - \bar{x})^3 \right]$$

$$\text{Kurtosis, } g_2 = \sigma^{-4} \; E\left[(x - \bar{x})^4 \right] - 3$$

For a normal population of n samples, the skewness g_1 is approximately normally distributed with a zero mean and a standard deviation of $\sqrt{(6/n)}$ (Snedecor, 1967 p86). For the five sets of residuals here, g_1 is not significantly greater than its standard deviation (σ) except in the range 70-84° where $g_1/\sigma = 3.7$.

A further estimate of any departure from normality is given by the kurtosis, g_2. Values of g_2 at different significance levels for various sample sizes are tabulated by Snedecor. Except for the range 30-44°, all the values of kurtosis are greater than the upper 1% level of significance, showing the populations to be more peaked than the normal distribution.

Calculations of the skewness and kurtosis show that the normality assumption has been violated in some cases, and this will have an effect on inferences made using normality. However, inferences about means are only slightly

affected by departures from normality, (Scheffé 1964 p 336) and the estimates of the regression coefficients should not be biased.

95% concidence limits will also be affected by non-normality, and in particular values of kurtosis, g_2 that are not negligible. Tables showing the effect of non-normality on the nominal 95% concidence limits not covering the true confidence limits are given by Scheffé. These show the probability is less than 0.1 within each distance range for the magnitude of kurtosis encountered here.

For the slowness curve to be treated as a world average, the underlying assumption is made that all the observations have been drawn from the same world, population which is distributed about the same mean with similar standard deviations.

The standard test (Bartletts' 1937 test) for equivalence of sample variances is usually very sensitive but tends to find differences in variances where none exist for positive values of kurtosis (Scheffé, p 362). The test was therefore not applied in this case.

It is concluded that the five sets of corrected onset time observations have been drawn from generally normal populations, the departures from which are not great enough to affect either the estimates of the regression coefficients, or the 95% confidence limits.

1.3 ERROR ANALYSIS

There are several sources of error which affect the calculation of slowness and arise from the assumptions made in Appendix A where the basic formula for $dT/d\Delta$ is derived. These are

(1) Assumption of plane wavefront

(2) Changes in apparent slowness with changes in epicentre.

(3) Changes in slowness arising from the spread of the arrays.

(4) Random reading errors.

It is shown that errors arising from 1-3 may be disregarded for events at epicentral distances greater than 30° and errors in epicentre no larger than 20 Kms.

(1) Assumption of plane wavefront

It is assumed that the wavefront traversing an array from an event with slowness S at an epicentral distance Δ° is planar. If the centre of the array is taken as the reference point, then the time difference between the curved wavefront and the theoretical planar front at the extremities of the array is negligible when $\Delta > 30^{\circ}$. This can be seen from the following argument.

If the length of one arm of the array is $2a^{\circ}$ then the time difference δ is given by

$$\delta = S\left[\left(a^2 + \Delta^2\right)^{\frac{1}{2}} - \Delta\right]$$

which on expansion reduces to $\delta = \frac{Sa^2}{2\Delta}$ secs

δ will be largest for the largest arrays (YKA and WRA) where a is approximately 12 Kms, and when Δ is a minimum of 30°, corresponding to S = 8.9 secs/deg. The effect of neglecting curvature δ is therefore less than 2 ms., and so is negligible.

(2) Changes in apparant slowness (and azimuth) with changes in epicentre

The epicentres were taken as those given by the USCGS Preliminary Determination of Epicentres (PDE) cards. Only events greater than magnitude 4.9 were used, and these are conservatively assumed to be in

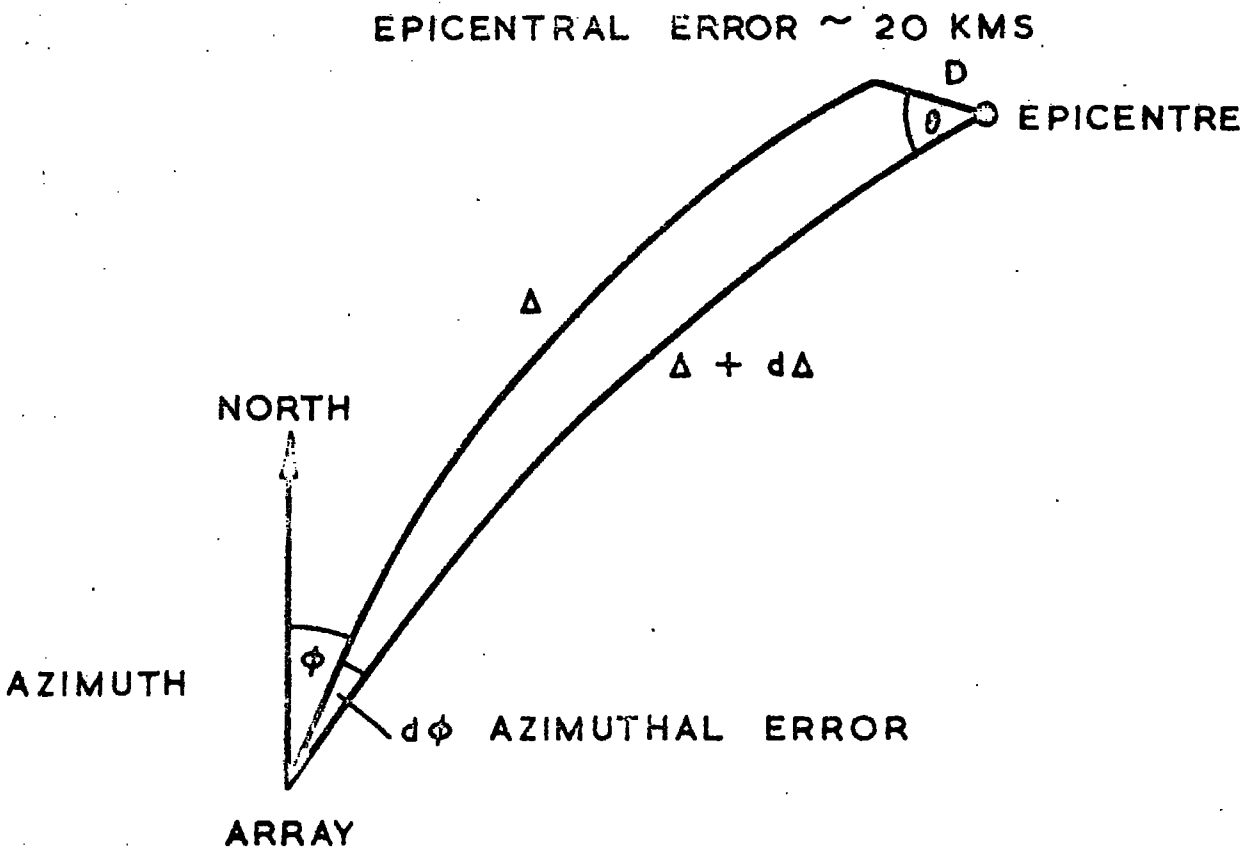

FIGURE 5 . ERRORS IN EPICENTRE LOCATION

error by up to 20 Kms. Tables show the maximum change in slowness will be at small distances, and when $\Delta = 30^{\circ}$, $d^2T/d\Delta^2 = -0.05$ secs/deg^2, the error in slowness will be less than 0.01 secs/degree.

Errors in azimuth will also be small. Referring to Fig. 5 and applying the sine theorem, the azimuthal error $d\phi$ for an event at epicentral distance Δ is given by

$$\frac{\sin d\phi}{\sin D} = \frac{\sin \theta}{\sin \Delta}$$

$d\phi$ is therefore a maximum when $\Delta = 30^{\circ}$ and when θ is a maximum. If the error in epicentre $D = 20$ kms then $d\phi$ will be less than 0.4° and so is negligible.

(3) Changes in slowness arising from the spread of the arrays

The terms epicentral distance and azimuth are ambiguous when referred to an array of seismometers spread over the finite distance of approximately 12 kms for the smaller arrays (EKA & GBA) and 25 kms for the larger arrays (YKA & WRA). Azimuths and distances are calculated from the hypocentres given by the USCGS PDE cards to the centre points of each array using geocentric coordinates and GEDESS (Young and Gibbs 1968). It has already been shown in paragraph 2 that the variations in slowness are greatest when Δ is less than 30°. For an array spread over 25 kms the maximum error in slowness will be of the order of 0.1 secs/deg. at most.

It can therefore be concluded that errors arising from the slight mis-locations in epicentres at distances greater than 30° may be safely ignored, and consequently inhomogeneities near the focii of the events will not affect the azimuth and slowness estimates. Any errors arising from mislocation of epicentres are still further reduced when the results from several arrays are used and slowness estimates averaged over discrete distance intervals of 2°, as they were here.

FIGURE 6 CALCULATED RMS ANOMALY IN $dT/d\Delta$ σ RMS SECONDS

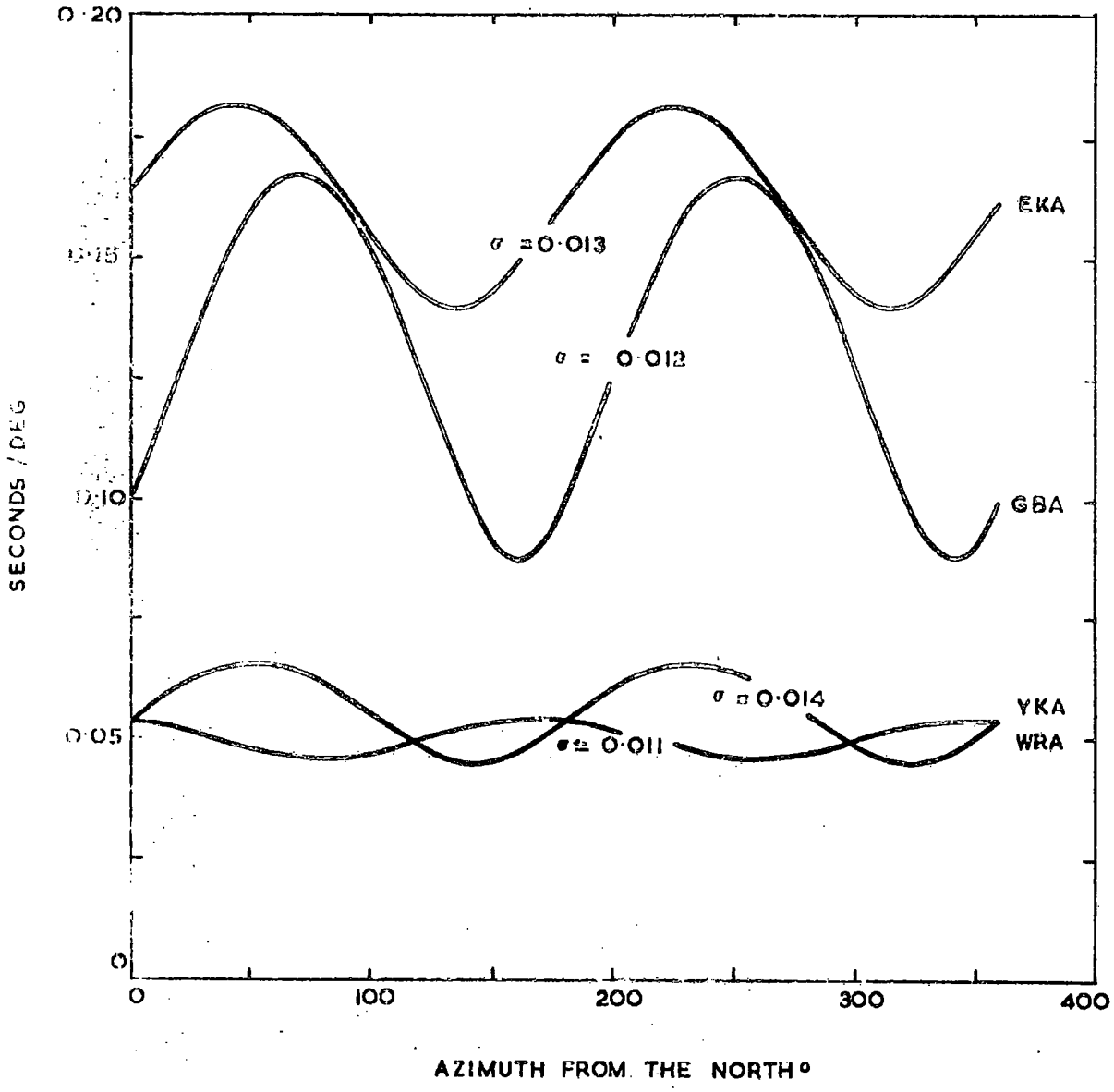

(4) Random Reading Errors

Errors in calculated slowness are propagated if it is assumed that the arrival times at individual seismometers of an array are accompanied by random errors arising from reading the records. Kelly (1964) has derived formulae to compute the error in slowness (and azimuth) when the reading errors are independent Gaussian variables with a variance σ^2 (secs^2).

The root mean square error ds in slowness S (secs/deg) is then

$$ds = \frac{\sigma K}{\sqrt{ND}} \left[\text{var } x.\cos^2\beta - 2 \text{ cov } (x,y).\sin\beta.\cos\beta + \text{var } y.\sin^2\beta \right]^{\frac{1}{2}}$$

where N is the number of seismometers in the array

$D = \text{var } x.\text{var } y - \text{cov } (x,y)^2$

K = number of kms. per deg.

β = azimuth of epicentre from array

x,y = cartesian coordinates of the seismometers with respect to N-S and E-W.

The rms error in calculated azimuth $d\beta$ is given by

$$\delta\beta = \frac{\sigma K}{S\sqrt{ND}} \left[\text{var } x.\sin^2\beta + 2 \text{ cov } (x,y) \sin\beta.\cos\beta + \text{vary}.\cos^2\beta \right]^{\frac{1}{2}}$$

It is shown in section 1.4 that the minimum value of σ that can be obtained when reading the records is, for each array

σ = 0.013 secs. for EKA

σ = 0.011 secs. for YKA

σ = 0.014 secs. for WRA

σ = 0.012 secs. for GBA

A computer program was written to calculate the corresponding values of ds, and values of ds are shown in Fig. 6 for each array. It is concluded that the individual estimates of slowness should be no larger than 0.18 secs/deg for the smaller arrays (GBA and EKA) and can be assumed to be less for a combination of results.

1.4 READING ONSET TIMES AND RANDOM READING ERRORS

Sources of errors affecting the calculation of slowness which arise from assumptions of a plane wavefront and epicentre location have already been discussed.

In this section an estimate is made of the random errors that arise from reading the onset times and also those that arise from the recording and play-back system.

Because of the relatively small apertures of the arrays (the smallest being 12 Kms in extent, the largest 25 Kms) it is essential to find a method of measuring the time taken by the P wave to cross the array that is repeatable to plus or minus a few hundredths of a second. An experiment was conducted whereby three different methods of reading onset times were compared, viz.(1) estimating the relative arrival time of the first peak (2) estimating the time of the first cross-over and (3) estimating the relative arrival time by matching waveforms. Method (3) is shown to give the lowest repeatable error in onset time and therefore matching waveforms were used to measure all the data.

Data from 22 presumed underground explosions fired in E. Kazakh, USSR, were used. These occured within an area of a few hundred square kms (Blamey and Gibbs, 1968), so the ray paths from each event to a given recording station should be very nearly constant and the explosions considered as identical repetitions of the same experiment. The only sources of error in the observed onset times are therefore in the recording and playback system and the reading error. An estimate of the variance of the errors can then be found for each method of reading the records for arrivals at each array.

Transcribing and Reading the Records

The facilities available at UKAEA, Blacknest for the handling and processing of seismic data are described in AWRE Pamphlet No.2.

FIG. 7

METHOD OF READING RECORDS.

P = IST. PEAK, X = IST. CROSS-OVER

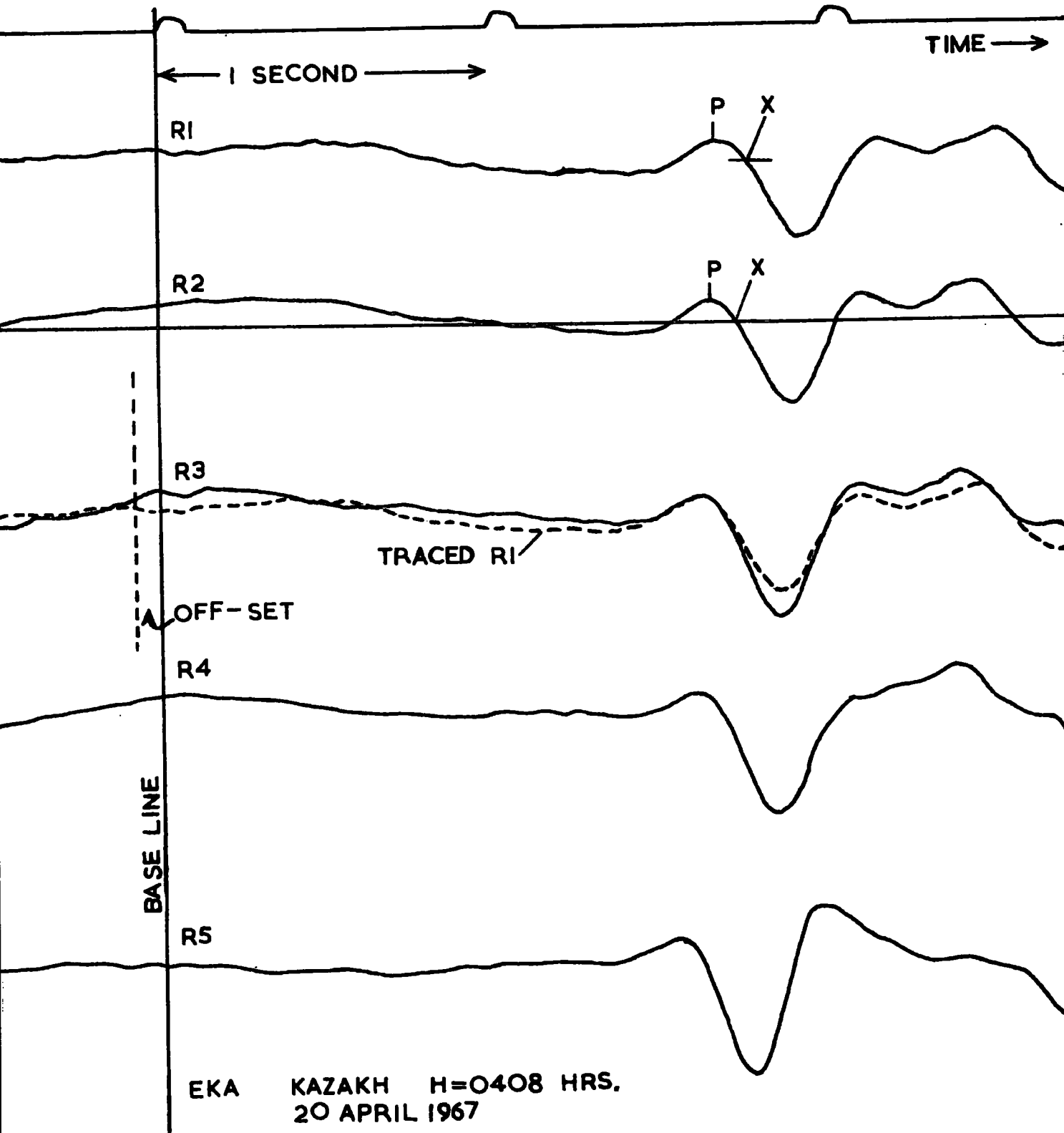

The outputs from the seismometers of each array are recorded continuously on 1 inch wide magnetic tape and consist of 21 signal channels, two error correction channels for wow and flutter, and one channel for timing. Frequency modulation is the recording technique used, with a tape speed of 0.3 inches/second, which provides for 3 days continuous recording using 14 inch diameter reels. The tapes are stored for two years, after which they are compressed by a factor of 8 and transcribed onto a library tape.

Reading the Records

Unfiltered, original recordings of the events were played out from the magnetic tape onto paper using an eight channel Mingograph recorder. The speed of playout was adjusted so that approximately 60 mm. was equivalent to 1 second of recording. It should then be possible to estimate onsets to within 0.01 seconds if the records are read to an accuracy of a few tenths of a mm. The playout speed was accurately determined by measuring the distance between second markers with a mm. graticule.

Fig 7 shows a full-size reproduction of 5 record channels and the time channel of an event that occurred on 20 April 1967, recorded at EKA. A base line has been drawn perpendicular to the traces and P shows the position of the first peak. By measuring the distance from the base line to each P and knowing the playout speed, the relative onset times with respect to the base line of the 5 channels can be calculated. The outputs from all 20 channels were played out in 3 groups of 7, each with the time trace. The base line could then be drawn relative to all the traces. The arrow X indicates the positions of the first cross-over points, the relative onset times of which were estimated in a similar way.

The method of matching waveforms involves tracing one of the curves (eg. R1, here) onto transparent paper, and using the paper as an overlay, matching the traced curve by eye with each of the recordings in turn. The relative displacements with respect to the arbitrary datum line

TABLE 1.4

EVENTS RECORDED AT THE E. KAZAKH TEST SITE SSR.

APPROXIMATE LATITUDE = 49.8 DEGS. N
APPROXIMATE LONGITUDE= 78.1 DEGS. E

E------RECORDED AT EKA.
Y------RECORDED AT YKA.
W------RECORDED AT WRA.
G------RECORDED AT GBA.

	DATE	ORIGIN TIME H MIN SEC				
1	21.11.65	4 57 57.9		Y		
2	13.02.66	4 57 57.9		Y	W	G
3	20.03.66	C5 50 .		Y	W	G
4	21.04.66	3 57 58.1		Y	W	G
5	29.06.66	6 57 58.1	E	Y	W	G
6	21.07.66	3 57 57.9	E		W	G
7	05.08.66	3 57 57.5	E	Y	W	G
8	19.10.66	3 57 57.9	E		W	G
9	03.12.66	C5 02 .				G
10	18.12.66	4 57 58.7	E	Y	W	G
11	25.03.67	C5 58 .	E	Y	W	G
12	20.04.67	4 07 58.1	E	Y	W	G
13	28.05.67	C4 08 .	E	Y	W	G
14	29.06.67	C2 57 .	E		W	
15	15.07.67	3 26 57.4	E	Y	W	G
16	04.08.67	C6 58 .	E	Y	W	
17	16.09.67	4 03 58.0	E	Y	W	
18	22.09.67	5 03 57.9		Y	W	G
19	17.10.67	5 03 58.0	E	Y	W	G
20	30.10.67	6 03 57.9	E	Y	W	G
21	08.12.67	6 03 57.1	E	Y	W	
22	07.01.68	C3 47 .	E			

can then be determined. All channels recording onsets for the 22 events listed in Table 1.4 were read using the three methods described.

Analysis of Variance

An analysis of variance was performed to estimate the random reading error associated with a single determination of onset time using the 22 Kazakh explosions.

For any array the arrival relative time at the ith seismometer of the jth event is taken to be of the form

$$t_{ij} = P_i + C_j + \bar{t} + \varepsilon_{ij} \qquad (1.6)$$

Assuming there is no event-seismometer interaction, then P_i depends on the position of the ith seismometer in the array, C_j depends on the arbitrary zero from which the relative onset times have been measured (the base line in Fig 7). t_{ij} will usually be associated with an error ε_{ij}. Because t_{ij} is a relative value, the constant $\bar{t}$ is introduced. Equation (1.6) however cannot be solved as written because any change in either one of the sets P_i or C_j can be compensated for by adjustments in the other. The following constraints are therefore applied:

$$\sum_{i}^{r} P_i = 0 \quad , \quad \sum_{j}^{c} C_j = 0$$

The model describes a simple two way analysis of variance with the onset times displayed in the Matrix of Observations:

	C_1	C_2	----------	C_c
P_1	t_{11}	t_{12}	----------	t_{1c}
P_2	t_{21}		t_{ij}	
.				
.				
P_r	t_{r1}			t_{rc}

The average onset time of the average event is $\bar{t} = \left(\sum_{ij}^{rc} t_{ij}\right)/rc$

the average onset time at the ith seismometer for all explosions is

$P_i = \left(\sum_{j=1}^{c} t_{ij}\right)/c - \bar{t}$ and the average onset time of the jth explosion at

all seismometers is given by $\left(\sum_{i=1}^{r} t_{ij}\right)/r - \bar{t}$ where c is the number of explosions and r the number of seismometers.

By substituting P_i, C_j and $\bar{t}$ into equation (1), the unassigned or unknown variation due to random errors ε_{ij}, can be found. An estimator of the variance S^2 is then given by

$$S^2 = \frac{\sum_{ij}^{rc} \left(s_{ij}\right)^2}{m - n}$$

where m-n is the number of degrees of freedom obtain from the number of equations of condition m with n unknowns. This method can be used if all t_{ij} are known. Unfortunately this was not always so, as not all the seismometers were working for all of the events. The equations have therefore to be solved by least squares, which does not require that all t_{ij} to be known and a special purpose least squares program (LSMF Douglas 1966) used to derive S^2. Using the 22 Kazakh explosions listed in the Table 1.4 the variance S^2 of the random reading errors was estimated at each array for each of the three methods of reading onset times.

For S^2 to be an efficient estimator of the population variance σ^2 the errors ε_{ij} should be normally distributed. The program TRUNCATE was used to eliminate residuals larger than three standard deviations when the Kolmogorov-Smirnov statistic was exceeded at the 95% level. For the 9 estimates of S^2, the number of residuals rejected were as follows (expressed as a percentage):

Array	Matching Waveforms	1st Peak	1st Crossover
EKA	0	1.2	0
YKA	3.2	1.8	2.4
WRA	0	0	1.2
GBA	0	1.4	0

After elimination of the onset times associated with these gross residuals, the analysis of variance was repeated. The standard deviations (in seconds) of a single estimate of the relative onset times for the normalised samples are:

Array	Matching Waveforms	1st Peak	1st Crossover
EKA	0.013	0.012	0.019
YKA	0.011	0.017	0.020
WRA	0.014	0.017	0.024
GBA	0.012	0.018	0.016

The technique of matching waveforms is seen to be marginally better than the other two methods for reading records and was therefore used to read all subsequent recordings.

DISCUSSION OF ERRORS

The technique of matching waveforms was first described by Evernden (1958) for the calculation of surface wave phase velocities across tripartite arrays. The advantage of this technique over the other two is that it does not depend on an accurate recognition of the first motion or cross-over, as the times can be computed from any part of the waveform. Records with fairly emergent onsets can then, in theory, also be used. The velocity filtering methods (Birtill and Whiteway, 1965) gives inferior results to the manual method because correlation has to be carried out over a fixed length of record for each trace. Correlating the records by eye, although a slow process, overcomes this difficulty.

The accurate estimation of onset times by either of the three methods described assumes the recorder pens are not displaced relative to each other. The Mingograph recorder is equipped with ink jets that operate in a plane perpendicular to the direction of the trace. They are therefore unaffected by displacements between traces which is a disadvantage

G. 8

MULATED POWER FAILURE YKA 2252 HRS. 19 JULY 1968.

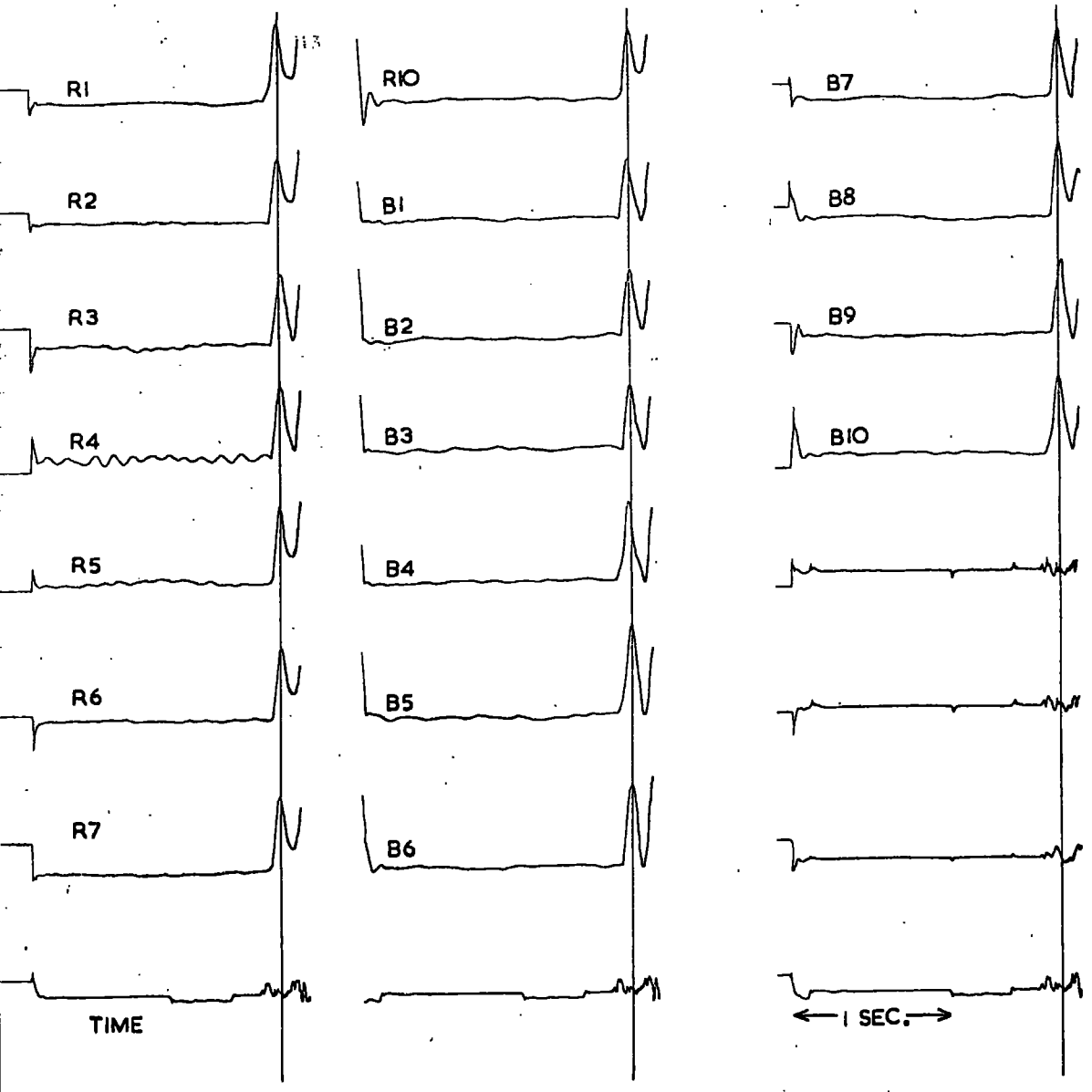

encountered with recorders equipped with pens pivoting around a radius. Any relative displacement of the ink jets can be checked by observing a pulse such as a lightning flash or a power failure that is recorded simultaneously on all channels. Displacements introduced by misaligned magnetic tape heads and also "snaking" as the magnetic tape passes across the heads can similarly be estimated.

Fig 8 shows a simulated power failure at YKA played out at 60 mm/second and recorded on all available channels. No displacements of the onsets are observable within the limits of reading error, and a similar conclusion was reached for recordings from the other 3 arrays. It is therefore concluded that the recording and transcription does not introduce significant errors into the reading of the onset times.

Muirhead (1968) discusses variations in the onset times introduced by variations in seismometer characteristics at the WRA array: (1) a phase shift produced by the finite pass band of the seismometer, (2) variations in seismometer damping. He found that (2) could be neglected. However, over a number of days at random the spread of the natural frequency of the seismometers varied between 0.9 and 1.1 Hz. It was computed that this variation could introduce an error of up to 0.04 seconds at the first cross-over point for a signal with a fundamental frequency of 1 Hz. Muirhead concluded that to overcome this variation, only high frequency events should be used, and the first convenient part of the waveform used to measure onset times. Consequently impulsive, high frequency events were used throughout the analysis wherever possible.

1.5 NORMAL ERROR THEORY AND ELIMINATION OF EXTREME VALUES

This section discusses the assumptions made when the least squares technique is used and describes a method of rejecting data to obtain a normally distributed set of residuals.

The estimation of slowness from the large number of equations of condition (approximately 1400 in each of the five distance ranges) uses the technique of least squares. The basic assumption behind this method is that the set of onset time measurements is actually the most probable set of measurements. In other words, it is hoped that the probability of obtaining the particular set of onset times observed has been maximised. This is the Principle of Maximum Likelihood. If the observations are distributed normally, then the probability is maximised by minimising the sum of the squares of the deviations from the most probable value.

On estimating the regression coefficients $^{dT}/_{d\Delta_k}$, C_{hj} and S_{hi} from the equation of condition.

$$S_{hi} + C_{hj} - \left(x_{hi} \sin \alpha_{hj} + y_{hi} \sin \alpha_{hj} \right) \frac{dT}{d\Delta_k} = t_{hij} + \varepsilon_{hij} \qquad 1.7$$

it is assumed that the errors ε_{hij} associated with the observed onset times t_{hij} are normally distributed, so justifying the use of least squares.

Any departure from the underlying assumption of normality will bias the estimates of the regression coefficients and also the estimates of the confidence limits (Scheffe' 1964 p.331). It is therefore necessary to test the distribution of residuals ε_{hij} for normality.

The computer program (Appendix H) written to solve (1.7) gives a list of the residuals. Relatively large values are easily spotted and misreadings and mispunchings can be corrected by recourse to the original records. However, a few large residuals will still remain and it is necessary to derive a technique for dealing with them.

The problem of truncation of data to eliminate large residuals is a controversial one, and there is no agreement among authorities as to a definite answer. If a relatively large residual is retained it can bias the estimate of the mean and have an even greater effect on the variance. If it is discarded, then a degree of subjective judgement is introduced.

Criteria for the rejection of observations have been given by Peirce and Chauvenet and alternative methods are discussed by Tukey (1962). Between the extreme views of Chauvenet and the principle of not rejecting any observation at all are more moderate views. A technique that has a better theoretical justification is the method of uniform reduction (Jeffreys 1961), although it is complicated to use. A comprehensive discussion of methods for dealing with contaminated seismic data is contained in Freedman (1968).

In order to, at least, partially eliminate the contaminated population, the following procedure was adopted, which is a modification of the subroutine TRUNCATE (Herrin et al 1968).

(1) The goodness of fit of the observed data to an assumed theoretical (normal) distribution was tested by the Kolmogorov-Smirnov distance at the 95% significance level.

(2) If the distribution was found to be contaminated by gross errors, then the data was truncated at plus and minus three mean deviations from the median.

(3) The sample mean and variance from the mean were calculated for the truncated sample, and the sample variance corrected for truncation (Freedman 1966).

To test whether or not a sample is drawn from a population having a specific distribution, the χ^2 test of goodness of fit is usually employed. To carry out this test, the null hypothesis is first set up that the sample has been drawn from a universe with a known distribution, e.g. the normal

distribution. The observed and the theoretical distributions are then divided into analogous classes, and a table of relative frequencies or probabilities in each class calculated. If the set of frequencies to be tested is O_1, O_2 .....O_n and the reference set C_1, C_2.....C_n, where n is the arbitrary number of classes, then the χ^2 statistic is given by

$$\chi^2 = \sum_{i=1}^{n} \frac{(O(i) - C(i))^2}{C(i)}$$

The calculated value of χ^2 with n-1 degrees of freedom is compared with the tabled value of χ^2_α at a selected level of significance (α). If the computed value of χ^2 is equal to or exceeds χ^2_α, the null hypothesis is rejected.

Although widely used, the test has some serious limitations (Williams 1950). One such drawback is that the choice of number and width of class interval can seriously affect the result of the test. An alternative test was therefore used based on the maximum difference between the observed and the hypothetical cumulative distributions. This distance (d) is known as the Kolmogorov-Smirnov distance. As the test is based on the continuous cumulative distribution of the population, it has the advantage that there need not be any arbitrary grouping of the data.

To use the test, it is supposed that the population has a specified cumulative frequency distribution function $F_o(x)$. For a given value of x, $F_o(x)$ will be the proportion of individuals in the population with measurements less than or equal to x. The observed cumulative step-function $S_N(x)$ of N observations in the sample is expected to be fairly close to the specified distribution, and the sampling distribution of

$$d = \text{maximum}/F_o(x) - S_N(x)/$$

is known and is independent of $F_o(x)$ if $F_o(x)$ is continuous. If $S_N(x)$ is not close enough, then this is evidence that the hypothetical distribution is not the correct one.

A graph of $F_o(x)$ is first drawn and curves at a distance $d_\alpha(N)$ are drawn above and below the hypothetical curve. If the observed cumulative distribution $S_N(x)$ passes outside of this acceptance band at any point, the hypothesis that the true distribution is $F_o(x)$ is rejected at the α level of significance.

Tables of the maximum distance $d_\alpha(N)$ for various sample sizes N and for different significance levels α have been compiled by Owen (1962). The asymptotic value (for a sample size N greater than 35) at the 95% significance level (which was the level used throughout) is:

$$d_{.95} = \frac{1.36}{\sqrt{N}}$$

Indications are that the test, which is considerably easier to use than the χ^2 statistic, is also superior to χ^2 (Massey 1951). Any sample population which failed the Kolmogorov-Smirnov test was truncated to remove non-normal errors using the sample median and the mean deviation about the median. These estimators are preferred to those of the sample mean and standard deviation from the mean when working with contaminated data (Tukey 1960, Herrin et al 1968). The sample median is less affected by extreme values than the mean, which may no longer be the appropriate estimator of the population mean.

It was considered a reasonable procedure to discard all data beyond three times the square root of the mean square deviation about the median. When the sample median is near the population mean in the normal case, the probability of observing data outside these limits is less than 0.003 and so any data rejected can be assumed to be caused by gross errors.

This procedure results in the rejection of a fraction (1-k) of the data. If the population of the central k per cent is considered normal, then the variance of this central portion is $\sigma_k^2 = \sigma^2 p(k)$ where σ^2 is the population variance and p (k) is a function independent of the

population mean and variance. On obtaining p(k) for the fraction k (Freedman 1966), an estimate of the population variance in the normal case after symmetrical truncation is given by

$$\sigma^2 = \frac{S^2(K)}{p(k)}$$

where $S^2(K)$ is the sample variance of the central K per cent.

A computer program (TRUNCATE) was written to perform the operations (1) to (3) to test the distribution of residuals and is listed in Appendix H.

FIG. 9

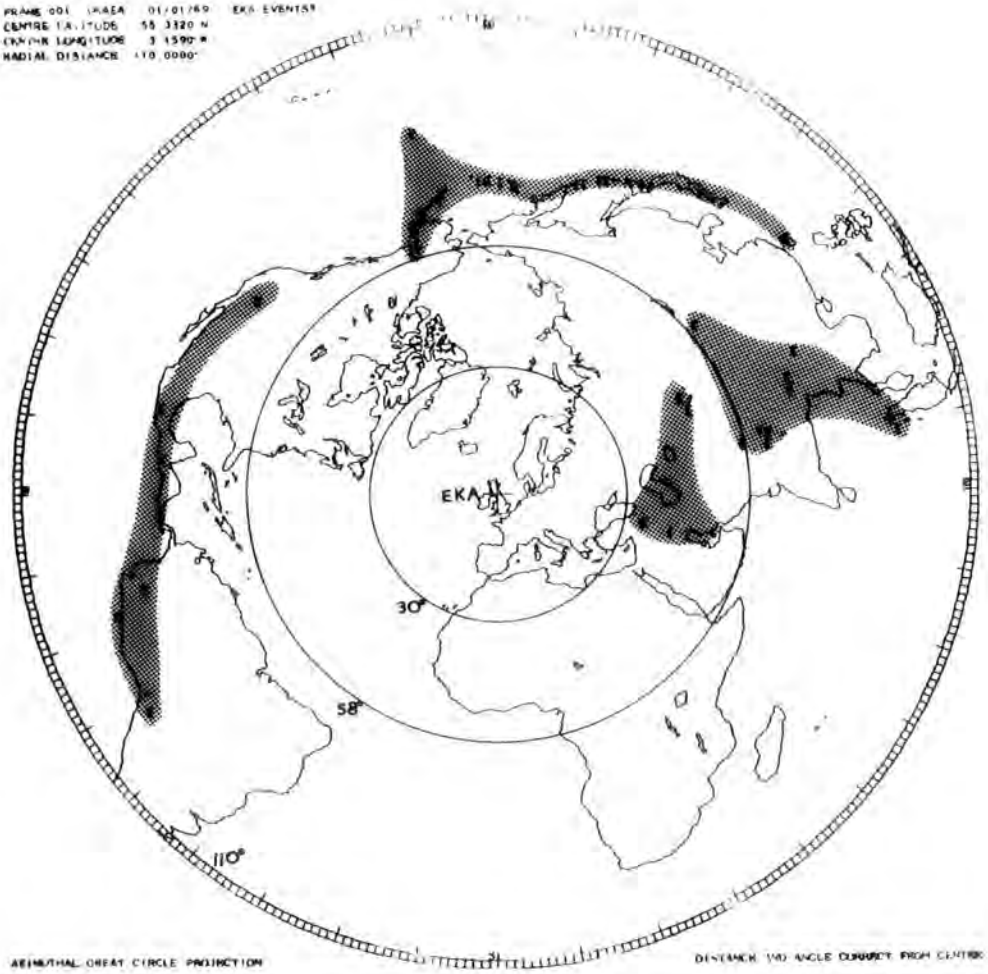

AZIMUTHAL GREAT CIRCLE PROJECTION

DISTANCE AND ANGLE CORRECT FROM CENTRE

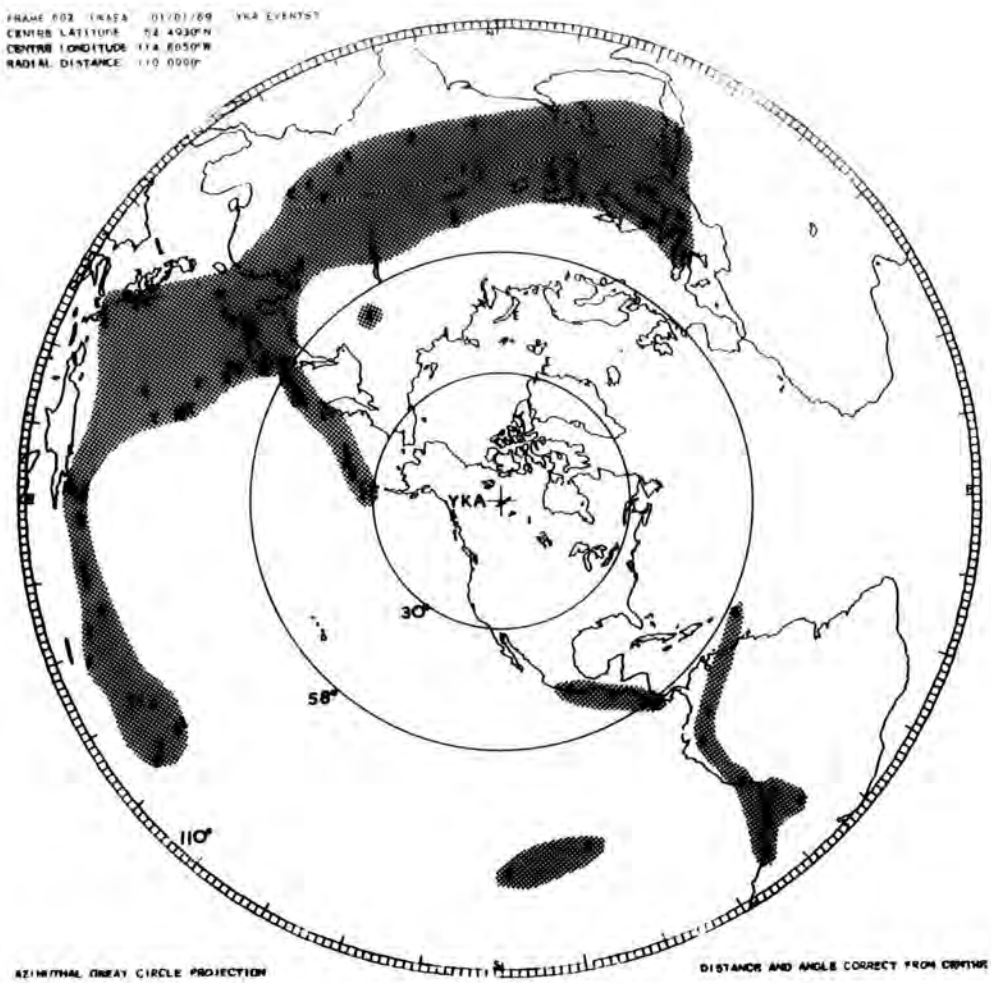

AZIMUTHAL GREAT CIRCLE PROJECTION

DISTANCE AND ANGLE CORRECT FROM CENTRE

FIG. 10

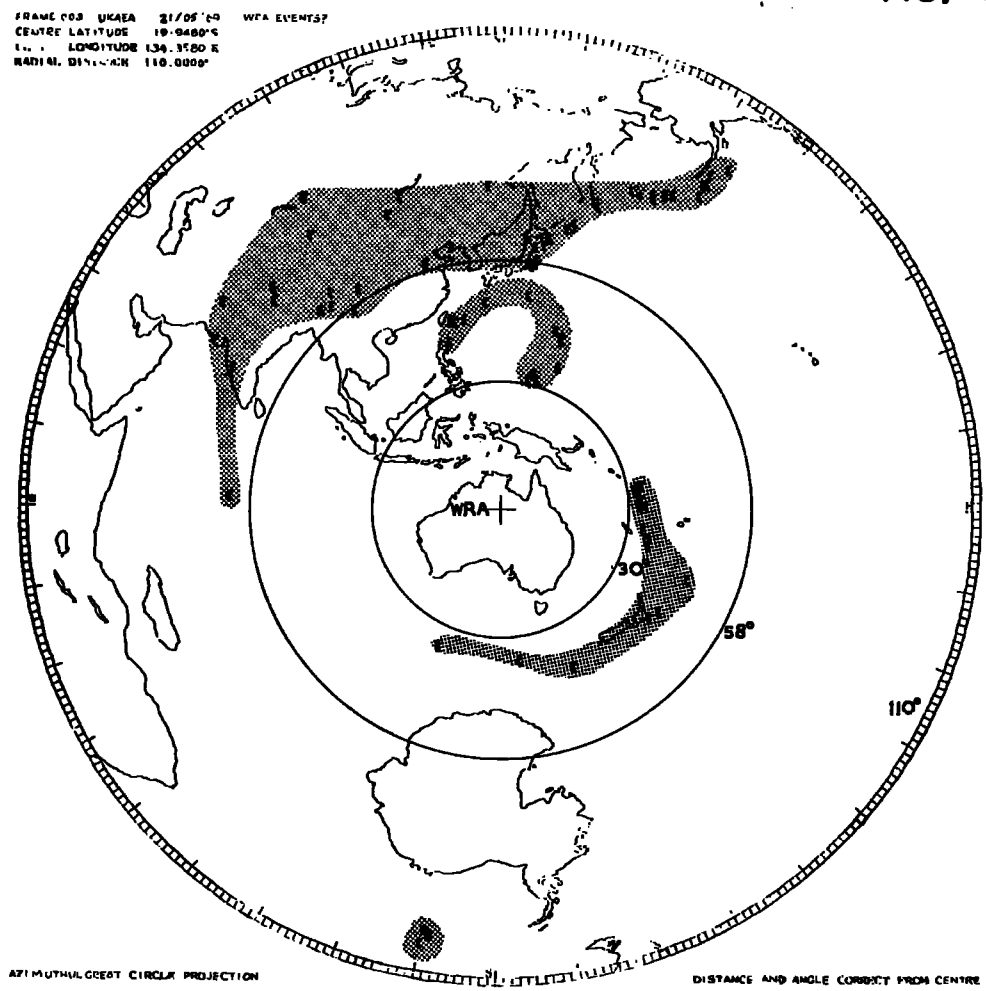

AZIMUTHAL GREAT CIRCLE PROJECTION

DISTANCE AND ANGLE CORRECT FROM CENTRE

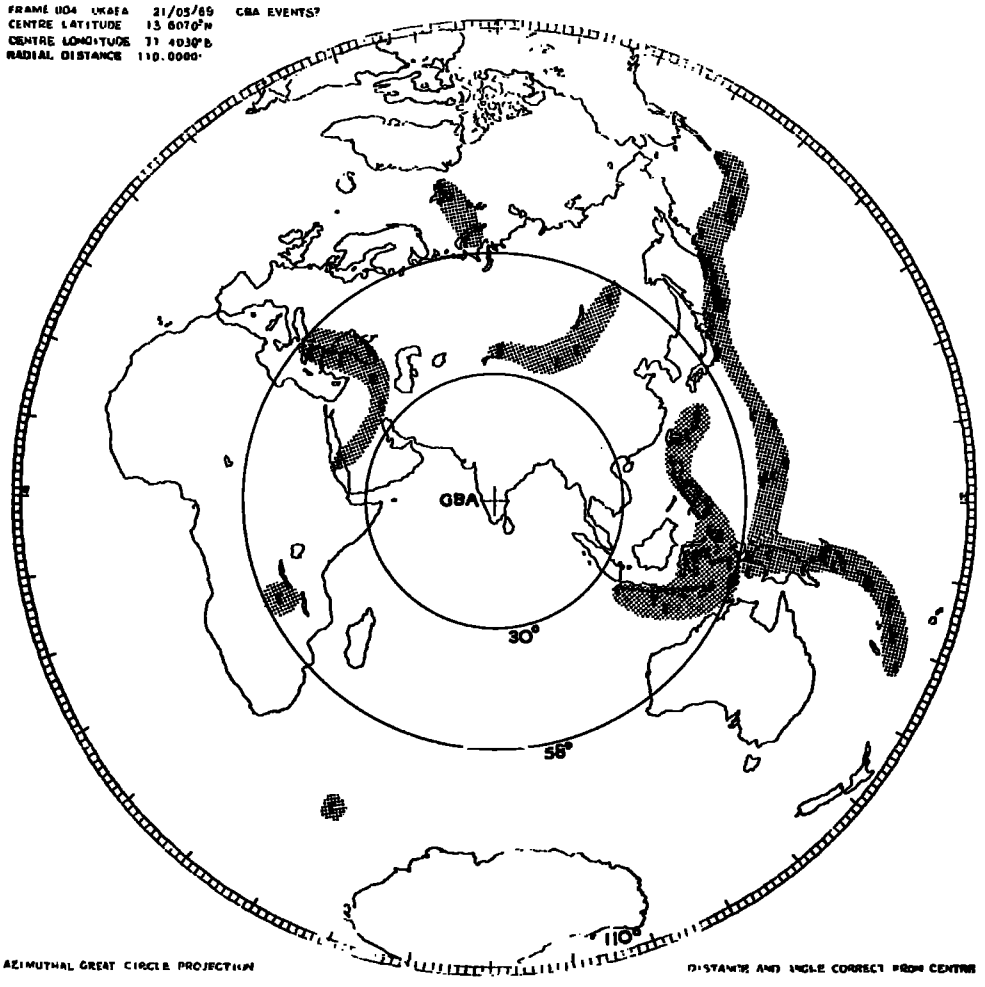

AZIMUTHAL GREAT CIRCLE PROJECTION

DISTANCE AND ANGLE CORRECT FROM CENTRE

CHAPTER 2

RESULTS

2.1 SLOWNESS CURVE

Values of slowness were estimated for 478 recordings, comprising 61 at EKA, 145 at YKA, 129 at WRA and 143 at GBA. The azimuthal distribution of the events at each array is shown in the shaded areas of Figures 9 and 10. It is apparent that the distributions at arrays WRA and GBA are different when events in the first two distance ranges ($\Delta = 30^\circ - 58^\circ$) are compared with events at distances greater than 58°. There is a greater spread of azimuths for the events in the first two distance ranges.

This change in the azimuthal distribution of events with distance affects the values of the azimuthal site corrections derived from the event residuals. Two sets of corrections were therefore estimated; one set for the distance range $\Delta = 30^\circ - 58^\circ$ and a further set for $\Delta = 30^\circ - 104^\circ$.

By using two sets of two-term azimuthal site corrections it was found the reduction in scatter of slowness is greater for the inner range $\Delta = 30^\circ - 58^\circ$ than when all events are corrected with the same corrections.

Calculation of the slowness estimates results in a reduction of the variance from 0.00054 to 0.00044 secs^2 ($\Delta = 30^\circ - 44^\circ$) and from 0.00035 to 0.00032 secs^2 ($\Delta = 43^\circ - 58^\circ$) when the site corrections for the inner ranges are used.

As only events with clear P onsets and a large signal to noise ratio were used, only a low number of events were selected at EKA, with most concentrated at distances greater than 58°. Events at distances greater than 58° are well distributed in azimuth at YKA, while those at a smaller distance are few but distributed at opposite azimuths, and are less likely to produce biased estimates of the azimuthal corrections.

The mean estimates of slowness, $dT/d\Delta_k$ and 95% confidence limits

FIG. 11

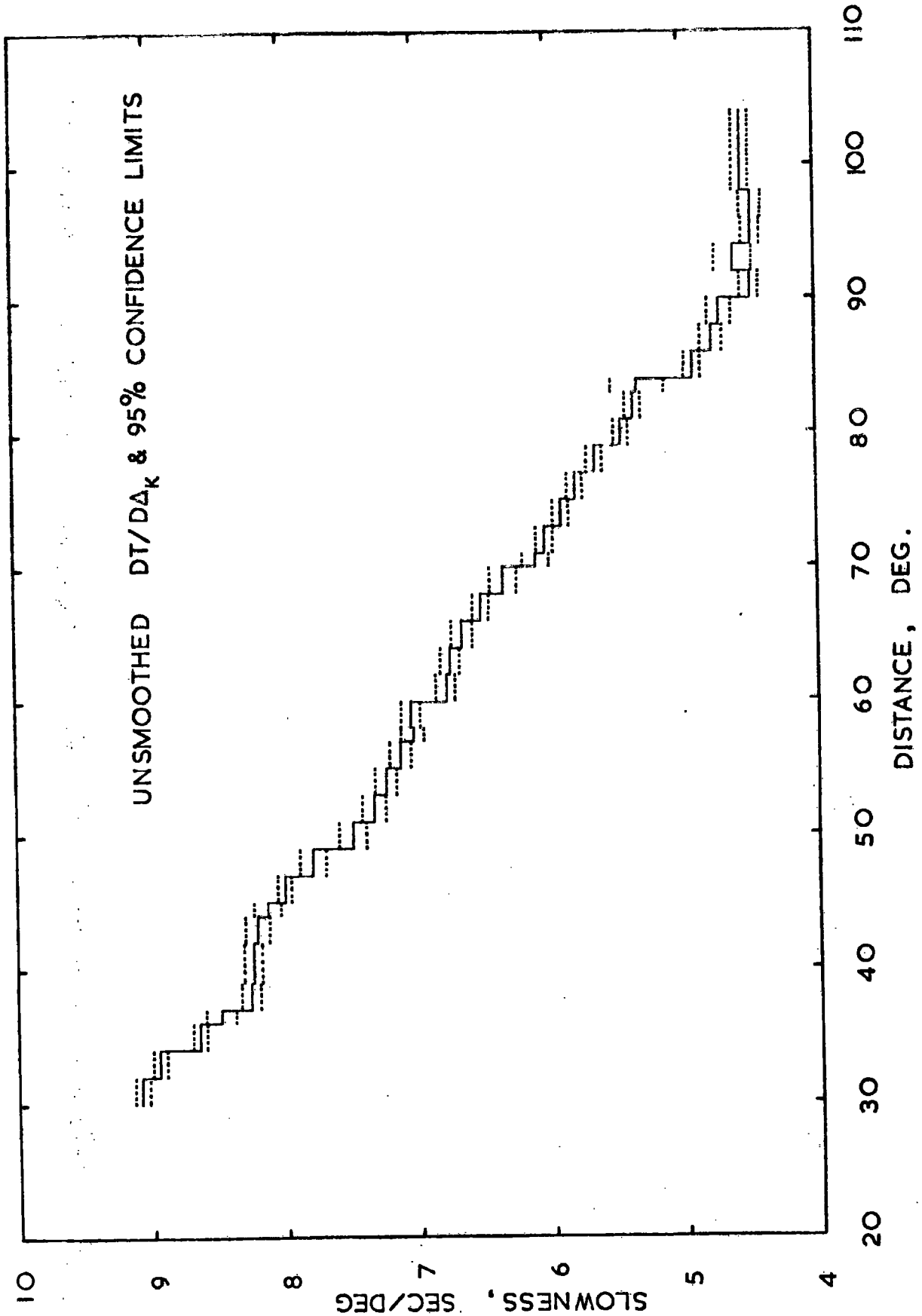
UNSMOOTHED DT/DΔ_K & 95% CONFIDENCE LIMITS
SLOWNESS, SEC/DEG
10
9
8
7
6
5
4
DISTANCE, DEG.
20
30
40
50
60
70
80
90
100
110

for all five distance ranges, corrected by removal of second order azimuthal corrections computed from $\Delta = 30^\circ - 58^\circ$ and $\Delta = 30^\circ - 104^\circ$ distance ranges are shown in Figure 11.

The curve has been estimated in two degree distance intervals except where the curve appears to be rapidly varying, when the interval was decreased to one degree and except when the data is sparse (between $\Delta = 39^\circ - 42^\circ$ and $98^\circ - 104^\circ$) when the interval was increased. Estimates of slowness made with the intervals all reduced to one degree and all increased to three degrees resulted in an increase in variance. For the data available, a two degree distance interval is considered optimum.

Individual estimates of slowness were also made for all events. The uncorrected values obtained using equation 1.1 are shown in Figure 12. Figure 13 shows slowness estimates after correcting for non-azimuthal site corrections (equation 1.3), Figure 14 the estimates after applying azimuthal site corrections containing a single sinusoidal term (equations 1.3 and 1.4) and Figure 15 shows the slowness estimates after correcting for azimuthal site corrections containing a two-term sinusoidal approximation (equations 1.3 and 1.5) for the two distance ranges $\Delta = 30^\circ - 58^\circ$ and $\Delta = 58^\circ - 104^\circ$. This last figure corresponds to the unsmoothed $dT/d\Delta_k$ estimates of Figure 11.

The striking reduction in scatter as the site corrections are successively applied sufficiently illustrates the power of the method.

The value of the second order azimuthal term in reducing scatter is clearly illustrated if portions in the curve in Figures 13 and 15 are compared between 70 and 74°: six events in Figure 13 have values of slowness which are much lower than the mean curve. One event is from the Greenland Sea and recorded at GBA, the other 5 are from the Aleutian Islands, recorded at EKA with azimuths of 349.0°, 349.6°, 356.8°, 358.0°, 360.5°.

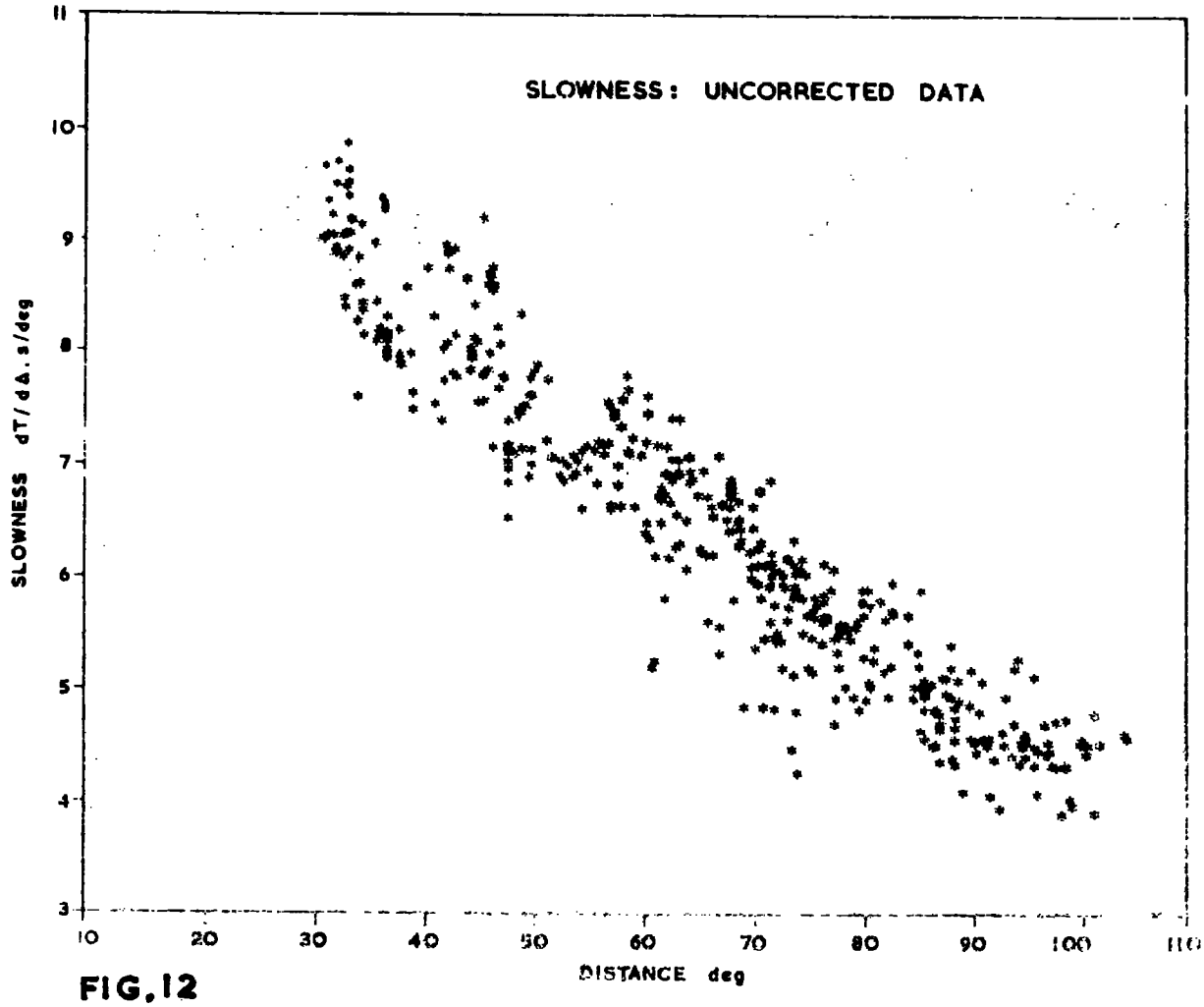
SLOWNESS: UNCORRECTED DATA
SLOWNESS dT/dΔ, s/deg
DISTANCE deg
11
10
9
8
7
6
5
4
3
10
20
30
40
50
60
70
80
90
100
110

FIG. 12

FIG. 13

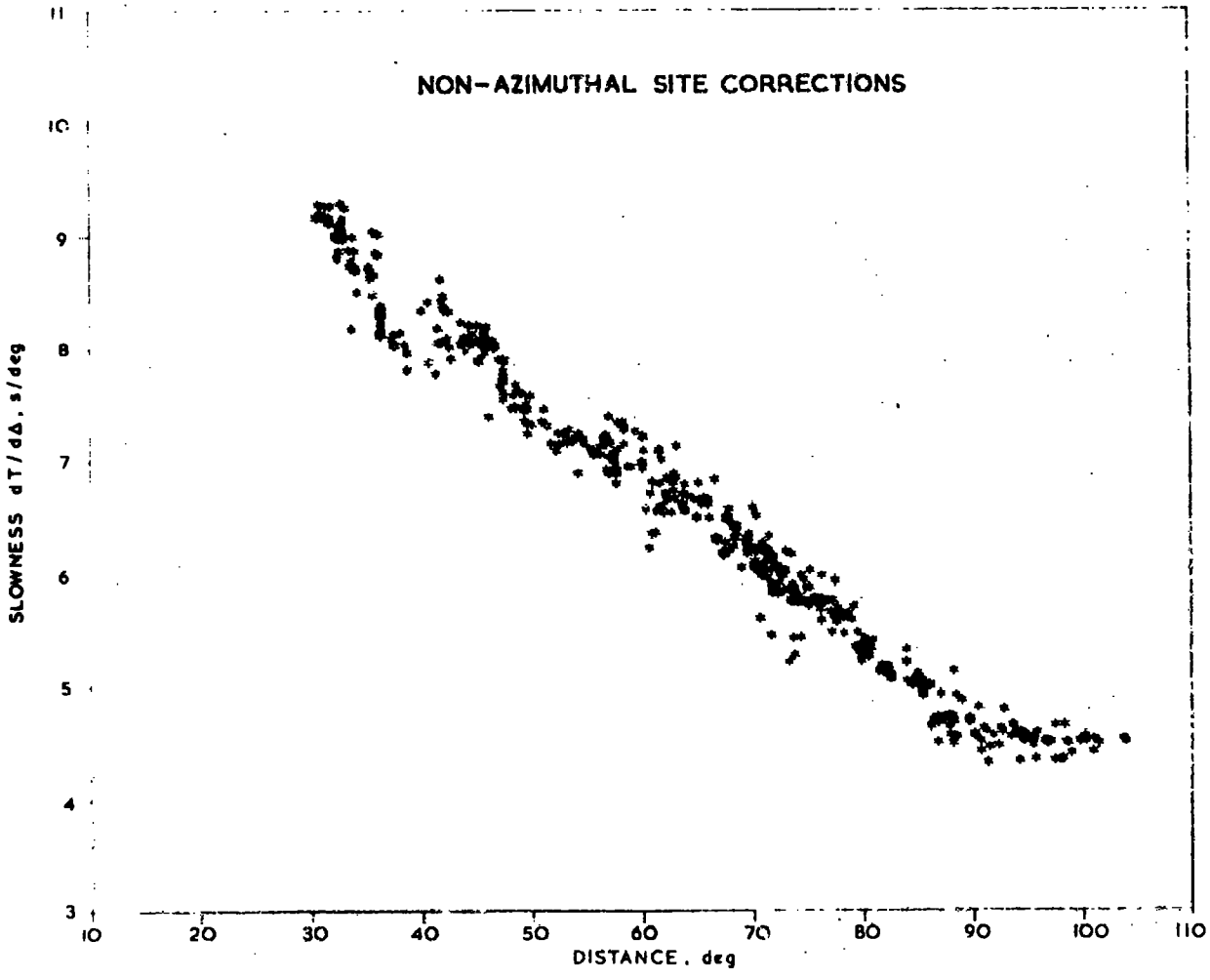
NON-AZIMUTHAL SITE CORRECTIONS
SLOWNESS dT/dΔ, s/deg
DISTANCE, deg
11
10
9
8
7
6
5
4
3
10
20
30
40
50
60
70
80
90
100
110

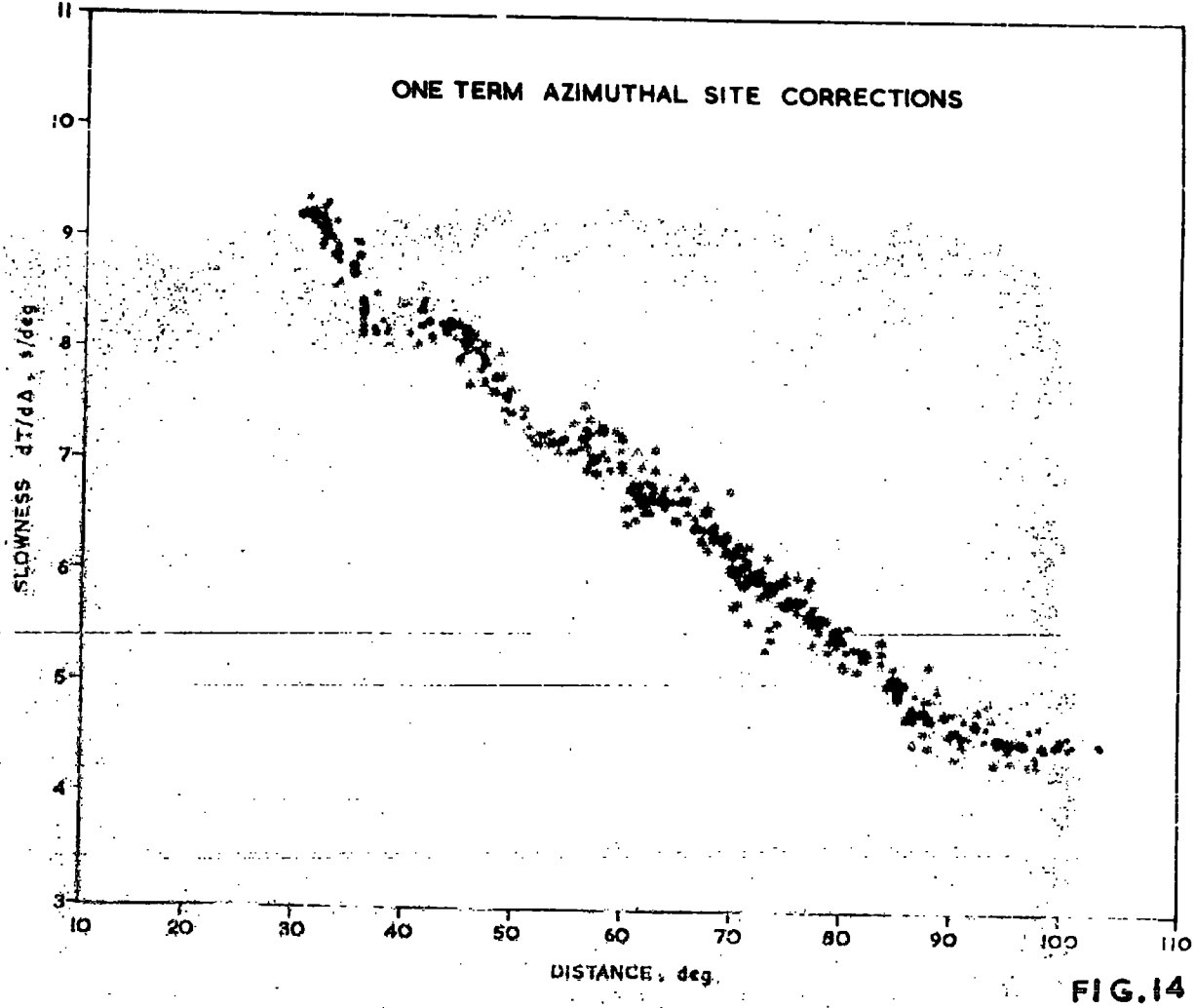
ONE TERM AZIMUTHAL SITE CORRECTIONS
SLOWNESS dT/dΔ, s/deg
DISTANCE, deg.

FIG.14

FIG.15

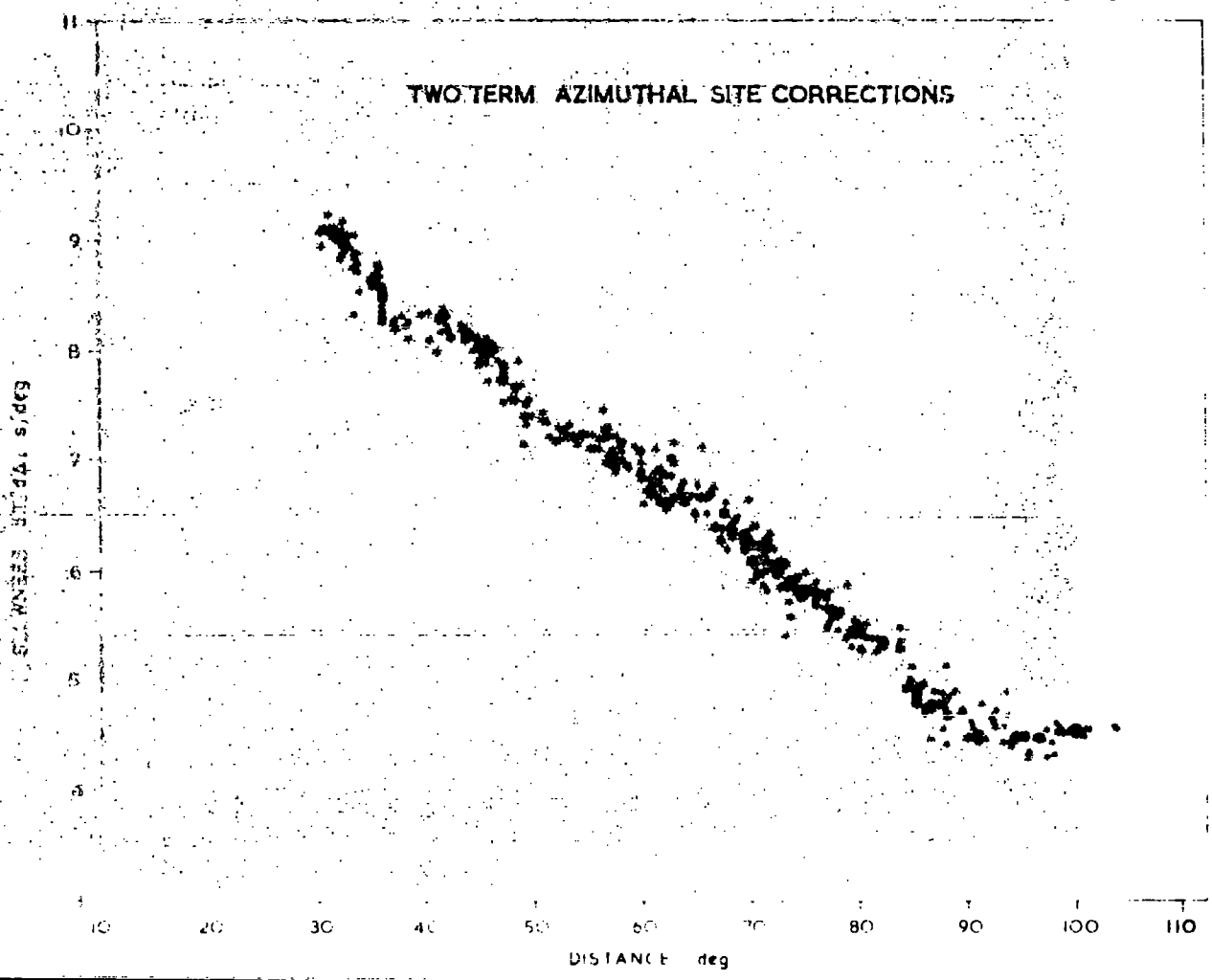
TWO TERM AZIMUTHAL SITE CORRECTIONS
DISTANCE deg

Possible explanations are that these low values are evidence for lateral inhomogeneity in the mantle between EKA and the Aleutian Islands, anomalous velocities beneath the Aleutian Islands, or inadequate corrections for the effects of array structure. However, the reduction in scatter (Figure 15) when two-term azimuthal site corrections are used shows that the last possibility to be more likely.

It is noted that although the three events with azimuths greater than 356° still lie below the mean curves, this may be due to the approximation used in deriving the site corrections. If the slowness of the same group of events corrected using one-term azimuthal corrections (Figure 14) is compared with Figure 13, the reduction in scatter is seen to be only marginal. The inclusion of the second order term in the site corrections is seen therefore, to be an essential feature of the method. A similar explanation may provide the reason for the anomalously large values of slowness observed by Johnson (1969) for 7 earthquakes in the region of the mid-Atlantic ridge between $\Delta = 55^{\circ} - 63^{\circ}$. Johnson was unable to account for these observations and left open the question of whether they are due to anomalous velocities near the axis of the mid-Atlantic ridge, in the deep mantle or due to inadequate sits corrections at TFSO array.

Other regions of high scatter in the corrected slowness curve (Figure 15) besides that already mentioned near $\Delta = 70^{\circ}$ are near 40°, 60° and as the core is approached beyond 88°. As will be seen later, these regions are all associated with large gradients in the slowness curve.

The mean slowness values $dT/d\Delta_k$ for each distance interval (Figure 2.13) were smoothed at the mid-point of each cell by Jeffreys Method of Summary Values (Jeffreys 1961), which is now described.

Smoothing the slowness curve

The tendency of random errors is to always increase the irregularities in the observed data, and attempts were made to estimate those parts of the irregularities that are attributable to random errors and remove them. The technique adopted for smoothing data must not however remove useful information and so must provide for some form of control over the amount of smoothing to be applied.

The fitting of a series of polynomials to the data by least squares can be used. However, the coefficients of the function chosen do not generally have any physical significance and the standard errors in the coefficients are not a very convenient method of measuring the reduction in error.

A technique that does provide a form of control is Jeffreys Method of Summary Values which can be used to smooth data at any tabular intervals. The method assumes that most of third or even second or first differences at the actual tabular intervals, are no larger than the known uncertainty in the individual values, but that values at wider intervals show these differences to be systematic. The method of summary values is used to establish how wide the intervals must be so that information on the second deviative of the function can be safely ignored while retaining the information provided by systemmatic differences.

The data curve is therefore divided into intervals. A linear solution (which is uniquely determined by two points) is used to find the points in the range where the difference between the linear solution and a quadratic solution is negligible. The two points where the two solutions agree are the "summary values" and are independent of the curvature. Jeffreys method finds the two points within each interval. To test the goodness of fit, the summary values are interpolated at the original tabular values and the χ^2 test applied at the 95% significance level.

A computer program was written to accept the unsmoothed data of Figure 11, along with twelve arbitrarily chosen ranges. Values of slowness were taken at the mid point of each two degree cell and the ranges were between 3° and 6° long. The program calculated the summary values and interpolated them using third divided differences at the original tabular values and calculated χ^2. The ranges were then adjusted until χ^2 was within the appropriate range. For 16 degrees of freedom, χ^2 was found to be 18.5 which is well within the 95% confidence region of 8.0 to 26.3 for the data of Figure 11.

Table 2.11 presents the summary values and Table 2.12 shows the smoothed slowness values interpolated at the original tabular values with their 95% confidence limits. Table 2.13 gives values of slowness interpolated at one degree intervals.

TABLE 2.11

SUMMARY VALUES

Range $^{\circ}$	First Summary Point		Second Summary Point	
	Δ	Slowness	Δ	Slowness
31 - 36.5	31.600	9.052 $\pm$ .020	35.099	8.662 $\pm$ .021
38 - 41	38.275	8.262 $\pm$ .029	40.725	8.248 $\pm$ .029
43 - 48	43.831	8.178 $\pm$ .027	46.762	7.893 $\pm$ .023
50 - 54	50.487	7.445 $\pm$ .039	53.686	7.250 $\pm$ .034
56 - 59	56.272	7.104 $\pm$ .034	58.796	7.041 $\pm$ .031
61 - 65	61.413	6.775 $\pm$ .029	64.567	6.685 $\pm$ .030
67 - 70.5	67.131	6.514 $\pm$ .030	70.162	6.166 $\pm$ .036
72 - 78	72.696	5.992 $\pm$ .021	77.168	5.711 $\pm$ .021
80 - 83.5	80.081	5.445 $\pm$ .027	82.506	5.345 $\pm$ .041
85 - 89	85.228	4.892 $\pm$ .027	88.540	4.713 $\pm$ .034
91 - 95	91.127	4.490 $\pm$ .034	94.866	4.496 $\pm$ .035
97 - 103	98.021	4.480 $\pm$ .024	102.276	4.480 $\pm$ .022

Table 2.12

Smoothed values of dT/d Δ and 95% confidence limits

(Degs)	dT/d Δ (secs/deg)	95% c.l.	(Degs)	dT/dΔ (secs/deg)	95% c.l.
30			68		
	9.089	.054		6.321	.096
32			70		
	8.966	.048		6.161	.092
34			71		
	8.700	.054		6.057	.056
36			73		
	8.483	.112		5.937	.060
37			75		
	8.308	.072		5.815	.058
39			77		
	8.264	.072		5.652	.061
42			79		
	8.235	.086		5.474	.056
44			81		
	8.149	.098		5.400	.080
45			83		
	8.003	.046		5.214	.198
47			84		
	8.762	.100		4.952	.060
49			86		
	7.520	.102		4.803	.078
51			88		
	7.365	.086		4.694	.088
53			90		
	7.253	.080		4.522	.072
55			92		
	7.139	.084		4.492	.136
57			94		
	7.103	.086		4.518	.074
58			96		
	7.046	.072		4.508	.078
60			98		
	6.839	.074		4.499	.062
62			100		
	6.746	.068		4.497	.062
64			102		
	6.686	.076		4.510	.062
66			104		
	6.548	.064			

Table 2.13

dT/d Δ values interpolated to one degree intervals

Distance (degs)	dT/d Δ (secs/deg)	Distance (degs)	dT/d Δ (secs/deg)	Distance (degs)	dT/d Δ (secs/deg)
30	9.128	55	7.191	80	5.474
31	9.089	56	7.139	81	5.444
32	9.053	57	7.114	82	5.400
33	8.966	58	7.089	83	5.286
34	8.843	59	7.046	84	5.126
35	8.700	60	6.946	85	4.952
36	8.553	61	6.839	86	4.860
37	8.415	62	6.783	87	4.803
38	8.308	63	6.746	88	4.750
39	8.269	64	6.719	89	4.694
40	8.264	65	6.686	90	4.603
41	8.270	66	6.628	91	4.522
42	8.261	67	6.548	92	4.495
43	8.235	68	6.438	93	4.492
44	8.184	69	6.321	94	4.504
45	8.105	70	6.211	95	4.518
46	8.002	71	6.122	96	4.515
47	7.885	72	6.057	97	4.508
48	7.762	73	5.995	98	4.503
49	7.635	74	5.937	99	4.499
50	7.520	75	5.878	100	4.497
51	7.434	76	5.815	101	4.497
52	7.365	77	5.737	102	4.501
53	7.307	78	5.652	103	4.510
54	7.253	79	5.558	104	4.523

FIG. 16

RESIDUAL SITE CORRECTIONS S_{HI}

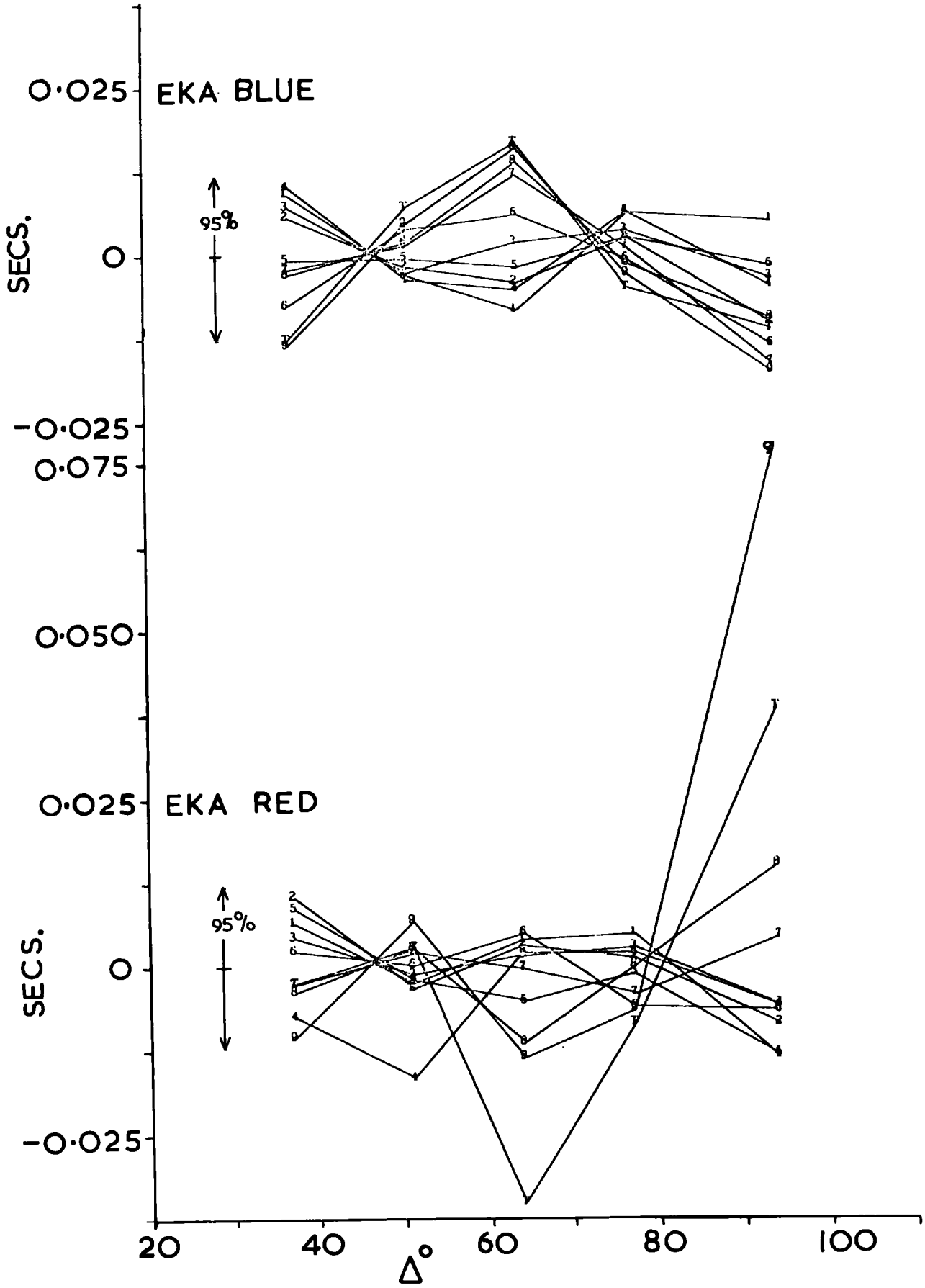

FIG. 17

RESIDUAL SITE CORRECTIONS S_{HI}

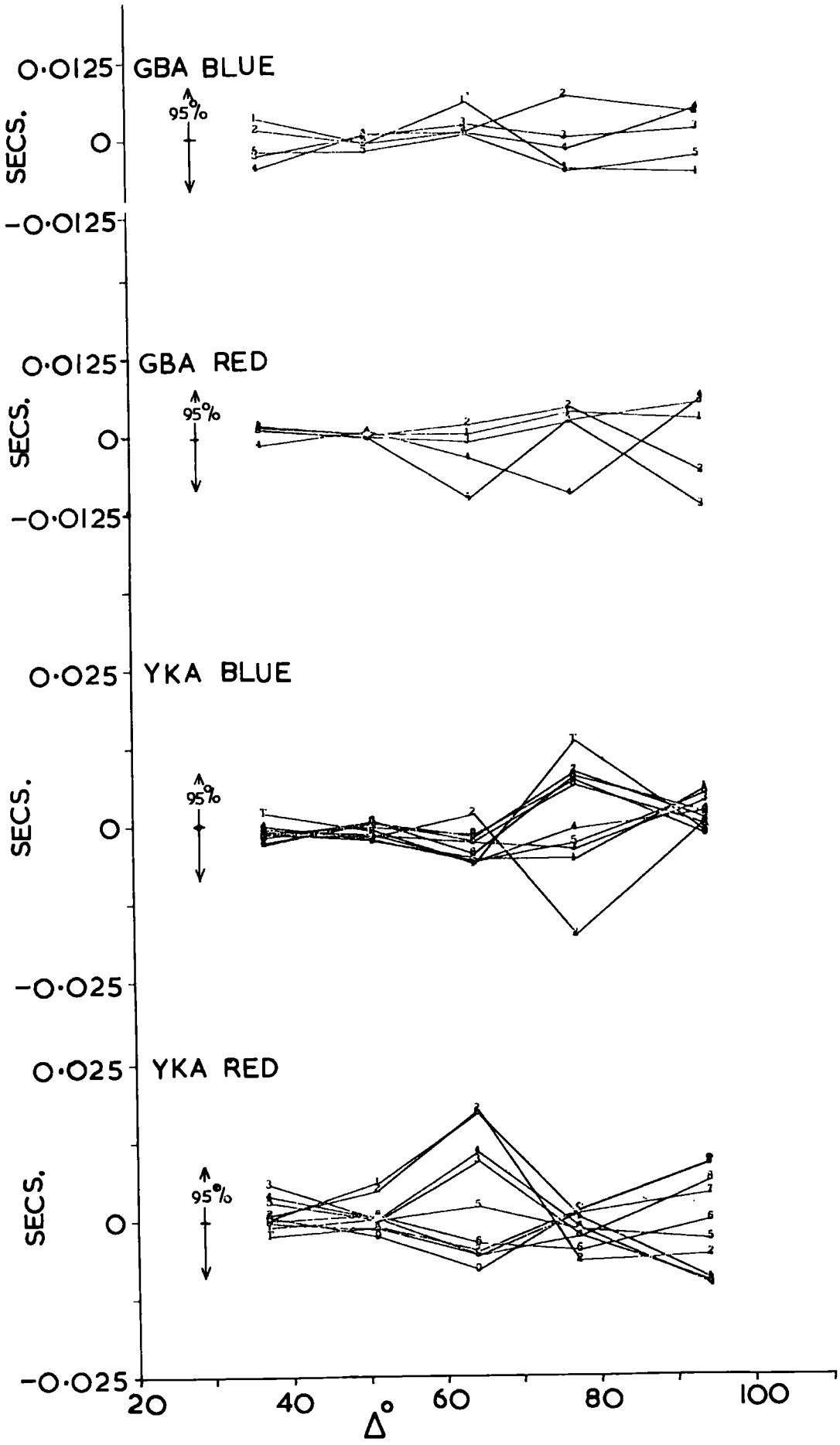

FIG. 18

RESIDUAL SITE CORRECTIONS S_{HI}

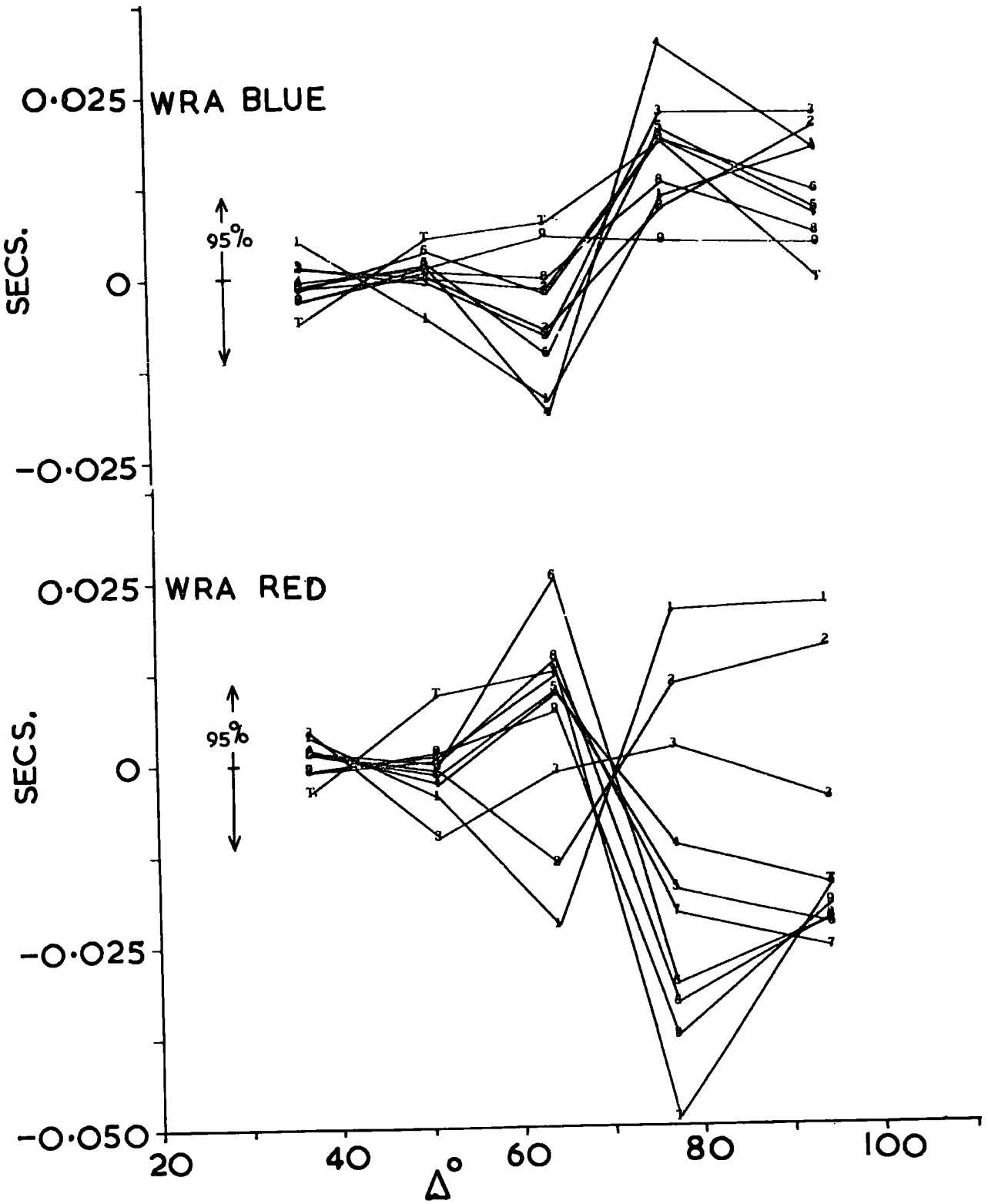

2.2 SITE CORRECTIONS

Time residuals ε_{hij} at each seismometer are obtained from the observed onset times after subtraction of the calculated onset times. When added to the DC site correction, S_{hi}, they can be expressed as a function of azimuth and termed "azimuthal site corrections". A corrected mean slowness-distance curve can then be estimated for epicentres in the five distance ranges using these azimuthal site corrections. Further "residual" site corrections are obtained for each site from this second calculation in each of the five distance ranges from the observed (corrected) onset times and the calculated onset times. These residual site corrections should then be free of any azimuthal bias.

However, as a different set of residuals is obtained for each distance range, a distance dependence may still be present in the corrections. The residual site corrections for each distance range are plotted against distance in Figs 16 to 18 for each seismometer site. Each correction is obtained with its 95% confidence limits and an average value of this error is also shown.

The corrections are generally small (less than $\pm$ 0.03 seconds), and the diagrams clearly show that at three arrays there is no significant distance dependence. Any trend is within the magnitude of the 95% confidence limits. The Warramunga corrections show a slight distance dependence and these are discussed below.

FIGURE 19 ESKDALEMUIR SITE CORRECTIONS ("A" TERM)

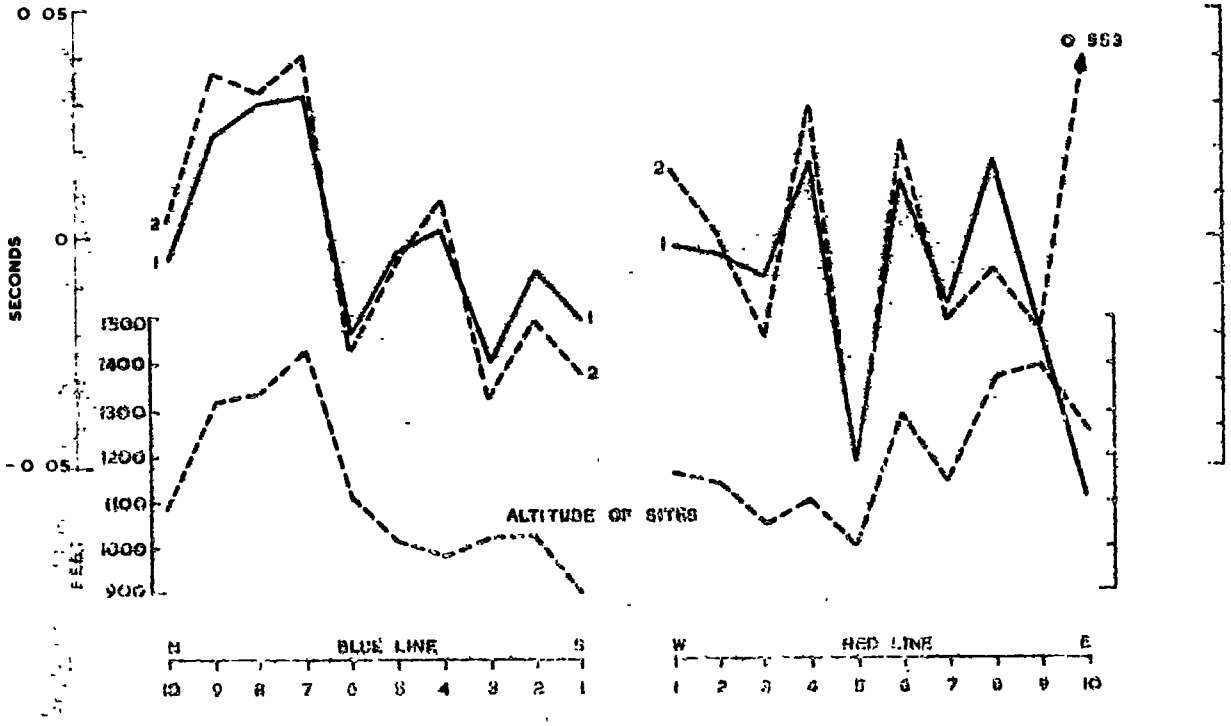

1 R = A + B SIN (α + Φ)₁ Δ = 30°– 104°
2 R = A + B SIN (α + Φ) + C SIN (2α + λ)₂ Δ = 30°– 104°
3 R = A + B SIN (α + Φ) + C SIN (2α + λ)₃ Δ = 30°– 58°

YELLOWKNIFE SITE CORRECTIONS ("A" TERM)

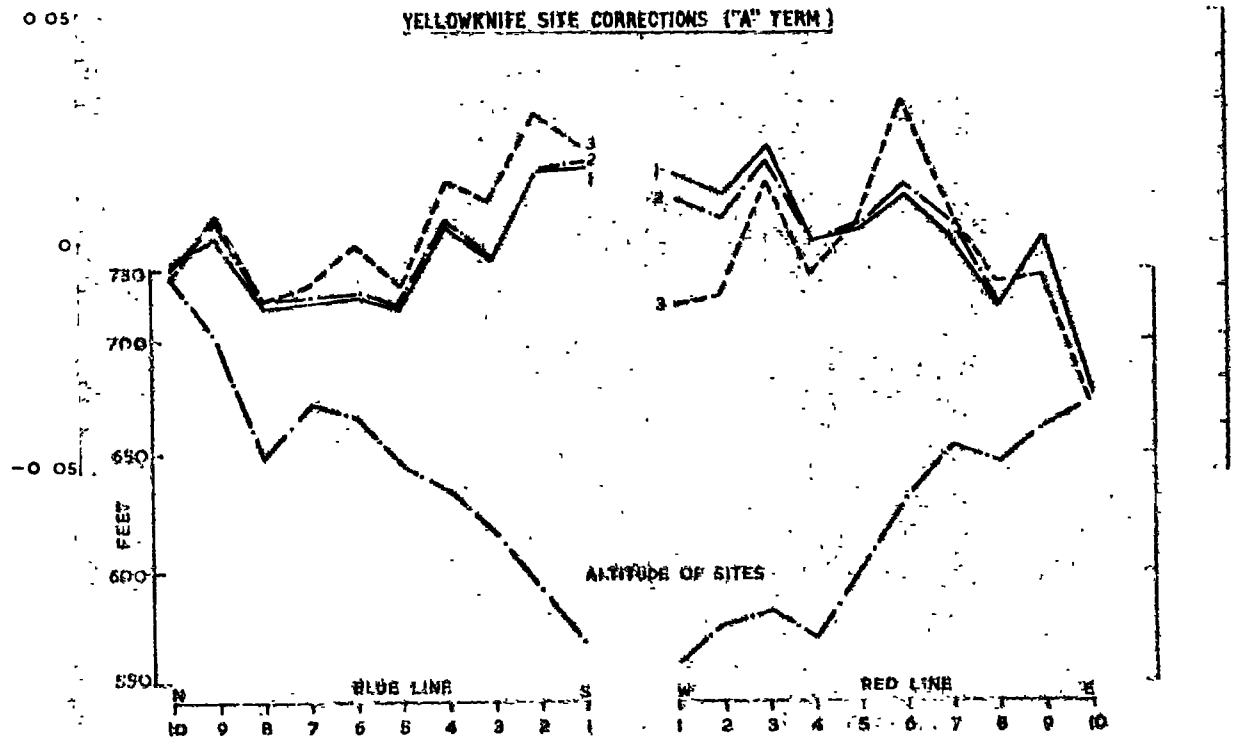

FIGURE 20 GAURIBIDANUR SITE CORRECTIONS ("A" TERM)

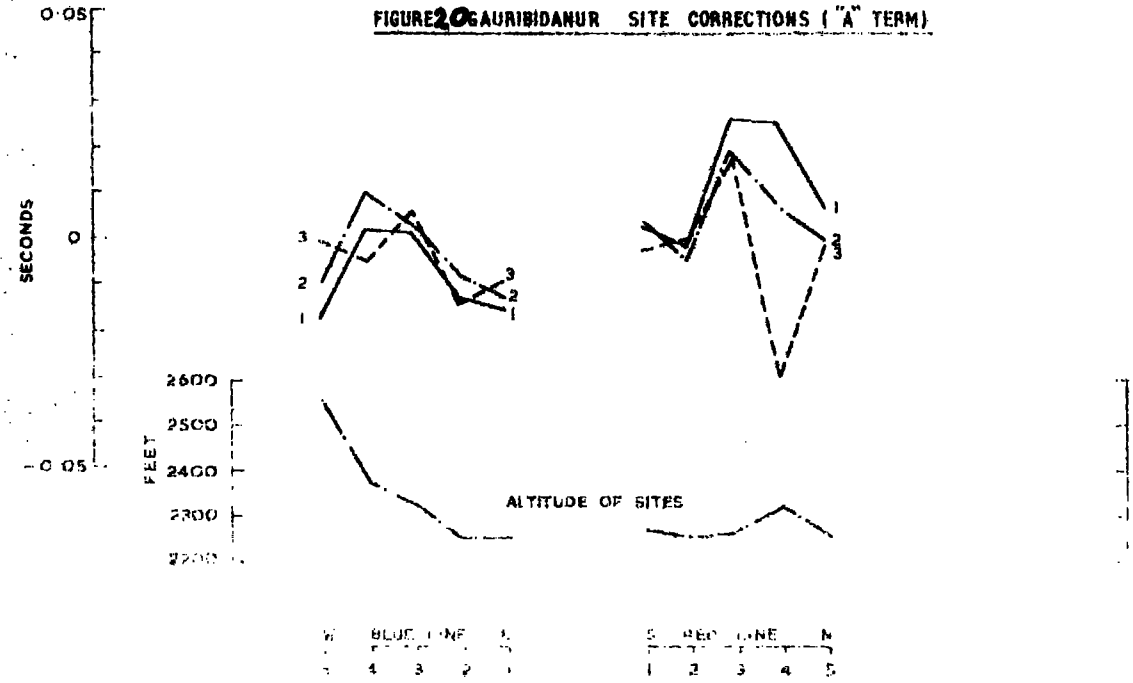

1 — $H = A + B \sin(\alpha + \phi) + C \sin(2\alpha + \lambda)$; $\Delta = 20° - 104°$

2 — $H = A + B \sin(\alpha + \phi) + C \sin(2\alpha + \lambda)$; $\Delta = 42° - 104°$

3 — $H = A + B \sin(\alpha + \phi) + C \sin(2\alpha + \lambda)$; $\Delta = 30° - 58°$

WARRAMUNGA SITE CORRECTIONS ("A" TERM)

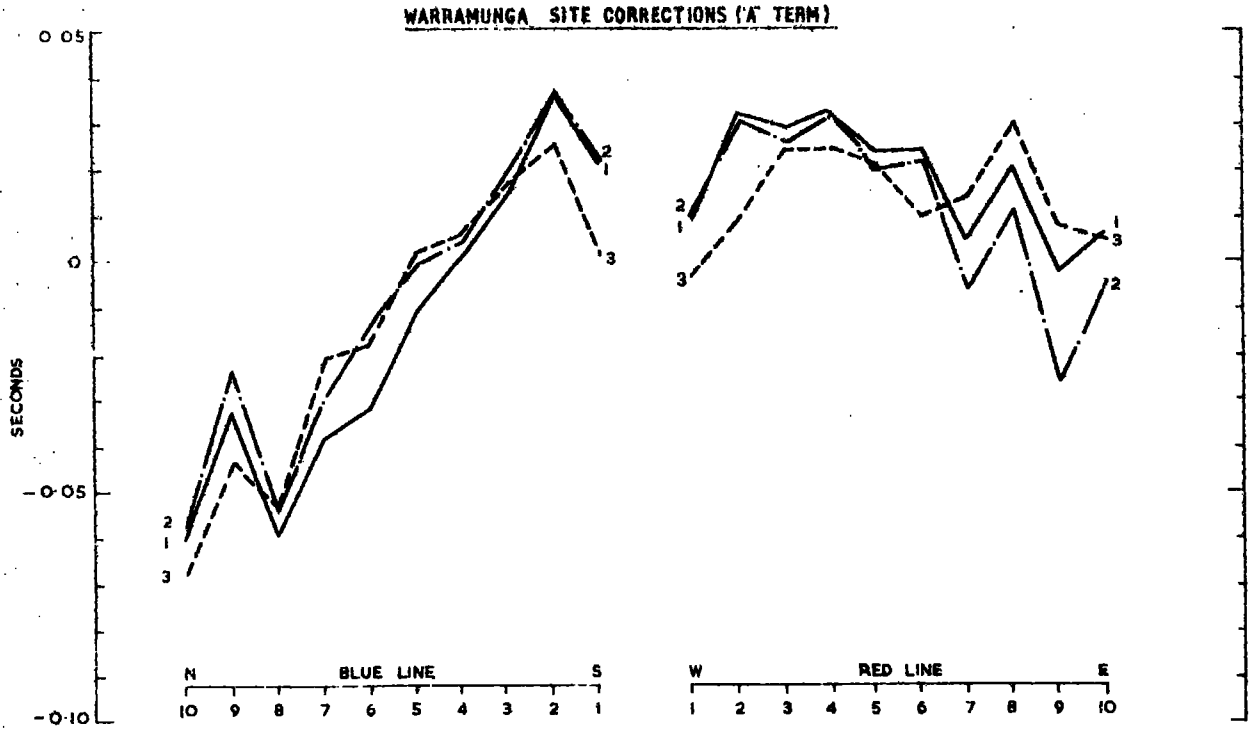

The cause of the site corrections can be attributed to inhomogeneities in the Earth. However, it is difficult to establish which part of the Earth is making the major contribution to the site corrections. It is hoped that as many events in many azimuths have been analysed for a widely distributed set of arrays, the average effect of the mantle has been removed and any lateral variations in the mantle or source effects will manifest themselves as individual values of slowness which are higher or lower than the world average curve. Variations in time corrections at individual sites are then assumed to be due only to geological variations in the crust beneath the array.

Expressing the azimuthal site corrections in the form

$$\left(S_{hi} + \varepsilon_{hij}\right) = A + B \sin(\alpha + \phi) \qquad (2.1)$$

or

$$\left(S_{hi} + \varepsilon_{hij}\right) = A + B \sin(\alpha + \phi) + C \sin(2\alpha + \lambda) \qquad (2.2)$$

facilitates the handling of the residuals in the computer program, as the number of independent parameters is reduced to 3 and 5 respectively. Equation (2.1) also has the advantage that it can be simply interpreted as the anomaly associated with a single dipping layer beneath the array. Equation 2.2, incorporating a second order term was found to give a better fit to the data (as the variance was reduced) than the first order corrections. However, the physical significance of the expression is more complex than a single dipping layer, and the ideal fit would be an even more complex mathematical expression. Any model made up of a series of dipping layers will not be unique, as a series of layers dipping in different directions can give rise to identical residuals as a single layer (Kelly, 1969).

Equations (2.1) can be thought of as the average site correction A, perturbed by the azimuthally varying term. The A terms are not identically equal, in equations 2.1 and 2.2.

It has already been mentioned that because of the significant change in distribution with distance of events recorded at GBA and WRA, equation 1.3 was

solved twice, once for events in the distance range $30^{\circ} - 58^{\circ}$, and once for events in the total distance range $30^{\circ} - 104^{\circ}$.

Figures 19 and 20 show the values of the DC term A for each array obtained from data in the distance ranges:

(1) $\Delta = 30^{\circ} - 104^{\circ}$ using equation 2.1

(2) $\Delta = 30^{\circ} - 104^{\circ}$ using equation 2.2

(3) $\Delta = 30^{\circ} - 58^{\circ}$ using equation 2.2

Values of A for all the arrays are given in Appendix F.

It is noted that generally there is very little difference between the values of A for each array except at EKA, where extreme values obtained using events in group (3) are due to the lack of data and are countered by generally larger values of B.

As pointed out previously, scatter in slowness is significantly reduced by using onset times corrected using equation (2.1), and further reduced when equation (2.2) is employed. Although C is generally small, this further reduction in scatter is brought about by the presence of the second order term in equation (2.2). 95% confidence limits on the A terms are of the order of $\pm$ 0.01 seconds. The variation in the A terms across the arrays therefore represents significant variations in the sub-array geology.

FIGURE21 ESKDALEMUIR DC SITE CORRECTIONS

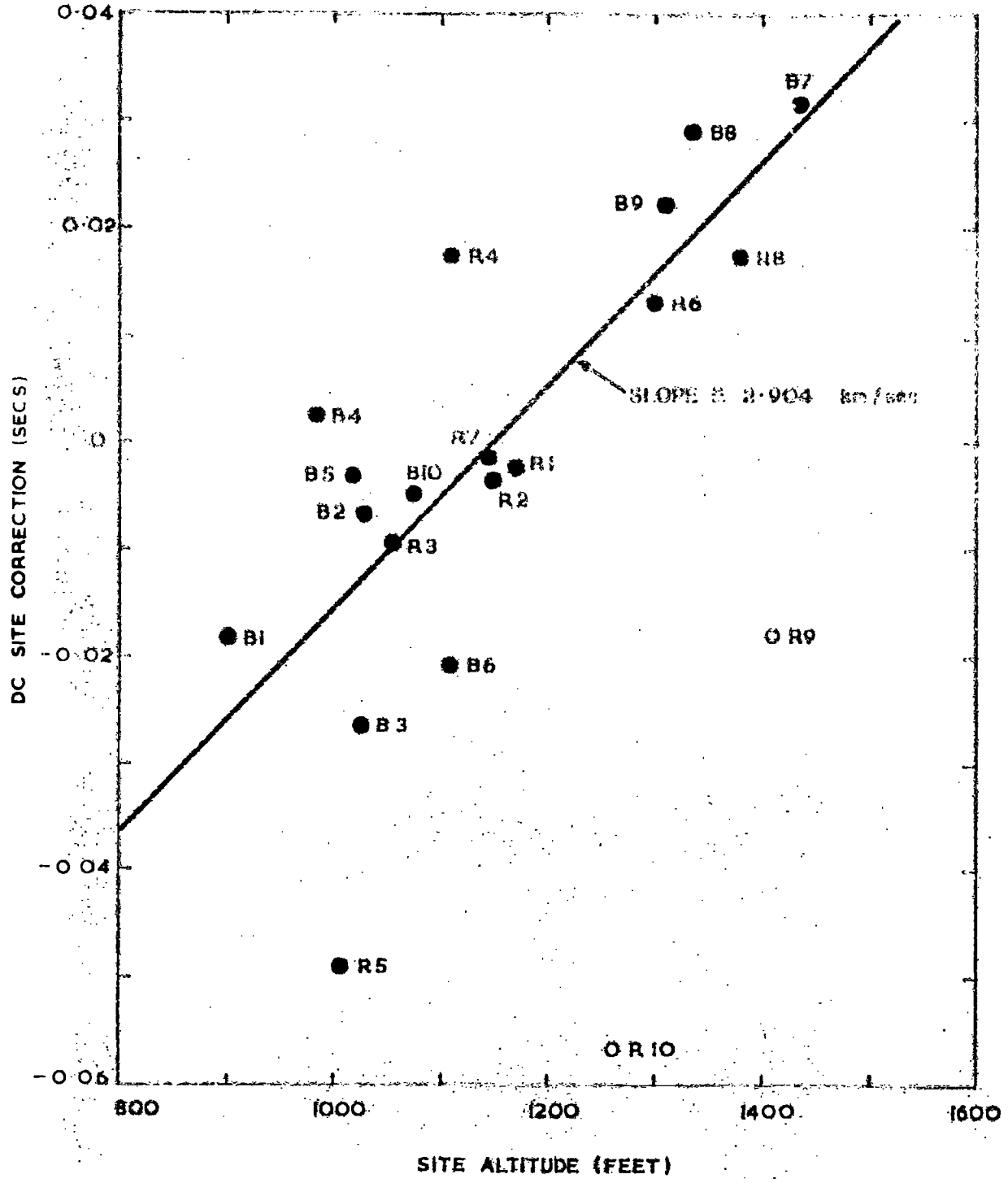

Site Corrections for EKA

Figure 19 shows the values of the DC site correction terms and also the altitude of the seismometer sites, which range between 900 and 1400 feet above mean sea level. To obtain a general picture of the correspondence between the average site correction and altitude, the A terms (equation 2.1 and Appendix F) have been plotted against altitude and a least squares line fitted to the points (Figure 21). Values of A for sites R9 and R10 are shown, although they were not included in the regression because they are associated with standard deviations greater than twice the average. This is a reflection on the lack of data used to derive these two corrections. The correlation coefficient is = 0.77 with 16 degrees of freedom. Values tabulated by Fisher (1958, p.209) show that for n = 16, the probability is less than 0.01 and so a significant linear relationship exists between the magnitude of the site corrections and their altitude. The gradient of the line is $V_o = 2.90 \pm 1.27$ kms/sec and represents the seismic velocity in the topmost surface layers beneath the array.

It has been assumed in this calculation that the rays are incident vertically beneath the array, however teleseismic events at distances of 30° to 100° have angles of incidence (i) beneath a 3 km/sec crust of between 6° and 14°. A better estimate of the velocity in thus

$$V = \frac{V_o}{\cos i} = \frac{2.90}{\cos (10^\circ)} = 2.94 \pm 1.3 \text{ km/sec}$$

Removal of the height effect by assuming a near surface velocity of 2.94 km/sec reduces the average site corrections to less than $\pm$ 0.02 secs, except for R5 where the corrections still remain high (- 0.035 secs) and which is probably associated with the seismometer coupling, the state of the rock immediately beneath the site, or possibly an incorrect estimate of the seismometer altitude. The reduced site corrections show no trend

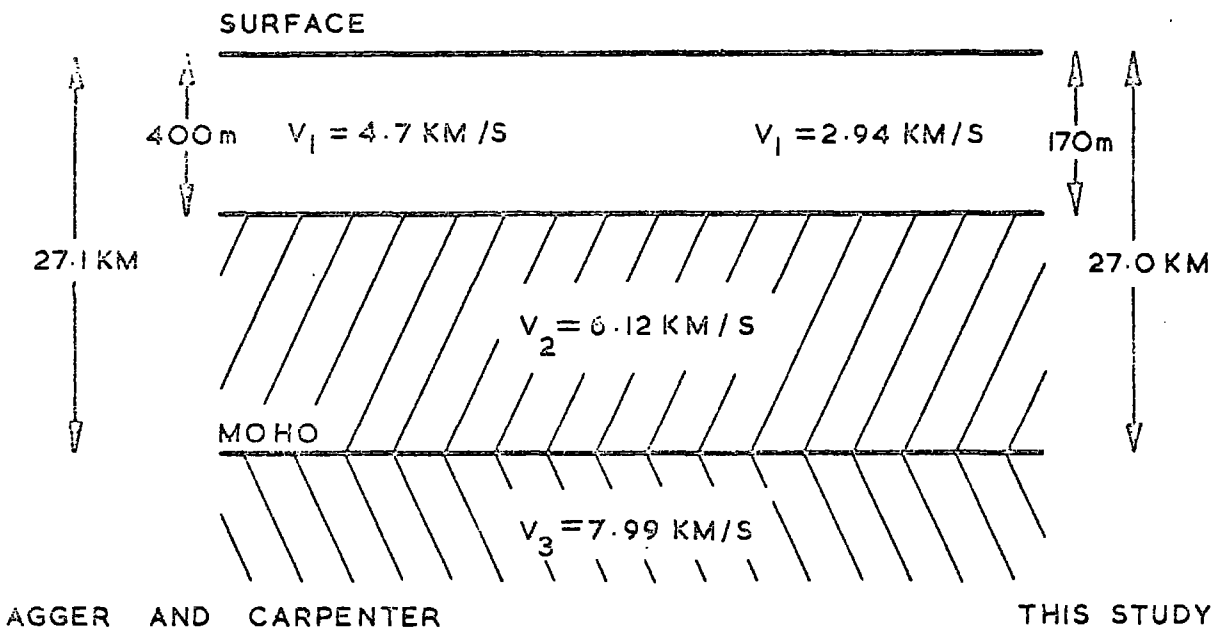

FIGURE 22 .CRUSTAL MODEL OF EKA FROM STATION TIME TERMS (AGGER AND CARPENTER, 1964)

across the array which is confirmed by the small magnitude of the azimuthal component. The only exception is R10 which has already been explained as being due to the lack of data recorded by that seismometer. Residual site corrections analysed as a function of distance (Figure 16) are also generally small, with the exception of R9 and R10 and less than 0.02 seconds.

The array at EKA has been described in detail by Truscott (1964) and a crustal study in the vicinity described by Agger and Carpenter (1964). Jacob (1969) describes crustal phase velocities recorded at EKA from first zone explosions.

The crustal model obtained by Agger and Carpenter is shown in Figure 22. The near surface velocity of 4.7 km/sec was obtained from geological evidence. If this velocity is modified to 2.94 km/sec., then the time terms they estimated can be used to re-compute the depths to the various layers, assuming Pg = 6.12 km/sec. and Pn = 7.99 km/sec. The depth to the Moho is found to remain unchanged at 27.0 kms. while that of the surface layer is 170 m. This assumes plane layering, which because of the small azimuthal terms in the site corrections is justified. Both models are shown in Figure 22.

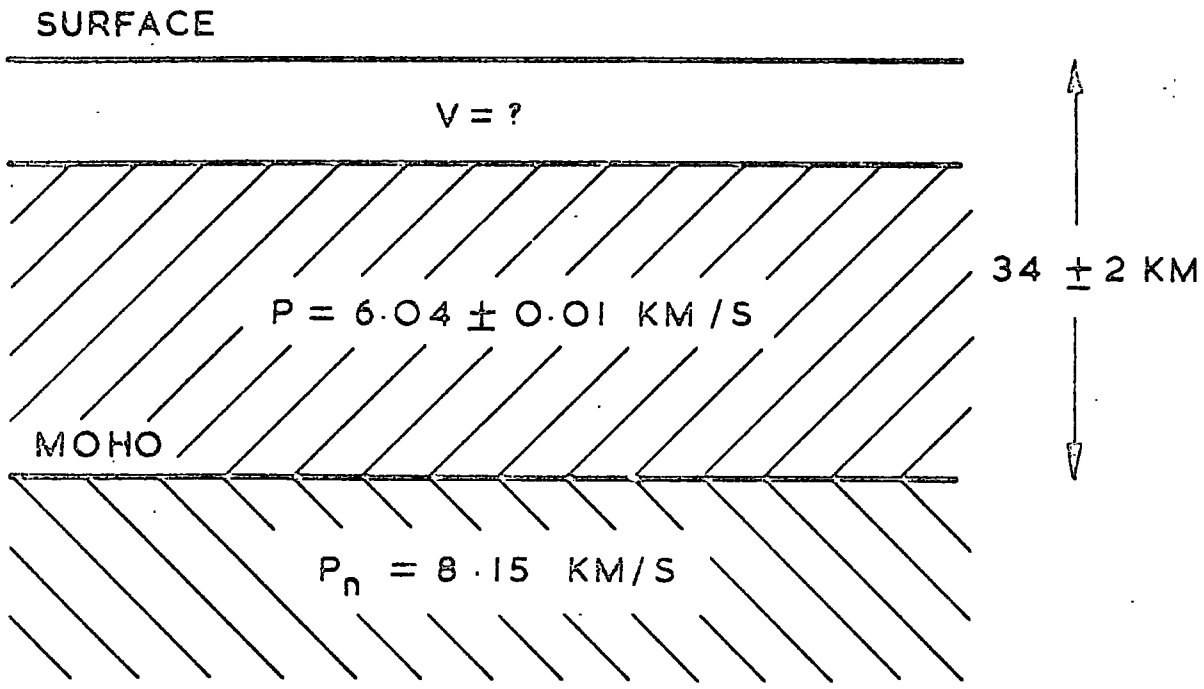

FIGURE 23 . YELLOWKNIFE — CRUSTAL MODEL

(WEICHERT AND WHITHAM 1969)

Site Corrections at YKA

Site corrections at YKA show very little dependence on azimuth (less than 0.01 secs) and the average corrections are generally small and less than $\pm$ 0.02 secs (Fig. 19). There is no preferred direction of trend and they do not appear to be related to altitude. Figure 17 shows the residual site corrections plotted as a function of distance, and no distance dependence is observed within the limit of accuracy (95% confidence limits = $\pm$ 0.08 secs). It must be concluded therefore, that as far as teleseismic data is concerned YKA is situated in a region of very uniform crustal material with horizontal layering.

A crustal seismic experiment carried out in the vicinity of the array (Weichert and Whitham 1969) confirms this uniformity and proposes the structure shown in Figure 23. They found the Moho to be essentially horizontal, or possibly sloping slightly upwards to the SE and NW of the array. Known faults approach to within 5 km of the east end of the array but are assumed to have a negligible effect on velocities. Slight crustal inhomogenities are observed at 30 kms SE of the array and a few tens of kms. further SE into the Great Slave Lake, where there are known faults. It was concluded that teleseismic rays with angles of incidence in the crust of 15°-30° should not therefore be affect and an essentially horizontally stratified crust could be assumed.

EXAMPLES OF ONE-TERM FIT TO RESIDUALS:

FIG.24

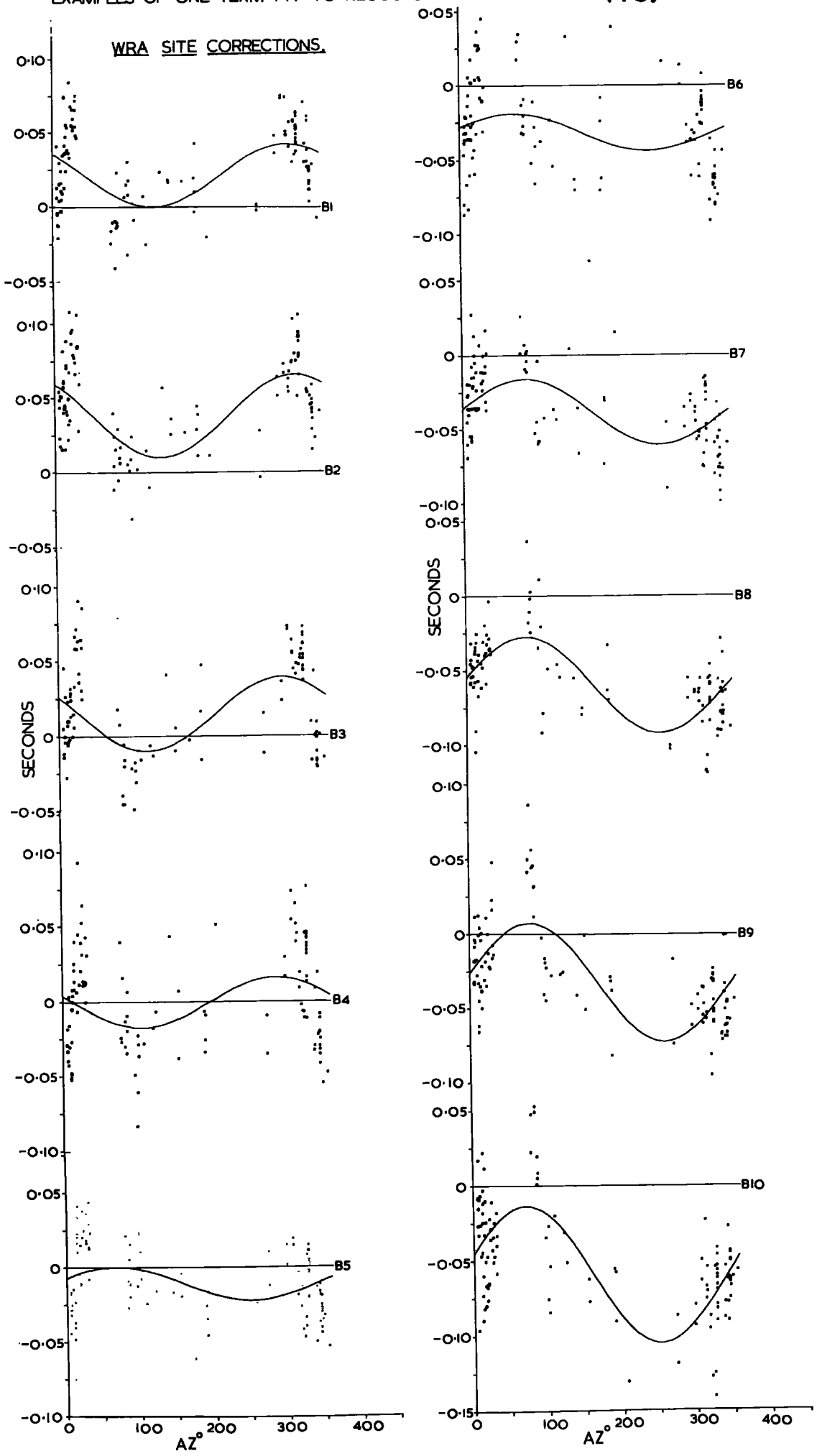

EXAMPLES OF ONE-TERM FIT TO RESIDUALS:

FIG. 25

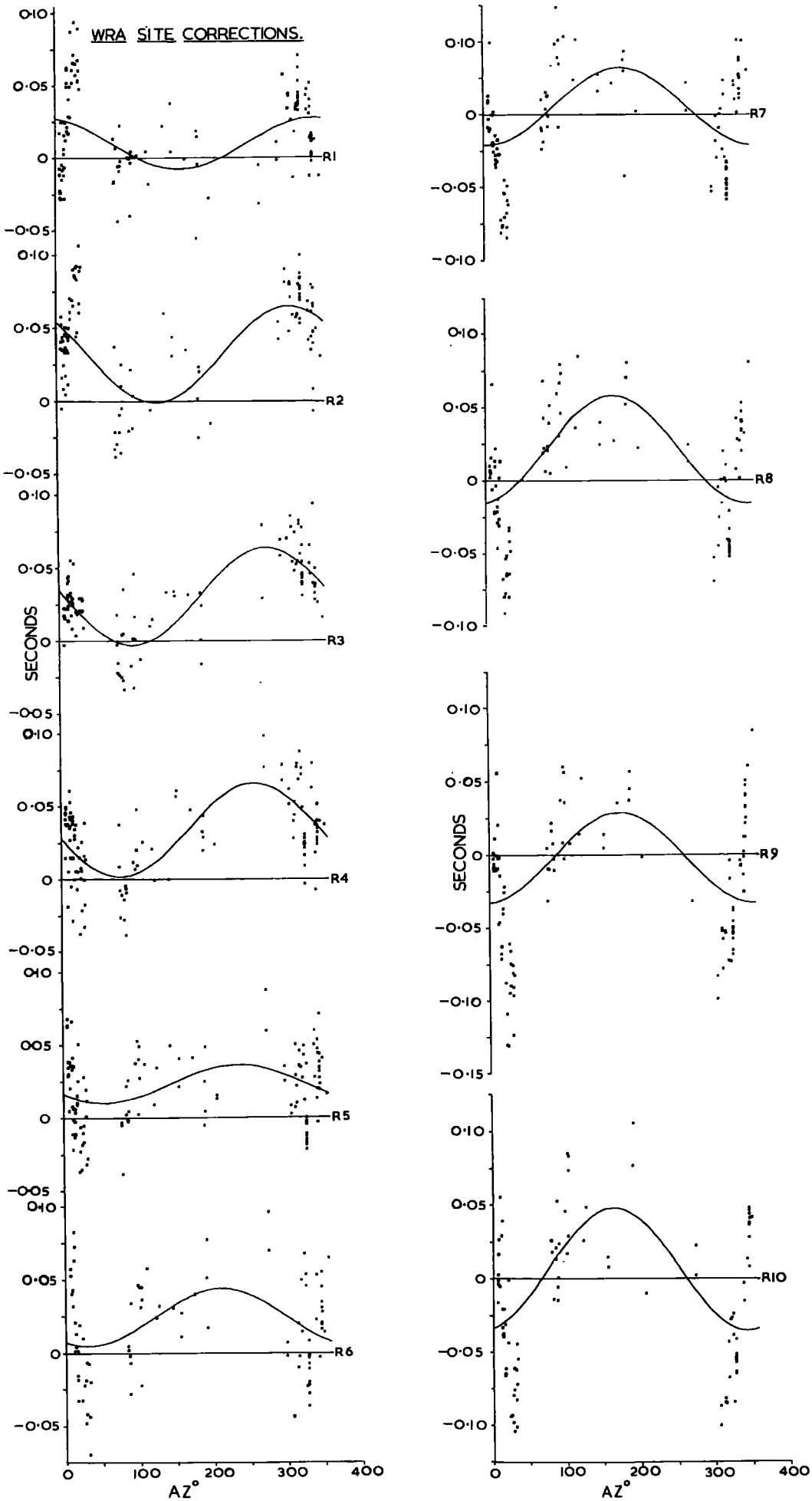

Site Corrections at WRA

The average site corrections at WRA show the greatest variation of any of the arrays, ranging from around 0.04 seconds at B2 to - 0.06 seconds at B10 (Figure 20). The distinct linear trend in the blue line (N - S) corrections is not repeated along the red line (E - W) where the corrections are more variable. Distinct departures are also noted at B9 and in the region of the cross-over point.

The trend of the site corrections across the array hints that a sloping layered structure may be the cause. On fitting a least squares plane through the average site corrections plotted in Fig 20 (equation 2.1), the plane was found to have a gradient of 0.0045 secs/km in the direction N 194.7°E. To interpret this gradient in terms of a dip angle it is necessary to know the velocity ratio at the dipping interface.

Underwood (1967), from a time term analysis of shots fired near the WRA array interpreted his results as being consistant with a two layer model (V_1 = 5.42, V_2 = 6.10 km/sec) dipping at 5.3° in the direction N 205.5°E. Cleary, Wright and Muirhead (1968), however, from the analysis of five teleseismic events recorded at WRA, favoured a higher velocity contrast of 0.7, rather than the 0.9 of Underwood's model.

From the observed gradient of 0.0045 secs/km and assuming a velocity ratio of 0.7 with a velocity below the dipping interface of 6.1 km/sec, the dip of the structure is found to be 3.6° in the direction N 194.7°E. This compares with the value of 6.0° found by Cleary et al. Figures 24 and 25 show the corrections for each seismometer site approximated by the one term series:

$$R = A + B \sin (\alpha + \phi)$$

This series has the advantage that it represents the observational anomaly from a single dipping interface, where the 'phase angle' ϕ is related to the maximum angle of dip as

$$\text{Dip direction} = 90^\circ - \phi^\circ. \quad \text{(from North)}$$

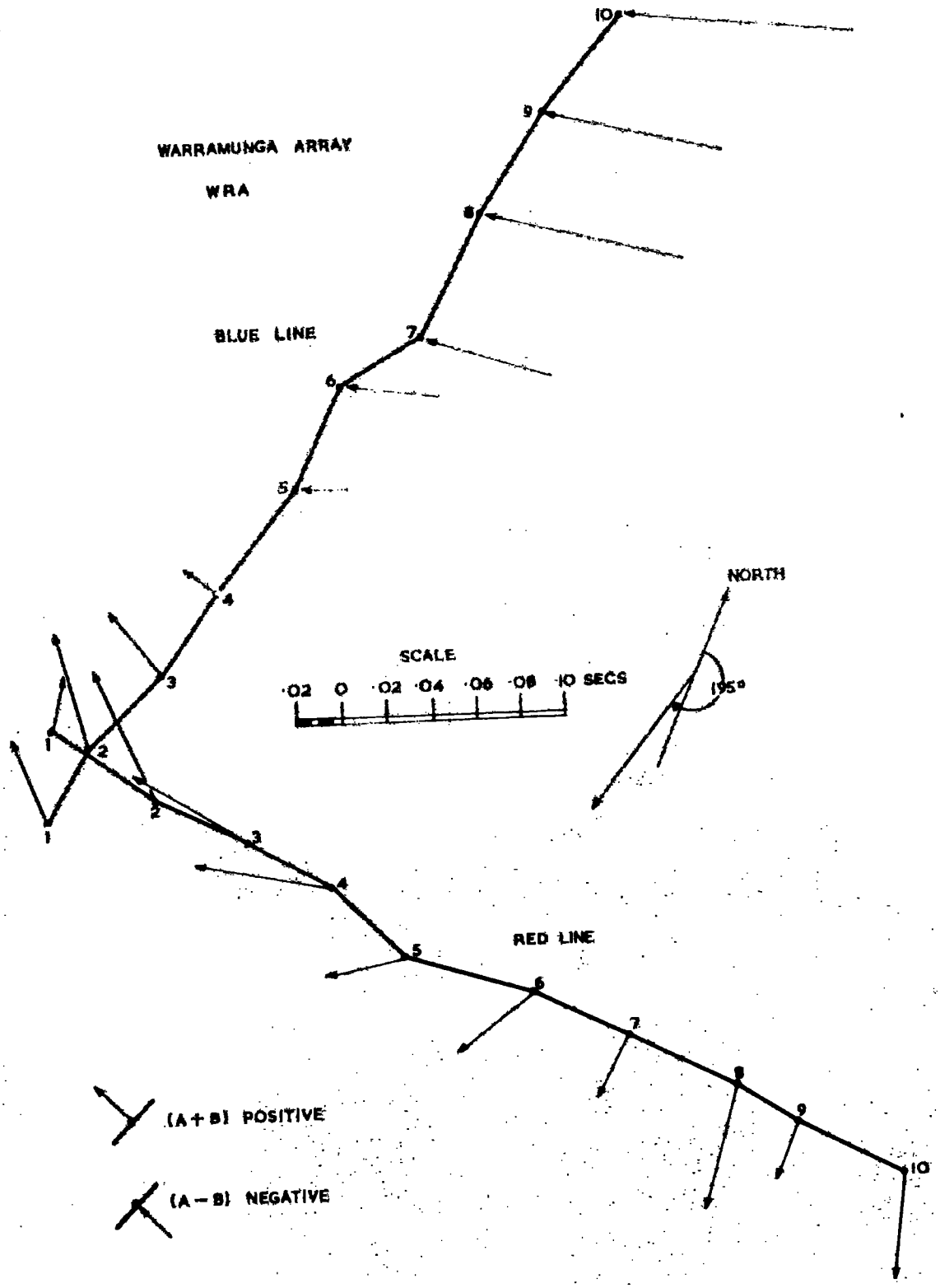

FIGURE 26 MAXIMUM DIP DIRECTION AND MAGNITUDE OF AZIMUTHAL SITE CORRECTION

Residuals and DC site corrections are calculated to sum to zero and so the average correction A varies from + ve to - ve values across the array, (Figure 20). When the term (A - B) is negative, the direction of maximum dip is given by

$$\text{Dip direction} = (90^\circ - \phi^\circ) + 180^\circ$$

Figure 26 is a plot of the maximum direction of dip marked as vectors of length (A + B) when A is positive and (A- B) when A is negative. The directions of the vectors show a consistent dip to the west along the blue arm and a dip to the south along the red arm. At the crossover point the trend is NW for the sites R1, R2 and B1, B2 and B3. The general increase in site corrections along the blue arm from North to South implies an increase in depth to the structure from North to South. The plots imply that the anomaly is shaped in the form of a syncline, whose axis trends north-easterly, and deepening towards the south-west. At the cross-over point the general trend is north-westerly.

The anomalous results for the region near the crossover point are also confirmed in Figure 18. This shows the residual site corrections after removal of the azimuthal term, plotted as a function of distance. The blue line shows a general increase with distance, while the red line decreases with distance. At R1, R2 and R3 however, there is a general increase with distance

Evidence for an anomalous region near the cross-over point has also been deduced from two independent studies.

An aeromagnetic survey of the area (ABMR, 1962) shows the presence of an anomaly to the west of the crossover point of the array and trending towards the north-west. A possible interpretation (Worthington, 1969) shows a rise in a magnetic basement from a depth of 2.16 kms to within 0.34 kms of the surface. A similar thinning of the crust in the region of the crossover point is also supported by Cleary et al (1968) from their analysis of teleseismic signals from the Aleutian Islands and south of Africa.

Site Corrections at GBA

The average value of the site corrections is small (less than 0.025 seconds) (Figure 20) and the azimuthal component is also small (Appendix F). Any trend in the site corrections would favour a gently dipping structure, dipping in the direction N 306°E at an angle of less than 1.5° (assuming velocities at the interface of 4 and 6 km/sec) Residual site corrections show no trend with distance and it is concluded that the GBA array is situated on a very uniform crustal structure

FIG. 27

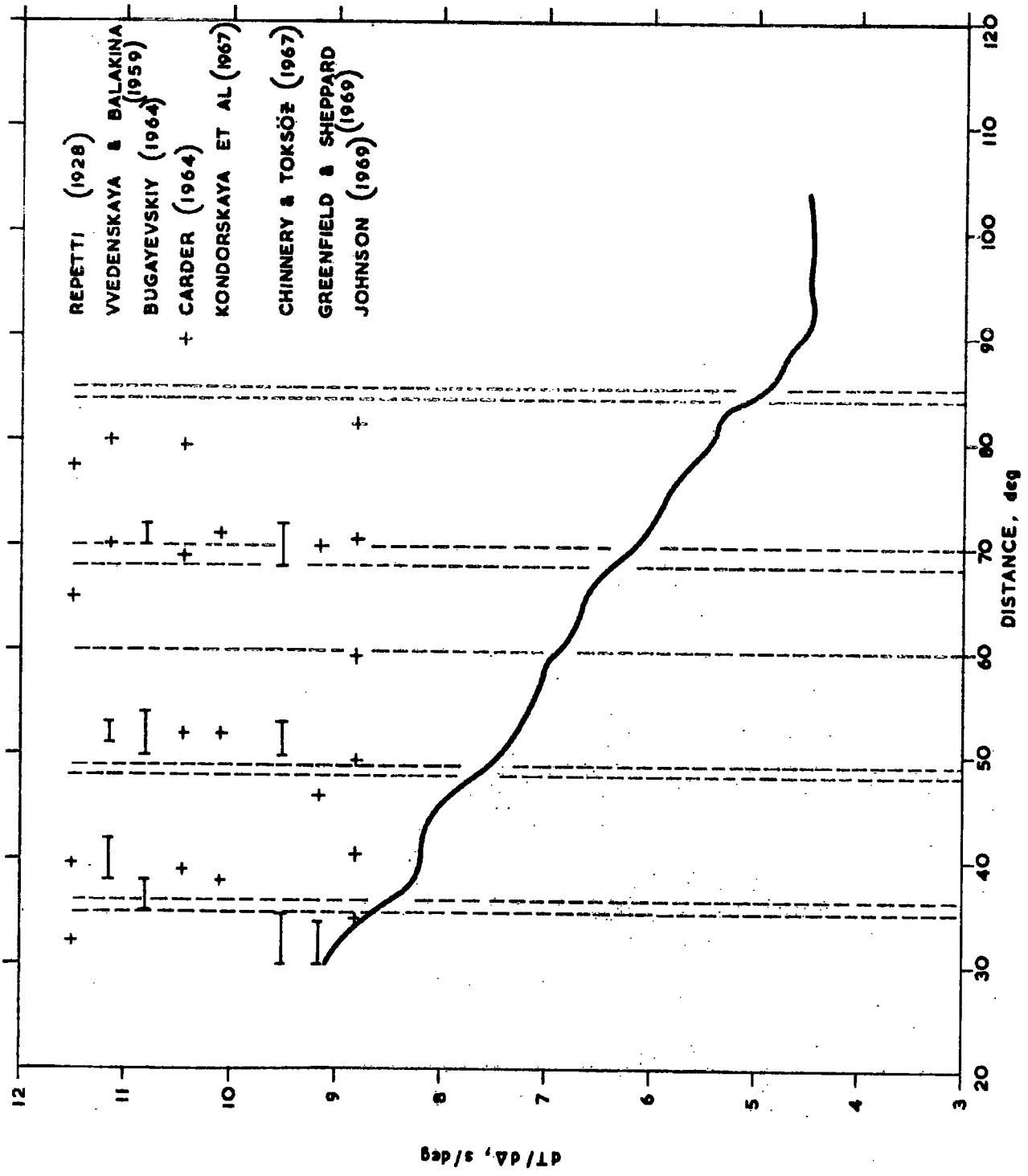
REPETTI (1928)
VVEDENSKAYA & BALAKINA (1959)
BUGAYEVSKIY (1964)
CARDER (1964)
KONDORSKAYA ET AL (1967)
CHINNERY & TOKSÖZ (1967)
GREENFIELD & SHEPPARD (1969)
JOHNSON (1969)
dT/dΔ, s/deg
DISTANCE, deg
12
11
10
9
8
7
6
5
4
3
20
30
40
50
60
70
80
90
100
110
120

2.3 DISCUSSION

When the assumption is made that the deep mantle has radial symmetry, it follows that the slowness should be constant for events falling within the same small distance intervals. Events from all azimuths can be included in the computation, the time corrections and azimuthal terms for unknown near surface geological variations having been included in the equations of condition. The problem of bias due to the restriction of seismic zones to particular areas is overcome by using several well distributed arrays. The validity of the method has already been pointed out by the remarkable reduction in scatter after applying the time terms in the Figures 12 to 15.

The smoothed version of the mean slowness values was interpolated at one degree intervals (Figure 27 and Table 2.13) using third divided differences.

The curve should be sufficiently free of local effects to be treated as a standard slowness-distance curve. Along with other geophysical data, it can be used to establish significant changes in velocity gradient with depth, and used for locating regional differences from the average.

Figure 28 graphs the integrated area under the smoothed slowness curve minus the Jeffreys-Bullen travel times and compares it with the curve obtained by Lilwall and Douglas (1969) from 81 events recorded by the WWSSN. To provide a better fit to the Lilwall & Douglas curve, the integrated travel-time curve has been rotated by an amount that corresponds to an upward DC shift of 0.023 secs/deg in the slowness curve. This figure is well within the 95% confidence limits. Chinnery and Toksöz (1967) shifted their slowness curve by 0.05 secs/deg to fit their observed travel time data from LONGSHOT, and a shift of 0.8 secs/deg is required if Greenfield and Sheppard's (1969) slowness curve is to be made compatable with J-B travel times.

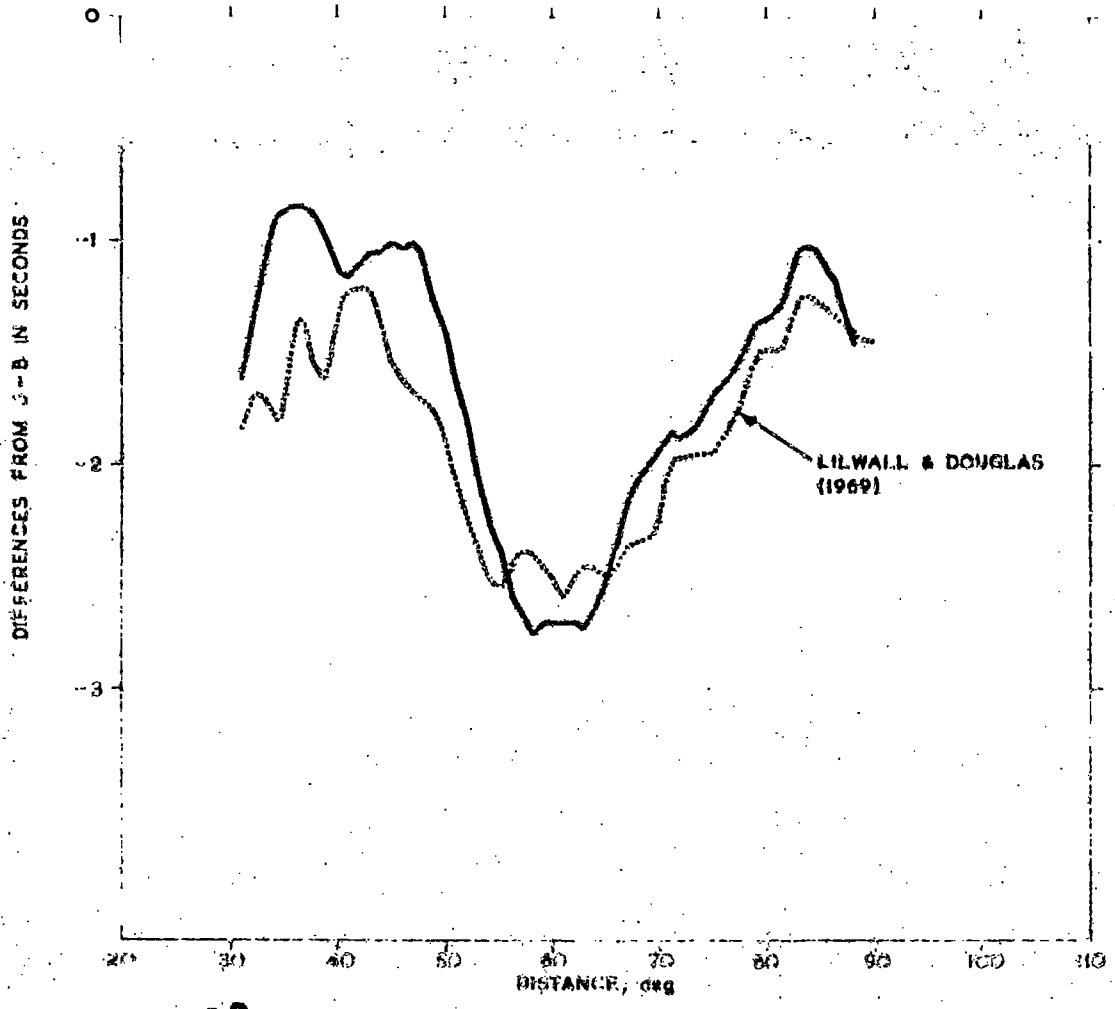
0
-1
-2
-3
DIFFERENCES FROM J-B IN SECONDS
LILWALL & DOUGLAS (1969)
20
30
40
50
60
70
80
90
100
110
DISTANCE, deg

FIG. 28

FIG. 29

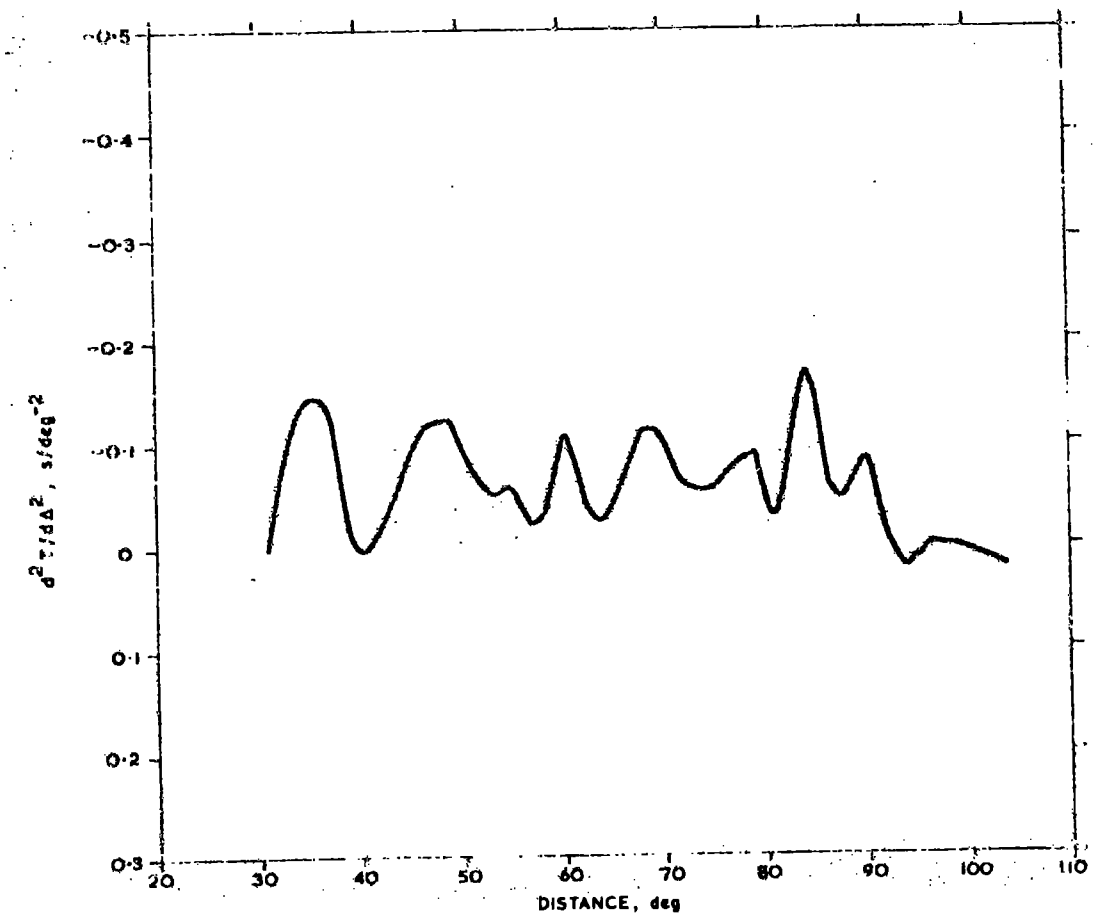
-0·5
-0·4
-0·3
-0·2
-0·1
0
0·1
0·2
0·3
$d^2T/d\Delta^2$, s/deg^{-2}
20
30
40
50
60
70
80
90
100
110
DISTANCE, deg

The correspondence of the travel times from the slowness distance curve to the standard travel times of Lilwall and Douglas is further evidence for the success of the method. The Lilwall-Douglas curve is the best available (in that it predicts the travel times and epicentres of known explosions better than any other curve), and the accuracy of the intergrated residual travel time curve is not high. However, the agreement between the two beyond 60° is remarkably good, while between 48° - 59° the fit is poorer and this is thought to reflect the lack of data in the second distance interval. An increase of 0.1 secs/degree in slowness near 50° brings the two travel time curves into agreement.

The smoothed slowness curve shows that there are several regions where the gradient is changing rapidly. On referring to the smoothed histogram version of Figure 11 there are several regions where there is a significant difference between this curve, and the average curve of Herrin et al (1968). Herrin's curve lies outside the 95% confidence limits of the smoothed curve in the distance ranges 30° - 36°, 42° - 47°, 58° - 60°, 66° - 68° and 81° - 83°. These five regions represent a flattening of the curve and have values of slowness that are all higher than Herrin's. At distances immediately beyond these flat regions there are regions where there is an anomalous steepening of the slowness curve and the gradient is changing rapidly. These five regions are near 35° - 36°, 48° - 49°, 60°, 68° - 70° and 84° - 85°, and are more clearly indicated in the curve of $d^2T/d\Delta^2$ (Figure 29) by the five pronounced relative maxima. The difference between the mean values of the curve at these distances all show significant decreases in the curve at these points.

The 95% confidence limits on the difference between adjacent mean values of slowness are found from the covariance matrix of results (Appendix D) and are calculated in the computer program. Forming the

t-ratio of differences between means and the standard error of the difference for the smoothed curve, t = 7.6, 4.6, 4.1, 4.4 and 3.2 for the five regions respectively. All these values exceed the limit t = 1.96 and show the five distance ranges correspond to regions where there is a significant decrease in the slowness curve.

The curve attains a minimum value of 4.492 secs/deg at $\Delta = 93^\circ$, increases slightly to 4.518 at 95° and then decreases to a minimum of 4.497 at $\Delta = 100^\circ$.

These figures compare with Herrin (ed.) (1968) who considered core-mantle grazing occurs at 99.3° (slowness = 4.5643 secs/degree) using smoothed P travel time data, Johnson (1968) who assumes 97°, and Sacks who puts the shadow boundary of the core at $\Delta = 96^\circ$ using diffracted P arrivals. Beyond 100° the curve slightly increases once more.

Although the final value of slowness (4.523 km/sec at $\Delta = 104^\circ$) is obtained because of the extrapolation involved in the smoothing program, the unsmoothed curve also shows indications of an increase in velocity over the last two distance ranges $96^\circ - 98^\circ$ and $98^\circ - 104^\circ$. The covariances give the standard error on the difference between the unsmoothed slowness values (4.470 and 4.538 secs/deg respectively) as being 0.48. The t statistic of 1.42 is thus just below the level needed to show a significant rise in slowness. Ansell (1969) has shown that an increase in slowness within the core shadow zone is possible if diffraction is taken into account. Beyond 95° the higher frequencies are attenuated at a greater rate than lower frequencies (Sacks, 1966), which results in an apparent delay in the arrival time of a pulse propagated round the core, and hence an increase in slowness. This frequency dependent effect also perturbs waves of different periods at the same distance resulting in a general increase in scatter of observed slowness as the core is approached. The scatter beyond 88° is clearly seen in the plot of the individual slowness estimate (Figure 15) and by the higher variance estimated for the final distance interval ($\Delta = 83^\circ - 104^\circ$). Johnson (1969) measured the

period of all waves arriving at distances greater than 90° and applied the appropriate correction to the observed slowness values. Although lateral variations at the mantle-core boundary are thought to be responsible for some scatter, the scatter in the corrected slowness values was reduced.

The five regions of anomalously steep slowness gradient near 35° - 36°, 48° - 49°, 60°, 68° - 70° and 84° - 85° are the result of high gradients in the lower mantle velocity structure, that is, when Bullens parameter - ζ = rdv/vdr, representing the non-dimensional velocity gradient, is a maximum (Bullen 1963, p. 112). These regions are indicated by dotted lines in Figure 27 which also shows the results from three studies of slowness using single arrays. The criterion for selecting anomalous gradients is not made clear by Chinnery and Toksöz (1967) and Greenfield and Sheppard (1969), partly because there are serious gaps in their data, but the regions they consider anomalous are included in Figure 27.

Lateral inhomogeneities in the lower mantle

Further evidence for the sharp change in slope near 35° from array measurements is given by Fairborn (1967), who analysed 400 slowness observations in both the north-west and south east azimuths from LASA. Changes in slope for events from the north-west azimuth were also observed at distances of 55° and 70°. The two curves derived from opposite azimuths show distinct differences between 65° and 75°, which Fairborn attributes to lateral inhomogeneities within the lower mantle.

The problem of detecting lateral inhomogeneities can only be solved if the corrections applied to the slowness observations sufficiently correct for the effects of array geology. The method of analysing the observations described in this thesis has been to obtain a world average curve and lateral variations have not been specifically looked for. Lateral variations in the lower mantle can however, be tested by combining observations from events in the same geographical area and testing them against the world average curve shown in

Figure 27. Fairborn's analysis, which is similar to that of Chinnery and Toksoz (1967), does not use any corrections for the upper mantle structure below LASA, but relies on assuming the structure can be approximated by a constantly dipping interface. If this is correct, then the differences between his curves from opposite azimuths will represent real lateral variations. The failure of seismic refraction and gravity data (Steinhart and Meyer, 1961; Borcherdt and Roller, 1967) to detect any large scale structural anomaly suggests the true picture may be more complicated.

Vinnik and Nikolayev (1969) used two networks of seismometers in Siberia and Kirgizia with 200 km apertures to directly measure slowness for 200 earthquakes mainly in the Pacific seismic belt. They did not correct for subcrustal effects, but found that events from both arrays fell near an average curve except for observations at Kirgiz from the north-easterly azimuth. These values had to be increased by 0.3 secs/degrees to fit the other data. They attributed some of the scatter on their curve to lateral inhomogeneities and found that events from Europe and North America gave values of slowness generally larger than those from the Pacific area. Lower mantle inhomogeneities, resulting in a flattening of the average curve were observed at distances of 30 - 36°, 40 - 45° and beginning at 92°. A steepening in the gradient of their curve therefore occurs between 36 - 40°, which is in good agreement with Figure 27.

The clustering of slowness values for events from the Aleutian Islands measured at EKA has already been mentioned (Figure 14). When sub-array corrections containing a two-term azimuthal component are used, the events move nearer to the average curve, although they still have slowness values less than average. Further analysis is needed to establish whether these results are due to path differences or mearly inadequate site corrections. It is however, worth mentioning that the same events from the Aleutian Islands recorded at the GBA array (at distances of 88° and 98°) also have slowness values less than average. Low slowness values are also recorded at GBA for Kurile Island events at distances between 68° and 70°.

Evidence for deep mantle structure

Figure 27 also compares the work of others who have found evidence for variations in deep mantle structure.

Repetti (1928) from a study of Mohorovicic's travel times found evidence for abrupt changes in slowness at distance of 32.2°, 39.4°, 65° and 77.5°. Vvedenskaya and Balakina (1959) investigated the amplitude P waves to SH waves and SV to SH waves and found anomalously large values near $38 - 42^{\circ}$, $51 - 55^{\circ}$ 70° and 80°. Bugayevskiy (1964) performed a least squares analysis of empirical travel time curves and noted discontinuities at epicentral distances of $35 - 38^{\circ}$, $50 - 54^{\circ}$ and $70 - 72^{\circ}$ Carder (1964) interpreted travel time data from nuclear explosions in the Central Pacific as having breaks at distances of 39°, 52°, 69°, $79\frac{1}{2}^{\circ}$ and $89\frac{1}{2}^{\circ}$. Kondorskyaya et al (1967) studied the spectra of P waves and found discontinuities at distances of 38°, 52°, and 71°. All the regions that are interpreted by these workers as being "anomalous" are included in Figure 27.

Kondorskaya and Slavina (1969) have recently made a statistical analysis of travel time residuals from 1144 earthquakes recorded at 15 stations throughout the USSR. Similar variations in the residuals were found for different stations at distances of 30°, $60 - 70^{\circ}$ and 85°, and it was inferred that their cause was inhomogeneities in the mantle with a world-wide distribution.

The comparison of distances at which anomalies are observed to occur by different workers is made more difficult because different parameters have been measured and different qualities are being compared whose effects may be observable at different distances.

Johnson (1969) used the same criterion to define anomalies as has been used here - that is apparent steep portions of the slowness curve. The fit of Johnson's curve to that of Figure 27 is particularly good over the greater part of the distance range beyond about 45°, and with the exception of 84° - 85°, the regions of his anomalous gradients correspond almost exactly with the curve presented here. Although not a very striking anomaly in this work, all other studies agree that velocities at 68° - 70° (about 1800 km depth) are smaller than expected and the strong inflexion in the Lilwall-Douglas travel time, which begins in this distance range is strong corroborative evidence for this feature.

On the other hand, only Johnson agrees with the anomaly at 60°, and, with the exception of Johnson, most of the other studies suggest that the change at 48° - 49° is observed at slightly greater distances. Only two of the four array studies present evidence for anomalous velocities within the range 80° - 90°, and Johnson's result agrees with those of the earlier studies in finding the anomaly at about 80° rather than 84° - 85° as here.

At distances less than 45°, Johnson's curve does not fit the average curve especially well. At 40° for example, the high gradient found by Johnson coincides with the well developed minimum on the average curve. Between 30° and 40° the results of the earlier studies are scattered but there is a slight suggestion in the array studies of two separate anomalous gradients around 35° and 40°. The former is strongly confirmed by all but one of the four array studies, as well as by the Lilwall-Douglas travel time curve.

The reasons for the significant deviations, at the shorter distances, of Johnson's curve from the average derived from combining the four arrays

is not known. One possibility is that there is bias which is caused by insufficient data and/or inadequate azimuthal corrections in one or both curves. The point has been discussed in the case of GBA and WRA in the section on results; the geological model for the Tonto Forest array used by Johnson may not be sufficiently exact. A second more interesting possibility is that if bias from these sources has been minimised in the average curve, and if the Tonto Forest model is good enough, the Johnson curve may indicate real differences from the assumed spherically symmetric earth at depths between 800 kms and 1200 km. Such conjecture will only be resolved after a standard set of slowness tables has been agreed.

The correlation of the regions where velocity gradients are changing rapidly, with the amplitude-distance curve of Carpenter et al (1967) is not as good as one would expect. The five large relative maxima of Figure 29 should correspond to maxima in amplitude (Bullen 1963, p.130) (it is for this reason the curve has been plotted with the sign of the y-axis reversed). In fact, only the amplitude maxima at 35° and at 48° - 54° show high correlation, and except at 94° the minima in Figure 29 do not correlate well. This may be due to the overall lack of data in the amplitude-distance curve, which was estimated in 3° intervals. Now that new data from explosions is available, the revised curve may show a better correlation.

Comparison with a recent amplitude distance curve derived from long period P observations at LRSM stations in the region near 40° (Willey, 1969) is especially good. His curve coincides very closely to the Gutenberg and Richter curves (Richter 1958) beyond 45° but near 40° it shows a significant drop in amplitudes as is predicted here. A similar flattening of the amplitude distance curve near 40° has been observed by Cleary (1967) for short period P arrivals at LRSM stations.

CHAPTER 3

3.1 INVERSION

The problem of obtaining a unique velocity model of the Earth from geophysical data is still unsolved. If the classical method of Weichert-Herglotz is used to obtain a velocity-depth distribution from the seismic travel times, then only an approximate result will be obtained. This is because there are always many velocity-depth curves that correspond to any real set of seismic observations. The range of possible solutions can only be limited by incorporating additional geophysical data, or by making the assumption that the travel-time curve is continuous and has a continuous derivative. The slowness curve must therefore have no violent changes in gradient. Bullen (1963, p. 112) has discussed the conditions for a wave to exist within a given layer.

For a ray with a velocity v at a radius r from the centre of the Earth, the radius of curvature is dv/vdr, while the radius of curvature at that level is $^1/r$. For a discontinuity at the radius r, a change in the shape of the rays of a given family will result when the ratio of the two radii of curvature defined by:

$$\zeta = \frac{r}{v}\frac{dv}{dr}$$

pass through 1. ζ defines the maximum velocity gradient within each layer for a wave to emerge into the next layer. For a ray to exist, ζ must be less than 1. Provided there are no low velocity layers where this condition is violated, the Weichert-Herglotz method may be used to integrate the slowness-distance curve.

A description of the method is given by Byerly (1942, p179 for further references), and a computer program (listed in Appendix H) written to obtain the velocity-depth curve from the slowness observations.

FIGURE 30

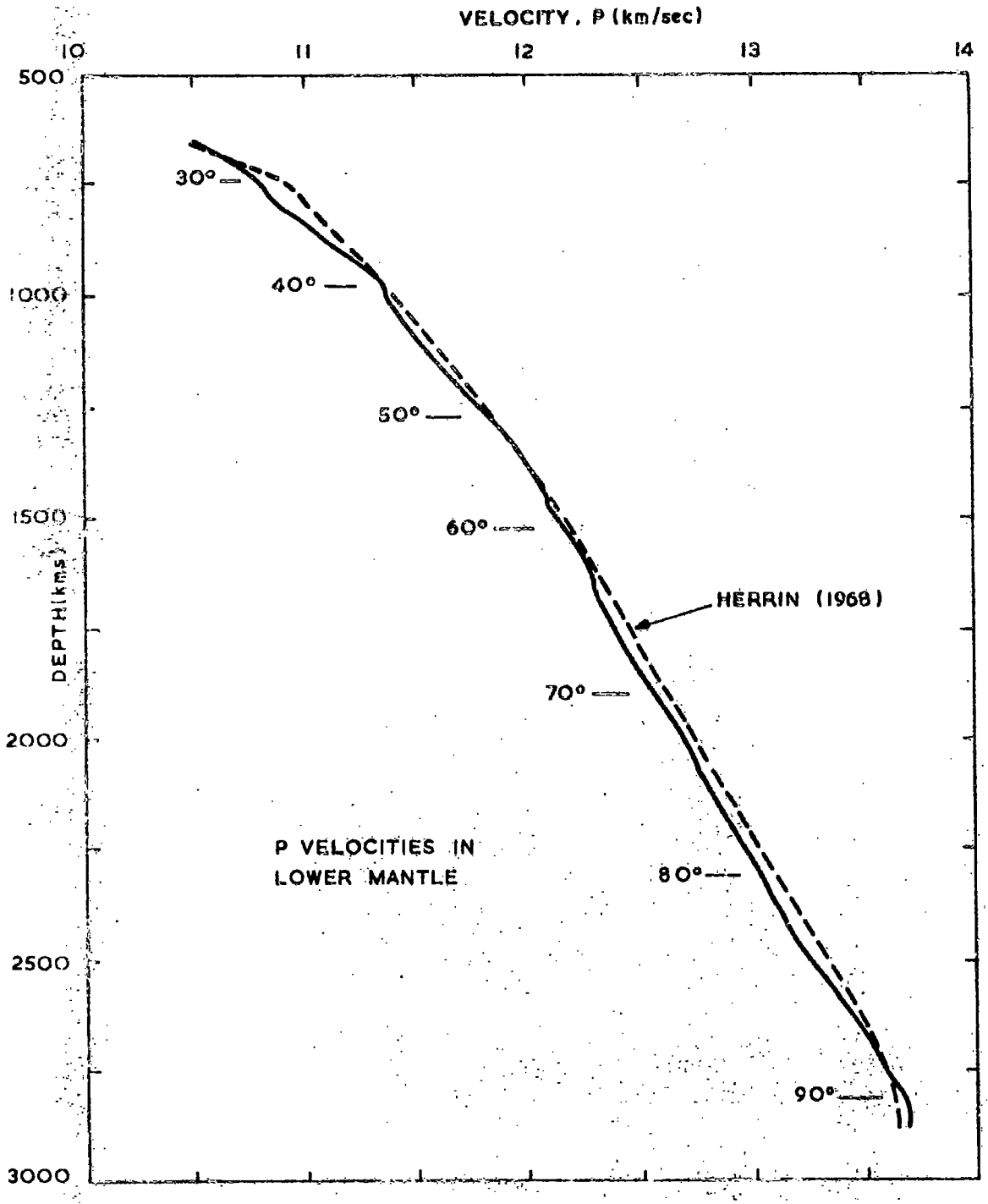
VELOCITY, P (km/sec)
10
11
12
13
14
500
1000
1500
2000
2500
3000
DEPTH (kms)
30°
40°
50°
60°
70°
80°
90°
HERRIN (1968)
P VELOCITIES IN
LOWER MANTLE

The method depends on evaluating the integral

$$\log \frac{r_o}{r_1} = \frac{1}{\pi r_o} \int_o^{\Delta_1} \cosh^{-1} \frac{p}{P_1} \, d\Delta$$

where p are the values of slowness tabulated at each Δ up to p_1 at an epicentral distance Δ_1 . r_o is the radius of the Earth. The equation gives r_1, the distance from the centre of Earth to the bottom of the ray emerging at Δ_1, that is, the depth at which the velocity $v = r_1/(r_o p_1)$. The accuracy of the method will depend on how accurately the integral can be evaluated, since the area under the $\cosh^{-1} p/p_1$ against distance curve must be evaluated for each pair of r_1, v values required.

From the integral, it can be seen that slowness values are required from an epicentral distance of 0^o. Herrin's (1968) values of slowness for the upper mantle were therefore smoothed into the observed, correct values of Figure 27. Herrin's model is an average for the upper mantle and is representative of the stable, continental region under the central United States but is not intended to represent the actual velocity structure anywhere on the Earth. The actual upper mantle structure chosen is unimportant as long as the angles of incidence of the rays within the model are small and the corresponding travel-times are average and do not contain discontinuities. The composite slowness curve was interpolated at $\frac{1}{2}$ degree intervals to enable the Weichert-Herglotz integral to be evaluated with sufficient accuracy.

The observed slowness curve contains a discontinuity near $\Delta = 40^o$ and this was smoothed between 39^o and 41^o to remove the inflexion and fulfill Bullen's condition $\zeta < 1$. Figure 30 shows the corresponding average BN1 velocity model for the lower mantle. For comparison the model of Herrin, et al (1968) is also shown, which was derived from average travel-time curves. This model is very smooth, with no anomalous features and against it the high gradient regions of BN1 show up clearly at the depths of

FIGURE 31 GRADIENTS OF P VELOCITIES IN THE LOWER MANTLE

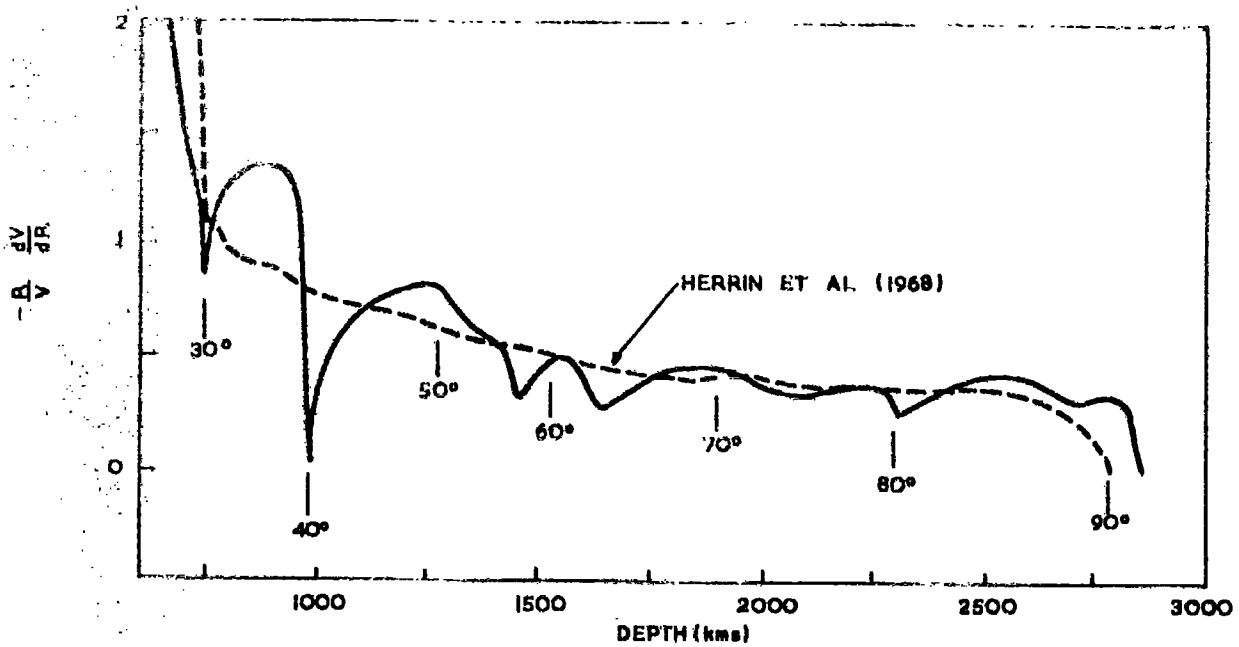

850 - 900, 1200, 1550, 1800 - 1900 and 2500 kms, corresponding to the epicentral distances 35 - 36°, 48 - 49°, 60°, 68 - 70° and 84 - 85° respectively. In general BN1 has velocities that are less than Herrin's below 1500 kms.

In an attempt to make the high velocity gradients of Figure 30 more conspicuous, the non dimensional velocity gradient - $\zeta = -r/v\ (^{dv}/dr)$ has been plotted as a function of depth (Figure 31), and these regions of high velocities can be seen as peaks against the values derived from Herrin's model which shows no anomalous features in the lower mantle. Minima in the plot of $-\zeta$ show the positions of unusually flat portions or low velocities in the velocity structure.

3.2 ELASTICITY OF THE LOWER MANTLE

The results from the slowness-distance curve strongly support the hypothesis that there are anomalies in the lower mantle. In this section, variations of the elastic parameters of the earth that are implied by the BNT velocity structure are discussed in the light of the classical theory of elasticity and assumptions of homogeneity.

The classical theory of elasticity for an isotropic, homogeneous medium relates the adiabatic bulk modules (k_s) and the ridgidity modules (μ) to the compression (α) and shear (β) body waves (Bullen 1963):

$$\alpha^2 = (k_s + \tfrac{4}{3}\mu)/\rho$$

$$\beta^2 = \mu/\rho$$

writing $\phi = \alpha^2 - \frac{4}{3}\beta^2$, then the ratios

$$k_s/\rho = \phi, \quad \mu/\rho = \beta^2$$

and Poisson's Ratio, σ

$$\sigma = \tfrac{1}{2}(\alpha^2 - 2\beta^2)/(\alpha^2 - \beta^2)$$

can all be found directly from the seismic velocities.

K_s and μ cannot be calculated without a knowledge of how the density ρ varies with depth. An estimate of the variation in density through the Earth's interior can be obtained from a study of P and S wave velocities if it is assumed that the change in density with depth is the result of adiabatic compression alone. Adams and Williamson (1923) showed

$$d\rho/\rho = -g\frac{dr}{\phi}$$

when g and ϕ are the values of gravity and the seismic parameter at a radius r, respectively. Although this equation will give the change of density within each layer, absolute densities must be adjusted to satisfy the conditions of mean density and moment of inertia.

Density can now be obtained directly from the study of long period surface waves and free oscillations.

Information on the viscosity, chemical and mineralogical properties of the lower mantle, and its temperature is, however, most inadequate at present. The temperature in the D layer will lie somewhere between the adiabatic pressure and melting point curves, but both of these quantities are unreliably determined for the lower mantle and leave a range of uncertainty of several thousand degrees.

The composition of the lower mantle can be inferred from the analysis of meteorites. The results of high pressure measurements, information on seismic velocities and densities can then be extrapolated by means of equations of state to give the properties of rocks that are stable at temperatures and pressures below the Moho.

Under the equations of state, the pressure, volume and temperature of a body can be related. Bridgman (1950) began experimental studies of the properties of matter at pressures of several dozen kilobars. The isothermal curves for the static compressibility of many elements and compounds were obtained using devices consisting of a piston and cylinder.

Measurements in the high pressure range approaching the actual pressures encountered in the interior of the Earth (of the order of 1 M bar) can only be made using dynamic methods. In these methods, the velocity of a shock wave and of the material behind the shockwave are determined as the wavefront passes through the material.

The two velocities, which experience shows to be linearly related, are then related to the density, pressure and volume by means of conservation laws. However, the compression of matter in the shock wave is followed by intense heating, resulting in the pressure, volume and temperature changing simultaneously on the adiabatic shock curve. This change is much more rapid than in the Earth's interior and in the region of the lower mantle it is almost impossible to obtain systematically theoretical equations of state. For this reason, semi-empirical methods based on potential theory have been employed.

The concept of this method is to obtain a quantitative relationship between the potential energy of a crystal and the lattice constants (or volume of the body). The numerical values of the parameters entering into the relation can then be found from experimental data. Equations of state for ionic crystals have been found by Born and Mayer (1931). Once the equations of state of a sufficiantly large number of rocks and minerals are known then the method can be used for the determination of the chemical composition of deep sections of the Earth.

The results of the preceding chapters of this thesis have enabled the compressional velocity (α) to be determined. Provided β is well known then the depth dependence of the seismic parameter ($\emptyset$) can be found quite accurately. It has already been mentioned that the depth dependence of the density is known less accurately and for this reason, comparisons are made using $\emptyset$ only.

The question of how far the mantle is homogeneous has been investigated by Birch (1952). He compared observed values of the rate of change of $\emptyset$ with depth with the values predicted for a homogeneous layer. A test of uniformity of composition can then be made.

Following Bullen (1949), Birch introduces Γ, a function that can be calculated directly from $\emptyset$-depth tables:

$$\Gamma = 1 - \frac{1}{g}\frac{d\emptyset}{dr} \qquad 3.21$$

where r is the radius and g the acceleration due to gravity at r (which departs very little from 10^3 cm sec^{-2} throughout the mantle). Birch shows that for a homogeneous layer in which changes of density and compressibility result from self compression in a gravity field and variation of temperature, then

$$\Gamma = \left(\frac{\partial K_T}{\partial \rho}\right)_T + T\alpha\gamma A + (T\alpha\gamma)^2 B + \frac{\alpha\emptyset\varepsilon C}{g}$$

Bullen (1949) gives simply dKs/dP for the right hand side. However, to allow for the effect of temperature and temperature gradient, Birch introduces the isothermal incompressibility K_T. Here, α is the coefficient of thermal expansion; γ is Gruneisen's ratio = $\alpha Ks/\rho Cp$ where Cp is the specific heat at constant pressure; T is the absolute temperature; ε the difference between the actual and adiabatic temperature gradients. A, B and C are functions of the homogeneous material. From a review of the parameters of many solids, Birch (1952) found that although the absolute magnitude of compressibility varies some hundredfold, and in spite of the differences in chemical binding between

various compounds, there are sytematic relations which enable A, B and C to be found. If the assumptions made are valid then a "law of corresponding states" holds for a wide range of substances.

The numerical values for the D region of the lower mantle enable the second order term to be ignored and A and C are of the order of -5 and -2, respectively. The equation therefore becomes

$$1 - \frac{1}{g}\frac{d\phi}{dr} = \left(\frac{\partial K_T}{\partial P}\right)_T - 5T\alpha\gamma - \frac{2\varepsilon\alpha\phi}{g} \qquad 3.22$$

To evaluate the left hand side of equation 3.22, g was assumed to be 10^3 cm sec^{-2} and the compressional velocity structure of section 3.1 used. To investigate the effect of the high velocity regions in this model on the elastic parameters in the lower mantle, a composite shear velocity model was constructed that also represented an average world structure.

A study of shear velocities to a similar degree of accuracy as that of compressional velocities has yet to be made. However, Ibrahim and Nuttli (1957) have made a study of S wave travel times out to about 50° using a polarization technique to identify arrivals.

They determined a shear velocity structure that was in gross agreement with the upper mantle P structure determined by Johnson (1967). Doyle and Hales (1967) have determined a new shear travel-time curve between 28° and 80°, and in a recent paper by Anderson and Julian (1969), these two shear travel times have been inverted to yield a shear velocity structure that is compatible with Johnson's

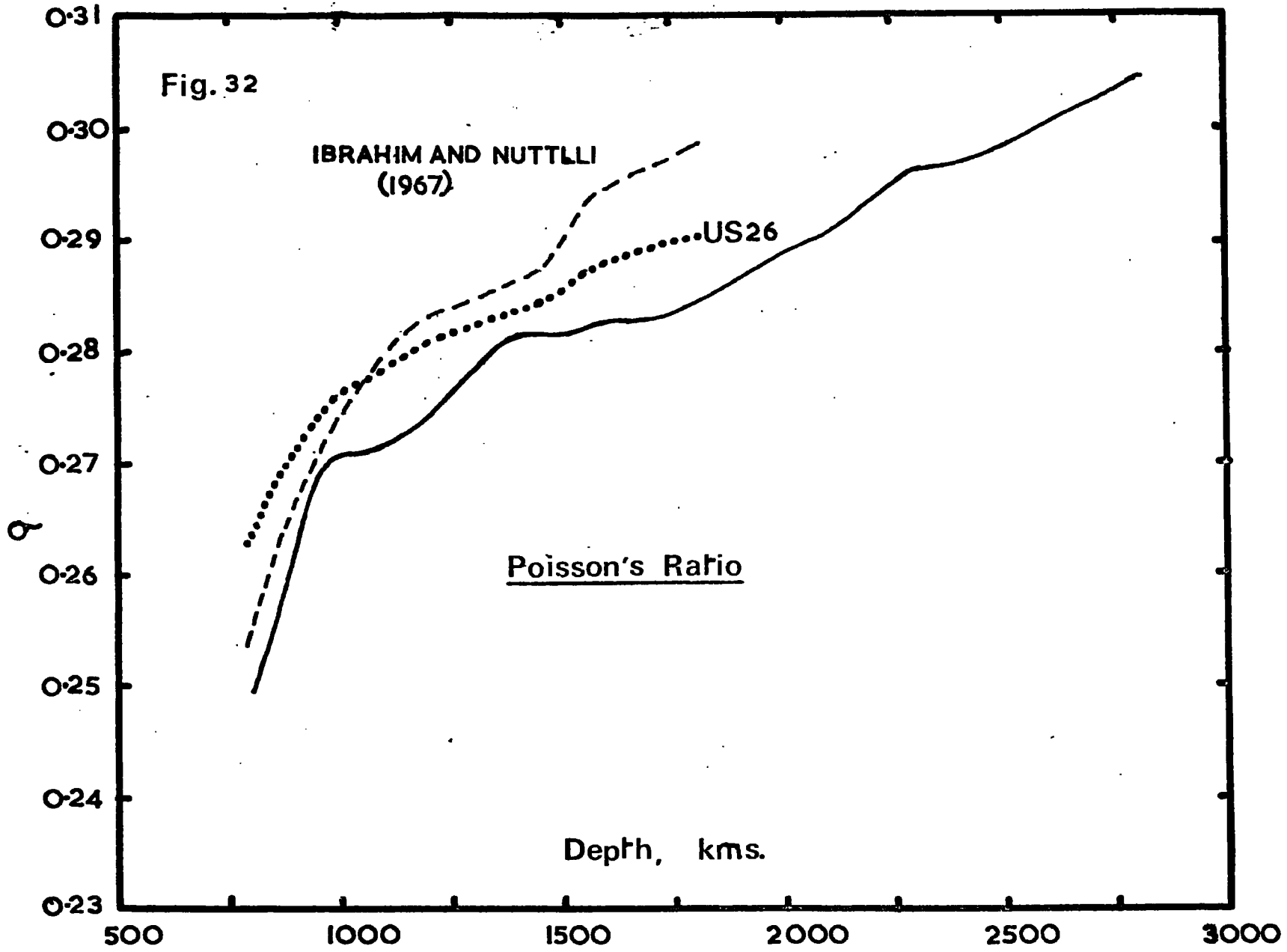
Fig. 32
IBRAHIM AND NUTTLLI
(1967)
US26
Poisson's Ratio
σ
Depth, kms.
0·31
0·30
0·29
0·28
0·27
0·26
0·25
0·24
0·23
500
1000
1500
2000
2500
3000

model. The model obtained by Anderson and Julian (US26) specifies velocities to a depth of 1800 kms. Velocities below this depth were taken from the Gutenberg-Birch II model (Anderson, 1964). The combined shear wave model is one with no pronounced discontinuities below 800 kms. At this depth, β = 6.30 km/sec and increases smoothly to the core boundary at 2898 kms, where β = 7.24 kms/sec. The model was interpolated at depths of 50 kms and along with the compressional velocity model (BN1), used to obtain the depth variation of the seismic parameter $\emptyset$. Because of the smooth form of the shear model, all rapid variations in the elastic parameters with depth must be due to variation in BN1.

The results show there is a relatively uniform increase of $\emptyset$ with depth below 1000 kms. k/μ and σ also increases uniformly within this region, except near 1200 kms, where σ shows a marked increase. This is the region of the high P-velocity gradient, and an increase in Poisson's ration is consistent with an increase in temperature and pressure. Poisson's ratio shows a marked flattening near 1500 kms depth (Figure 32), followed by an increase in value. Values of σ obtained by Anderson and Julian for their US26 model and the data of Ibrahim and Nuttli are also shown. Decreases in σ in the upper mantle observed by Anderson and Julian were thought to be due to changes in crustal structure. Shock wave data shows that for a given crystal coordination, Poisson's ratio decreases as the packing index of Fairbairn (1943)

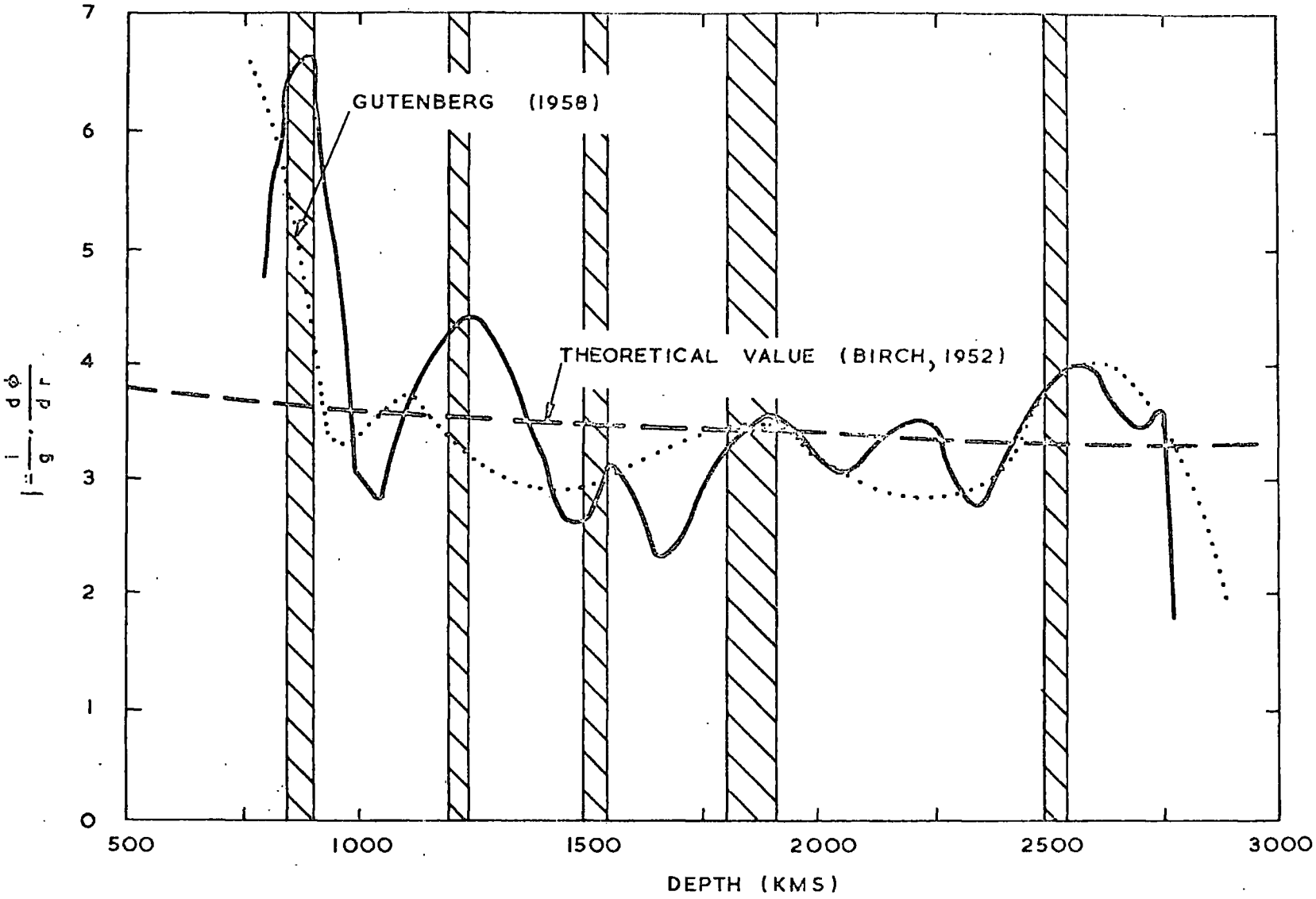

FIGURE 33 . REGIONS OF INHOMOGENEITY IN THE LOWER MANTLE

increases, and for a given mean atomic weight, Poisson's ratio decreases as the coordination increases. For simple oxide phase changes there is such an increase in packing index. The phase changes are also necessary to produce model densities that agree with the observed values (Clark and Ringwood, 1964). It is then unnecessary to postulate an increase in density near the lower mantle by increasing the FeO/(FeO + MgO) ratio as suggested by Anderson (1967).

The geophysical and geochemical implications rely heavily on the reliability of the estimates of the lower mantle velocities. Until a study of shear wave velocities has been made with an accuracy comparable to that of body waves it will be difficult to estimate how far the trends in Figure 33 are real and how far they are just due to random scatter. High pressure laboratory data is also very limited at present, and unavailable for the lower mantle regions and so any hypothesis produced to explain the high velocity gradients cannot be checked. Figure 33 shows the rate of change of ϕ with depth for the lower mantle, plotted as the function $1 - \frac{1}{g}\frac{d\phi}{dr} = \Gamma$. For comparison, the values obtained from Gutenberg's (1958) data are shown.

Theoretical values, obtained by Birch (1952), using equation 3.22 are also shown. For T of the order of several thousand degrees $T\alpha\gamma$ will be about 0.1 - 0.2. The quantity $\varepsilon\alpha\phi/g$ lies between 0.2 and 0.1 for a super adiabatic gradient of 1°/km. These two terms form corrections to $(\partial^{K}T/\ P)_{T}$ which is about 3.5 for the lower mantle, decreasing with depth. The calculations assume

that the mantle material is homogeneous and isotropic. Regions where there are gross departures from the theoretical curve indicate that the region is either not isothermal or not homogeneous or both.

A conspicuous feature of both of the observed curves is the high value of γ in the region above 800-900 kms which represents Bullen's "C" region of rapid rise of velocity. If the layer were homogeneous, values would be expected in the neighbourhood of 4 from equation 3.22, decreasing with pressure. The high value of γ cannot be explained by high temperatures, as this would have the effect of reducing the observed values. In the transition region, both the density and seismic velocities increase more rapidly than they would by compression of a homogeneous solid. It is therefore thought that in this region there is a change in composition or a phase change with a resulting rearrangement of the atoms in the lattice.

Gutenberg interpreted relatively straight sequents of the travel-time curve between 40° and 44°, and 53° and 63° as being anomalous, as they represent a relatively slow increase in velocity with depth within the mantle. These regions are seen between 900 and 1000 km and 1400 and 1500 km, and are indicated as minima in γ in Figure 33. As pointed out in Chapter 2, anomalous regions in this study have been taken as meaning those regions where the velocity is changing rapidly with depth and these regions are shown as the shaded areas in Figure 33.

The region of the upper mantle above 1000 kms has already been discussed. The observed values of Γ also show a marked increase near 1200, 1550, 1800-1900 and 2500 kms. Within these regions Γ is varying rapidly with depth, although in the two regions near 1550 and 1800-1900 kms, the actual value of Γ is not significantly different from Birch's calculated value. The increase in Γ above the theoretical value near 1200 kms is most pronounced. As the core is approached, both Gutenberg's and the observed curve increase above the theoretical value.

The discontinuity near 1000 kms has been investigated by Ringwood (1969) and interpreted as phase changes in oxides of magnesium and iron with coordinations higher than six. Similar transformations are postulated for increases in seismic velocities below 1000 kms.

CHAPTER 4

CONCLUSIONS

4.1 THE DATA

A slowness-distance curve has been derived using all available data recorded by the four UKAEA arrays.

As more data are collected the curve, which is estimated in intervals of two degrees, will be revised and the intervals reduced to give more information of the fine structure. With the construction of further arrays it will also be possible to obtain a far greater coverage of azimuths than is possible with the present distribution. From Figures 9 and 10 it can be seen that there is a general lack of events to the south of each array. An array situated in Brazil would be able to remedy this to some extent. Ideally, results from a location in Siberia would provide the necessary coverage.

The arrays used have a sufficiently small aperture to minimise structure corrections and still produce a stable estimate of slowness. It is however necessary to read the events to an accuracy of a few hundredths of a second, and the laborious method of matching waveforms, described in Section 1.4 was used. For the large number of events available, the reading of onset times (approximately 9000) also took a considerable length of time. If events were available in digital form and the data handling performed with the aid of a video screen, then the process of reading arrivals could be speeded up, while still allowing the operator the very necessary facility of being able to match the waveforms by eye. Signal processing techniques

could also be easily incorporated to enhance the onsets, and so make available a larger population of events that at present have to be discarded because of low signal to noise ratios and ill-defined P onsets.

4.2 SITE CORRECTIONS

The site corrections are attributed to inhomogeneities in the geology beneath the arrays. The corrections derived for each array show the crustal layering beneath YKA and GBA to be horizontal and to have very little effect in perturbing the slowness of the wavefronts crossing the arrays. The magnitude of the corrections, especially at GBA, is small (less than ± 0.025 seconds). GBA has now been extended from 10 to 20 instruments and the number of events recorded warrants the experiment to be repeated to obtain corrections for all channels. This should also remove any possible weighting effect that may have biased the slowness estimates by using an array with only half the number of seismometers.

The corrections at EKA have been shown to be a function of the relative height of the instruments. By assuming a crustal velocity of 2.94 kms/second in the top 170 m this height effect can be effectively removed, with the exception of R5. The correction at this pit still remains large after the removal of the height effect, and it is suggested that this is due to the seismometer coupling or an erroneous value for the altitude. Because of the lack of data recorded by seismometers R9 and R10, no conclusions could be reached for these two pits.

The corrections derived for WRA array show that to a first approximation the layering in the crust is dipping at 3.6° in the direction N195°E. The corrections therefore have a relatively large azimuthal component. The directions of dip beneath individual seismometers show a trend towards the NW for the seismometers near the cross-over point. The available geophysical evidence from the area confirms a rise in the basement near the NW of the cross-over point.

4.3 SLOWNESS ESTIMATES

The slowness curve obtained from the available data should represent the best average for the world. The curve is in good agreement with the results of observed travel times and shows several anomalous features.

These correspond to regions of anomalously high velocity gradients at the distances of $35\text{-}36^{\circ}$, $48\text{-}49^{\circ}$, 60°, $68\text{-}70^{\circ}$ and $84\text{-}85^{\circ}$.

The features have been interpreted as radially anomalous velocity gradients within the lower mantle near the depths of 900, 1200, 1550, 1900 and 2500 kms. Those near 900, 1200 and 1900 kms. are confirmed by other array studies and also independent studies; the consistency of the evidence near 1900 kms. is especially noteworthy.

By estimating slowness in narrow distance ranges, using data from all azimuths, a single model can be estimated against which it is possible to test the existence of lateral mantle variations. Comparison with a single array study (Johnson, 1969) suggest the possibility of differences from the world average structure at depths

of 800 to 1200 kms. Below 1200 kms. the assumption that the mantle structures are very close to radial symmetry is strongly supported by this and other array studies.

The P wave velocities for the lower mantle have been combined with shear velocities to obtain an estimate of the rate of change of the seismic parameter $\emptyset$ with depth. This quality can be used as a measure of the degree of homogeneity. Because the scatter in this curve (Figure 33) is unknown, the significance of the departures from homogeneous behaviour is difficult to estimate. The results confirm Gutenberg's (1958) observations near the depths of 900-1000 kms. and 1400-1500 kms. The features near the depths of 1200 and 2500 kms. show the greatest departure from homogeneity. However, until a shear velocity structure has been derived with an accuracy comparable to that of the compressional wave studies no reliable conclusions regarding the geochemical nature of the fine structure in the lower mantle can be drawn.

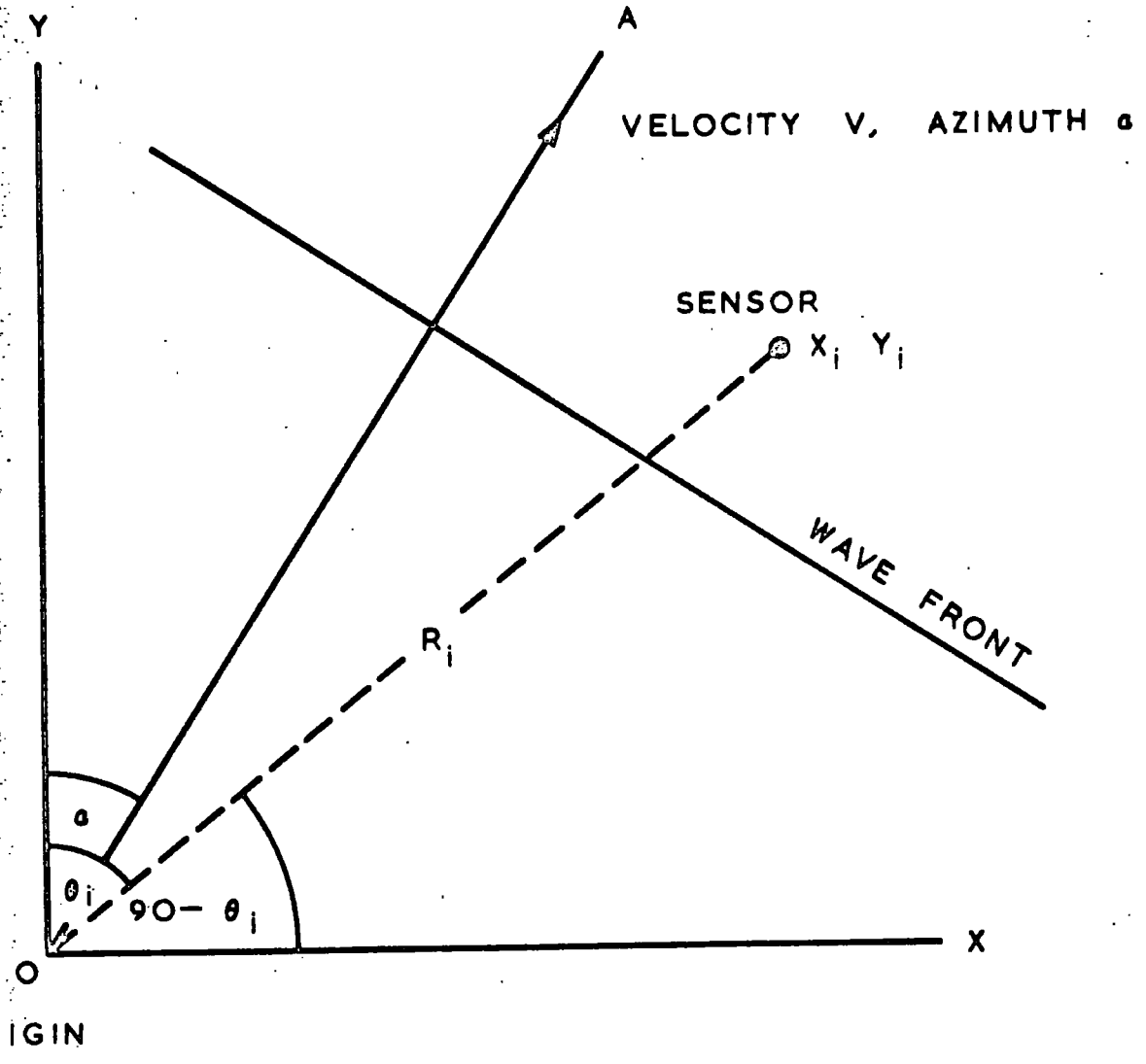

FIGURE A1. SCHEMATIC DIAGRAM OF ARRAY

APPENDIX A

The equation to estimate the slowness and azimuth of a plane wave propagated across an array of seismometers is derived.

Consider an array of n seismometers, with cartesian coordiantes (x_i , y_i) -------- (x_n , y_n) with respect to the arbitary origin (0, 0) at 0, the Y-axis N-S and the X-axis E-W.

The wavefront of a seismic signal from the direction OA at an aximuth α^o from north with respect to 0, traverses the array with a constant velocity V. The distance travelled by the wave is assumed to be large so that the wavefront can be approximated by a plane and the velocity of the wavefront V is constant for all the seismometers (Figure A1).

If the seismometer i is at a radial distance R_i and azimuth θ_i from the centrepoint 0, the apparent or phase velocity of the wave along R_i is $\frac{V}{\cos(\theta - \alpha)}$.

The arrival time of the wave at x_i y_i relative to that at the origin is:

$$O_i = - \frac{R_i}{V/\cos(\theta_i - \alpha)} \qquad A1$$

Now coordinates $R_i \cos \theta_i = Y_i$ and $R_i \sin \theta_i = X_i$, and on expanding equation A1 and substituting:

$$O_i = - \frac{(X_i \sin \alpha + Y_i \cos \alpha)}{V} \qquad A2$$

The arrival time relative to an arbitary zero time (which preceeds the onset time at i) will be:

$$t_i = O_i + t_o + \varepsilon_i$$

where t_o = arrival time at the origin, and ε_i is the error in the observed arrival time t_i

Hence from A2 $t_i = t - \frac{(X_i \sin \alpha + Y_i \cos \alpha)}{V} + \varepsilon_i \qquad A3$

For n seismometers there are t_i ----------t_n relative arrival times, and n equations of condition, and three unknowns α, V and t_o. These equations can be solved in the presence of the errors ε_i by least squares if ε_i are normally distributed, to yield the solutions $(\sin \alpha/v)$, $(\cos \alpha/v)$ and t_o, from which α and V can be obtained, viz

$$\alpha = \arctan \frac{\frac{\cos\alpha}{v}}{\frac{\sin\alpha}{v}}$$

$$v = \frac{1}{\frac{1}{\left(\frac{\sin\alpha}{v}\right)} + \frac{1}{\frac{\cos\alpha}{v}}}$$

The phase velocity is simply the reciprocal of the travel time derivative "slowness", and putting $t_o = C$ we have from A3

$$t_i = C - R_i \cos(\theta_i - \alpha) \cdot \frac{dT}{d\Delta} + \varepsilon_i$$

APPENDIX B

The equation to be solved has the form

$$1 \cdot S_{hi} + 1 \cdot C_{hj} - R_{hi} \cdot \cos\left(\theta_{hi} - \alpha_{hj}\right) \cdot p_i = t_{hij} \qquad \text{B.1}$$

which is a simple series of linear equations in S_{hi}, C_{hi}, p_k

In the case considered h = 1, 2 --- 4 arrays ; i = 1, 2 ---- I_h (no. of seismometers in array h) ; j = 1, 2 --- J_h (no. of events recorded at array h). $p_k = \left(dT/d\Delta\right)_k$ the slowness of event j at a distance K = Δ. t_{hij} is the appropriate onset time.

The matrix of coefficients comprising the equations of condition B.1 can be set up. The A matrix is:

$\leftarrow I_1\text{-x-}I_2\text{-x-}I_3\text{-x-}I_4\text{-x-}J_1\text{-x-}J_2\text{-x-}J_3\text{-x-}J_4\rightarrow$

$J_1 \times I_1$ equations	S				C				K
$J_2 \times I_2$		T				D			L
$J_3 \times I_3$			U				E		M
$J_4 \times I_4$				V				F	N

B.2

S is a matrix containing the coefficients of the site corrections. There are J_1 sets of $I_1 \times I_1$ coefficients, derived from the LHS of the equation of condition (1) ie

I_1 equations

$$\left\{\begin{array}{l} 1S_1 + 0S_2 + 0S_3 \text{ ------ } 0S_{I_1} \\ 0S_1 + 1S_2 + 0S_3 \text{ ------ } 0S_{I_1} \\ 0S_1 + 0S_2 + 1S_3 \text{ ------ } 0S_{I_1} \\ \\ 0S_1 + 0S_2 + 0S_3 \text{ ------ } 1S_1 \\ 1S_1 + 1S_2 + 1S_3 \text{ ------ } 1S_{I_1} \end{array}\right\} \quad \text{for array h = 1}$$

T, U, V are similar matrices for the site corrections at arrays 2, 3 & 4. The additional terms in the I_1 + 1 row of the S matrix is included with zero on the R.H.S. of the equals sign to include the condition $\sum_i S_i = 0$.

Three similar equations are included in matrices T, U and V, so that $\sum_i Si = 0$ for all h. C is a matrix containing the constants and consists of J_1 sets of J_1 x I_1 matrices, derived from the LHS of equation B.1.

I_1 equations $\begin{pmatrix} 1C_1 + OC_2 + OC_3 \text{ --------- } OC_{J_1} \\ 1C_1 + OC_2 + OC_3 \text{ --------- } OC_{J1} \\ 1C_1 + OC_2 + OC_3 \text{ --------- } OC_{J_1} \end{pmatrix}$ for array h = 1

D, E, F are similar matrices for the constants for the other 3 arrays. If event 1 at array 1 falls in the Δ_2 (say) distance range, then K is a matrix containing the terms:

$$- R_i \left(\theta_i - \alpha_j \right) = -\left(x_i \sin \alpha_j + y_i \cos \alpha_j \right) = K_i \qquad B.3$$

I_1 equations

Δ_1	Δ_2	Δ_3 ----------	Δ_k
	K_i		
	K_i		

for array h=1

There are thus J_1 sets of k x I_1 matrices. L, M, N are similar matrices for the 3 other arrays, all with the same number of columns K.

The elements of the matrices comprising the STUV, CDEF terms will all be ones or zeros and the KLMN terms will be of the form given by equation B.3.

The unknowns form the column vector X =

$$\left.\begin{array}{l} S_{11} \\ S_{12} \\ \vdots \\ S_{1I_1} \\ S_{21} \\ S_{22} \\ \vdots \\ S_{2I_2} \\ \text{etc} \end{array}\right] \text{site corrections for each array}$$

$$\left.\begin{array}{l} C_{11} \\ C_{13} \\ \vdots \\ C_{1J_1} \\ C_{21} \\ C_{22} \\ \vdots \\ C_{2J_2} \\ \text{etc} \end{array}\right] \text{constants for each array}$$

$$\left.\begin{array}{l} P_k \equiv \Delta_1 \\ P_k \equiv \Delta_2 \\ \vdots \\ P_k \equiv \Delta_k \end{array}\right] \; dT/d\Delta \text{ values in discrete distance intervals.}$$

If Y is a column vector comprising the observed onset times t_{hij}, then the system is overdetermined and characterised by the linear set: $AX = Y$ where A has HIJ rows and (HI + HJ + K) columns. The most probable values of X are obtained by choosing the values that minimise the sum of the squares of the deviations of these values. Forming the residual vector

$$AX - Y = r$$

The condition for the least squares solution is that r^2 is a minimum.

The least squares solution becomes

$$\tilde{A}AX = \tilde{A}Y \qquad \tilde{A} \equiv \text{transpose of } A$$

$\tilde{A}A$ is now a symmetric matrix with (HI + HJ + K) rows and columns. The vector X is thus given by

$$X = (\tilde{A}A)^{-1}\,\tilde{A}Y$$

where $(\tilde{A}A)^{-1}$ is the inverse matrix of $\tilde{A}A$.

A is a HIJ x (HI + HJ + K) matrix. For H = 4 arrays, I = 20 seismometers per array and approximately J = 120 events recorded per array in K = 31 distance intervals (assuming $\Delta = 30^{\circ} - 104^{\circ}$ in 2° intervals) then A will have approximately 4.9×10^{6} locations. A more efficient method is to set up the normal equations $\tilde{A}A$, directly. The number of equations is thus reduced to the number of unknowns, with a corresponding reduction in storage locations.

As an example, consider equation B.1 rewritten in the form:

$$\varepsilon + a_1 x_1 + a_2 x_2 + a_3 x_3 = Y \qquad \text{B.4}$$

where x_1, x_2, x_3 are the unknowns (regression coefficients) $\equiv S_{hi}, C_{hj}, P_k$ $a_1\ a_2\ a_3$ are the independent variates, and if $y \equiv t_{hij}$ is the dependent variate which will usually be in error ε.

In the example quoted here three normal equations can be constructed from (4), and if $\sum$ stands for summation over all observations

$$x_1 \sum (a_1)^2 + x_2 \sum (a_1 a_2) + x_3 \sum (a_1 a_3) = \sum (a_1 y_1)$$

$$x_1 \sum (a_1 a_2) + x_2 \sum (a_2)^2 + x_3 \sum (a_2 a_3) = \sum (a_2 y_2)$$

$$x_1 \sum (a_1 a_3) + x_2 \sum (a_2 a_3)^2 + x_3 \sum (a_3)^2 = \sum (a_3 y_3)$$

or $$(\tilde{A}A)\ X = AY$$

(AA) is a matrix symmetrical about the leading diagonal.

It is noted that in order to restrain the parameters to the condition $\sum_{i}^{3} x_i = 0$ it is only necessary to add 1 to each coefficient of a on the LHS of the normal equations.

The matrix $\tilde{A}A$ containing the elements of the normal equations can be solved by matrix inversion giving the covariance matrix C, which will also be symmetrical about the leading diagonal.

Matrix C is related to the normal matrix by the relationship $C(\tilde{A}A) = I$, the unit matrix.

$$\begin{pmatrix} C_{11} & C_{12} & C_{13} \\ C_{12} & C_{22} & C_{23} \\ C_{13} & C_{32} & C_{33} \end{pmatrix} \begin{pmatrix} \sum(a_1)^2 & \sum(a_1a_2) & \sum(a_1a_3) \\ \sum(a_1a_2) & \sum(a_2)^2 & \sum(a_2a_3) \\ \sum(a_1a_3) & \sum(a_2a_3) & \sum(a_3)^2 \end{pmatrix} = \begin{pmatrix} 1 & 0 & 0 \\ 0 & 1 & 0 \\ 0 & 0 & 1 \end{pmatrix}$$

B.5

Once the six values of C are known then the regression coefficients may be found from $X = C\,\tilde{A}Y$

ie
$$\begin{aligned} x_1 &= C_{11}\sum(a_1y_1) + C_{12}\sum(a_2y_1) + C_{13}\sum(a_3y_1) \\ x_2 &= C_{12}\sum(a_1y_2) + C_{22}\sum(a_2y_2) + C_{23}\sum(a_3y_2) \\ x_3 &= C_{13}\sum(a_1y_3) + C_{23}\sum(a_2y_3) + C_{33}\sum(a_3y_3) \end{aligned}$$

B.6

APPENDIX C

The method of solving the equation of condition:

$$S_{hi} + C_{hj} - \left(X_{hi} \sin \alpha_{hj} + y_{hi} \cos \alpha_{hj} \right) {}^{dT}/_{d\Delta k} = t_{hij} \qquad C.1$$

for S_{hi}, C_{hj} and ${}^{dT}/_{d\Delta k}$ has already been described. (Appendix B). In this section the equations of condition are derived for the corrected values of slowness for individual events.

The observed relative onset times t_{hij} are measured with respect to an arbitrary zero line (which is represented by C_{hj} in equation C.1). On solving C.1, corrected onset times can be obtained by subtraction of the site correction term:

$$t_i = t_{hij} - S_{hi}$$

Values of ${}^{dT}/_{d\Delta}$ for individual events can then be obtained from the equation

$$C - \left(x_i \sin \alpha + y_i \cos \alpha \right) \frac{dT}{d\Delta} = t_i \qquad C.2$$

C_{hj} will generally be a better estimate of the constant time-shift C, and so in deriving ${}^{dT}/_{d\Delta}$, C was made equal to C_{hj}. The corrected relative onset times are now

$$t_i = t_{hij} - S_{hi} - C_{hj}$$

and the equation of condition

$$-\left(x_i \sin \alpha + y_i \cos \alpha \right) \frac{dT}{d\Delta} = t_i$$

putting $-\left(x_i \sin \alpha + y_i \cos \alpha \right) = F_i$, the least squares estimate of ${}^{dT}/_{d\Delta}$ for $i = 1, 2 \ldots\ldots n$ onset times is

$$\text{slowness } \frac{dT}{d\Delta} = \frac{\sum_i^n F_i \, t_i}{\sum_i^n F_i^{\,2}} \qquad \text{for each event.}$$

APPENDIX D

CONFIDENCE LIMITS

The normal error law shows that any item picked at random from a normal population distributed with a variance σ^2 and mean $\bar{x}$ will lie between $\pm$ 1.96 σ with a probability of 95%. Hence $\pm$ 1.96 are called the 95 per cent confidence limits.

However, the distribution we are dealing with is usually only a sample of the total population, $\bar{x}$ and σ are therefore unknown, and have to be estimated. An estimate of σ^2 ($= S^2$) can be made from the errors ε:

$$S^2 = \frac{\sum_i^m \varepsilon_i^2}{m-n}$$

where m-n is the number of degrees of freedom obtained from m equations of condition with n unknowns. The errors ε_i can be obtained by substituting the regression coefficients x into the equations of condition B.4 (Appendix B Confidence limits for the regression coefficients x can be estimated from the covariance matrix C

$$\begin{Bmatrix} C_{11} & C_{12} & C_{13} \\ C_{12} & C_{22} & C_{23} \\ C_{13} & C_{23} & C_{33} \end{Bmatrix}$$

Rearranging B.6, it can be shown that x is a linear function of y :

$$\left.\begin{aligned} x_1 &= \sum y_1 \left[C_{11} a_1 + C_{12} a_2 + C_{13} a_3 \right] \\ x_2 &= \sum y_2 \left[C_{12} a_1 + C_{22} a_2 + C_{23} a_3 \right] \\ x_3 &= \sum y_3 \left[C_{13} a_1 + C_{23} a_2 + C_{33} a_3 \right] \end{aligned}\right\} \quad \text{D.1}$$

Now the variance V[x] of any linear combination of uncorrelated random variables:

$$x = k_o + k_1 y_1 + k_2 y_2 + k_3 y_3 \text{ -------- } k_n y_n$$

is given by $$V\left[x_i\right] = \sigma^2 \sum_i^n k_i^2$$

when σ^2 is the variance of y_i (Douglas 1966 p 23). It is now shown that $\sum k_i^2$ is simply equal to the appropriate diagonal element of the covariance matrix.

If the quantity in brackets in equation D.1 is represented by k_i, the variance of x is:

$$V\left[x\right] = \sigma^2 \sum \left[c_{11}\, a_1 + c_{12}\, a_2 + c_{13}\, a_3 \right]^2$$

where σ^2 is the variance of y, ie the variance of the errors ε which has been estimated to be S^2.

Expanding the term in the brackets:

$$V\left[x\right] = \sigma^2 \sum k_i \left[c_{11}\, a_1 + c_{12}\, a_2 + c_{13}\, a_3 \right]$$

$$= \sigma^2 \left\{ c_{11} \sum k_i\, a_1 + c_{12} \sum k_i\, a_2 + c_{13} \sum k_i\, a_3 \right. \qquad \text{D.2}$$

considering only the first term, and expanding once move:

$$= \sigma^2 \left\{ c_{11} \sum \left[c_{11}\, a_1 + c_{12}\, a_2 + c_{13}\, a_3 \right] a_1 \right\}$$

$$= \sigma^2 \left\{ c_{11} \left[c_{11} \sum a_1^2 + c_{12} \sum a_1\, a_2 + c_{13} \sum a_1\, a_3 \right] \right\}$$

It is noted that the term inside the square brackets is equal to the product of the first row and the first column of equation B.5 (= 1). Similarly the other terms of equation D.2 can be obtained by expanding equation B.5 and are thus zero.

Hence $V\left[x_1\right] = \sigma^2 c_{11}$, or more generally

$V\left[x_i\right] = \sigma^2 c_{ii}$ where c_{ii} is the ith diagonal element of the covariance matrix.

Now if x_i is normally distributed, then the confidence limits will be

$$x_i \pm t_\infty \sqrt{V\left[x_i\right]}$$

ie $$x_i \pm t_\infty S \sqrt{C_{ii}}$$ where S is an estimate of σ.

For large numbers of degrees of freedom t_∞ = 1.96 for 95% confidence limits

= 2.58 for 99% confidence limits

= 1.04 for 66.7% confidence limits

for small numbers of degrees of freedom, t can be found from tables.

In a similar way, the confidence limits on the difference of two x's i.e. x_1 and x_2 can be obtained from the appropriate elements of the covariance matric C_{ii}. The 95% confidence limits on the difference between x_1 and x_2 is:

$$\pm t_\infty \left(s^2 C_{11} + s^2 C_{22} - 2s^2 C_{12} \right)$$

where C_{11} and C_{22} are the diagonal elements of the covariance matrix as previously defined, and C_{12} is the appropriate off-diagonal element. $s^2 C_{12}$ is thus the covariance of x_1 and x_2.

The 95% confidence limits on all means and differences between means are formed when the values of slowness are computed, and can be obtained from the computer print-out.

FIG. E1

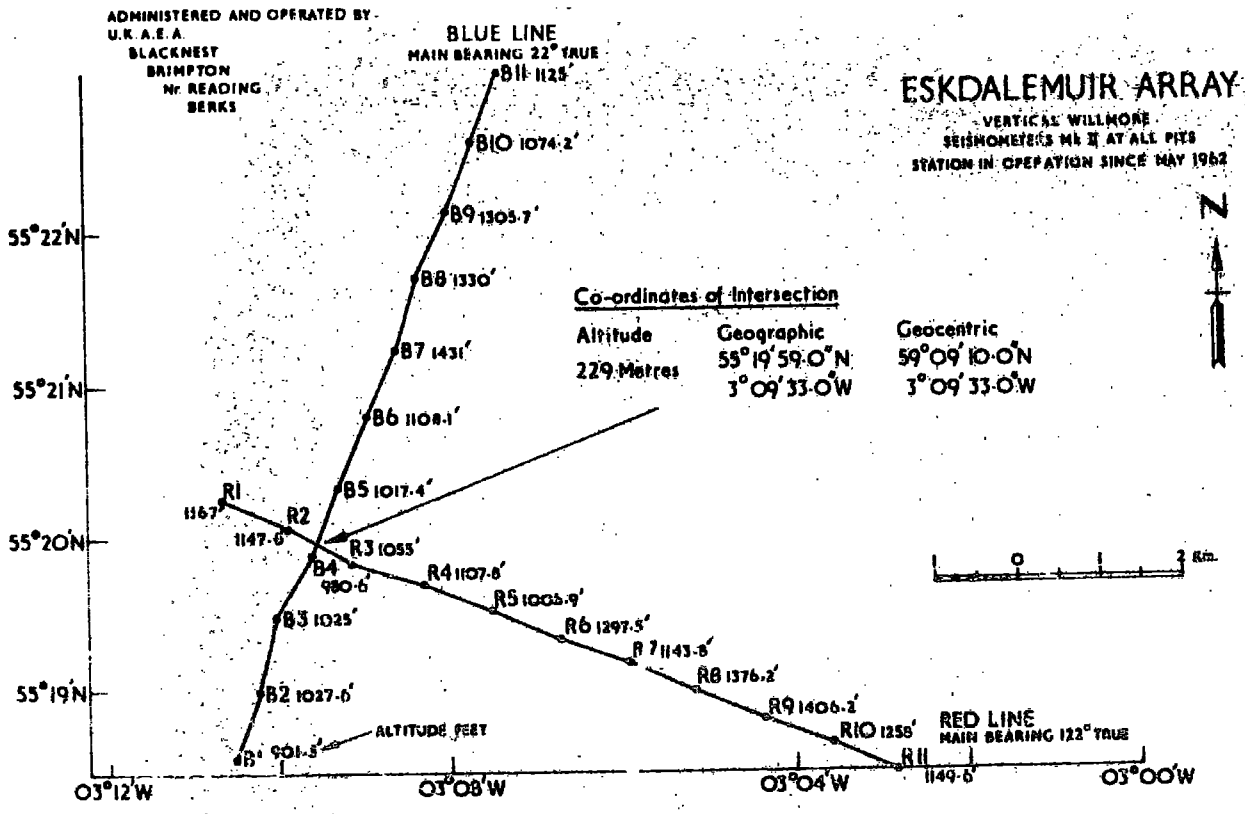
ADMINISTERED AND OPERATED BY:
U.K.A.E.A.
BLACKNEST
BRIMPTON
Nr. READING
BERKS
BLUE LINE
MAIN BEARING 22° TRUE
ESKDALEMUIR ARRAY
VERTICAL WILLMORE SEISMOMETERS Mk II AT ALL PITS
STATION IN OPERATION SINCE MAY 1962
B11 1125'
B10 1074·2'
B9 1305·7'
B8 1330'
B7 1431'
B6 1108·1'
B5 1017·4'
B4 980·6'
B3 1025'
B2 1027·6'
B1 901·5'
R1 1167'
R2 1147·6'
R3 1055'
R4 1107·6'
R5 1005·9'
R6 1297·5'
R7 1143·8'
R8 1376·2'
R9 1406·2'
R10 1259'
R11 1149·6'
RED LINE
MAIN BEARING 122° TRUE
Co-ordinates of Intersection
Altitude
229 Metres
Geographic
55°19'59·0"N
3°09'33·0"W
Geocentric
59°09'10·0"N
3°09'33·0"W
N
0 1 2 Km.
ALTITUDE FEET
55°22'N
55°21'N
55°20'N
55°19'N
03°12'W
03°08'W
03°04'W
03°00'W

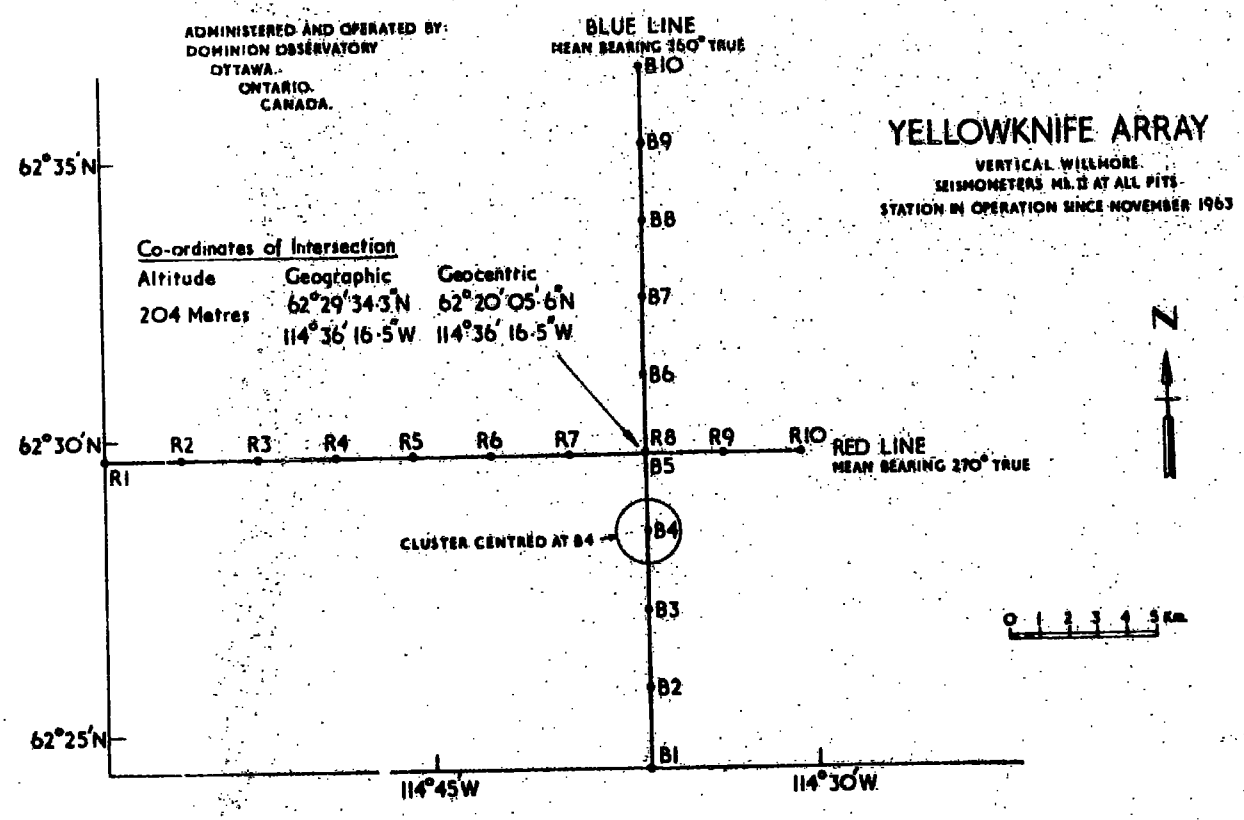
ADMINISTERED AND OPERATED BY:
DOMINION OBSERVATORY
OTTAWA.
ONTARIO.
CANADA.
BLUE LINE
MEAN BEARING 360° TRUE
YELLOWKNIFE ARRAY
VERTICAL WILLMORE SEISMOMETERS Mk II AT ALL PITS
STATION IN OPERATION SINCE NOVEMBER 1963
B10
B9
B8
B7
B6
B5
B4
B3
B2
B1
R1
R2
R3
R4
R5
R6
R7
R8
R9
R10
RED LINE
MEAN BEARING 270° TRUE
CLUSTER CENTRED AT B4
Co-ordinates of Intersection
Altitude
204 Metres
Geographic
62°29'34·3"N
114°36'16·5"W
Geocentric
62°20'05·6"N
114°36'16·5"W
N
0 1 2 3 4 5 Km.
62°35'N
62°30'N
62°25'N
114°45'W
114°30'W

APPENDIX E

The four UKAEA-designed seismic arrays

Seismic signals have to be detected against a continual background of seismic noise. For teleseismic signals in the range 30° - 100°, the noise should not be greater than 10^{-6} cm/sec rms. in the frequency band 1-2 Hz. Noise levels generally decrease with distance from oceans, and so inland rather than coastal sites are to be favoured. Other factors to be considered are proximity to vehicle traffic, industrial areas and trees, all of which tend to increase noise levels. Sites should also be chosen in regions that are geologically stable and free from elastic discontinuities and with low relief.

The configuration chosen for the four UKAEA arrays is L-shaped, which has advantages in being able to differentiate between seismic signals coming from different directions. The two lines of seismometers (designated "red" E-W and "blue" N-S) are spaced at 2.5 Kms at each array, except EKA where the spacing is 986 m. Each array has 20 seismometers except GBA where 10 were operating for the duration of the experiment. Willmore Mk II short period verticle component seismometers, with a damping factor of 0.6 and a natural period of 1 Hz, are used throughout the system. A description of the recording system has been given by Keen et al (1965) and in AWRE Pamphlet No 2.

Eskdalemuir (EKA)

EKA is situated in Scotland and possesses the highest background noise levels of the four arrays, varying from 3.5×10^{-6} cm/sec to 2×10^{-5} cm/sec in the $\frac{1}{3}$ to 3 Hz band under typical conditions (Truscott 1964). The number of events recorded with well defined onsets was therefore fewer at this array than the other three. During some periods of its operation, a Hall-Sears HS 2 geophone was used at position R4. As onset times recorded by the geophone

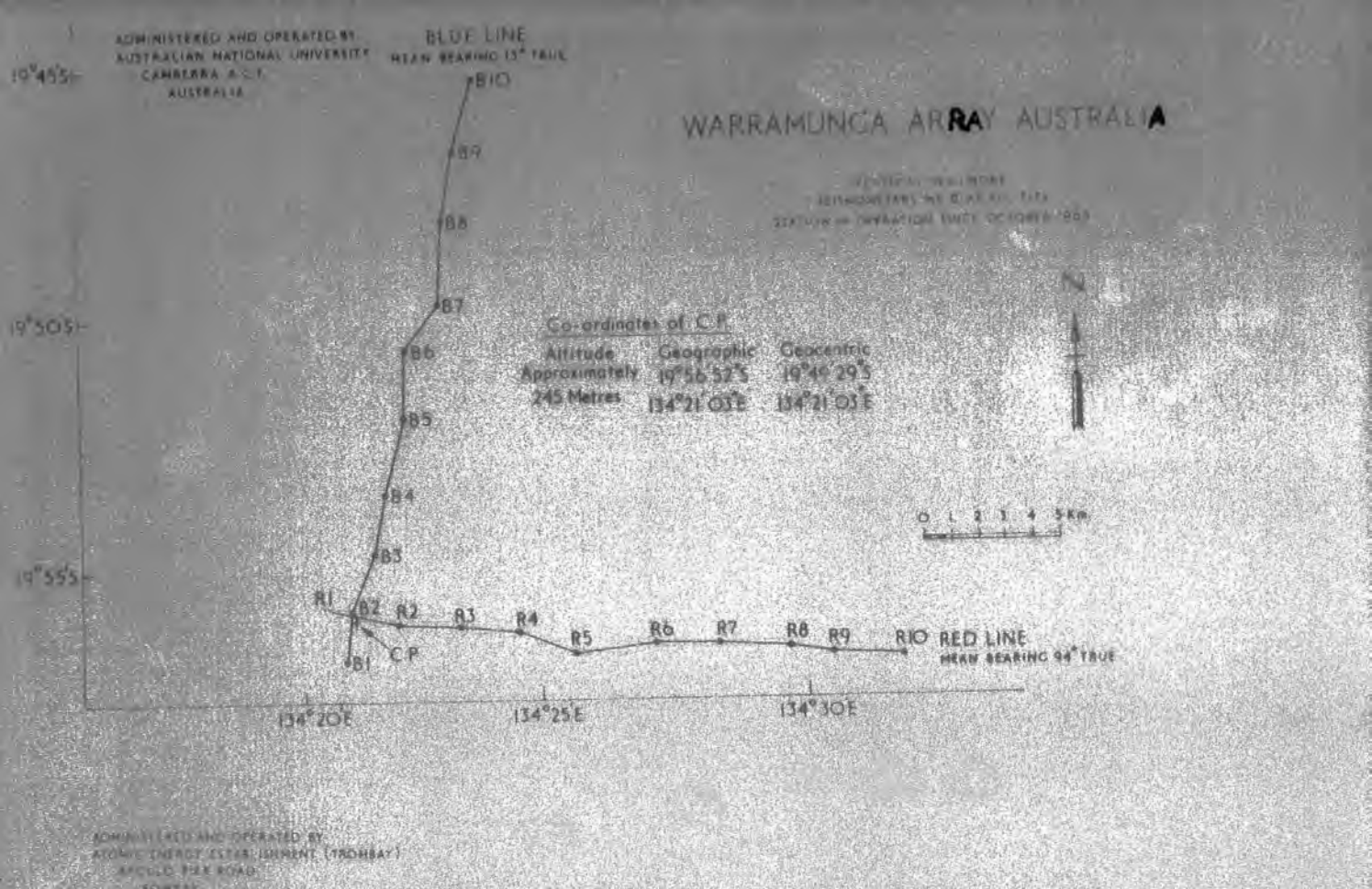
ADMINISTERED AND OPERATED BY
AUSTRALIAN NATIONAL UNIVERSITY
CANBERRA A.C.T.
AUSTRALIA
BLUE LINE
MEAN BEARING 13° TRUE
WARRAMUNGA ARRAY AUSTRALIA
VERTICAL WILLMORE
SEISMOMETERS MK II AT ALL PITS
STATION IN OPERATION SINCE OCTOBER 1965
Co-ordinates of C.P.
Altitude Approximately 245 Metres
Geographic 19°56'52"S 134°21'03"E
Geocentric 19°4' 29"S 134°21'03"E
N
0 1 2 3 4 5Km
B10
B9
B8
B7
B6
B5
B4
B3
B2
B1
R1
R2
R3
R4
R5
R6
R7
R8
R9
R10
C.P
RED LINE
MEAN BEARING 94° TRUE
19°45'S
19°50'S
19°55'S
134°20'E
134°25'E
134°30'E

ADMINISTERED AND OPERATED BY
ATOMIC ENERGY ESTABLISHMENT (TROMBAY)
ANUSHAKTI NAGAR
BOMBAY
INDIA
GAURIBIDANUR ARRAY
(MYSORE STATE — INDIA)
VERTICAL WILLMORE
SEISMOMETERS MK II AT ALL PITS
STATION IN OPERATION SINCE 1965
RED LINE
MEAN BEARING 302° TRUE
PROPOSED EXTENSION OF RED LINE
Co-ordinates of C.P.
Altitude 686 Metres
Geographic 13°36'15·0"N 77°26'10·0"E
Geocentric 13°30'59·0"N 77°26'10·0"E
N
0 1 2 3 4 5Km
R5
R4
R3
R2
R1
C.P
B1
B2
B3
B4
B5
PROPOSED EXTENSION OF BLUE LINE
BLUE LINE
MEAN BEARING 212° TRUE
13°40'N
13°35'N
13°30'N
13°25'N
77°15'E
77°20'E
77°25'E

FIG. E2

were found to be significantly altered, data was only used when a Willmore Mk II was sited at the R4 position.

The configuration of the array is shown in Figure E1 and the site coordinates and altitudes listed in Table E1.

Yellowknife (YKA)

The array is situated on the Northern shore of the Great Slave Lake, Canada. The configuration is shown in Figure E1 and the relative coordinates of the site positions used in the experiment are given in Table E2. The array has recently been re-surveyed with a precision of 4m. using low level air photography. The new co-ordinates are significantly different from those shown in Table E2 (the average site being moved approximately 75 m north-west). Seismologically the shift is negligible for slowness measurements, except very short range crustal measurements (Weichert and Manchee, 1969).

The Precambrian granite in the vicinity of the array is thought to be very uniform for teleseismic rays (Weichert and Whitham, 1969).

Warramunga

The array is sited approximately 300 miles north of Alice Springs. The geometry is shown in Fig E2 , and the relative coordinates given in Table E3. The seismometer sites are situated on granite outcrops and the microseismic noise level is low. Slowness and azimuth measurements made at the array are perturbed by variations in the structure under the array (Cleary, Wright and Muirhead 1968; Underwood 1967).

Gauribidanur

The array is situated approximately 50 Km north of Bangalore. Data was utalised from 10 sites, before the array was extended to 20 seismometers. The array is shown in Fig E2 , and the coordinates given in Table E4. The array is situated on deep rooted granite gneiss with relatively shallow weathering. Noise levels are low (approximately 1.2×10^{-5} cm/sec at 0.75 Hz).

TABLE E1

ESKDALEMUIR ARRAY (EKA)

GEOGRAPHIC COORDINATES OF INTERSECTION

LONGITUDE 55.332 DEGS
LATITUDE -3.159 DEGS

CARTESIAN COORDINATES AND ALTITUDES OF SEISMOMETERS

SITE	X KMS	Y KMS	ALTITUDE FEET
B1	-1.049	-2.659	901
B2	-.717	-1.829	1028
B3	-.521	-.952	1025
B4	-.056	-.168	981
B5	.276	.662	1017
B6	.606	1.493	1108
B7	.937	2.323	1431
B8	1.313	3.281	1330
B9	1.598	3.984	1306
B10	1.929	4.814	1074
R1	-1.174	.471	1167
R2	-.342	.136	1148
R3	.489	-.199	1055
R4	1.320	-.534	1108
R5	2.151	-.869	1007
R6	2.983	-1.204	1297
R7	3.814	-1.540	1144
R8	4.645	-1.874	1376
R9	5.477	-2.210	1406
R10	6.308	-2.545	1258

TABLE E2

YELLOWKNIFE ARRAY (YKA)

GEOGRAPHIC COORDINATES OF INTERSECTION

LONGITUDE 62.493 DEGS
LATITUDE -114.605 DEGS

CARTESIAN COORDINATES AND ALTITUDES OF SEISMOMETERS

SITE	X KMS	Y KMS	ALTITUDE FEET
B1	20.000	10.000	565
B2	20.000	12.500	590
B3	20.000	15.000	615
B4	20.000	17.500	633
B5	20.000	20.000	645
B6	20.000	22.500	664
B7	20.000	25.000	670
B8	20.000	27.500	649
B9	20.000	30.000	699
B10	20.000	32.500	726
R1	2.500	20.000	557
R2	5.000	20.000	574
R3	7.500	20.000	580
R4	10.000	20.000	568
R5	12.500	20.000	600
R6	15.000	20.000	630
R7	17.500	20.000	652
R8	20.000	20.000	645
R9	22.500	20.000	659
R10	25.000	20.000	672

TABLE E3

WARRAMUNGA ARRAY (WRA)

GEOGRAPHIC COORDINATES OF INTERSECTION

LONGITUDE -19.948 DEGS
LATITUDE 134.358 DEGS

CARTESIAN COORDINATES AND ALTITUDES OF SEISMOMETERS

SITE	X KMS	Y KMS	ALTITUDE FEET
B1	-.310	-1.476	0
B2	.183	.373	0
B3	.638	2.558	0
B4	1.025	4.724	0
B5	1.762	7.519	0
B6	1.863	10.095	0
B7	3.150	11.662	0
B8	3.291	14.635	0
B9	3.623	17.132	0
B10	4.554	19.816	0
R1	-1.033	.391	0
R2	1.552	-.140	0
R3	3.934	-.264	0
R4	5.998	-.465	0
R5	8.052	-1.314	0
R6	10.998	-.846	0
R7	13.263	-1.004	0
R8	15.826	-1.074	0
R9	17.334	-1.281	0
R10	20.016	-1.502	0

TABLE E4

GAURIBIDANUR ARRAY (GBA)

GEOGRAPHIC COORDINATES OF INTERSECTION

LONGITUDE 13.607 DEGS
LATITUDE 77.403 DEGS

CARTESIAN COORDINATES AND ALTITUDES OF SEISMOMETERS

SITE	X KMS	Y KMS	ALTITUDE FEET
B1	.000	.000	2250
B2	-1.503	-1.844	2250
B3	-2.856	-4.302	2325
B4	-3.908	-6.454	2375
B5	-5.412	-8.297	2550
R1	-1.202	.615	2260
R2	-3.457	1.844	2240
R3	-5.411	3.534	2250
R4	-7.515	4.456	2300
R5	-9.468	5.992	2240

APPENDIX F

List of first and second order azimuthal site corrections derived from the Multiple-Array Slowness Analysis program to correct for the sub-array structure beneath each seismometer at each array.

The first order corrections are for all events $\Delta = 30^{\circ} - 104^{\circ}$.

The second order corrections were derived in two groups: (1) for all events $\Delta = 30^{\circ} - 104^{\circ}$ and (2) events $\Delta = 30^{\circ} - 58^{\circ}$.

ESKDALEMUIR ARRAY (EKA)

FIRST ORDER AZIMUTHAL SITE CORRECTIONS. (DELTA = 30 - 104 DEGS
EQUATION IS

R = A + B*SIN(AZIMUTH+E) SECS.

WHERE

SITE	A	B	E
B1	-.01830	.01666	-87.38
B2	-.00666	.00548	-52.52
B3	-.02672	.00947	77.90
B4	.00236	.00773	129.63
B5	-.00324	.00475	-140.66
B6	-.02086	.01210	149.75
B7	.03141	.01307	65.43
B8	.02868	.02187	68.59
B9	.02213	.01995	86.12
B10	-.00476	.02267	140.32
R1	-.00218	.01155	154.46
R2	-.00358	.01147	140.80
R3	-.00939	.01029	61.90
R4	.01743	.00420	58.71
R5	-.04924	.01598	-66.90
R6	.01297	.00921	-12.37
R7	-.00154	.00719	-45.65
R8	.01723	.00644	-84.45
R9	-.01793	.01708	67.83
R10	-.05661	.11148	70.08

ESKDALEMUIR ARRAY (EKA)

SECOND ORDER AZIMUTHAL SITE CORRECTIONS. (DELTA = 30 - 58 DEGS

EQUATION IS

R = A + B*SIN(AZIMUTH+E) + F*SIN(2*AZIMUTH+G) SECS

WHERE

SITE	A	B	E	F	G
B1	14.01201	14.91823	-170.04		
B2	5.11962	5.44457	-170.24		
B3	.23006	.27464	-168.56		
B4	.43207	.46215	-168.45		
B5	-.23101	.23535	9.31		
B6	-.20290	.19030	18.53		
B7	.29627	.27353	-167.10		
B8	-.10849	.16053	2.36		
B9	-4.51327	4.83890	9.14		
B10	-.91983	.95376	8.70		
R1	.02632	.05342	-128.30		
R2	.03392	.04730	-144.74		
R3	.23050	.24901	-170.11		
R4	.03125	.01172	-45.00		
R5	-.05596	.03054	56.18		
R6	.10271	.07625	-174.18		
R7	-.17257	.19050	10.30		
R8	.75137	.78450	-173.79		
R9	-.25069	.26165	19.06		
R10	.44300	.48087	179.96		

INSUFFICIENT DATA FOR F AND G TERMS

ESKDALEMUIR ARRAY (EKA)

SECOND ORDER AZIMUTHAL SITE CORRECTIONS. (DELTA = 30 - 104 DEG

EQUATION IS

R = A + B*SIN(AZIMUTH+E) + F*SIN(2*AZIMUTH+G) SECS

WHERE

SITE	A	B	E	F	G
B1	-.02879	.00350	154.78	.01076	-68.29
B2	-.01813	.01599	95.61	.01269	-69.10
B3	-.03527	.02464	92.95	.00966	-78.28
B4	.00901	.00703	-115.87	.00770	89.86
B5	-.00505	.00632	-169.77	.00517	4.88
B6	-.02433	.01636	120.36	.01067	-142.68
B7	.03970	.01520	7.15	.02116	168.07
B8	.03167	.02803	45.49	.02628	-174.73
B9	.03564	.01523	-3.52	.02726	162.22
B10	.00384	.00605	166.41	.02182	161.09
R1	.01534	.02631	-104.20	.01820	93.71
R2	.00116	.00573	-175.42	.00634	135.47
R3	-.02125	.03109	87.66	.01372	-91.50
R4	.02834	.01844	-64.40	.01244	114.07
R5	-.04901	.01788	-86.88	.01341	13.58
R6	.02100	.02001	-62.67	.01154	64.43
R7	-.01763	.02355	93.92	.01818	-74.23
R8	-.00682	.03417	111.09	.02877	-52.33
R9	-.02125	.02391	124.11	.03102	-18.21
R10	.24836	.55267	-102.63	.32311	32.03

YELLOWKNIFE ARRAY (YKA)

FIRST ORDER AZIMUTHAL SITE CORRECTIONS. (DELTA = 30 - 104 DEGS
EQUATION IS

R = A + B*SIN(AZIMUTH+E) SECS.

WHERE

SITE	A	B	E
B1	.01597	.00227	153.72
B2	.01526	.01221	-107.95
B3	-.00352	.00586	-144.22
B4	.00383	.00597	115.07
B5	-.01540	.00289	51.24
B6	-.01178	.00533	-56.46
B7	-.01316	.01073	-41.70
B8	-.01329	.00916	-29.83
B9	.00166	.00801	-28.81
B10	-.00395	.00712	-6.02
R1	.01535	.00537	154.73
R2	.01018	.00317	-140.17
R3	.02121	.00278	171.21
R4	.00022	.00501	82.12
R5	.00166	.00136	-43.70
R6	.00986	.00404	-13.63
R7	.00023	.01037	5.97
R8	-.01540	.00289	51.24
R9	-.00074	.01364	156.49
R10	-.03350	.02237	132.58

YELLOWKNIFE ARRAY (YKA)

SECOND ORDER AZIMUTHAL SITE CORRECTIONS. (DELTA = 30 - 58 DEGS

EQUATION IS

R = A + B*SIN(AZIMUTH+E) + F*SIN(2*AZIMUTH+G) SECS

WHERE

SITE	A	B	E	F	G
B1	.02008	.01675	30.00	.01292	-81.67
B2	.02664	.00480	38.98	.00430	69.87
B3	.00763	.01745	-103.74	.01867	8.19
B4	.01347	.02052	21.94	.02046	-65.34
B5	-.01015	.02173	-149.91	.02820	41.05
B6	-.00089	.02453	-93.92	.02587	-12.89
B7	-.00978	.02537	-78.17	.02017	-35.90
B8	-.01308	.01398	-70.91	.00896	-32.43
B9	.00580	.01293	.65	.01487	-66.68
B10	-.00810	.00965	1.78	.00877	-170.29
R1	-.01418	.05022	178.99	.05578	133.02
R2	-.01153	.01219	72.20	.04464	167.42
R3	.01182	.01336	68.84	.03372	-172.48
R4	-.00765	.02217	129.00	.01873	145.87
R5	.00299	.01941	55.86	.00997	-163.10
R6	.02862	.07024	19.80	.04591	-100.63
R7	.00576	.00595	-1.35	.01629	14.69
R8	-.01015	.02173	-149.91	.02820	41.05
R9	-.00763	.03300	-173.66	.02532	69.42
R10	-.03649	.01199	142.10	.01956	-40.94

YELLOWKNIFE ARRAY (YKA)

SECOND ORDER AZIMUTHAL SITE CORRECTIONS. (DELTA = 30 - 104 DEG

EQUATION IS

R = A + B*SIN(AZIMUTH+E) + F*SIN(2*AZIMUTH+G) SECS

WHERE

SITE	A	B	E	F	G
B1	.01718	.00380	51.60	.00515	-79.80
B2	.01610	.01556	-118.11	.00489	49.58
B3	-.00330	.01720	-149.01	.01178	67.67
B4	.00430	.01583	-173.47	.01562	66.31
B5	-.01362	.01349	-158.03	.01815	53.59
B6	-.01108	.00825	-108.00	.00675	60.02
B7	-.01218	.01036	-50.99	.00324	17.50
B8	-.01299	.01014	-22.41	.00160	-86.95
B9	.00477	.02176	5.59	.01587	-95.42
B10	-.00605	.00892	4.72	.00557	-170.30
R1	.00909	.02009	45.93	.02741	-136.46
R2	.00549	.01338	27.16	.02354	-124.45
R3	.01685	.00306	69.05	.01197	-163.64
R4	-.00005	.01974	40.80	.01641	-111.77
R5	.00309	.01028	20.19	.00981	-91.42
R6	.01226	.02263	24.33	.01917	-87.16
R7	.00392	.00465	-55.26	.01331	33.24
R8	-.01362	.01349	-158.03	.01815	53.59
R9	.00006	.02934	-173.44	.01967	62.35
R10	-.03411	.02734	154.03	.01082	73.38

WARRAMUNGA ARRAY (WRA)

FIRST ORDER AZIMUTHAL SITE CORRECTIONS. (DELTA = 30 - 104 DEGS
EQUATION IS

R = A + B*SIN(AZIMUTH+E) SECS.

WHERE

SITE	A	B	E
B1	.02082	.02112	135.91
B2	.03757	.02768	128.58
B3	.01443	.02477	151.94
B4	-.00077	.01681	164.09
B5	-.01102	.01139	21.55
B6	-.03151	.01225	16.17
B7	-.03840	.02230	5.89
B8	-.05994	.03215	9.34
B9	-.03252	.03942	8.72
B10	-.05959	.04581	18.03
R1	.00946	.01774	103.29
R2	.03172	.03301	138.10
R3	.03025	.03347	171.83
R4	.03341	.03224	-169.27
R5	.02318	.01294	-145.35
R6	.02418	.01965	-119.59
R7	.00536	.02666	-94.60
R8	.02086	.03686	-81.38
R9	-.00219	.03084	-86.04
R10	.00584	.04183	-73.40

WARRAMUNGA ARRAY (WRA)

SECOND ORDER AZIMUTHAL SITE CORRECTIONS. (DELTA = 30 - 58 DEGS

EQUATION IS

R = A + B*SIN(AZIMUTH+E) + F*SIN(2*AZIMUTH+G) SECS

WHERE

SITE	A	B	E	F	G
B1	.00171	.01618	46.29	.01829	104.67
B2	.02478	.01257	113.76	.01182	77.95
B3	.01650	.04136	-160.33	.02265	-10.44
B4	.00572	.04207	-147.23	.03123	-16.35
B5	.00205	.02248	-139.97	.03357	-29.20
B6	-.01819	.02983	-166.72	.05412	-37.46
B7	-.02143	.02136	-124.72	.04665	-22.82
B8	-.05426	.01568	16.91	.02853	-43.80
B9	.04296	.08579	-145.77	.08718	-31.73
B10	-.06845	.04876	31.65	.02169	-84.97
R1	-.00279	.01208	45.99	.01192	118.62
R2	.00884	.01599	56.11	.03087	119.75
R3	.02368	.02004	164.88	.01557	144.61
R4	.02523	.00834	-152.85	.02337	130.98
R5	.02106	.00543	38.32	.02148	144.77
R6	.01030	.02129	29.13	.02598	145.82
R7	.01383	.00604	-156.47	.03644	-171.29
R8	.02996	.00330	-134.76	.02609	-156.47
R9	.00817	.00065	-175.16	.03184	-179.66
R10	.00484	.02156	16.91	.02971	-178.92

WARRAMUNGA ARRAY (WRA)

SECOND ORDER AZIMUTHAL SITE CORRECTIONS. (DELTA = 30 - 104 DEG

EQUATION IS

R = A + B*SIN(AZIMUTH+E) + F*SIN(2*AZIMUTH+G) SECS

WHERE

SITE	A	B	E	F	G
B1	.02163	.02169	141.41	.00267	15.89
B2	.03735	.02485	132.38	.00661	77.73
B3	.02020	.03320	166.59	.01256	-14.08
B4	.00446	.02888	167.73	.01710	-42.19
B5	-.00149	.01148	152.59	.02848	-39.71
B6	-.01442	.02324	171.15	.04489	-40.18
B7	-.02957	.00412	-.67	.02385	-26.32
B8	-.05401	.02179	15.70	.01609	-41.10
B9	-.02407	.02293	21.14	.02536	-44.10
B10	-.05800	.04317	25.63	.01060	-66.03
R1	.01023	.01762	108.97	.00213	-5.30
R2	.03134	.03179	140.39	.00409	70.21
R3	.02591	.02669	162.40	.00929	170.01
R4	.03181	.02861	-169.28	.00448	158.56
R5	.01990	.00782	-109.89	.01095	153.91
R6	.02189	.01996	-106.04	.00898	115.95
R7	-.00621	.03416	-42.50	.03341	157.44
R8	.01165	.04476	-52.38	.02684	149.78
R9	-.02553	.06094	-30.89	.05860	140.09
R10	-.00358	.05689	-49.50	.03307	139.25

GAURIBIDANUR ARRAY (GBA)

FIRST ORDER AZIMUTHAL SITE CORRECTIONS. (DELTA = 30 - 104 DEGS
EQUATION IS

R = A + B*SIN(AZIMUTH+E) SECS.

WHERE

SITE	A	B	E
B1	-.01688	.01368	-15.65
B2	-.01429	.02498	27.99
B3	-.00078	.00205	51.40
B4	.00106	.01178	-3.17
B5	-.01834	.01976	94.36
R1	.00070	.01281	16.56
R2	-.00303	.01255	-34.95
R3	.02359	.02808	-155.73
R4	.02304	.02708	-142.09
R5	.00437	.02703	168.75

GAURIBIDANUR ARRAY (GBA)

SECOND ORDER AZIMUTHAL SITE CORRECTIONS. (DELTA = 30 - 58 DEGS

EQUATION IS

R = A + B*SIN(AZIMUTH+E) + F*SIN(2*AZIMUTH+G) SECS

WHERE

SITE	A	B	E	F	G
B1	-.01124	.01444	-70.70	.00381	-74.04
B2	-.01451	.00906	33.45	.01007	-62.03
B3	.00513	.02140	-152.45	.01654	-46.90
B4	-.00568	.00790	22.54	.00887	-58.98
B5	-.00119	.01689	-142.84	.02269	24.48
R1	-.00445	.01384	35.67	.00756	-140.30
R2	-.00208	.02648	-30.81	.02138	126.32
R3	.01621	.00999	129.05	.01687	159.86
R4	-.03265	.07389	55.32	.04405	-177.24
R5	-.00263	.02720	118.09	.00636	171.46

GAURIBIDANUR ARRAY (GBA)

SECOND ORDER AZIMUTHAL SITE CORRECTIONS. (DELTA = 30 - 104 DEG

EQUATION IS

$$R = A + B*SIN(AZIMUTH+E) + F*SIN(2*AZIMUTH+G) \text{ SECS}$$

WHERE

SITE	A	B	E	F	G
B1	-.01362	.00706	-74.97	.01350	-43.11
B2	-.00882	.01148	13.69	.01312	-21.98
B3	.00220	.01211	-178.34	.01633	-50.52
B4	.00856	.01393	-71.61	.00913	11.78
B5	-.00984	.00891	147.59	.00977	29.95
R1	.00207	.00867	14.17	.00446	-39.53
R2	-.00613	.02318	-13.19	.01467	130.90
R3	.01651	.01446	177.74	.01423	166.35
R4	.00474	.00921	30.03	.02615	156.11
R5	-.00034	.01948	143.76	.01264	148.71

APPENDIX G

List of all events used to compute slowness. Latitudes, longitudes and depths were taken from USCGS PDE cards, and the distance and azimuth of each event relative to the arrays calculated using GEDESS (Young and Gibbs, 1968).

EVENTS RECORDED AT ESKDALEMUIR

	DATE	DELTA DEGS.	AZ. DEGS.	DEPTH KMS.	LAT. DEGS	LONG. DEGS.
1	26.07E67	32.8	.400	33	39.5	40.4
2	19.08E66	33.8	99.600	26	39.2	41.7
3	11.01E67	39.7	1.700	34	34.1	45.7
4	21.07E66	47.4	60.400	0	49.8	78.1
5	05.08E66	47.4	60.400	0	49.8	78.1
6	18.12E66	47.4	60.400	0	49.8	78.1
7	25.03E67	47.4	60.400	0	49.8	78.1
8	20.04E67	47.4	60.400	0	49.8	78.1
9	15.07E67	47.4	60.400	0	49.8	78.1
10	30.10E67	47.4	60.400	0	49.8	78.1
11	08.12E67	47.4	60.400	0	49.8	78.1
12	18.09E66	49.2	99.600	16	27.8	54.3
13	20.02E67	56.7	77.700	24	33.7	75.3
14	05.01E67	59.8	48.200	33	48.1	102.8
15	20.01E67	59.9	48.300	33	48.0	102.9
16	30.08E66	60.4	41.100	36	61.3	-147.5
17	07.10E66	60.5	42.600	56	61.6	-150.1
18	06.03E66	61.2	75.400	44	31.6	80.5
19	15.08E66	62.5	78.700	50	28.7	78.9
20	27.06E66	62.9	76.500	37	29.7	80.9
21	16.12E66	63.0	76.500	9	29.6	81.0
22	16.04E66	65.5	42.700	33	57.0	-153.6
23	07.02E67	66.3	44.700	67	56.7	-157.2
24	01.07E67	68.7	44.500	33	54.4	-158.0
25	16.01E66	69.8	6.800	15	54.9	165.8
26	01.06E67	70.4	49.000	60	53.7	-165.6
27	15.09E67	70.6	69.900	57	27.4	91.8
28	01.06E67	70.4	49.000	60	53.7	-165.6
29	15.09E67	70.6	69.900	57	27.4	91.8
30	26.09E66	71.0	69.200	33	27.5	92.6
31	14.03E67	71.2	67.400	24	28.4	94.3
32	19.06E67	71.5	49.600	33	52.7	-166.9
33	02-06E66	71.7	9.600	0	37.4	-116.6
34	30.06E66	71.7	9.600	0	37.4	-116.6
35	18.10E67	71.7	9.600	0	37.4	-116.6
36	14.07E66	71.8	3.600	29	53.1	171.1
37	19.01E68	72.2	9.600	0	37.4	-166.6
38	13.09E67	72.3	2.800	34	52.7	172.5
39	27.05E67	73.1	.500	34	51.9	176.1
40	04/07E66	73.3	58.000	13	51.7	179.9
41	29.10E65	73.6	58.000	0	51.4	179.2
42	29.04E67	73.6	56.800	50	51.4	-178.3
43	11.05E66	74.7	14.000	13	48.9	156.2
44	03.03E66	75.0	15.400	45	48.3	154.3
45	28.09E66	75.0	63.600	33	27.4	100.1
46	09.04E66	77.0	68.100	30	9.6	-84.1
47	01.04E67	77.0	17.700	40	45.8	151.8
48	08/09E66	77.2	18.700	32	45.4	150.5
49	10.08E67	77.2	18.800	37	45.4	150.3
50	18.08E66	77.3	77.200	76	14.6	-91.7
51	07.08E66	78.6	24.900	66	42.3	143.0
52	12.11E66	79.3	24.300	33	41.8	144.1
53	09.12E65	79.8	85.500	57	17.3	-100.0
54	04.11E67	83.6	55.700	99	-2.8	-77.7
55	04.11E67	83.6	55.700	99	-2.8	-77.7
56	28.05E66	88.1	47.800	33	24.4	122.5
57	23.03E66	88.7	47.900	51	23.8	122.8
58	12.04E67	91.2	79.100	55	5.3	96.5
59	03.09E67	91.2	53.100	38	-10.6	-79.8
60	21.08E67	92.2	80.600	33	3.6	95.8
61	11.05E67	93.4	38.700	67	-20.3	-68.5

EVENTS RECORDED AT YELLOWKNIFE

	DATE	DELTA DEGS.	AZ. DEGS.	DEPTH KMS.	LAT. DEGS	LONG. DEGS.
1	28/01Y67	30.2	76.200	50	52.4	-169.4
2	28.01Y67	30.3	75.900	32	52.3	-169.3
3	07/08Y66	30.7	79.800	33	31.8	-114.5
4	07.08Y66	32.3	75.100	39	50.6	-171.3
5	22.07Y66	32.6	78.400	56	51.7	-173.5
6	23.11Y67	32.8	16.900	10	80.2	-1.0
7	11.06Y66	34.9	82.000	60	51.6	-178.4
8	27.11Y66	34.9	17.500	33	78.5	6.4
9	29.04Y67	35.0	81.700	50	51.4	-178.3
10	04/07Y66	35.6	83.400	13	51.7	179.9
11	04.07Y66	37.1	86.100	28	51.8	176.4
12	27.05Y67	37.2	86.400	34	51.9	176.1
13	17.08Y66	37.4	87.700	32	52.3	174.9
14	02.06Y66	37.8	85.500	41	51.1	176.0
15	13.09Y67	38.2	89.800	34	52.7	172.5
16	27.10Y66	44.2	4.300	0	73.4	54.8
17	13/04Y67	44.9	99.200	50	52.1	157.6
18	13.04Y67	45.1	60.500	86	18.5	-100.2
19	25.09Y66	45.2	61.400	60	18.3	-100.8
20	21.06Y66	46.4	97.700	14	50.1	157.8
21	18.08Y66	50.5	50.800	76	14.6	-91.7
22	21/11Y66	51.2	98.100	40	46.7	152.5
23	01.04Y67	52.2	98.000	40	45.8	151.8
24	01/04Y67	52.3	97.900	40	45.7	151.8
25	20/03Y67	52.6	98.100	51	45.6	151.4
26	08.09Y66	53.1	98.600	32	45.4	150.5
27	10.08Y67	53.2	98.700	37	45.4	150.3
28	07.12Y66	53.5	96.900	26	44.3	151.7
29	18.01Y67	53.7	25.600	11	56.6	120.8
30	22.09Y67	54.3	98.800	60	44.5	149.4
31	12.10Y66	55.1	45.300	43	11.2	-86.2
32	03.10Y67	55.5	45.100	21	10.9	-85.9
33	19.03Y66	56.7	.600	11	43.3	145.8
34	09.04Y66	57.2	43.500	30	9.6	-84.1
35	19.09Y67	57.2	.800	84	43.0	145.2
36	04/11Y67	57.2	1.900	30	43.5	144.1
37	09.04Y66	57.2	43.500	30	9.6	-84.1
38	19.09Y67	57.2	.800	84	43.0	145.2
39	04/11Y67	57.2	1.900	30	43.5	144.1
40	27.03Y66	58.1	42.900	40	8.9	-83.4
41	24/12Y67	58.1	15.600	20	17.4	-61.3
42	24.12Y67	58.2	15.400	24	17.4	-61.1
43	12.11Y66	58.7	.900	33	41.9	144.1
44	24.01Y67	59.9	2.200	69	41.4	141.9
45	17.01Y67	62.4	.300	44	38.3	142.1
46	04.11Y67	63.4	.100	46	37.4	141.6
47	03.04Y66	64.3	.400	68	36.7	140.8
48	08.01Y66	64.8	2.600	10	37.3	138.3
49	05/01Y67	65.4	33.400	33	48.4	103.1
50	05.01Y67	65.8	33.500	33	48.1	102.8
51	20.01Y67	65.9	33.400	33	48.0	102.9
52	09.02Y67	66.3	35.800	58	2.9	-74.9
53	27.11Y65	67.5	98.500	74	32.9	140.6
54	21.11Y65	67.6	51.100	0	49.8	78.1
55	20.03Y66	67.6	51.100	0	49.8	78.1
56	21.04Y66	67.6	51.100	0	49.8	78.1
57	29.06Y66	67.6	51.100	0	49.8	78.1
58	18.12Y66	67.6	51.100	0	49.8	78.1
59	20-04Y67	67.6	51.100	0	49.8	78.1
60	28.05Y67	67.6	51.100	0	49.8	78.1
61	26.11Y65	68.3	97.900	64	32.1	140.9
62	10.06Y66	69.3	34.700	33	45.1	99.7
63	09.06Y66	69.5	95.700	12	30.1	142.2
64	25.06Y66	70.0	95.600	49	29.6	142.1
65	12/11Y65	70.0	97.600	40	30.5	140.2
66	30.11Y67	70.3	34.300	29	41.5	20.5
67	23.05Y66	70.6	97.600	28	30.0	139.8
68	25.06Y66	70.0	95.600	49	29.6	142.1
69	12.11Y65	70.0	97.600	40	30.5	140.2
70	30.11Y67	70.3	34.300	29	41.5	20.5
71	23.05Y66	70.6	97.600	28	30.0	139.8
72	04.11Y67	70.9	40.600	99	-2.8	-77.7
73	08/02Y66	71.5	30.900	33	41.4	25.1
74	22.03Y66	72.7	20.600	11	37.5	115.0
75	05.02Y66	72.8	34.000	38	39.2	22.0
76	22.07Y67	73.5	26.800	4	40.7	30.8
77	02.03Y66	73.7	14.900	24	43.0	45.8
78	05.01Y66	74.9	87.900	34	21.8	146.6
79	28.02Y66	75.1	5.100	33	29.2	130.1
80	20.04Y66	75.2	13.200	19	41.7	48.2
81	29.03Y66	75.2	92.700	79	23.7	142.1
82	10.02Y66	75.9	87.700	43	20.8	146.3
83	06.04Y67	76.1	86.600	22	20.1	147.2
84	05.04Y67	76.2	86.500	50	20.0	147.2
85	05/04Y67	76.2	86.600	50	20.0	147.1
86	25.04Y66	76.6	57.000	33	41.2	69.3
87	07.03Y66	77.0	18.700	13	39.1	41.7

88	20/04Y66	77.4	86.200	55	18.8	146.9
89	13.04Y67	77.4	5.400	38	27.3	128.7
90	14.02Y66	78.1	31.300	46	35.0	27.2
91	28.01Y66	78.4	53.900	20	39.3	73.1
92	11.04Y66	79.0	55.900	29	38.9	70.6
93	25.11Y65	80.1	66.200	29	-17.1	-100.4
94	16.11Y65	80.4	7.600	77	25.4	125.2
95	10.07Y66	81.5	7.100	28	24.2	125.2
96	30.08Y67	82.0	30.500	3	31.7	100.3
97	20.05Y66	82.0	84.600	66	13.9	146.1
98	14.07Y67	83.6	40.100	99	-14.9	-73.4
99	14.07Y67	83.6	40.100	99	-14.9	-73.4
100	06.11Y65	84.3	79.300	33	-22.1	-113.8
101	03.11Y65	84.5	79.500	12	-22.3	-114.1
102	26.08Y67	85.9	89.500	33	12.2	140.7
103	28/09Y66	86.2	29.500	33	27.4	100.1
104	14.03Y67	86.5	34.700	24	28.4	94.3
105	13.02Y66	86.7	26.500	33	26.1	103.2
106	05.02Y66	86.7	26.600	15	26.1	103.1
107	27.06Y66	87.3	46.500	37	29.7	80.9
108	16.12Y66	87.4	46.400	9	29.6	81.0
109	24.01Y66	87.9	56.300	12	29.9	69.7
110	15.09Y67	88.0	36.700	57	27.4	91.8
111	07.02Y66	88.0	56.600	33	29.9	69.7
112	21/06Y65	89.4	8.300	28	28.1	56.0
113	07.11Y67	89.5	35.400	43	-14.9	-173.0
114	18.09Y66	89.6	9.800	16	27.9	54.3
115	14.06Y67	90.0	35.800	11	-15.2	-173.6
116	01.01Y67	90.1	35.800	33	-15.3	-173.6
117	11.05Y67	90.2	37.400	67	-20.3	-68.5
118	03.02Y66	90.4	8.600	69	16.6	120.9
119	25.12Y67	90.7	39.500	53	-21.5	-70.4
120	21.12Y67	91.1	39.300	33	-21.8	-70.0
121	19.01Y67	91.7	40.600	18	-14.8	-178.8
122	27.07Y66	93.3	40.300	35	-24.2	-70.3
123	18.05Y67	94.1	.500	32	10.0	126.1
124	21.06Y67	94.2	40.800	23	-25.2	-70.5
125	09.03Y67	94.3	55.500	30	-10.6	164.3
126	11.03Y67	94.5	55.500	49	-10.7	166.2
127	10.08Y66	95.1	35.400	96	-20.1	-175.3
128	21.08Y66	95.2	99.400	67	8.5	126.7
129	13.03Y67	95.4	25.000	7	19.7	98.9
130	31.01Y66	95.7	35.400	43	-24.8	-64.4
131	15.06Y66	96.3	60.200	33	-10.2	161.1
132	27.11Y65	96.5	61.700	51	-9.7	159.7
133	13.01Y67	96.6	59.800	32	-10.6	161.4
134	28.09Y67	96.7	68.700	44	-6.6	153.4
135	27.12Y67	96.9	34.000	33	-22.3	-174.8
136	15.11Y67	97.3	42.500	15	-28.7	-71.2
137	17.02Y67	98.3	33.800	19	-23.7	-175.2
138	23/12Y66	99.5	73.000	43	-7.1	148.3
139	14.12Y66	99.5	78.000	74	-4.8	143.9
140	10.04Y66	99.9	43.400	64	-31.5	-71.2
141	08.09Y66	100.0	95.300	96	2.4	128.4
142	13.12Y67	100.8	49.500	51	-19.1	168.7
143	08.03Y66	101.3	96.900	33	1.9	126.4
144	18/08Y66	103.6	97.300	33	-.1	125.1
145	18.08Y66	103.7	97.300	56	-.2	125.1

EVENTS RECORDED AT WARRAMUNGA

	DATE	DELTA DEGS.	AZ. DEGS.	DEPTH KMS.	LAT. DEGS	LONG. DEGS.
1	02.01W67	30.7	79.200	33	-11.7	165.1
2	01/01W67	31.1	80.900	33	-12.4	165.8
3	01-01W67	31.2	78.300	33	-11.1	165.5
4	01.06W66	31.4	83.900	48	-13.8	166.6
5	23.11W66	31.4	86.000	48	-14.9	166.9
6	07/06W66	31.5	9.900	50	11.3	139.6
7	03.05W66	31.5	14.100	30	10.9	141.8
8	29.06W66	31.5	83.900	35	-13.8	166.7
9	01-06W66	31.6	86.700	93	-15.2	167.2
10	11.03W67	32.0	78.100	49	-10.7	166.2
11	09.03W67	32.1	78.100	59	-10.7	166.3
12	06.06W66	32.3	86.400	37	-14.9	167.8
13	28.10W66	32.3	96.300	19	-20.1	168.8
14	17.05W67	32.5	86.900	36	-15.1	168.1
15	25.08W67	32.6	11.900	33	12.2	140.9
16	26*08W67	32.6	11.600	33	12.2	140.7
17	26+08W67	32.6	11.600	14	12.2	140.7
18	26-08W67	32.6	11.800	30	12.2	140.8
19	25.05W66	33.2	99.200	35	-21.6	169.9
20	26/08W66	33.3	.100	33	-22.1	170.0
21	05.04W67	33.5	73.200	33	-53.2	140.6
22	07.01W67	33.6	6.100	33	-48.8	112.7
23	12.09W66	33.8	1.900	49	-23.1	170.6
24	13.09W66	33.8	1.800	28	-23.0	170.6
25	22.08W66	33.8	.700	39	-22.4	170.6
26	15.08W66	35.4	37.700	14	13.3	121.3
27	20.05W66	35.6	19.900	66	13.9	146.1
28	23/05W66	35.6	20.400	39	13.8	146.4
29	26.10W66	35.7	37.400	51	13.5	121.0
30	25/05W66	38.4	55.000	33	-52.9	160.0
31	21.07W66	38.5	54.700	34	-52.8	160.3
32	20/05W66	41.1	42.100	96	19.6	122.0
33	27.06W66	41.2	25.300	54	-38.0	177.2
34	05/04W67	41.6	18.300	50	20.0	147.2
35	05-04W67	41.6	18.200	50	20.0	147.1
36	06.04W67	41.7	18.300	22	20.1	147.2
37	28.08W66	41.7	21.700	94	-35.8	178.5
38	10/02W66	42.2	17.600	33	20.7	146.9
39	27/10W66	43.4	15.700	29	22.2	145.9
40	27/10W66	43.4	15.700	29	22.2	145.9
41	26.08W66	44.7	9.300	59	-27.5	-177.3
42	23.08W66	44.8	45.400	37	23.8	123.2
43	10/07W66	45.3	48.400	58	24.8	125.3
44	07.06W66	45.4	44.700	41	24.2	122.5
45	29/06W66	45.4	44.700	33	24.2	122.5
46	05.05W66	45.5	44.900	60	24.4	122.6
47	25/10W67	45.5	44.400	67	24.3	122.2
48	28.05W66	45.6	44.800	33	24.4	122.5
49	30.06W66	45.6	44.400	47	24.4	122.2
50	25.10W67	45.7	44.500	65	24.5	122.2
51	26.11W67	48.4	54.900	33	28.6	130.0
52	23.05W66	49.9	6.200	28	30.0	139.8
53	03.04W66	56.7	6.200	68	36.7	140.8
54	04.11W67	57.4	6.800	46	37.4	141.6
55	28.09W66	57.6	23.600	33	27.4	100.1
56	03.04W66	56.7	6.200	68	36.7	140.8
57	04.11W67	57.4	6.800	46	37.4	141.6
58	28.09W66	57.6	23.600	33	27.4	100.1
59	17.01W67	58.4	7.200	44	38.3	142.1
60	07.03W66	59.8	42.000	33	37.2	114.8
61	22-03W66	59.8	42.300	40	37.3	115.1
62	22/03W66	59.9	42.400	33	37.5	115.1
63	22.03W66	60.0	42.300	11	37.5	115.0
64	30.08W67	60.9	26.900	3	31.7	100.3
65	24.01W67	61.4	6.500	69	41.4	141.9
66	14.03W67	61.7	19.900	24	28.4	94.3
67	26.09W66	62.1	18.000	33	27.5	92.6
68	12.11W66	62.1	8.200	33	41.8	144.1
69	11/11W67	62.5	73.500	33	-6.1	71.4
70	15.09W67	62.6	17.400	57	27.4	91.8
71	11.11W67	62.7	73.600	34	-6.0	71.3
72	19.09W67	63.4	8.900	84	43.0	145.2
73	19.03W66	63.8	9.300	11	43.3	145.8
74	04/11W67	63.8	7.900	30	43.5	144.1
75	15.08W67	64.0	21.600	33	31.1	93.7
76	10.08W67	66.6	12.200	37	45.4	150.3
77	08.09W66	66.7	12.300	32	45.4	150.5
78	20.03W67	67.1	12.900	51	45.6	151.4
79	01/04W67	67.2	13.200	40	45.7	151.8
80	01.04W67	67.3	13.100	40	45.8	151.8
81	04.06W66	68.1	13.400	27	46.5	152.5
82	10.12W67	70.1	98.100	33	17.7	73.9
83	10.12W67	70.1	98.100	33	17.7	73.9
84	18.12W66	71.2	12.400	25	29.6	81.0
85	27/06W66	71.3	12.500	40	29.7	81.0
86	27.06W66	71.3	12.500	37	29.7	80.9
87	06.03W66	72.7	13.800	44	31.6	80.5

88	20.01W67	73.3	38.500	33	48.0	102.9
89	06.12W66	73.3	16.800	27	50.1	159.8
90	23.10W66	73.9	16.000	28	51.0	159.2
91	05.08W66	74.0	14.200	55	32.6	79.6
92	23/10W66	74.0	16.000	33	51.1	159.2
93	19.04W66	75.9	15.200	62	53.1	159.3
94	30.08W66	76.0	41.300	33	51.7	104.4
95	20.11W66	77.4	44.200	33	55.1	129.4
96	22.07W66	77.5	24.800	33	42.8	84.5
97	08.06W66	79.4	21.500	20	53.1	171.1
98	08.11W66	79.5	22.900	41	52.4	173.0
99	02.06W66	79.6	25.200	41	51.1	176.0
100	13.09W67	79.6	22.500	34	52.7	172.5
101	01.08W66	80.2	6.700	33	29.9	68.9
102	01/08W66	80.3	6.700	33	30.0	68.7
103	27.05W67	80.3	24.700	34	51.9	176.1
104	29.10W65	81.2	26.600	0	51.4	179.2
105	04.07W66	81.7	26.700	13	51.7	179.9
106	29.04W67	82.2	27.700	50	51.4	-178.3
107	15.05W66	82.3	27.600	31	51.5	-178.4
108	11.06W66	82.3	27.500	60	51.6	-178.4
109	07.08W66	84.9	31.300	39	50.6	-171.3
110	29/06W66	85.4	27.400	0	49.9	78.1
111	21.07W66	85.4	27.400	0	49.8	78.1
112	05.08W66	85.4	27.400	0	49.8	78.1
113	19.10W66	85.4	27.400	0	49.8	78.1
114	18.12W66	85.4	27.400	0	49.8	78.1
115	20.04W67	85.4	27.400	0	49.8	78.1
116	28.05W67	85.4	27.400	0	49.8	78.1
117	15.07W67	85.4	27.400	0	49.8	78.1
118	16.09W67	85.4	27.400	0	49.8	78.1
119	17.10W67	85.4	27.400	0	49.8	78.1
120	30.10W67	85.4	27.400	0	49.8	78.1
121	18.01W67	87.6	31.000	37	52.5	-168.3
122	06.07W67	87.7	31.000	14	52.6	-168.2
123	19.06W67	88.4	31.400	33	52.7	-166.9
124	19.05W66	90.6	31.200	28	54.1	-164.1
125	01.07W67	93.8	32.800	33	54.4	-158.9
126	22.08W67	97.8	90.200	33	-60.8	-24.6
127	11.10W66	98.5	89.700	37	-60.3	-26.0
128	14.09W66	98.8	89.300	33	-60.1	-27.0
129	02.02W67	100.7	90.700	81	-57.9	-25.7

EVENTS RECORDED AT GAURIBIDANUR

	DATE	DELTA DEGS.	AZ. DEGS.	DEPTH KMS.	LAT. DEGS	LONG. DEGS.
1	26.02G67	33.5	24.300	33	-6.2	104.7
2	11.01G67	35.3	10.900	34	34.1	45.7
3	22.09G67	36.2	.900	0	49.8	78.1
4	19.10G66	36.2	.900	0	49.8	78.1
5	29.06G66	36.2	.900	0	49.8	78.1
6	21.04G66	36.2	.900	0	49.8	78.1
7	13.02G66	36.2	.900	0	49.8	78.1
8	20.03G66	36.2	.900	0	49.8	78.1
9	21.07G66	36.2	.900	0	49.8	78.1
10	18.12G66	36.2	.900	0	49.8	78.1
11	03.12G66	36.2	.900	0	49.8	78.1
12	17.10G67	36.2	.900	0	49.8	78.1
13	30.10G67	36.2	.900	0	49.8	78.1
14	13/03G67	37.4	84.700	7	19.7	38.9
15	05.01G67	40.3	26.300	33	48.1	102.8
16	19.08G66	40.5	15.700	26	39.2	41.7
17	20.08G66	41.1	15.400	37	39.3	40.9
18	04.01G67	41.2	74.700	33	20.3	120.0
19	24.11G67	41.3	19.500	80	-8.1	112.9
20	15.08G66	42.6	85.100	14	13.3	121.3
21	19.02G67	42.0	20.700	80	-9.2	113.1
22	26.10G67	43.5	68.700	63	24.5	122.2
23	25.10G67	43.5	68.700	65	24.5	122.2
24	23.02G67	43.7	69.200	48	24.2	122.5
25	28/05G66	43.8	68.900	33	24.4	122.5
26	26.10G67	43.5	68.700	63	24.5	122.2
27	25.10G67	43.5	68.700	65	24.5	122.2
28	23.02G67	43.7	69.200	48	24.2	122.5
29	28/05G66	43.8	68.900	33	24.4	122.5
30	05.05G66	43.9	68.900	60	24.4	122.6
31	23.08G66	44.4	69.800	37	23.8	123.2
32	11/01G67	44.4	4.400	23	-.1	120.1
33	30.03G67	45.0	21.100	33	-11.0	115.5
34	12.07G66	45.9	20.300	26	44.6	37.4
35	10.07G66	46.2	69.500	28	24.2	125.2
36	10/07G66	46.3	68.700	58	24.8	125.3
37	23/04G66	46.5	3.900	79	-.5	122.2
38	23.04G66	46.8	4.300	45	-.9	122.4
39	10.11G67	47.8	88.200	53	10.4	126.3
40	25.02G67	48.0	2.500	70	.0	123.9
41	06.06G66	48.1	89.200	45	9.6	126.4
42	06.04G66	48.2	90.200	69	8.9	126.4
43	07.04G66	48.3	67.100	46	26.1	127.4
44	21.08G66	48.6	90.600	67	8.5	126.7
45	22.07G67	48.7	12.700	4	40.7	30.8
46	07.10G66	48.8	96.000	86	4.5	126.1
47	18.08G66	49.2	2.300	56	-.2	125.1
48	23/02G67	49.3	67.200	30	26.1	128.5
49	26/10G67	49.3	2.200	42	-.2	125.2
50	13.03G67	49.4	97.000	35	3.6	126.5
51	13.04G67	49.6	65.700	38	27.3	128.7
52	26.11G67	50.9	64.200	33	28.6	130.0
53	02.12G66	51.1	96.900	92	3.2	128.1
54	08.09G66	51.6	97.800	96	2.4	128.4
55	02.01G67	54.0	46.500	33	-10.2	28.5
56	18.01G67	54.1	27.900	11	56.6	120.8
57	02.03G66	54.5	3.600	41	-2.9	129.8
58	01.05G67	55.5	9.000	15	39.7	21.3
59	19.03G67	55.9	7.900	60	-6.7	129.9
60	12.10G67	55.9	8.400	45	-7.1	129.8
61	23.06G67	56.1	6.600	85	-5.8	130.5
62	09.08G67	56.2	7.300	89	-6.4	130.4
63	30.11G67	56.4	10.900	29	41.5	20.5
64	25.05G66	56.9	7.000	39	-6.4	131.1
65	25.05G66	56.9	7.000	39	-6.4	131.1
66	22.08G66	58.3	.700	13	-1.8	134.2
67	08.11G67	59.2	4.700	33	-5.3	134.0
68	07.06G66	60.6	84.600	50	11.3	139.6
69	03.04G66	60.7	55.500	68	36.7	140.8
70	27.10G66	61.2	52.700	0	73.4	54.8
71	21.10G67	61.2	52.700	0	73.4	54.8
72	04.11G67	61.4	54.700	46	37.4	141.6
73	06.04G66	61.5	65.200	33	45.9	96.1
74	26.08G67	61.5	83.400	33	12.2	140.7
75	29.03G66	61.7	70.300	79	23.7	142.1
76	17.01G67	61.9	53.700	44	38.3	142.1
77	24.01G67	62.0	50.200	69	41.4	141.9
78	04.09G66	62.9	.000	39	-2.5	138.8
79	07.01G67	63.5	83.500	36	11.8	142.7
80	12.11G66	63.7	50.000	33	41.8	144.1
81	19.09G67	64.6	48.700	84	43.0	145.2
82	19/03G66	65.1	48.400	11	43.3	145.8
83	27/10G66	65.3	71.700	29	27.2	145.9
84	10.02G66	65.8	73.100	43	20.8	146.3
85	11.12G66	66.4	81.200	50	13.4	146.0
86	22.09G67	67.7	47.300	60	44.5	149.4
87	18/12G65	68.1	47.100	33	44.7	149.9

88	13/12G65	68.3	47.100	35	44.7	150.1
89	13.12G65	68.3	47.800	33	44.1	150.2
90	18.12G65	68.3	47.600	36	44.3	150.2
91	10.08G67	68.4	46.400	37	45.4	150.3
92	20.03G67	69.2	46.200	51	45.6	151.4
93	07.12G66	69.4	47.600	26	44.3	151.7
94	07/12G66	69.4	47.600	26	44.3	151.7
95	01.04G67	69.5	46.000	40	45.8	151.8
96	01/04G67	69.5	46.100	40	45.7	151.8
97	04.06G66	70.0	45.300	27	46.5	152.5
98	27.04G66	70.1	44.700	65	47.0	152.7
99	04.06G66	70.0	45.300	27	46.5	152.5
100	27.04G66	70.1	44.700	65	47.0	152.7
101	07-12G65	71.2	1.700	109	-6.4	146.3
102	03.03G66	71.2	43.400	45	48.3	154.3
103	05.02G66	71.8	41.400	98	50.2	155.1
104	11.12G65	71.9	41.100	110	50.5	155.3
105	11-05G66	72.5	42.600	28	49.0	156.2
106	11.05G66	72.5	42.700	13	48.9	156.2
107	11/05G66	72.6	42.800	33	48.8	156.3
108	28.01G66	73.0	39.900	107	51.6	157.0
109	08.04G66	73.4	40.300	47	51.2	157.7
110	21.06G66	73.5	41.500	14	50.1	157.8
111	08/04G66	73.5	40.300	48	51.2	157.8
112	18.10G67	74.1	49.700	33	79.8	2.4
113	23/10G66	74.4	40.500	38	51.0	159.2
114	19.04G66	74.4	38.300	62	53.1	159.3
115	22.10G66	75.9	36.100	59	55.2	162.0
116	22.02G66	75.9	99.200	28	-5.4	151.5
117	28.09G67	78.0	99.800	44	-6.6	153.4
118	16.01G66	78.1	36.200	15	54.9	165.8
119	14.07G66	78.9	8.200	33	-52.9	27.5
120	23.10G66	79.7	99.300	34	-6.5	155.2
121	26.09G67	80.4	99.700	94	-7.1	155.8
122	27.05G67	84.7	38.000	34	51.9	176.1
123	07.06G66	84.8	38.800	41	51.1	176.0
124	15/06G66	85.9	1.500	33	-10.2	160.7
125	15.06G66	86.1	1.600	31	-10.4	160.8
126	15-06G66	86.3	1.400	33	-10.2	161.1
127	13.01G67	86.7	1.700	32	-10.6	161.4
128	29.10G65	86.7	38.000	0	51.4	179.2
129	04.07G66	87.0	37.500	13	51.7	179.9
130	05.08G66	87.6	1.700	93	-10.9	162.3
131	11.06G66	88.0	37.200	60	51.6	-178.4
132	15.05G66	88.1	37.300	31	51.5	-178.4
133	29.04G67	88.2	37.400	50	51.4	-178.3
134	08.03G66	92.4	3.600	37	-13.9	166.6
135	07.08G66	92.6	36.500	39	50.6	-171.3
136	29.06G66	92.5	3.500	35	-13.8	166.7
137	18.01G67	93.4	33.900	37	52.5	-168.3
138	01.06G67	94.3	32.100	60	53.7	-165.6
139	16.02G66	94.5	7.000	31	-17.7	167.9
140	13.12G67	95.5	8.200	51	-19.1	168.7
141	22.12G65	97.3	24.200	50	58.4	-153.0
142	16.04G66	98.0	25.400	33	57.0	-153.6
143	12.09G66	98.1	11.800	49	-23.1	170.6

APPENDIX H

This Appendix contains three computer program listings written or adapted by the author.

The programs are written in FORTRAN IV for an IBM 7030 (Stretch) computer that has approximately an 80,000 word store.

1. Multi-Array Slowness Analysis Program.

2. Inversion of Phase Velocity-Distance Curve.

   This program uses the Wiechert-Herglotz integral method to invert the $dT/d\Delta$ against Δ curve to a velocity-depth curve.

3. Truncate.

   This program computes the cumulative distribution of residuals and checks the distribution against the normal curve. A description has already been given in Section 1.5.

MULTI-ARRAY SLOWNESS ANALYSIS PROGRAM

This section describes the program that computes the corrected slowness values $^{dT}/_{d_{\Delta k}}$ from the observed relative onset times.

The program consists of a MAIN program used to read in data and seventeen associated subroutines as well as subroutines used to graph output on a SC 4060 plotter and which have already been described elsewhere (Young & Douglas 1968). The programs are written in FORTRAN IV for an IBM 7030 (Stretch) computer and will accept data from up to 120 events recorded at 4 arrays that each possessing up to 20 seismometers.

1. INPUT

The first part of the input consists of cards containing standard tables:

(1) Students t tables for the 95% probability level.

(2) Travel time and slowness-distance tables at 1° intervals (from Herrin 1968).

(3) Jeffreys-Bullen (1939) travel times at 1° intervals.

2. There follows an instruction card defining the slowness-distance curve:

RANGE (1) - the lower limit of epicentral distance in degrees.

RINT - the unit increment in distance

NP - number of increments

eg if $^{dT}/_{d\Delta_k}$ is to be estimated from 70° to 84° in 2° intervals, then RANGE (1) = 70, RINT = 2 and NP = 8, and INSTR 2 = EVEN. If the curve is to be estimated over unequal intervals, then RINT and INSTR 2 are left blank and then follows card(s) with each distance interval tabulated from 70° to 84°.

The remainder of the card contains switches enabling the calculated travel time to be restrained to any fixed value and $dt/d\Delta_k$ to be restrained to fixed values at both ends. The card also contains switches to produce cards punched with results, residuals and site corrections, and also full printouts of normal and inverted matrices.

3. The next section consists of 4 sets of cards, one for each array with the cartesian coordinates in kms (referred to N-S and E-W axis) of the seismometer sites constituting each array. If the first card of each set is punched with the velocity in the top 500 feet of the array (VEL), then the onset times will be corrected for site altitudes (ALTIT), (if known).

4. If ICOR = 1 is punched on card 2 then cards follow with parameters A, B, E, F, G for each seismometer which correct onset times for azimuthal site effects. The correction for an event at azimuth α from an array is (Appendix F)

$$= A + B \sin(\alpha + E) + F \sin(2\alpha + G)$$

If only first order corrections are known, then F & G should be left blank.

5. A directory follows listing all events recorded by the 4 arrays, with details of their epicentres. Data that is essential for the running of the program is:

AZ - azimuth α of the event from the array

TFACT - the playout speed of the paper records used to measure the onset times - ie the conversion factor from distance (usually mm) to seconds

EVENT - a unique code defining the event

DELTU - hypocentral distance from the array.

If DEPTH of the event is also punched then DELTU will be corrected for depth and put equal to DELTA.

6. Four blocks of cards, one block for each array then follow. Each block of cards contains the relative stepouts measured in mm. from each record. The events should be arranged in the same order as the directory (paragraph 5) for speed of operation.

PROGRAM MAIN

This program reads in all the data listed above and converts the step-outs to relative onset-times, applies all corrections and prints out the input data. The following corrections may be applied to the onset times:

(1) Altitude correction

If values of altitude (ALTIT) are known for individual sites, as well as the seismic velocity (VEL) in the top 500 feet of the array, then individual onset times are corrected by

$$\text{correction} = \frac{\text{ALTIT} - \text{ALTIT}_o}{\text{VEL}}$$

where ALTIT_o is the lowest site altitude at an array.

(2) Depth Correction

If the hypocentre of the event is known then the epicentral distance (DELTU) is corrected for the depth of the event using subroutine DEPTHA. The corrections are made using the upper mantle model of Herrin et al (1968) shown in Fig H1.

(3) Azimuthal Corrections

Onset times of an event at azimuth α can be corrected for azimuthal site corrections defined by the parameters A, B, E, F, G, (see paragraph 4). If azimuthal site corrections are used, they will include the altitude corrections (1).

The matrix of coefficients of the normal equations (the A matrix) is then set up in subroutine NORMAL. As explained previously, if the equations of condition were set up, a prohibitively large amount of computer storage would be needed; this is avoided when the matrix of normal coefficients are formed directly. NORMAL checks that each epicentral distance is in the correct distance range and also sets up the condition that the site corrections at each array sum to zero $\left(\sum_i S_{hi} = 0 \text{ for all } h \right)$. Without this condition the normal equations are insoluble. If restraints are to be placed on the slowness and travel time curves, these are also

included at this stage. The restraints that may be applied to the data are contained in the following subroutines:

SHOLDS

The value of slowness in the first distance interval $^{dT}/_{d\Delta}\ _{k=1}$ can be restrained to any value , that may be read in, by including the equation of condition

$$\sqrt{H} \cdot \frac{dT}{d\Delta}_{k=1} = \sqrt{H} \cdot \phi_1$$

where H is a number, large with respect to , and taken to be 10^5. (see Payne and Irones 1967).

SHOLDF

The value of slowness in the last distance interval can be similarly restrained to any value by including

$$\sqrt{H} \cdot \frac{dT}{d\Delta}_{k=n} = \sqrt{H} \cdot \phi_n$$

The total slowness curve ($\Delta = 30^\circ - 104^\circ$) was estimated in five sections each overlapping by one degree at the ends. At the overlaps there was found to be slight differences in the slowness estimates. SHOLDS and SHOLDF were used to restrain the value of slowness to the mean of the two estimates, and the curve re-estimated.

JBTIME

An independent check on the slowness distance curve is to compare its integral (travel time) with known values or alternatively to restrain the travel time to a fixed value. JBTIME is used to include in the matrix the equation of condition

$$D_1\left(\frac{dT}{d\Delta}\right) + D_2\left(\frac{dT}{d\Delta}\right) \ldots\ldots D_k\left(\frac{dT}{d\Delta}\right) \ldots\ldots D_m\left(\frac{dT}{d\Delta}\right) = TJB_m$$

where D_k is the interval in Kms, over which the slowness is $\left(^{dT}/_{d\Delta}\right)_k$ and TJB_m is the Jeffreys-Bullen travel time across the range D_1 to D_m.

TTTIME

This is a subroutine similar to JBTIME that allows the travel time to be restrained to any value (= THOLD).

The complete matrix of coefficients of the normal equations are inserted using subroutine SOLVE derived from the Harwell Program Library (No. MB01A). This uses the method of traingular decomposition (HMSO, 1961) to form the inverted matrix, which is stored on disk. From the inverted matrix, subroutine RESIDL computes the site corrections S(HI), constants C(HJ) and slowness S(K) for each distance interval K. On subsituting these values into the original equations of condition, the error terms RESID (HIJ), and hence S^2 the estimate of the variance of the errors can be found. From S^2 and the diagonal elements of the inverted matrix, the 95% confidence limits on S(HI), C(HJ) and S(K) are computed.

The observed onset times AT(HIJ) corrected for S(HI) and C(HJ) are used to calculate the individual estimates of slowness for all events, from the equation

$$dT/d\Delta = \frac{\Sigma_i F_i t_i}{\Sigma_i F_i^2}$$ (see Appendix C)

where $F_i = -(x_i \text{ sm } \alpha + yi \cos \alpha)$ and t_i is the corrected onset time t_i = AT(HIJ) - C(HJ) - S(HI). Printed output from the program is:

(1) Tables of slowness S(K), (secs/deg) for each distance interval K with 95% confidence limits, and the reciprocal of slowness, "phase velocity" V (km/sec).

(2) Tables showing the best estimates of S(HI) and C(HJ) with 95% confidence limits.

(3) Tables showing the residuals for each site RESID (HIJ)

(4) Tables showing the calculated onset times for each site

CT(HIJ) = AT(HIJ) - RESID(HIJ)

(5) The integrated area under S(K), ie, the total travel time across K distance intervals and 95% confidence limits and differences from the Jeffreys-Bullen (1939) and Herrin (1968) travel time tables.

(6) Tables showing the values of $^{dT}/_{d\Delta}$ for individual events corrected for sub array structure.

(7) Tables of 95% confidence limits on the differences between S(K)'s.

Output available on punched cards is:-

(1) Corrected epicentral distance DELTA, corrected individual estimate of slowness $^{dT}/_{d\Delta}$, corresponding phase velocity V, event code ECODE.

(2) RESID (HIJ)

(3) RESID (HIJ) + S(HI). These cards are used to derive the azimuthal site corrections.

Graphical output is also available using the SC 4060 plotter. Subroutine GRAPH plots all graphs using the standard package POLGRF derived from the subroutine CARGRF described by Young and Douglas (1968).

Graphical output is:-

(1) Area under S(K) - DELTA curve plotted with Jeffreys-Bullen and Herrin 1968 travel times.

(2) Observed travel time - J.B. plotted against distance.

(3) V(K) - DELTA curve, 95% confidence limits and phase velocity from Herrin (1968).

(4) V(K) - DELTA curve, 95% confidence limits and individual estimates of V corrected for sub array structure.

(5) S(K) - DELTA curve, 95% confidence limits and $^{dT}/_{d\Delta}$ from Herrin (19

(6) S(K) - DELTA curve, 95% confidence limits and individual estimates of $^{dT}/_{d\Delta}$.

```
B       TYPE,COMPILGO,F4
T       SUBTYPE, F100
B     2410D, DISK
        END
T       SUBTYPE,FORTRAN,LMAP,LSTRAP
C
C
C
C     MULTI-ARRAY SLOWNESS ANALYSIS PROGRAM.        DEREK J. CORBISHLEY.
C     **************************************        ********************
C
C
C
C
C     THIS PROGRAM ESTIMATES  THE DERIVATIVE OF THE TRAVEL-TIME CURVE
C     DT/DX(SLOWNESS) AND ITS RESIPROCAL (PHASE VELOCITY) IN DISCRETE
C     DISTANCE INTERVALS. THE DATA READ IN IS ONSETTIMES FROM UP TO 120
C     EVENTS RECORDED AT 4 SEISMIC ARRAYS. THE PLANE WAVEFRONT APPROXIMA
C     TION IS ASSUMED FOR EVENTS AT A EPICENTRAL DISTANCE GREATER THAN
C     30 DEGREES. ALL DATA IS INVERTED SIMULTANEOUSLY USING LEAST SQUARE
C     S. ONSET TIMES CAN BE CORRECTED FOR AZIMUTHAL PIT CORRECTIONS,
C     AND ALTITUDE. EPICENTRAL DISTANCE IS CORRECTED FOR FOCAL DEPTH.
C
C     OUTPUT INCLUDES GRAPHS OF DT/DX WITH 95 PER CENT CONFIDENCE LIMITS
C     (95 PCCL) , PHASE VELOCITY WITH 95 PCCL, TRAVEL TIME OBTAINED BY
C     INTEGRATING AND CORRECTED VALUES OF DT/DX FOR ALL EVENTS AND SITE
C     CORRECTIONS.
C
C     THE EQUATION OF CONDITION FOR AN EVENT(J) IN THE DISTANCE INTERVAL
C     (K) ARRIVING AT A SEISMOMETER(I) AT THE ARRAY(H) IS
C
C     T(HIJ) = S(HI) + C(HJ) - R(HI)*COS(THET(HI)-AZ(HJ))*(DT/DX)K
C
C     WHERE
C          S(I) = TIME CORRECTION FOR STRUCTURE UNDER SEISMOMETER(I)
C          C(J) = A CONSTANT
C          R(HI)COS(THET(HI)-AZ(HJ)) = X(HI)*SIN(AZ(HJ)) + Y(HI)*COS(AZ
C          (HJ)). FOR SEISMOMETER COORDINATES X(HI),Y(HI) AND EVENT AT
C          AZIMUTH AZ(HJ).
C
C     THE PROGRAM SOLVES FOR S, C, DT/DX.
C
C     THE PROGRAM IS WRITTEN FOR  H = 4 ARRAYS (ONLY)
C                                 I = 20 SEISMOMETERS / ARRAY (OR LESS)
C                                 J = 120 TOTAL EVENTS (OR LESS)
C                                 K = 30 DISTANCE INTERVALS (OR LESS)
C
C     SEE
C     (DOUGLAS AND CORBISHLEY, NATURE, 30/3/68, PAGE 1243)
C
C
C
C
C                  THE ORDER OF THE INPUT DECK IS
C
C     ******************************************************************
C
C     THE FIRST 3 INSTRUCTIONS REMAIN CONSTANT FOR ALL RUNS
C
C        1  CARDS WITH
C     ST(I)     57 VALUES OF STUDENTS T.
C               THE FORMAT FOR PUNCHING IS IN STATEMENT NO.89.
C
C        2  CARDS WITH
C     TIMEH(I) TRAVEL-TIMES AND SLOWNESS OF P FOR DISCRETE EPICENTRAL
C     SLOWH(I) DISTANCES FROM 0 TO 108 DEGREES AT 1 DEGREE INTERVALS
C               OBTAINED FROM HERRIN (1968).
C               THE FORMAT FOR PUNCHING IS IN STATEMENT NO. 90.
C
C        3  CARDS WITH
C     TIMEJ(I) 112 VALUES OF TRAVEL-TIMES(JEFFREYS-BULLEN)  FROM 0 TO
C               111 DEGREES AT 1 DEGREE INTERVALS.
C
C     ******************************************************************
C
C     THE FOLLOWING INSTRUCTIONS DEFINE THE DT/DX - X CURVE.
C
C        4  CARD WITH
C     RANGE(1) LOWER LIMIT OF EPICENTRAL DISTANCE FROM STATIONS. PUNCH
C               IN COLS 7-8.
C     RINT      INCREMENT IN DELTA.   PUNCH IN COL 11.
C     NP        NUMBER OF INCREMENTS. PUNCH IN COLS 13-14.
C     INSTR2    PUNCH -EVEN- IF INCREMENT IN DELTA IS CONSTANT OVER ALL
C               NP. OTHERWISE OMIT. (PUNCH IN COLS. 16-19)
C              IF INSTR2 = BLANK, THEN CARDS FOLLOW WITH VALUES OF RANGES
C               (AFTER INSTRUCTION 5)TO A MAXIMUM OF 30 (SEE FORMAT 96)
C     IHOLD     PUNCH 1 TO HOLD TRAVEL-TIME ACROSS DISTANCE RANGE TO THAT
C               GIVEN IN COLS 23-29. (F6.3).  PUNCH IN COL 21.
C     THOLD     CURVE RESTRAINED TO THIS TIME(SEE -IHOLD-)
C     ISTART    PUNCH 1 TO HOLD START OF SLOWNESS CURVE TO VALUE GIVEN IN
```

```
C              COLS 33-38 (F6.3)  PUNCH 1 IN COL 31
C      SSTART  START OF CURVE RESTRAINED TO THIS SLOWNESS (SEE -ISTART-)
C      IENDS   PUNCH 1 TO HOLD END OF SLOWNESS CURVE TO VALUE GIVEN IN
C              COLS 43-48 (F6.3)  PUNCH 1 IN COL 41
C      SENDS   END OF CURVE RESTRAINED TO THIS SLOWNESS (SEE -IENDS-)
C      IRSTRN  PUNCH 1. TO RESTRAIN TOTAL TRAVEL-TIME ACROSS DISTANCE
C              RANGE TO THAT GIVEN BY J.B. (PUNCH IN COL. 52)
C      IBODG   PUNCH 1 TO REMOVE HERRIN SLOWNESS EFFECT FROM ARRIVAL
C              TIMES.(PUNCH IN COL.54) BY PUNCHING -IBODG- EACH ONSETTIM
C              E IS CORRECTED BY SUBTRACTING THE THEORETICAL ONSET TIME
C              OBTAINED FROM HERRINS(1968) TRAVEL TIMES, THE PROGRAM
C              THEN CALCULATES -SLOWNESS DEFECT- AND THE RESIDUALS AND
C              PIT CORRECTIONS WILL BE INDEPENDENT OF ANY DISTANCE TERM.
C      IRESID  PUNCH 1.FOR CARDS PUNCHED WITH TOTAL RESIDUAL = (RESIDUAL
C              + PIT CORRECTION). OTHERWISE LEAVE BLANK. (PUNCH IN COL
C              56).
C      IMTREX  PUNCH 1.FOR PRINTOUTS OF MATRICES.OTHERWISE LEAVE BLANK.
C              (PUNCH IN COL. 58)
C      IVEL    PUNCH 1.FOR CARDS PUNCHED WITH (DISTANCE,SLOWNESS,PHASE
C              VELOCITY,EVENT CODE)
C                      OTHERWISE LEAVE BLANK. (PUNCH IN COL. 60)
C      ICOR    PUNCH 1.TO READ IN CARDS PUNCHED WITH AZIMUTHAL PIT
C              CORRECTIONS----SEE STATEMENT 7 BELOW.(PUNCH IN COL 62)
C      IPUNCH  PUNCH 1.FOR CARDS PUNCHED WITH PIT RESIDUALS. OTHERWISE
C              LEAVE BLANK. (PUNCH IN COL. 66)
C              THE FORMAT FOR PUNCHING IS IN STATEMENT NO.88.
C
C     ****************************************************************
C
C     THE FOLLOWING INSTRUCTIONS GIVE DETAILS OF THE FOUR ARRAYS.
C
C        5  ONE CARD WITH
C     STN       THREE LETTER CODE OF ARRAY STATION(I).
C     NPIT(I)   NUMBER OF PITS AT STATION.
C     SLAT(I)   LATITUDE OF STATION.
C     SLONG(I)  LONGITUDE OF STATION.
C     VEL(I)    VELOCITY IN TOP 500 FT. OF STATION OF P WAVE. FOR HEIGHT
C               CORRECTIONS (IF KNOWN)
C               THE FORMAT FOR PUNCHING IS IN STATEMENT NO.31.
C
C        6  (J) CARDS WITH
C     STN(I)    NAME OF STATION(I)
C     PIT(I,J)  REFERENCE NUMBER OF PIT(J) AT STATION (I).
C     X(I,J)    X-COORDINATE OF PIT POINT.
C     Y(I,J)    Y-COORDINATE OF PIT POINT.
C
C     ALT(I,J) ALTITUDE OF PIT POINT IN FEET.FOR HEIGHT CORRECTIONS.
C     COR(I,J) CORRECTION TO ONSET TIME(SECS).LEAVE BLANK FOR NO
C              CORRECTION
C     THERE MUST BE 20 SETS OF COORDS. IF J LT. 20 THEN THE NUMBER
C     SHOULD BE MADE UP WITH BLANKS.
C              THE FORMAT FOR PUNCHING IS IN STATEMENT NO.41.
C
C        THERE ARE (I)   BLOCKS OF CARDS.EACH BLOCK HAS ONE CARD PUNCHED
C        AS IN 5(ABOVE),FOLLOWED BY(J)CARDS PUNCHED AS IN 6(ABOVE).
C
C        7  CARDS WITH
C              IF -ICOR- HAS BEEN PUNCHED AS IN 4.ABOVE, THEN FOLLOW ONE
C              CARD FOR EACH PIT WITH AZIMUTHAL PIT CORRECTIONS OF THE
C              FORM
C
C                  CORRECTION = ALPH1 + BET1*(AZ + GAMM1) + BET2(AZ +
C                                                              GAMM2)
C
C              IF CORRECTIONS ARE OF ONLY THE FIRST ORDER THEN LEAVE
C              BET2 AND GAMM2 BLANK.
C
C     ALPH1     AZIMUTHAL PIT CORRECTIONS      1ST ORDER
C     BET1      AZIMUTHAL PIT CORRECTIONS      1ST ORDER
C     GAMM1     AZIMUTHAL PIT CORRECTIONS      1ST ORDER
C     BET2      AZIMUTHAL PIT CORRECTIONS      2ND ORDER
C     GAMM2     AZIMUTHAL PIT CORRECTIONS      2ND ORDER
C              FORMAT FOR PUNCHING IS IN STATEMENT NO.41
C
C     IF PIT CORRECTIONS HAVE, OR HAVE NOT BEEN INCLUDED, THERE FOLLOWS-
C
C     ****************************************************************
C
C     THE FOLLOWING INSTRUCTIONS ARE A DIRECTORY OF THE EVENTS USED
C
C        8  ONE CARD WITH
C     NE(1)     NUMBER OF EVENTS RECORDED AT ARRAY (1)
C     NE(2)     NUMBER OF EVENTS RECORDED AT ARRAY (2)
C     NE(3)     NUMBER OF EVENTS RECORDED AT ARRAY (3)
C     NE(4)     NUMBER OF EVENTS RECORDED AT ARRAY (4)
C      TOTAL NE(1)+NE(2)+NE(3)+NE(4) MUST BE LESS THAN 121
C              THE FORMAT FOR PUNCHING IS IN STATEMENT NO.5.
C
C        9  4 BLOCKS OF CARDS EACH WITH
C     V(K)      PHASE VELOCITY(KM/SEC)OF SIGNAL FROM EVENT(K).
C              ACROSS ARRAY FROM USCGS, IF KNOWN.
```

```
C      AZ(K)     AZIMUTH(DEGREES)FROM USCGS.
C      TFACT(K)  FACTOR FOR CONVERTING ONSET TIMES TO SECONDS (IE. IF
C                ONSETS ARE IN MM. THEN TFACT = X MM./SEC)
C      EVENT(K)  DATE OF EVENT(K). ALL EVENTS MUST BE DEFINED UNIQUELY.
C      DEPTH(K)  DEPTH OF EVENT FROM USCGS, ASSUMED ZERO IF UNKNOWN.
C      DELTU(K)  EPICENTRAL DISTANCE FROM ARRAY.
C      ELAT(K)   LATITUDE(DEGREES)OF EPICENTRE IF KNOWN.NORTH IS POSITIVE.
C      ELONG(K)  LONGITUDE(DEGREES)OF EPICENTRE IF KNOWN.EAST IS POSITIVE.
C                FORMAT FOR PUNCHING IS IN STATEMENT NO.9.
C
C                THERE SHOULD BE ONE CARD FOR EACH EVENT, BLOCKS OF CARDS
C                FOR EACH ARRAY SHOULD BE IN THE SAME ORDER AS INSTRUCTION
C                                                                      5.
C      ********************************************************************
C
C      THE FOLLOWING INSTRUCTIONS CONTAIN ONSETTIME DATA RECORDED AT EACH
C      SEISMOMETER (PIT). THEIR SHOULD BE 4 BLOCKS OF DATA IN THE SAME
C      ORDER AS INSTRUCTION 5, EACH BLOCK OF DATA HAS
C
C         10 ONE CARD WITH
C      ASTN      NAME OF STATION.
C                FORMAT FOR PUNCHING IS IN STATEMENT NO.7.
C
C         11 ONE CARD WITH
C      AEVEN3    EVENT CODE.
C      ANAME     LOCATION OF EVENT.
C                FORMAT FOR PUNCHING IS IN STATEMENT NO.45.
C
C         12 CARDS WITH
C      APIT      NAME OF PIT.
C      T         ONSET TIME AT PIT
C                FORMAT FOR PUNCHING IS IN STATEMENT NO.12.
C
C        THERE SHOULD BE ONE CARD FOR EACH PIT.IF A PIT IS MISSING,THE
C        LAST CARD SHOULD BE A BLANK.
C
C
C      ********************************************************************
C      ********************************************************************
C      ********************************************************************
C
C
C      THIS -MAIN- PROGRAM READS IN THE DATA AND CORRECTS THE ONSET TIMES
C                      AND PRINTS OUT IN TABULAR FORM.
C
C
C
C      ********************************************************************
C
C
      COMMON /AMATRX/ ALT(4,20), COR(4,20), TFACT(120), ELAT(120),
     1 ELONG(120), AIND(120,2C)
      COMMON /ATT/ AT(4,120,20)
      COMMON /BMATRX/ B(231)
      COMMON /EVENTT/ EVENT(120), NEVENT, NE(4), AZ(120), DELTA(120),
     1 INDEX(120)
      COMMON /GRFF/ TITLE(2C), XMAX, XMIN,YMAX, YMIN, INDX, INDY, IND,
     1IDOT, INSTR1, XLIMIT, YLIMIT, SCALX, SCALY
      COMMON /PITT/ STN(4), PIT(4,20), X(4,20), Y(4,20), NPIT(4)
      COMMON /REST/ V(120), ENAME(120,3), VELOC(120), M
      COMMON /RJST/ S(231), D(231)
      COMMON /RNGE/ RANGE(30), RINT, NP
      COMMON /SLV/ N, IMTREX, IRESID, IRSTRN, IVEL, IBODG, IHOLD, ISTART
     1, IENDS, THOLD, SSTART, SENDS, IPUNCH
      COMMON /STATS/ ST(57)
      COMMON /TTCVS/ TIMEH(109), AMPV(24), TIMEJ(112), SLOWH(109)
      DIMENSION SLAT(4), SLONG(4), VEL(4), ANAME(3), BMIN(4), HMIN(4),
     1 DEPTH(120), DELTU(12C), ALPHA(4,20), BETA(4,20), GAMMA(4,20)
     2,  ALPH1(4,20), BET1(4,20), GAMM1(4,20),BET2(4,20), GAMM2(4,20)
C
      DATA EVEN(8HEVEN     )
      DATA STAR(8H*        )
      DATA BLANK(8H         )
      PI=4.*ATAN(1.)
      RTOD=180./PI
      DTOR = PI/180.
      RADIUS=6371.028
      REAL INSTR2
C
C     SPECIAL LIBRARY ROUTINES
      CALL SCLIBR
      CALL EBUMP
      CALL SDATE(DATE)
      CALL SECCLK(TS)
C
      DO 22 I=1,4
      DO 33 J=1,20
      X(I,J) = 0.0
      Y(I,J) = 0.0
      ALT(I,J) = 0.0
      COR(I,J) = 0.0
```

```
      ALPHA(I,J) = 0.
      BETA(I,J) = 0.
      GAMMA(I,J) = 0.
      ALPH1(I,J) = 0.
      BET1(I,J) = 0.
      GAMM1(I,J) = 0.
      BET2(I,J) = 0.0
      GAMM2(I,J) = 0.0
      DO 20 K = 1, 120
      AT(I,K,J) = 0.0
 20   CONTINUE
 33   CONTINUE
 22   CONTINUE
C
C     ******************************************************************
C
C                              READS IN FIXED TABLE OF CONSTANTS
C
      READ 89, (ST(I), I = 1, 57)
      PRINT89, (ST(I), I = 1, 57)
 89   FORMAT (1X, 15F5.2)
      READ 90, (TIMEH(I), SLOWH(I), I = 1, 109)
      PRINT90, (TIMEH(I), SLOWH(I), I = 1, 109)
 90   FORMAT ((5(F8.4, 1X, F7.4)))
      DO 99 I = 1, 109
      TIMEH(I-1) = TIMEH(I)
      SLOWH(I-1) = SLOWH(I)
 99   CONTINUE
      READ 91, (TIMEJ(I), I = 1, 112)
      PRINT91, (TIMEJ(I), I = 1, 112)
 91   FORMAT (2X, 7F10.2)
      DO 92 I = 1, 112
      TIMEJ(I-1) = TIMEJ(I)
 92   CONTINUE
C
C     SETS ARRAYS TO ZERO
      IHOLD = 0
      ISTART = 0
      IENDS = 0
      IRSTRN = 0
      IBODG = 0
      IRESID = 0
      IMTREX = 0
      IVEL = 0
      ICOR = 0
      IPUNCH = 0
C
C     ******************************************************************
C
C                              READS IN DETAILS OF DISTANCE INTERVALS AND
C                              SWITCHES
C
      READ 88, RANGE(1),RINT,NP,INSTR2,IHOLD,THOLD,ISTART,SSTART,IENDS,
     1SENDS,IRSTRN,IBODG,IRESID,IMTREX, IVEL, ICOR, IPUNCH
      PRINT88, RANGE(1),RINT,NP,INSTR2,IHOLD,THOLD,ISTART,SSTART,IENDS,
     1SENDS,IRSTRN,IBODG,IRESID,IMTREX, IVEL, ICOR, IPUNCH
 88   FORMAT (6X, I2, 2X, I1, 1X, I2, 1X, A4, 1X, I1, 1X, F7.3, 1X, I1,
     1 1X, F6.3, 2X, I1, 1X, F6.3, 3X, I1, 6(1X, I1))
      IHOLD = IHOLD + 1
      ISTART = ISTART + 1
      IENDS = IENDS + 1
      IRSTRN = IRSTRN + 1
      IBODG = IBODG + 1
      IRESID = IRESID + 1
      IMTREX = IMTREX + 1
      IVEL = IVEL + 1
      ICOR = ICOR + 1
      IPUNCH = IPUNCH + 1
C
      NP = NP + 1
      IF (INSTR2.EQ.EVEN)GO TO 95
      READ 96, (RANGE(I), I = 1, NP)
      PRINT96, (RANGE(I), I = 1, NP)
 96   FORMAT (9F8.2)
      GO TO 97
 95   DO 98 I = 2, NP
      RANGE(I) = RANGE(1) + FLOAT(I-1)*RINT
 98   CONTINUE
 97   CONTINUE
      NP = NP - 1
C
C     ******************************************************************
C
C                              READS IN ARRAY INFORMATION AND PRINTS OUT
C
      DO 1 I = 1, 4
      READ 31,STN(I),NPIT(I),SLAT(I),SLONG(I),VEL(I)
 31   FORMAT (1X, A4, 3X, I3, 4X, F8.3, 2X, F8.3, 3X, F6.2)
      READ 41, (STN(I),PIT(I,J),  X(I,J), Y(I,J), ALT(I,J), J = 1, 20)
 41   FORMAT  (1X, A4, 1X, A3, 6X, F10.5,F10.5,F10.5)
```

```
    1   CONTINUE
        PRINT 10,DATE
   10   FORMAT (1H1/3X, 29HMULTI-ARRAY VELOCITY PROGRAM , 30X, 20HDEREK J.
       1 CORBISHLEY., 30X, A8/3X, 29H******************************, 30X,
       2 20H********************, 30X, 8H********)
        PRINT 18
   18   FORMAT (    //3X, 24HCOORDINATES OF STATIONS.
       1/3X,24H-----------------------//30X,7HNAME OF,3X,5HNO.OF,3X,8HLAT
       2ITUDE,3X,9HLONGITUDE,3X,14HVELOCITY UNDER
       3                                  /30X,7HSTATION,4X,4HPITS,5X,6
       4H(DEGS),5X,6H(DEGS),6X,14HSTATION (FT/S)
       5                                 /30X,7H-------,3X,6H------,3X,8H-
       6-------,3X,9H---------,3X,14H--------------)
        PRINT 3,(STN(I),NPIT(I),SLAT(I),SLONG(I),VEL(I),          I=1, 4)
    3   FORMAT (32X, A4, 5X, I3, 5X, F8.3, 4X, F8.3, 5X, F6.2)
        PRINT 4, (PIT(1,J),    X(1,J), Y(1,J), ALT(1,J), COR(1,J),
       1                       X(2,J), Y(2,J), ALT(2,J), COR(2,J),
       2                       X(3,J), Y(3,J), ALT(3,J), COR(3,J),
       3                       X(4,J), Y(4,J), ALT(4,J), COR(4,J), J=1, 20)
    4   FORMAT(//3X,62HCARTESIAN COORDINATES,ALTITUDES AND CORRECTIONS OF
       1PIT POINTS./3X,63H-----------------------------------------------
       2---------------//17X,3HEKA,28X,3HYKA, 28X,3HWRA,28X,3HGBA//1X,3HPI
       3T,4(4X, 1HX, 7X,1HY,5X,6HALTIT.,2X,5HCORR.)
       4/1X,3H---, 4(2X, 29H----------------------------)
       5/(1X, A3, 2X, F6.3, 2X, F6.3, 4X, I4, 1X, F5.2, 3X,
       6              F6.3, 2X, F6.3, 4X, I4, 1X, F5.2, 3X,
       7              F6.3, 2X, F6.3, 4X, I4, 1X, F5.2, 3X,
       8              F6.3, 2X, F6.3, 4X, I4, 2X, F5.2))
        GO TO (110,111)ICOR
  111   PRINT 112
  112   FORMAT (1H1/3X, 99HAZIMUTHAL PIT CORRECTIONS OF THE FORM  CORR.= A
       1LPH1 + BET1*SIN(AZ.+ GAMM1) + BET2*SIN(2*AZ.+ GAMM2)/3X,25H********
       2**********************//3X, 23HTWO TERM FOURIER SERIES/3X, 23H********
       3**********//
       4 17X, 5HARRAY, 9X, 3HPIT, 10X, 5HALPH1, 10X, 4HBET1, 12X, 5HGAMM1,
       5  10X, 4HBET2, 12X, 5HGAMM2/)
        DO 113 I = 1, 4
        READ 115,(STN(I),PIT(I,J),ALPH1(I,J),BET1(I,J),GAMM1(I,J),
       1BET2(I,J), GAMM2(I,J), J = 1, 20)
  115   FORMAT (1X, A4, 1X, A3, 6X, 5F10.5)
  113   CONTINUE
        DO 114 I = 1, 4
        PRINT116,(STN(I),PIT(I,J),ALPH1(I,J),BET1(I,J),GAMM1(I,J),
       1BET2(I,J), GAMM2(I,J), J = 1, 20)
  116   FORMAT (18X, A4, 9X, A3, 7X, F10.5, 4X, F10.5, 6X, F10.2, 4X,
       1 F10.5, 6X, F10.2)
  114   CONTINUE
C
C       **************************************************************************
C
C                                 READS IN DIRECTORY OF EVENT INFORMATION ANC
C                                 PRINTS OUT
C
  110   READ 5, NE(1), NE(2), NE(3), NE(4)
    5   FORMAT (7X, I3, 7X, I3, 7X, I3, 7X, I3)
        NEVENT = NE(1)  + NE(2) + NE(3) + NE(4)
        READ 9, (V(K), AZ(K), TFACT(K), EVENT(K), DEPTH(K), DELTU(K),
       1 ELAT(K), ELONG(K),    K = 1, NEVENT)
    9   FORMAT (2X, F8.3, 2X, F8.3, 2X, F7.3, 2X, A8, 3X, I3, 6X, F5.1,
       1 2X, F6.1, 2X, F6.1)
C       CORRECTS FOR FOCAL DEPTH
        CALL CEPTHA(DEPTH, DELTU, DELTA, NEVENT)
C       ****************************************
        PRINT 51
   51   FORMAT (1H1/3X, 40HTABLE OF ALL EVENTS USED AT EACH STATION
       1/3X, 40H----------------------------------------
       2//12X, 7HDATE OF, 6X, 10HPHASE VEL., 4X, 7HAZIMUTH, 5X, 5HTFACT,
       3 3X, 5HDEPTH, 3X, 10HUSCGS DIST, 4X, 10HCORR. DIST, 4X, 8HLATITUDE
       4,4X,9HLONGITUDE/13X, 5HEVENT, 8X, 8H(KM/SEC), 4X, 9H(DEGREES),
       5 12X, 5H(KMS), 4X, 9H(DEGREES), 4X, 9H(DEGREES), 4X, 9H(DEGREES),
       6 4X, 9H(DEGREES))
        LIM1 = NE(1)
        LIM2 = NE(2) + LIM1
        LIM3 = NE(3) + LIM2
        LIM4 = NE(4) + LIM3
        LLIM1 = LIM1 + 1
        LLIM2 = LIM2 + 1
        LLIM3 = LIM3 + 1
        PRINT 39, STN(1)
        PRINT 17, (EVENT(K),V(K),AZ(K),TFACT(K), DEPTH(K), DELTU(K),
       1 DELTA(K), ELAT(K), ELONG(K), K = 1, LIM1)
        PRINT 39, STN(2)
        PRINT 17, (EVENT(K),V(K),AZ(K),TFACT(K), DEPTH(K), DELTU(K),
       1 DELTA(K), ELAT(K), ELONG(K), K = LLIM1, LIM2)
        PRINT 39, STN(3)
        PRINT 17, (EVENT(K),V(K),AZ(K),TFACT(K), DEPTH(K), DELTU(K),
       1 DELTA(K), ELAT(K), ELONG(K), K = LLIM2, LIM3)
        PRINT 39, STN(4)
        PRINT 17, (EVENT(K),V(K),AZ(K),TFACT(K), DEPTH(K), DELTU(K),
       1 DELTA(K), ELAT(K), ELONG(K), K = LLIM3, LIM4)
```

```
 39   FORMAT (1X, 8HSTATION , A4/1X, 11H----------)
 17   FORMAT (12X,A8,6X,F6.1,8X,F5.1,5X,F6.2, 4X, I3, 5X, F5.1, 9X, F5.1
     1, 8X, F6.1, 6X, F6.1)
C
C     ****************************************************************
C
C                            PROGRAM NOW READS IN ARRAY, EVENT AND ONSET
C                           TIMES CHECKING EACH AGAINST THE DIRECTORY,
C                            IF A MISTAKE OCCURS THE JOB IS REJECTED
C
      KEVENT = 1
      LEVENT = NE(1)
C
C     SELECTS ARRAY
      DO 14 I = 1, 4
      READ 7, ASTN
 7    FORMAT (1X, A4)
      DO 50 IS = 1, 4
      IF (ASTN.EQ.STN(IS)) GO TO 42
 50   CONTINUE
      PRINT 43, ASTN
 43   FORMAT (//4X, 37HJOB REJECTED, CANNOT IDENTIFY STATION, A8/4X,
     1 37H**************************************)
      CALL EXIT
 42   IO = IS
      NEVENT = NE(IO)
      NLIM = NPIT(IO)
C     FINDS HEIGHT OF LOWEST PIT
      CALL AAMIN(ALT, 20, HMIN, IO)
C     ****************************
      DO 70 J = 1, 20
      ALT(IO,J) = ALT(IO,J) - HMIN(IO)
 70   CONTINUE
      DO 21 K = 1, 120
      DO 26 J = 1, 20
      AIND(K,J) = BLANK
 26   CONTINUE
 21   CONTINUE
C
C     SELECTS EVENT
      DO 44 K = KEVENT, LEVENT
      READ 45, AEVENT, (ANAME(L), L = 1, 3)
 45   FORMAT (6X, A8, 26X, 3A8)
      DO 46 KS = KEVENT, LEVENT
      IF(AEVENT.EQ.EVENT(KS)) GO TO 47




 46   CONTINUE
 48   PRINT 49, AEVENT
 49   FORMAT (//4X, 35HJOB REJECTED, CANNOT IDENTIFY EVENT, A8/4X,
     1 35H**********************************)
      CALL EXIT
 47   KO = KS
      DO 93 IA = 1, 3
      ENAME(KO,IA) = ANAME(IA)
 93   CONTINUE
C
C     SELECTS PIT
      DO 15 J=1,20
      READ 12, APIT, T
 12   FORMAT (6X, A3, 3X, F10.2)
      IF(APIT.NE.BLANK) GO TO 6
      GO TO 44
 6    DO 2 JS = 1, 20
      IF (APIT.EQ.PIT(IO,JS))   GO TO 37
 2    CONTINUE
      PRINT 16, APIT
 16   FORMAT (//4X, 35HJOB REJECTED, CANNOT IDENTIFY PIT   , A8/4X,
     135H**********************************)
      CALL EXIT
 37   JO = JS
      AGAMMA = (AZ(KO) + GAMMA(IO,JO))*DTOR
      AGAMM1 = (AZ(KO) + GAMM1(IO,JO))*DTOR
      AGAMM2 = (2.*AZ(KO) + GAMM2(IO,JO))*DTOR
C     ONSETTIMES CORRECTED FOR PIT CORRECTIONS
      AT(IO,KO,JO) = T/TFACT(KO) - (ALPHA(IO,JO)*BETA(IO,JO)*SIN(AGAMMA)
     1) - (ALPH1(IO,JO)*BET1(IO,JO)*SIN(AGAMM1) + BET2(IO,JO)*SIN(AGAMM2
     2)) + 0.00001
      GO TO (106,107) IBODG
C     ONSETTIMES CORRECTED FOR TRAVEL TIMES
 107  CALL TIMOUT(IO,KO,JO)
C     **********************
 106  AIND(KO,JO) = STAR
      IF (VEL(IO)) 71, 71, 72
 71   GO TO 15
C     ONSET TIMES CORRECTED FOR HEIGHT OF PITS.
 72   AT(IO,KO,JO) = AT(IO,KO,JO) - ALT(IO,JO)/VEL(IO)
 15   CONTINUE
 44   CONTINUE
C
C
C     ****************************************************************
```

```
C                              PRINT OLT ONSET TIMES
C
      N9 = (MEVENT - 1)/9 + 1
      PRINT 23, STN(IO)
   23 FORMAT (1H1/3X, 31HOBSERVED ARRIVAL TIMES AT PITS.
     1/3X,31H------------------------------/3X,9HSTATION  ,A4/3X,13H---
     2----------)
      IF(VEL(IO) - 0.) 24, 25, 36
   36 PRINT 25, VEL(IO)
   25 FORMAT(//3X,50HOBSERVED ARRIVAL TIMES AT PITS HAVE BEEN CORRECTED/
     13X,41H----------------------------------------/3X,32HFOR ALTITUDE
     2 USING A VELOCITY OF,F6.0,8HFEET/SEC/3X,32H----------------------
     3---------
     4/3X,35HTHE LOWEST PIT BEING TAKEN AS REFERENCE
     5/3X,39H---------------------------------------
     6/3X)
      GO TO 28
   24 PRINT 34
   34 FORMAT (/55X, 24HONSET TIME AT PITS(SECS)
     1/55X, 24H------------------------)
   28 DO 30 IZ = 1, N9
      NLOW = (IZ -1)*9 + KEVENT
      NHY = NLOW + 8
      IF (NHY.GT.LEVENT)NHY = LEVENT
      PRINT 29, (EVENT(K), K = NLOW, NHY)
   29 FORMAT (//5X, 3HPIT, 9(4X, A8)/)
      DO 35 J = 1, NLIM
      PRINT32, PIT(IO,J),(AT(IO,K,J),AIND(K,J),K = NLOW, NHY)
   32 FORMAT (6X, A3, 9(3X, F8.3, A1))
   35 CONTINUE
   30 CONTINUE
      IO = IO + 1
      KEVENT = KEVENT + NE(IO - 1)
      LEVENT = LEVENT + NE(IO)
   14 CONTINUE
C
C
C     SETS UP NORMAL EQUATIONS
      CALL NORMAL
C     ************
C     INVERTS NORMAL EQUATIONS
      CALL SOLVE
C     ***********
C     OUTPUTS RESULTS.
      CALL RESIDL




C     ************
      GO TO(200,300) IBODG
C     THIS SUBROUTINE PLOTS THE GRAPHS ONLY.
  200 CALL GRAPH
C     ***********
C
C
C
C
      CALL SECCLK(TF)
      TS=TF-TS
      PRINT 227,TS
  227 FORMAT(////15X,20HTIME TAKEN FOR JOB =,F7.3,7HSECONDS)
C
  300 RETURN
      END
T        SUBTYPE,FORTRAN,LMAP,LSTRAP
C
C
C
      SUBROUTINE DEPTHA(H, X, XC, N)
C     ******************************
C
C     COMPUTES THE CORRECTED EPICENTRAL DISTANCE(XC) FROM THE OLD
C     DISTANCE(X) FOR AN EVENT AT A DEPTH(H). (N) IS THE NO.OF EVENTS.
C     THE STRUCTURE USED IS THAT OF HERRIN (1968), IE.
C
C                       C. KMS.  ****************************************
C
C                                          6.    KM/SEC.
C
C                      15. KMS.  ****************************************
C
C                                          6.75 KM/SEC.
C
C                      40. KMS. *****************************************
C
C                                          8.049KM/SEC.
C
C
      COMMON /TTCVS/ TIMEH(105), AMPV(24), TIMEJ(112), SLOWH(109)
      DIMENSION H(N), X(N), XC(N), RH(500)
C
      RADIUS = 6371.028
      ATOK = 1./111.19533839
C
```

```
      V1 = 6.0
      H1 = 15.0
      V2 = 6.75
      H2 = 40.0
      V3 = 8.049
      R1 = RADIUS - H1
      R2 = RADIUS - H2
      DO 2 I = 1, N
      B1 = 0.
      B2 = 0.
      B3 = 0.
      D1 = 0.
      D2 = 0.
      D3 = 0.
      IND = IFIX(X(I)+0.5) + 1
      P = SLOWH(IND)*RADIUS*ATOK
      RH(I) = RADIUS - H(I)
      IF(H(I).GT.H1) GO TO 3
      B1 = ASIN(V1*P/RH(I))
      D1 = H(I)*TAN(B1)*ATOK
      XC(I) = X(I) + D1
      GO TO 2
C
 3    B1 = ASIN(V1*P/R1)
      D1 = H1*TAN(B1)*ATOK
      IF(H(I).GT.H2) GO TO 5
      B2 = ASIN(V2*P/RH(I))
      D2 = (H(I)-H1)*TAN(B2)*ATOK
      XC(I) = X(I) + D1 + D2
      GO TO 2
C
 5    B2 = ASIN(V2*P/R2)
      D2 = (H2-H1)*TAN(B2)*ATOK
      B3 = ASIN(V3*P/RH(I))
      D3 = (H(I)-H2)*TAN(B3)*ATOK
      XC(I) = X(I) + D1 + D2 + D3
 2    CONTINUE
      RETURN
      END
T        SUBTYPE,FORTRAN,LMAP,LSTRAP
C
C
C
      SUBROUTINE AAMIN(X, N, XMIN, I)
C     **********************************
C
C     THIS SUBPROGRAM FINDS THE MINIMUM OF THE ARRAY X(N)  =  XMIN(I).
C
      DIMENSION X(N), XMIN(I)
C
      KQ = 1
 5    KP = KQ
 2    IF (KQ - N) 3, 4, 4
 3    KQ = KQ + 1
      IF (X(KP) - X(KQ)) 2, 5, 5
 4    XMIN(I) = X(KP)
      RETURN
      END
T        SUBTYPE,FORTRAN,LMAP,LSTRAP
C
C
C
      SUBROUTINE NORMAL
C     *****************
C
C     THIS SUBROUTINE SETS UP THE NORMAL EQUATIONS DIRECTLY, (THE
C     EQUATIONS OF CONDITION ARE NOT FORMED).
C
C
      COMMON /AMATRX/ A(231,231)
      COMMON /ATT/ AT(4,120,2C)
      COMMON /BMATRX/ B(231)
      COMMON /EVENTT/ EVENT(120), NEVENT, NE(4), AZ(120), DELTA(120),
     1 INDEX(120)
      COMMON /PITT/ STN(4), PIT(4,20), X(4,20), Y(4,20), NPIT(4)
      COMMON /REST/ V(120), ENAME(120,3), VELOC(120), M
      COMMON /RNGE/ RANGE(3C), RINT, NP
      COMMON /SLV/ N, IMTREX, IRESID, IRSTRN, IVEL, IBOUG, IHOLD, ISTART
     1, IENDS, THOLD, SSTART, SENDS
      DIMENSION FACT(4,12C)
C
      PI = 4.*ATAN(1.)
      DTOR = PI/180.
      DATA BLANK(8H
      DO 1 I = 1, 231
      DO 2 J = 1, 231
      A(I,J) = 0.
 2    CONTINUE
 1    CONTINUE
      N = 80 + NEVENT + NP
```

```
      NO = N + 1
      NP = NP + 1
      I = 1
      KPIT = 1
      LPIT = NPIT(1)
      KEVENT = 1
      LEVENT = NE(1)
      M = 0                1
 12   K = KEVENT
 11   IF(K-LEVENT)3,3,4
 3    JA = 70 + 5
C
C     ****************************************************************
C
C                              SELECTS CORRECT DISTANCE RANGE FOR EVENT.
C
      IF (DELTA(K).GT.RANGE(1).AND.DELTA(K).LE.RANGE(NP)) GO TO 5
      PRINT 6, DELTA(K), RANGE(1), RANGE(NP)
 6    FORMAT (/4X, 22HJOB REJECTED, DISTANCE, F6.2, 48HDEGREES LIES OUTS
     1IDE RANGE OF DISTANCE SPECIFIED/4X, 9HWHICH WAS, F6.2, 1X,   2HTO,
     2 F6.2, 7HDEGREES)
      CALL EXIT
 5    DO 7 JD = 2, NP
      IF (DELTA(K).GT.RANGE(JD-1).AND.DELTA(K).LE.RANGE(JD)) GO TO 8
 7    CONTINUE
 8    JD = JC - 1
      JB = 80 + NEVENT + JD
      INDEX(K) = JB
      THETA = AZ(K)*DTOR
      DO 9 J = KPIT, LPIT
      JE = J - KPIT + 1
      IF (AT(I,K,JE).EQ.0.) GO TO 9
      FACT(I,JE)= X(I,JE)*SIN(THETA) + Y(I,JE)*COS(THETA)
      FACT(I,JE) = -FACT(I,JE)
      L = J
      IF (I.EQ.4.AND.JE.GE.11) L = L - 5
C
C     ****************************************************************
C
C                              FORMS NORMAL EQUATIONS.
C
      A(L,L) = A(L,L) + 1.
      A(L,JA) = A(L,JA) + 1.
      A(L,JB) = A(L,JB) + FACT(I,JE)
      A(L,NO) = A(L,NO) + AT(I,K,JE)




      A(JA,JA) = A(JA,JA) + 1.
      A(JA,JB) = A(JA,JB) + FACT(I,JE)
      A(JA,NO) = A(JA,NO) + AT(I,K,JE)
      A(JB,JB) = A(JB,JB) + FACT(I,JE)*FACT(I,JE)
      A(JB,NO) = A(JB,NO) + FACT(I,JE)*AT(I,K,JE)
C
      M = M + 1
 9    CONTINUE
      K = K + 1
      GO TO 11
 4    I = I + 1
C
C     ****************************************************************
C
C                              SETS UP CONDITION  SUM S(J) = 0.
C
      CALL ADDER(KPIT,LPIT)
C     **********************
      IF (I.GT.4) GO TO 10
      KPIT = KPIT + NPIT(I - 1)
      LPIT = LPIT + NPIT(I)
      KEVENT = KEVENT + NE(I - 1)
      LEVENT = LEVENT + NE(I)
      GO TO 12
C
C
C     ****************************************************************
C                              RESTRAINING SWITCHES, SEE INSTRUCTION 4.
C
 10   GO TO (23,24)IRSTRN
 24   CALL JBTIME(NEVENT, N)
 23   GO TO (26, 27) IHOLD
 27   CALL TTTIME(NEVENT)
 26   GO TO (28, 29) ISTART
 29   CALL SHOLDS(NEVENT)
 28   GO TO (30, 31) IENDS
 31   CALL SHOLDF(NEVENT)
 30   DO 15 I = 1, N
      DO 16 J = I, N
      A(J,I) = A(I,J)
 16   CONTINUE
 15   CONTINUE
      NP = NP - 1
      DO 19 I = 1, N
      B(I) = A(I,NO)
```

```
 19   CONTINUE
C
C     ******************************************************************
C
C                              PRINTS NORMAL EQUATIONS IF REQUESTED.
      GO TO (17, 18) IMTREX
 18   PRINT 14
 14   FORMAT (1H1/3X, 16HNORMAL EQUATIONS/3X, 16H================)
      DO 25 I = 1, N
      PRINT 13, (A(I,J), J = 1, NU)
 13   FORMAT (1X, 12F10.5)
 25   CONTINUE
      GO TO 17
C
 17   RETURN
      END
T        SUBTYPE,FORTRAN,LMAP,LSTRAP
C
C
C
      SUBROUTINE ADDER(NL, NH)
C     ************************
C
C     THIS SUBROUTINE ADDS 1. TO THE UPPER DIAGONAL OF THE ARRAY A(N,N).
C
      COMMON /AMATRX/ A(231,231)
C
      DO 1  I = NL, NH
      DO 2 J = 1, NH
      A(I,JJ = A(I,J) + 1.
 2    CONTINUE
 1    CONTINUE
      RETURN
      END
T        SUBTYPE,FORTRAN,LMAP,LSTRAP
C
C
C
      SUBROUTINE SHOLDS(NEVENT)
C     *************************
C
C     THIS SUBROUTINE RESTRAINS THE SLOWNESS IN THE FIRST DISTANCE
C     INTERVAL TO = SSTART.
C
      COMMON /AMATRX/ A(231,231)
      COMMON /SLV/ N, IMTREX, IRESID, IRSTRN, IVEL, IBODG, IHOLD, ISTART
     1, IENDS, THOLD, SSTART, SENDS
C
      HUGE = 1.0E+5
      DTOK = 111.19533839
      I1 = 80 + NEVENT + 1
      NO = N + 1
      A(I1,I1) = A(I1,I1) + HUGE
      A(I1,NO) = A(I1,NO) + SSTART*HUGE/DTOK
      RETURN
      END
T        SUBTYPE,FORTRAN,LMAP,LSTRAP
C
C
C
      SUBROUTINE SHOLDF(NEVENT)
C     *************************
C
C     THIS SUBROUTINE RESTRAINS THE SLOWNESS IN THE LAST DISTANCE
C     INTERVAL TO = SENDS.
C
      COMMON /AMATRX/ A(231,231)
      COMMON /SLV/ N, IMTREX, IRESID, IRSTRN, IVEL, IBODG, IHOLD, ISTART
     1, IENDS, THOLD, SSTART, SENDS
C
      HUGE = 1.0E+5
      DTOK = 111.19533839
      NO = N + 1
      A(N,N) = A(N,N) + HUGE
      A(N,NO) = A(N,NO) + SENDS*HUGE/DTOK
      RETURN
      END
T        SUBTYPE,FORTRAN,LMAP,LSTRAP
C
C
C
      SUBROUTINE JBTIME(NEVENT, N)
C     ****************************
C
C     THIS SUBROUTINE RESTRAINS THE TOTAL TIME ACROSS NP INTERVALS TO
C     THE J.B. VALUE.
C
      COMMON /AMATRX/ A(231,231)
      COMMON /RNGE/ RANGE(30), RINT, NP
      COMMON /TJCVS/ TIMEH(109), AMPV(24), TIMEJ(112), SLOWH(109)
```

```
      DTOK = 111.19533839
C
      ISTRT = RANGE(1)
      IFINN = RANGE(NP)
      I1 = 80 + NEVENT + 1
      NO = N + 1
      DO 1 I = I1, N
      I2 = I - 80 - NEVENT
      DO 2 J = I, N
      I3 = J - 80 - NEVENT
      A(I,J) = A(I,J) + (RANGE(I2+1)-RANGE(I2))*(RANGE(I3+1)-RANGE(I3))*
     1DTOK*DTOK
    2 CONTINUE
      A(I,NO) = A(I,NO) + (RANGE(I2+1)-RANGE(I2))*(TIMEJ(IFINN)-
     1 TIMEJ(ISTRT))*DTOK
    1 CONTINUE
      RETURN
      END
T        SUBTYPE,FORTRAN,LMAP,LSTRAP
C
C
C
      SUBROUTINE TTTIME(NEVENT)
C     ************************
C
C     THIS SUBROUTINE RESTRAINS THE TOTAL TIME ACROSS NP INTERVALS TO
C     A VALUE = THOLD (SECS).
C
      COMMON /AMATRX/ A(231,231)
      COMMON /RNGE/ RANGE(80), RINT, NP
      COMMON /SLV/ N, IMTREX, IRESID, IRSTRN, IVEL, IBODG, IHOLD, ISTART
     1, IENDS, THOLD, SSTART, SENDS
      DTOK = 111.19533839
C
      I1 = 80 + NEVENT + 1
      NO = N + 1
      DO 1 I = I1, N
      I2 = I - 80 - NEVENT
      DO 2 J = I, N
      I3 = J - 80 - NEVENT
      A(I,J) = A(I,J) + (RANGE(I2+1)-RANGE(I2))*(RANGE(I3+1)-RANGE(I3))*
     1DTOK*DTOK
    2 CONTINUE
      A(I,NO) = A(I,NO) + (RANGE(I2+1)-RANGE(I2))*THOLD*DTOK
    1 CONTINUE




      RETURN
      END
T        SUBTYPE,FORTRAN,LMAP,LSTRAP
C
C
C
      SUBROUTINE TIMOUT(I,K,J)
C     ************************
C
C     THIS SUBROUTINE REMOVES THE EFFECT OF THE HERRIN SLOWNESS FROM
C     EACH ARRAYFOR EACH EVENT. THE HERRIN TIME CONTRIBUTION AT AN ARRAY
C     IS SUBTRACTED FROM EACH PIT FOR EACH EVENT AT ITS PARTICULAR
C     DISTANCE. -APVA- THEN EFFECTIVELY CALCULATES THE SLOWNESS DEFECT.
C
      COMMON /ATT/ AT(4,120,20)
      COMMON /EVENTT/ EVENT(120), NEVENT, NE(4), AZ(120), DELTA(120),
     1 INDEX(120)
      COMMON /PITT/ STN(4), PIT(4,20), X(4,20), Y(4,20), NPIT(4)
      COMMON /SLV/ N, IMTREX, IRESID, IRSTRN, IVEL, IBODG, IHOLD, ISTART
     1, IENDS, THOLD, SSTART, SENDS
      COMMON /TTCVS/ TIMEP(109), AMPV(24), TIMEJ(112), SLOWH(109)
      DIMENSION FACT(4,20)
C
      PI = 4.*ATAN(1.)
      RTOD = 180./PI
      ATOD = 1./111.19533839
C
      IDELT = IFIX(DELTA(K) + 0.5)
      THETA = AZ(K)/RTOD
      FACT(I,J) = X(I,J)*SIN(THETA) + Y(I,J)*COS(THETA)
      AT(I,K,J) = AT(I,K,J) - SLOWH(IDELT)*FACT(I,J)*ATOD
      RETURN
      END
T        SUBTYPE,FORTRAN,LMAP,LSTRAP
C
C
C
      SUBROUTINE SOLVE
C     ****************
C
C     THIS SUBPROGRAM INVERTS THE NORMAL EQUATIONS.
C
C     THE METHOD USED IS CALLED  TRIANGULAR DECOMPOSITION
C        FROM N.P.L. MODERN COMPUTING METHODS
C
```

```
C         BASED ON LIBRARY SUBROUTINE MB01A
C
      COMMON /AMATRX/ A(231,231)
      COMMON /BMATRX/ B(231)
      COMMON /RJST/ X(231), D(231)
      COMMON /RNGE/ RANGE(3C), RINT, NP
      COMMON /SLV/ M, IMTREX, IRESID, IRSTRN, IVEL, IBODG, IHOLD, ISTART
     1, IENDS, THOLD, SSTART, SENDS
      DIMENSION IND(231), C(231)
C
  100 AMAX=0.0                                                    MB01A003
      DO 2 I=1,M                                                  MB01A004
      IND(I)=I                                                    MB01A005
      IF(ABS (A(I,1))-AMAX)2,2,3                                  MB01A006
    3 AMAX=ABS (A(I,1))                                           MB01A007
      I4=I                                                        MB01A008
    2 CONTINUE                                                    MB01A009
      MM=M-1                                                      MB01A010
      DO 111 J=1,MM                                               MB01A011
      IF(I4-J)6,6,4                                               MB01A012
    4 ISTO=IND(J)                                                 MB01A013
      IND(J)=IND(I4)                                              MB01A014
      IND(I4)=ISTO                                                MB01A015
      DO 5 K=1,M                                                  MB01A016
      STO=A(I4,K)                                                 MB01A017
      A(I4,K)=A(J,K)                                              MB01A018
      A(J,K)=STO                                                  MB01A019
    5 CONTINUE                                                    MB01A020
    6 AMAX=0.0                                                    MB01A021
      J1=J+1                                                      MB01A022
      DO 11 I=J1,M                                                MB01A023
      A(I,J)=A(I,J)/A(J,J)                                        MB01A024
      DO 10 K=J1,M                                                MB01A025
      A(I,K)=A(I,K)-A(I,J)*A(J,K)                                 MB01A026
      IF (K-J1)14,14,10                                           MB01A027
   14 IF(ABS (A(I,K))-AMAX)10,10,17                               MB01A028
   17 AMAX=ABS (A(I,K))                                           MB01A029
      I4=I                                                        MB01A030
   10 CONTINUE                                                    MB01A031
   11 CONTINUE                                                    MB01A032
  111 CONTINUE                                                    MB01A033
   65 DO 140 I1=1,MM                                              MB01A034
      I=M+1-I1                                                    MB01A035
      I2=I-1                                                      MB01A036
      DO 41 J1=1,I2                                               MB01A037

      J=I2+1-J1                                                   MB01A038
      J2=J+1                                                      MB01A039
      W1=-A(I,J)                                                  MB01A040
      IF(I2-J2)141,43,43                                          MB01A041
   43 DO 42 K=J2,I2                                               MB01A042
      W1=W1-A(K,J)*C(K)                                           MB01A043
   42 CONTINUE                                                    MB01A044
  141 C(J)=W1                                                     MB01A045
   41 CONTINUE                                                    MB01A046
      DO 40 K=1,I2                                                MB01A047
      A(I,K)=C(K)                                                 MB01A048
   40 CONTINUE                                                    MB01A049
  140 CONTINUE                                                    MB01A050
      DO 150 I1=1,M                                               MB01A051
      I=M+1-I1                                                    MB01A052
      I2=I+1                                                      MB01A053
      W=A(I,I)                                                    MB01A054
      DO 56 J=1,M                                                 MB01A055
      IF (I-J)52,53,54                                            MB01A056
   52 W1=0.0                                                      MB01A057
      GO TO 55                                                    MB01A058
   53 W1=1.0                                                      MB01A059
      GO TO 55                                                    MB01A060
   54 W1=A(I,J)                                                   MB01A061
   55 IF(I1-1)156,156,57                                          MB01A062
   57 DO 58 K=I2,M                                                MB01A063
      W1=W1-A(I,K)*A(K,J)                                         MB01A064
   58 CONTINUE                                                    MB01A065
  156 C(J)=W1                                                     MB01A066
   56 CONTINUE                                                    MB01A067
      DO 50 J=1,M                                                 MB01A068
      A(I,J)=C(J)/W                                               MB01A069
   50 CONTINUE                                                    MB01A070
  150 CONTINUE                                                    MB01A071
      DO 60 I=1,M                                                 MB01A072
   63 IF(IND(I)-I)61,60,61                                        MB01A073
   61 J=IND(I)                                                    MB01A074
      DO 62 K=1,M                                                 MB01A075
      STO=A(K,I)                                                  MB01A076
      A(K,I)=A(K,J)                                               MB01A077
      A(K,J)=STO                                                  MB01A078
   62 CONTINUE                                                    MB01A079
      ISTO=IND(J)                                                 MB01A080
      IND(J)=J                                                    MB01A081
      IND(I)=ISTO                                                 MB01A082
```

```
      GO TO 63                                                          MB01A083
   60 CONTINUE                                                          MB01A084
C
 64   DO 66 J=1,M
      STO=0.
      DO 67 I=1,M
      STO=STO+A(I,J)*B(I)
 67   CONTINUE
      X(J)=STO
      D(J)=A(J,J)
 66   CONTINUE
C
C     PRINTS OUT THE MATRIX IF REQUIRED.
      GO TO (68, 102) IMTREX
 102  CONTINUE
      PRINT 80
 80   FORMAT (1H1/3X, 15HINVERTED MATRIX/3X, 15H===============)
      DO 81 J = 1, M
      PRINT 82, (A(I,J), I = 1, M), B(J)
 82   FORMAT (1X, 12F10.5)
 81   CONTINUE
      PRINT 21, (X(J), D(J), J = 1, M)
 21   FORMAT (//10X, 4HX(J), 10X, 17HDIAGONAL ELEMENTS/(2X, F15.5,
     1 9X, F15.5))
C
C     THE FOLLOWING PRINTS THE MATRIX REQUIRED FOR THE COVARIANCES.
      PRINT 83
 83   FORMAT (1H1/3X, 17HCOVARIANCE MATRIX/3X, 17H=================)
      PRINT 88, M, NP
 88   FORMAT (1X, 3HM =, F10.5, 5X, 4HNP =, F10.5)
      M = M - 1
      MM = M - NP + 1
      DO 87 J = MM, M
      PRINT 86, (A(I,J), I = MM, M)
 86   FORMAT (1X, 12F10.5)
 87   CONTINUE
 68   CONTINUE
C
C     STORE MATRIX ON DISC
      DO 84 J = MM, M
      WRITE(24) (A(I,J), I = MM, M)
 84   CONTINUE
      REWIND 24
      M = M + 1
      RETURN




      END
T        SUBTYPE,FORTRAN,LMAP,LSTRAP
C
C
C
      SUBROUTINE RESIDL
C     *****************
C
C
C
C     THIS SUBROUTINE CALCULATES THE RESULTS FROM THE INVERTED MATRIX.
C
C
      COMMON /AMATRX/ RESID(4,120,20), CT(4,120,20), FACT(4,120),
     1 CONST(120), VELC(50,4), DLT(50,4), TVELOC(120), ERR(120),
     2 CVM(120,120), COV(120,120), AIND(120), PS(260), PNS(260), PV(260)
     3, PNV(260), VBAR(120), TJB(112), TAT(112), VELH(109), TH(109),
     4SLOW(260), TDIFF(112), DIST(80),  PVEL(80),  ERLO(80),  ERHY(80),
     5 TPVEL(80), DDIST(80), TERLO(80), TERHY(80), EELO(80), VHERIN(30),
     6 SHERIN(30), ARANGE(30)
      COMMON /ATT/ AT(4,120,20)
      COMMON /EVENTT/ EVENT(120), NEVENT, NE(4), AZ(120), DELTA(120),
     1 INDEX(120)
      COMMON /GRFF/ TITLE(20), XMAX, XMIN,YMAX, YMIN, INDX, INDY, IND,
     1IDOT, INSTR1, XLIMIT, YLIMIT, SCALX, SCALY
      COMMON /PITT/ STN(4), PIT(4,20), X(4,20), Y(4,20), NPIT(4)
      COMMON /REST/ V(120), ENAME(120,3), VELOC(120), M
      COMMON /RJST/ S(231), D(231)
      COMMON /RNGE/ RANGE(30), RINT, NP
      COMMON /SLV/ N, IMTREX, IRESID, IRSTRN, IVEL, IBODG, IHCLD, ISTART
     1, IENDS, THOLD, SSTART, SENDS, IPUNCH
      COMMON /STATS/ ST(57)
      COMMON /TTCVS/ TIMEH(109), AMPV(24), TIMEJ(112), SLOWH(109)
C
      PI = 4.*ATAN(1.)
      RTOD = 180./PI
      DTOK = 111.19533839
      ATOD = 1./111.19533839
      REAL INSTR1
      DATA STAR(8H*       )
      DATA BLANK(8H       )
C
      CALL SDATE(DATE)
C     SET ARRAYS TO ZERO
      DO 1 J = 1, 20
      DO 2 K = 1, 120
```

```
      AIND(K) = 0.
      DO 3 I = 1, 4
      RESID(I,K,J) = 10000.
      CT(I,K,J) = 0.
    3 CONTINUE
    2 CONTINUE
    1 CONTINUE
      NO = N + 1
C
C     ****************************************************************
C                              CALCULATES RESIDUALS, CORRECTED ONSETTIMES
C
C      SELECT ARRAY
      I = 1
      KPIT = 1
      LPIT = NPIT(1)
      KEVENT = 1
      LEVENT = NE(1)
      SUM = 0.
      ADD = 0.
C
C      SELECT EVENT
    7 DO 4 K = KEVENT, LEVENT
      KA = K - KEVENT + 1
      THETA = AZ(K)/RTOD
      JA = 80 + K
      II = INDEX(K)
      T1 = 0.
      F1 = 0.
      F2 = 0.
      P1 = 0.
      FT = 0.
C
C      SELECT PIT
      DO 5 J = KPIT, LPIT
      JE = J - KPIT + 1
      FACT(I,JE) = X(I,JE)*SIN(THETA) + Y(I,JE)*COS(THETA)
      FACT(I,JE) = - FACT(I,JE)
      IF(AT(I,K,JE).EQ.0.) GO TO 5
      L = J
      CT(I,K,JE)=  S(II)*FACT(I,JE) + S(L) + S(JA)
      RESID(I,K,JE) = AT(I,K,JE) - CT(I,K,JE)
      SUM = SUM + RESID(I,K,JE)*RESID(I,K,JE)
      ADD = ADD + RESID(I,K,JE)
      AT(I,K,JE) = AT(I,K,JE) - S(L) - S(JA)




      T1 = T1 + AT(I,K,JE)
      F1 = F1 + FACT(I,JE)
      F2 = F2 + FACT(I,JE)*FACT(I,JE)
      P1 = P1 + 1.
      FT = FT + AT(I,K,JE)*FACT(I,JE)
    5 CONTINUE
      CONST(K) = (F2*T1-F1*FT)/(F2*P1-F1*F1)
      VELOC(K) = F2/FT
      VELC(KA,I) = VELOC(K)
      DLT(KA,I) = DELTA(K)
      TVELOC(K) = DTOK/VELOC(K)
    4 CONTINUE
C
C     ****************************************************************
C
      GO TO (100,101) IRESID
C     PUNCHES  (PIT CORRECTIONS + RESIDUALS)
  101 CALL SINCRV(KPIT, LPIT, KEVENT, LEVENT, I)
C     ********************************************
  100 GO TO (114,115) IPUNCH
C     PUNCHES (RESIDUALS)
  115 CALL RESOUT(KPIT, LPIT, KEVENT, LEVENT, I)
C     ********************************************
C
  114 I = I + 1
      IF (I.GT.4) GO TO 6
      KPIT = KPIT + NPIT(I - 1)
      LPIT = LPIT + NPIT(I)
      KEVENT = KEVENT + NE(I - 1)
      LEVENT = LEVENT + NE(I)
      GO TO 7
    6 CONTINUE
C
C     PUNCHES (DISTANCE,SLOWNESS,PHASE VELOCITY,EVENT CODE)
      GO TO (102,103) IVEL
  103 PUNCH 104, (DELTA(I),TVELOC(I),VELOC(I),EVENT(I),I = 1, NEVENT)
  104 FORMAT (5X, 3F10.5, 24X, A8)
C     PRINTS OUT RESULTS FOR INDIVIDUAL EVENTS.
  102 CALL OUTPUT
C     ***********
C
C     ****************************************************************
C
C                              PRINTS OUT RESIDUALS OF (OBSERVED - CALCULA
C                              TED) ONSET TIME FOR EACH EVENT AT EACH
```

```
C                                SEISMOMETER.
C
      I = 1
      KEVENT = 1
      LEVENT = NE(I)
   14 NLIM = NPIT(I)
      MEVENT = NE(I)
      N9 = (MEVENT - 1)/9 + 1
      PRINT 8, STN(I)
    8 FORMAT (1H1/4X, 23HTABLE OF RESIDUALS FOR ,A3/4X, 26H----------
     1----------)
      DO 9 IZ = 1, N9
      NLOW = (IZ - 1)*9 + KEVENT
      NHY = NLOW + 8
      IF (NHY.GT.LEVENT)NHY = LEVENT
      PRINT 10, (EVENT(K), K = NLOW, NHY)
   10 FORMAT (//5X, 3HPIT, 9(4X, A8)/)
      DO 11 J = 1, NLIM
      DO 87 K = NLOW, NHY
      AIND(K) = STAR
      IF(RESID(I,K,J).EQ.10000.) AIND(K) = BLANK
   87 CONTINUE
      PRINT 12, PIT(I,J), (RESID(I,K,J), AIND(K), K = NLOW, NHY)
   12 FORMAT (6X, A3, 9(3X, F8.3, A1))
   11 CONTINUE
    9 CONTINUE
      I = I + 1
      IF (I.GT.4) GO TO 13
      KEVENT = KEVENT + NE(I - 1)
      LEVENT = LEVENT + NE(I)
      GO TO 14
   13 CONTINUE
C
C     **********************************************************************
C
C
C                              PRINTS OUT CALCULATED ONSET TIMES FOR EACH
C                              EVENT AT EACH SEISMOMETER.
C
      I = 1
      KEVENT = 1
      LEVENT = NE(I)
   37 NLIM = NPIT(I)
      MEVENT = NE(I)
      N9 = (MEVENT - 1)/9 + 1
      PRINT 38, STN(I)

   38 FORMAT (1H1/4X,  36HTABLE OF CALCULATED ONSET TIMES FOR ,A3/4X,
     1 39H----------------------------------------)
      DO 39 IZ = 1, N9
      NLOW = (IZ - 1)*9 + KEVENT
      NHY = NLOW + 8
      IF (NHY.GT.LEVENT) NHY = LEVENT
      PRINT 40, (EVENT(K), K = NLOW, NHY)
   40 FORMAT (//5X, 3HPIT, 9(4X, A8)/)
      DO 41 J = 1, NLIM
      DO 90 K = NLOW, NHY
      AIND(K) = STAR
      IF(RESID(I,K,J).EQ.10000.) AIND(K) = BLANK
   90 CONTINUE
      PRINT 42, PIT(I,J), (CT(I,K,J), AIND(K), K = NLOW, NHY)
   42 FORMAT (6X, A3, 9(3X, F8.3, A1))
   41 CONTINUE
   39 CONTINUE
      I = I + 1
      IF(I.GT.4) GO TO 43
      KEVENT = KEVENT + NE(I - 1)
      LEVENT = LEVENT + NE(I)
      GO TO 37
   43 CONTINUE
C
C     **********************************************************************
C
C
C                              COMPUTES STATISTICS AND 95 PCCL.
C
      DF = FLOAT(M - N)
      MDF = DF
      IF (MDF.LT.30) GO TO 19
      IF (MDF.GE.300) GO TO 20
      MDF = MDF/10 + 27
      GO TO 19
   20 MDF = 57
   19 T = ST(MDF)
      SUMSQ = SUM
      AVSQ = SUMSQ/DF
      SD = T*SQRT(AVSQ)/2.
      DO 21 I = 1, N
      ERR(I) = T*SQRT(AVSQ*D(I))
   21 CONTINUE
      PRINT 22
   22 FORMAT (1H1/4X, 33HCONFIDENCE LIMITS ON ALL UNKNOWNS
     1/4X, 33H--------------------------------
```

```
     2//30X, 3HEKA, 32X, 3HYKA, 32X, 3HNRA
     3//8X, 3HPIT,   10X, 11HCORRECTIONS, 4X, 10HCON.LIMITS, 10X,
     411HCORRECTIONS, 4X, 10HCON.LIMITS, 10X, 11HCORRECTIONS, 4X,
     5 10HCON.LIMITS
     6/38X, 6H* OR -, 29X, 6H* OR -, 29X, 6H* OR -)
C
C     ******************************************************************
C
C                          }
C                            PRINTS OUT PIT CORRECTIONS AND 95 PCCL.
C
      DO 23 I = 1, 20
      J = I + 20
      K = J + 20
      PRINT 24, PIT(1,I), S(I), ERR(I), S(J), ERR(J), S(K), ERR(K)
 24   FORMAT (8X, A3, 3(1CX, F10.5, 5X, F8.3, 2X))
 23   CONTINUE
      PRINT 25
 25   FORMAT (//30X, 3HGBA//8X, 3HPIT, 10X, 11HCORRECTIONS, 4X,
     1 10HCON.LIMITS/38X, 6H* OR -)
      DO 26 I = 1, 20
      J = I + 60
      PRINT 27, PIT(4,I), S(J), ERR(J)
 27   FORMAT (8X, A3, 10X, F10.5, 5X, F8.3)
 26   CONTINUE
C
C     ******************************************************************
C
C
C                            PRINTS OUT CONSTANTS,VELOCITY,SLOWNESS WITH
C                            95 PCCL FOR EACH EVENT.
      PRINT 29
 29   FORMAT (////6X, 5HEVENT, 7X, 10HCONSTANT C,  7X, 6H* OR -, 12X,
     1 10H1/VELOCITY, 7X, 6H* OR -, 8X, 8HVELOCITY, 8X,14HV LIES BETWEEN
     2,6X, 8HDISTANCE/)
C
      DO 30 JP = 1, NEVENT
      JQ = 80 + JP
      II = INDEX(JP)
      VBAR(JP) = 1./S(II)
      PS(II) = S(II) + ERR(II)
      PNS(II) = S(II) - ERR(II)
      PV(II) = 1./PS(II)
      PNV(II) = 1./PNS(II)
      PRINT 31, JP, EVENT(JP), S(JQ), ERR(JQ), S(II), ERR(II), VBAR(JP),
     1 PV(II), PNV(II), DELTA(JP)
 31   FORMAT (1X, I3, 2X, A8, 4X, F8.3, 7X, F8.3, 12X, F9.4, 6X,
     1 F9.4, 6X, F8.2, 5X, F8.2, 2X, 4H AND,F8.2,4X,F5.1)
 30   CONTINUE
      PRINT 29
C
C     ******************************************************************
C
C
C                            PRINTS DT/DX - X TABLE WITH 95PCCL
C
      PRINT 32
 32   FORMAT (1H1/3X, 34HTABLE OF DISTANCE AGAINST VELOCITY/3X,
     1 34H----------------------------------//10X, 18HDISTANCE (DEGREES)
     2, 5X, 17HVELOCITY (KM/SEC), 5X, 14HV LIES BETWEEN, 8X, 24HHERRIN V
     3ELOCITY (KM/SEC),          6X, 19HSLOWNESS (SECS/DEG)/)
      DO 61 I = 1, 112
      TJB(I) = 0.
      TAT(I) = 0.
 61   CONTINUE
      NP = NP + 1
      EE = 0.
      TT = 0.
      I4 = RANGE(1)
      AA = TIMEJ(I4)
      TAT(1) = S(NEVENT+71)*(RANGE(2)-RANGE(1))*DTDK + AA
      DO 33 I = 2, NP
      I2 = I - 1
      I3 = I2 + 70 + NEVENT
      I4 = RANGE(I2)
      I5 = 2*I2 - 1
      I6 = RANGE(I)
      TT = TT + S(I3)*(RANGE(I2+1) - RANGE(I2))
      EE = EE + ERR(I3)*(RANGE(I2+1) - RANGE(I2))
      VBAR(I3) = 1./S(I3)
      TPVEL(I3) = S(I3)*DTDK
      EELO(I3) = ERR(I3)*DTDK
      VELH(I4) = DTDK/SLOWH(I4)
      VHERIN(I2) = VELH(I4)
      SHERIN(I2) = SLOWH(I4)
      ARANGE(I2) = RANGE(I2+1)
      TAT(I2+1) = TAT(I2) + S(I3+1)*(RANGE(I+1)-RANGE(I))*DTDK
      TJB(I2) = TIMEJ(I4)
      TJB(I2+1) = TIMEJ(I6)
      TH(I2) = TIMEH(I4)
      TH(I2+1) = TIMEH(I6)
      TDIFF(I2) = TAT(I2) - TJB(I2+1)
      PRINT 34, RANGE(I2), VELH(I4),  VBAR(I3), PV(I3), PNV(I3),
```

```
     1 TPVEL(I3), EELO(I3)
  34   FORMAT (17X, F5.1, 64X, F8.2  /35X, F8.2, 4X, F8.2, 2X,
     1 4H AND, F8.2, 38X, F6.3,5H +OR-, F5.3)
  33   CONTINUE
       INP = RANGE(NP)
       VELH(INP) = DTOK/SLOWH(INP)
       PRINT 34, RANGE(NP), VELH(INP)
       TJB(NP) = TIMEJ(INP)
       TH(INP) = TIMEH(INP)
C
C      **********************************************************************
C
C                              PRINTS(OBSERVED - J.B.)TRAVEL TIMES
C
       PRINT 211, RANGE(1)
  211  FORMAT (1H1/3X, 78HTABLE OF DIFFERENCES FROM J.B. TRAVEL TIMES (J.
     1B. - CALCULATED) NORMALISED TO , F5.1, 1X, 7HDEGREES/3X, 91H------
     2----------------------------------------------------------------
     3------------------//)
       PRINT 209
  209  FORMAT (10X, 18HDISTANCE (DEGREES), 5X, 22HTIME DIFFERENCE (SECS)/
     1)
       PRINT 210, (ARANGE(I), TDIFF(I), I = 1, NP)
  210  FORMAT (17X, F5.1, 13X, F6.3)
       NP = NP + 1
       DIS = RANGE(NP) - RANGE(1)
       DIFJ = TJB(NP) - TJB(1)
       DIFH = TH(NP) - TH(1)
       EEE = EE*DTOK
       TTT = TT*DTOK
       PRINT 48, DIS, TTT,EEE, DIFJ, DIFH
  48   FORMAT (////19X, 29HTHE TOTAL TRAVEL TIME ACROSS ,I3, 1X,
     1 12HDEGREES IS =,F8.2, 1X, 5H+OR- ,   F4.2, 1X, 5HSECS./57X,
     2 7H(J.B. =,F8.2, 1X, 5HSECS)/48X,16H(HERRIN (1968) =, F8.2, 1X,
     3 5HSECS))
       GO TO (204,205)IRSTRN
  205  PRINT 206
  206  FORMAT (53X, 28H**RESTRAINED TO J.B. VALUE**)
  204  NP = NP - 1
C
C      **********************************************************************
C
C                              CALCULATES COVARIANCE DT/DX MATRIX AND
C                              PRINTS WITH STATISTICS.
C
       PRINT 59
  59   FORMAT (1H1/3X, 11HCOVARIANCES/3X, 11H===========)
       N = N - 1
       MM = N - NP + 1
       DO 64 J = 1, 120
       DO 65 I = 1, 120
       COV(I,J) = 0.
  65   CONTINUE
  64   CONTINUE
       NN = N - MM + 1
       DO 68 J = 1, NN
       READ(24) (CVM(I,J), I = 1, NN)
  68   CONTINUE
       DO 55 J = 1, NN
       DO 56 I = 1, NN
       COV(I,J) = T*SQRT(AVSQ*(CVM(I,I) + CVM(J,J) - 2.*CVM(I,J)))
  56   CONTINUE
  55   CONTINUE
       DO 57 J = 1, NN
       PRINT 58, (COV(I,J), I = 1, J)
  58   FORMAT (1X, 12F10.5)
  57   CONTINUE
       N = N + 1
       PRINT 18, SUMSQ, AVSQ, SD, DF, N, T, ADD
  18   FORMAT (1H1///9X, 26HSUM OF SQUARED RESIDUALS =,F10.5
     1//9X, 26HAVERAGE SQUARED RESIDUAL =,F10.5
     2//15X, 20HSTANDARD DEVIATION =,F10.5
     3//5X, 30HNUMBER OF DEGREES OF FREEDOM =,I5
     4//15X, 20HNUMBER OF UNKNOWNS =,I5
     5//23X, 12HSTUDENTS T =,F6.2
     6//17X, 18HSUM OF RESIDUALS =,E20.10)
       RETURN
       END
T         SUBTYPE,FORTRAN,LMAP,LSTRAP
C
C
C
       SUBROUTINE OUTPUT
C      ******************
C
C      THIS SUBPROGRAM PRINTS OUT THE SLOWNESS FOR EACH INDIVIDUAL EVENT.
C
       COMMON /EVENTT/ EVENT(120), NEVENT, NE(4), AZ(120), DELTA(120),
     1 INDEX(120)
       COMMON /REST/ V(120), ENAME(120,3), VELOC(120), M
```

```
      COMMON /RJST/ S(231), D(231)
      DIMENSION VBAR(120), STC(120)
C
      RADIUS = 6371.028
      PI = 4.*ATAN(1.)
      RTOD = 180./PI
C
      PRINT 15
 15   FORMAT (1H1, 4X, 15HTABLE OF EVENTS/4X, 15H---------------////)
      PRINT 9
 9    FORMAT (    5X, 7HDATE OF, 12X, 8HLOCATION, 8X, 9HT-T SLOPE, 1X,
     1 7HUSCGS V, 2X, 8HUSCGS AZ, 2X, 8HLUMPED V, 2X, 8HLUMPED C, 2X,
     2 10HCORR. DIST, 2X, 9HINDIVID V, 2X,                        /6X,
     3 5HEVENT,29X, 9H(SEC/DEG), 2X, 6HKM/SEC, 3X, 6H(DEGS), 3X,
     4 8H(KM/SEC), 3X, 6H(SECS), 3X, 9H(DEGREES), 3X, 8H(KM/SEC))
      DO 10 JP = 1, NEVENT
      JQ = 80 + JP
      II = INDEX(JP)
      VBAR(JP) = 1./S(II)
      STC(JP) = RADIUS/(VBAR(JP)*RTOD)
      PRINT 13, JP, EVENT(JP), (ENAME(JP,I),I=1,3),STC(JP),V(JP),AZ(JP),
     1 VBAR(JP), S(JQ), DELTA(JP), VELOC(JP)
 13   FORMAT (1X, I3, 1X, A8, 2X, 3A8,-3X, F5.2, 4X, F5.1, 4X, F5.1,
     1 5X, F5.2, 4X, F6.3, 6X, F5.1, 6X, F5.2)
 10   CONTINUE
      PRINT 9
      RETURN
      END
T        SUBTYPE,FORTRAN,LMAP,LSTRAP
C
C
C
      SUBROUTINE SINCRV(KPIT, LPIT, KEVENT, LEVENT, I)
C     ************************************************
C
C     THIS SUBPROGRAM PUNCHES CARDS WITH (PIT CORRECTION + RESIDUAL)
C     AND ALSO PRINTS OUT WHEN INDICATOR IRESID = 1. (SEE INSTRUCTION 4)
C
      COMMON /AMATRX/ RESID(4,120,20)
      COMMON /ATT/ AT(4,120,20)
      COMMON /EVENTT/ EVENT(120), NEVENT, NE(4), AZ(120), DELTA(120),
     1 INDEX(120)
      COMMON /PITT/ STN(4), PIT(4,20), X(4,20), Y(4,20), NPIT(4)
      COMMON /RJST/ S(231), D(231)
C
      DO 3 J = KPIT, LPIT
      JE = J - KPIT + 1
      PUNCH 8, PIT(I,JE), STN(I)
      PRINT 8, PIT(I,JE), STN(I)
 8    FORMAT (6X, 19HRESIDUALS FOR PIT  , A3, 13H    AT ARRAY , A4)
      DO 4 K = KEVENT, LEVENT
      JA = 80 + K
      IF (AT(I,K,JE).EQ.0.) GO TO 4
      L = J
      IF (I.EQ.4.AND.JE.GE.11) L = L - 5
      RESID(I,K,JE) = RESID(I,K,JE) + S(L)
      PUNCH 6, PIT(I,JE),RESID(I,K,JE), AZ(K), STN(I), EVENT(K)
      PRINT 6, PIT(I,JE),RESID(I,K,JE), AZ(K), STN(I), EVENT(K)
 6    FORMAT (2X, A3, 2X, F10.7, 4X, F7.3, 30X, A3, 2X, A8)
      RESID(I,K,JE) = RESID(I,K,JE) - S(L)
 4    CONTINUE
      PUNCH 7
 7    FORMAT (72X)
 3    CONTINUE
      RETURN
      END
T        SUBTYPE,FORTRAN,LMAP,LSTRAP
C
C
C
      SUBROUTINE RESOUT(KPIT, LPIT, KEVENT, LEVENT, I)
C     ************************************************
C
C     THIS SUBPROGRAM PUNCHES CARDS WITH (RESIDUAL) ONLY, WHEN INDICATOR
C     IPUNCH = 1 (SEE INSTRUCTION 4 -MAIN-)
C
      COMMON /AMATRX/ RESID(4,120,20)
      COMMON /ATT/ AT(4,120,20)
      COMMON /EVENTT/ EVENT(120), NEVENT, NE(4), AZ(120), DELTA(120),
     1 INDEX(120)
      COMMON /PITT/ STN(4), PIT(4,20), X(4,20), Y(4,20), NPIT(4)
      COMMON /RJST/ S(231), D(231)
C
      DO 3 J = KPIT, LPIT
      JE = J - KPIT + 1
      PRINT 8, PIT(I,JE), STN(I)
 8    FORMAT (6X, 19HRESIDUALS FOR PIT  , A3, 13H    AT ARRAY , A4)
      DO 4 K = KEVENT, LEVENT
      JA = 80 + K
      IF (AT(I,K,JE).EQ.0.) GO TO 4
```

```
      L = J
      IF (I.EQ.4.AND.JE.GE.11) L = L - 5
      PUNCH 6, PIT(I,JE),RESID(I,K,JE), AZ(K), STN(I), EVENT(K)
      PRINT 6, PIT(I,JE),RESID(I,K,JE), AZ(K), STN(I), EVENT(K)
    6 FORMAT (2X, A3, 2X, F10.7, 4X, F7.3, 30X, A3, 2X, A8)
    4 CONTINUE
    3 CONTINUE
      RETURN
      END
T        SUBTYPE,FORTRAN,LMAP,LSTRAP
C
C
C
      SUBROUTINE AMIN(X, N, XMIN)
C     ***************************
C
C     FINDS MINIMUM VALUE OF ARRAY X
C
      DIMENSION X(N)
C
      KQ=1
    5 KP=KQ
    2 IF(KQ-N)3,4,4
    3 KQ=KQ+1
      IF(X(KP)-X(KQ))2,5,5
    4 XMIN=X(KP)
      RETURN
      END
T        SUBTYPE,FORTRAN,LMAP,LSTRAP
C
C
C
      SUBROUTINE AMAX(X, N, XMAX)
C     ***************************
C
C     FINDS MAXIMUM VALUE OF ARRAY X
C
      DIMENSION X(N)
C
      KQ = 1
    2 KP = KQ
    5 IF(KQ - N) 3, 4, 4
    3 KQ = KQ + 1
      IF(X(KP) - X(KQ))2, 5, 5
    4 XMAX = X(KP)




      RETURN
      END
T        SUBTYPE,FORTRAN,LMAP,LSTRAP
C
C
      SUBROUTINE GRAPH
C     ****************
C
C     THIS SUBROUTINE IS FOR GRAPHING ONLY. THE GENERAL GRAPHING ROUTINE
C     IS -POLGRF(X,Y,N)- WHICH JOINS POINT X(1)Y(1) TO X(2)Y(2) TO.....
C     ..X(N)Y(N). A FULL DESCRIPTION OF THE USE OF THE ROUTINES IS GIVEN
C     IN -YOUNG AND DOUGLAS (1968) AWRE REPORT NO. 041/68.
C     SUBROUTINE -DOTLIN(X1,Y1,X2,Y2)- JOINS POINTS (X1,Y1) AND (X2,Y2)
C     WITH A DOTTED LINE.
C
C
C     INSTRUCTIONS FOR GRAPHING ARE
C                                  IDOT = 21  PLOTS  E
C                                         23  PLOTS  G
C                                         24  PLOTS  H
C                                         33  PLOTS  J
C                                         42  PLOTS  .
C                                         44  PLOTS  *
C                                         48  PLOTS  BLANK
C                                         54  PLOTS  W
C                                         56  PLOTS  Y
C                                  INDX   = 1     LINEAR X SCALE.
C                                  INDY   = 2     LOG10(Y) SCALE.
C                                  INSTR1 = AJOIN JOINS POINTS WITH LINE.
C                                         = ZERO  LEAVES POINTS OPEN.
C                                     IND = 0     CALLS AND FINISHES FRAME
C                                         = 1     CALLS AND LEAVES OPEN.
C                                         = 2     FINISHES FRAME
C                                         = 3     KEEPS FRAME OPEN.
C
C
      COMMON /AMATRX/ RESID(4,120,20), CT(4,120,20), FACT(4,120),
     1 CONST(120), VELC(50,4), DLT(50,4), TVELOC(120), ERR(120),
     2 CVM(120,120), COV(120,120), AIND(120), PS(260), PNS(260), PV(260)
     3, PNV(260), VBAR(120), TJB(112), TAT(112), VELH(109), TH(109),
     4SLOW(260), TDIFF(112), DIST(80),  PVEL(80),  ERLO(80),  ERHY(80),
     5 TPVEL(80), DDIST(80), TERLO(80), TERHY(80), EFLO(80), VHERIN(30),
     6 SHERIN(30), ARANGE(30)
      COMMON /ATT/ AT(4,120,20)
      COMMON /EVENTT/ EVENT(120), NEVENT, NE(4), AZ(120), DELTA(120),
```

```
      1 INDEX(120)
       COMMON /GRFF/ TITLE(20), XMAX, XMIN,YMAX, YMIN, INDX, INDY, IND,
      1IDOT, INSTR1, XLIMIT, YLIMIT, SCALX, SCALY
       COMMON /PITT/ STN(4), PIT(4,20), X(4,20), Y(4,20), NPIT(4)
       COMMON /REST/ V(120), ENAME(120,3), VELOC(120), N
       COMMON /RNGE/ RANGE(30), RINT, NP
       COMMON /TTCVS/ TIMEH(109), AMPV(24), TIMEJ(112), SLOWH(109)
       DIMENSION              ATITLE(10), BTITLE(10), CTITLE(10),
      1 DTITLE(10),              FTITLE(10), XTITLE(5),YTITLE(5),VMID(260)
C
C     **********************************************************************
C
C                              TITLES FOR GRAPHS.
C
       DATA AJOIN(8HJOIN    ), ZERO(8H        ),
      1 (ATITLE(I),I=1,10)(80HPHASE VEL-DISTANCE CURVE (H--HERRIN CURVE,
      2 --PHASE VEL,  ...95 PER CENT LIMITS)),
      3 (XTITLE(I),I=1,5)(40HDISTANCE IN DEGREES     VELOCITY  KM/SEC),
      4 (BTITLE(I),I=1,10)(80H1./PHASE VEL -DIST CURVE  (H--HERRIN CURVE,
      5  --SLOWNESS,  ...95 PER CENT LIMITS)),
      6 (YTITLE(I),I=1,5)(40HDISTANCE IN DEGREES     SLOWNESS SEC/DEG)
       DATA (CTITLE(I),I=1,10)(80HTRAVEL - TIME CURVE      (J--J.B. CURVE,
      1 --TRAVEL - TIME, H--HERRIN (1968) CURVE)),
      2(DTITLE(I),I=1, 4)(32H   (DATA POINTS)SECONDS          )
       DATA (FTITLE(I),I=1,10)(80HDIFFERENCE TRAVEL TIME CURVE (OBSERVED
      1 MINUS  J.B. CURVE IN SECONDS              )
       CALL SDATE(DATE)
       DTOK = 111.19533839
C
C     **********************************************************************
C
C                              SETS UP ARRAYS FOR PLOTTING.
C
       DO 51 I = 1, NP
       II = 2*I - 1
       I3 = I + 80 + NEVENT
       DIST(II) = RANGE(I)
       DIST(II+1) = RANGE(I+1)
       PVEL(II) = 1./S(I3)
       PVEL(II+1) = 1./S(I3)
       ERLO(II) = PV(I3)
       ERLO(II+1) = PV(I3)
       ERHY(II) = PNV(I3)
       ERHY(II+1) = PNV(I3)
       TERLO(II) = DTOK/ERHY(II)
       TERLO(II+1) = DTOK/ERHY(II+1)
       TERHY(II) = DTOK/ERLO(II)
       TERHY(II+1) = DTOK/ERLO(II+1)
       TPVEL(II) = DTOK*S(I3)
       TPVEL(II+1) = DTOK*S(I3)
 51    CONTINUE
       NUM = II + 1
       NUM1 = II
C
C     **********************************************************************
C
C                              PLOTS CALCULATED TRAVEL TIME CURVE AND J.B.
C                              AND HERRIN (1968) TRAVEL TIME CURVES.
C
       DO 52 I = 1, 3
       TITLE(I) = XTITLE(I)
 52    CONTINUE
       DO 53 I = 3, 4
       TITLE(I+1) = DTITLE(I)
 53    CONTINUE
       DO 54 I = 1, 10
       TITLE(I+5) = CTITLE(I)
 54    CONTINUE
       TITLE(16) = DATE
       INSTR1 = AJOIN
       IND = 1
       IDOT = 33
       XMAX = 0.
       XMIN = 0.
       YMAX = 0.
       YMIN = 0.
       INDX = 1
       INDY = 1
       CALL POLGRF(RANGE, TJB, NP)
       CALL NUMBER(NEVENT)
       CALL ENDFME
       IND = 3
       IDOT = 24
       NPC = NP
       DO 212 I = 1, NP
       IF (RANGE(I).GE.97.) NPC = I
       IF (RANGE(I).GE.97.) GO TO 213
212    CONTINUE
213    CONTINUE
       CALL POLGRF(RANGE, TH, NPC)
```

```
      CALL ENDFME
      IND = 2
      IDOT = 42
      NP = NP - 1
      CALL POLGRF(ARANGE, TAT, NP)
      CALL ENDFME
C     ******************************************************************
C
C                              PLOTS (OBSERVED-J.B.) TRAVEL TIMES.
C
      IND = 0
      IDOT = 42
      YMAX = 0.
      YMIN = 0.
      DO 200 I = 1, 10
      TITLE(I+5) = FTITLE(I)
  200 CONTINUE
      CALL POLGRF(ARANGE, TDIFF, NP)
      CALL NUMBER(NEVENT)
      CALL ENDFME
C     ******************************************************************
C
C                              PLOTS PHASE VELOCITY - X HISTOGRAM WITH
C                              95 PCCL AND HERRIN (1968) CURVE
      DO 71 I = 4, 5
      TITLE(I) = XTITLE(I)
   71 CONTINUE
      DO 72 I = 1, 10
      TITLE(I + 5) = ATITLE(I)
   72 CONTINUE
      IND = 1
      IDOT = 24
      XMAX = 0.
      XMIN = 0.
      CALL AMAX(ERHY, NUM1, YMAX)
      CALL AMIN(ERLO, NUM1, YMIN)
      CALL POLGRF(RANGE, VHERIN, NP)
      CALL NUMBER(NEVENT)
      CALL ENDFME
      INSTR1= AJOIN
      IND = 3
      IDOT = 48
      CALL POLGRF(DIST, PVEL, NUM)
      DO 70 I = 1, NUM1, 2




      XPLOT1 = (DIST(I)-XLIMIT)*SCALX + 123.
      YPLOT1 = 923. - (ERHY(I) - YLIMIT)*SCALY
      XPLOT2 = (DIST(I+1) - XLIMIT)*SCALX + 123.
      CALL DOTLIN(XPLOT1, YPLOT1, XPLOT2, YPLOT1)
      YPLOT1 = 923. -  (ERLO(I) - YLIMIT)*SCALY
      CALL DOTLIN(XPLOT1, YPLOT1, XPLOT2, YPLOT1)
   70 CONTINUE
      CALL ENDFME
C
C     ******************************************************************
C
C                              PLOTS PHASE VELOCITY - X HISTOGRAM WITH
C                              95 PCCL,VELOCITIES FOR INDIVIDUAL EVENTS
C                              CORRECTED FOR STRUCTURE. CODED  E - EKA
C                                                              Y - YKA
C                                                              G - GBA
C                                                              W - WRA
C
      DO 69 I = 1, 2
      TITLE(I + 8) = OTITLE(I)
   69 CONTINUE
      DO 73 I = 11, 15
      TITLE(I) = BLANK
   73 CONTINUE
      IND = 1
      CALL POLGRF(DIST, PVEL, NUM)
      CALL NUMBER(NEVENT)
      CALL ENDFME
      IDOT = 48
      DO 85 I = 1, NUM1, 2
      XPLOT1 = (DIST(I)-XLIMIT)*SCALX + 123.
      YPLOT1 = 923. - (ERHY(I) - YLIMIT)*SCALY
      XPLOT2 = (DIST(I+1) - XLIMIT)*SCALX + 123.
      CALL DOTLIN(XPLOT1, YPLOT1, XPLOT2, YPLOT1)
      YPLOT1 = 923. -  (ERLO(I) - YLIMIT)*SCALY
      CALL DOTLIN(XPLOT1, YPLOT1, XPLOT2, YPLOT1)
   85 CONTINUE
      CALL ENDFME
      INSTR1 = ZERO
      IND = 3
      DO 86 I = 1, 4
      NEE = NE(I)
      DO 93 KA = 1, NEE
      IF(I.EQ.1) IDOT = 21
      IF(I.EQ.2) IDOT = 56
```

```
      IF(I.EQ.3) IDOT = 54
      IF(I.EQ.4) IDOT = 23
      IF(I.EQ.4) IND = 2
 93   CONTINUE
      CALL POLGRF(DLT(1,I), VELC(1,I), NEE)
 66   CONTINUE
      CALL ENDFME
C
C     ***************************************************************
C
C                          PLOTS DT/DX-X HISTOGRAM WITH 95 PCCL ANC
C                          DT/DX FOR INDIVIDUAL EVENTS CORRECTED FOR
C                          SUB-ARRAY STRUCTURE
C
      DO 62 I = 4, 5
      TITLE(I) = YTITLE(I)
 62   CONTINUE
      DO 66 I = 1, 3
      TITLE(I+5) = BTITLE(I)
 66   CONTINUE
      DO 76 I = 1, 2
      TITLE(I+8) = DTITLE(I)
 76   CONTINUE
      DO 77 I = 11, 15
      TITLE(I) = BLANK
 77   CONTINUE
      XMAX = 0.
      XMIN = 0.
      CALL AMAX(TERHY, NUM1, YMAX)
      CALL AMIN(TERLO, NUM1, YMIN)
      IND = 1
      INSTR1 = AJOIN
      IDOT = 48
      CALL POLGRF(DIST, TPVEL, NUM)
      CALL NUMBER(NEVENT)
      CALL ENDFME
      DO 75 I = 1, NUM1, 2
      XPLOT1 = (DIST(I)-XLIMIT)*SCALX + 123.
      YPLOT1 = 923. -(TERHY(I) - YLIMIT)*SCALY
      XPLOT2 = (DIST(I+1) - XLIMIT)*SCALX + 123.
      CALL DOTLIN(XPLOT1, YPLOT1, XPLOT2, YPLOT1)
      YPLOT1 = 923. - (TERLO(I) - YLIMIT)*SCALY
      CALL DOTLIN(XPLOT1, YPLOT1, XPLOT2, YPLOT1)
 75   CONTINUE
      CALL ENDFME



      INSTR1 = ZERO
      IDOT = 44
      IND = 2
      CALL POLGRF(DELTA, TVELOC, NEVENT)
      CALL ENDFME
C
C     ***************************************************************
C
C                          PLOTS DT/DX-X HISTOGRAM WITH 95 PCCL AND
C                          HERRIN (1968) DT/DX CURVE.
C
      DO 67 I = 1, 10
      TITLE(I+5) = BTITLE(I)
 67   CONTINUE
      IND = 1
      INSTR1 = AJOIN
      IDOT = 24
      CALL POLGRF(RANGE, SHERIN, NP)
      CALL NUMBER(NEVENT)
      CALL ENDFME
      INSTR1 = AJOIN
      IND = 3
      IDOT = 48
      CALL POLGRF(DIST, TPVEL, NUM)
      DO 74 I = 1, NUM1, 2
      XPLOT1 = (DIST(I)-XLIMIT)*SCALX + 123.
      YPLOT1 = 923. -(TERHY(I) - YLIMIT)*SCALY
      XPLOT2 = (DIST(I+1) - XLIMIT)*SCALX + 123.
      CALL DOTLIN(XPLOT1, YPLOT1, XPLOT2, YPLOT1)
      YPLOT1 = 923. - (TERLO(I) - YLIMIT)*SCALY
      CALL DOTLIN(XPLOT1, YPLOT1, XPLOT2, YPLOT1)
 74   CONTINUE
      CALL ENDFME
 112  RETURN
      END
T        SUBTYPE,FORTRAN,LMAP,LSTRAP
C
C
C
      SUBROUTINE NUMBER(NEVENT)
C     *************************
C
C     THIS SUBROUTINE PRINTS THE NUMBER OF EVENTS IN THE GRAPHING
C                                                              ROUTINES
      CALL TSP(847, 48, 39)
```

```
      CALL C4020H
      PRINT 111
  111 FORMAT (16HNO. OF EVENTS = )
      CALL C4020I(NEVENT,3)
      CALL ENDFME
      RETURN
      END
C
C
C


//
```

```
T        SUBTYPE,FORTRAN,LMAP,LSTRAP
C      INVERSION OF PHASE VELOCITY-DISTANCE CURVE.   DEREK J. CORBISHLEY.
C      ******************************************   ********************
C
C      THIS PROGRAM INVERTS THE SLOWNESS (DT/DDELTA) CURVE FROM 0.TO N
C      DEGREES USING THE CLASSICAL METHOD OF WIECHERT AND HERGLOTZ
C      SEE BATEMAN,H., 1910, PHIL.MAG, 6, P576-587.
C         IT IS ESSENTIAL THAT VALUES OF SLOWNESS SHOULD BE GIVEN FROM
C      ZERO DISTANCE.
C
C         OUTPUT INCLUDES 4 GRAPHS
C                   1) SLOWNESS (SL) - DISTANCE(DELTA) INPUT.
C                   2) VELOCITY(V) - DEPTH(H=RO-R) OUTPUT
C                   3) V - H OUTPUT (LOWER MANTLE ONLY)
C                   4) BULLEN'S PARAMETER (R/V)*(DV/DR) - H (BULLEN,1963
C                      PAGE 112) THIS MYST ALWAYS BE LT. 1 FOR A RAY TO
C                      EXIST.
C      GRAPHS 2,3,AND 4 ALSO HAVE HERRINS  VALUES FOR COMPARISON.
C
C     1,CARDS WITH
C       OH         DEPTH-VELOCITY CURVE DERIVED FROM HERRIN (1968). THESE
C       VH         CARDS ARE CONSTANT FOR ALL RUNS.
C      FORMAT FOR READING IS ON STATEMENT NO.47
C
C     2,CARD WITH
C      FMT         FORMAT TO READ SLOWNESS CURVE IN WITH.
C      PUNCH IN COLS.1.TO 80.
C
C     3,CARDS WITH
C       DELTA      DISTANCE-SLOWNESS CURVE TO BE INVERTED. DELTA MUST BE
C       SL         IN 0.1 DEG.INTERVALS 0-5DEGS. AND 0.5 DEG. INTERVALS
C                  5-ETC.DEGS. NOT MORE THAN 500 CARDS.
C      LAST CARD MUST BE A BLANK.
C      PUNCH AS FORMAT ABOVE.
C
C
C      ********************************************************************
C
       COMMON/GRFF/TITLE(20),XMAX,XMIN,YMAX,YMIN,INDX,INDY,
      1IND,IDOT,ANSTR1,IF,XLIMIT,YLIMIT,SCALX,SCALY
       COMMON DELTA(500), SL(500), D(500), V(500), B(500), DH(600),
      1  VH(600), BH(600), MM
       DIMENSION THETA(500), R(500), FMT(10), DV(500), A(500), AH(600),
      1 DVH(600), RH(600)
C
C
       CALL SCLIBR
       CALL EDUMP
       CALL SCATE(DATE)
       CALL SECCLK(TS)
       DTOK=111.19533839
       RADIUS = 6371.028
       PI=4.*ATAN(1.)
C
C      ********************************************************************
C      READS IN DATA.
C      ********************************************************************
C
       READ 47, (DH(I), VH(I), I = 1, 574)
 47    FORMAT (4(2F10.5))
       READ 48, FMT
       PRINT48, FMT
 48    FORMAT (10A8)
       I = 1
 50    READFMT, DELTA(I), SL(I)
       IF(SL(I).EQ.0.) GO TO 51
       I = I + 1
       GO TO 50
 51    N = I - 1
C
       J=1
       NN = N
       MM = NN
 100   CONTINUE
C
C      ********************************************************************
C      EVALUATION OF W.H.B.INTEGRAL
C      ********************************************************************
C
       DO 10 I=1,NN
       X = SL(I)/SL(NN)
       THETA(I) = ACOSH(X)
 10    CONTINUE
C
C      ********************************************************************
C      COMPUTES AREA UNDER COSH-1 CURVE.
C      ********************************************************************
C
       IF(DELTA(NN).LE.5.0) GO TO 28
       CALL SIMPSN(AREA1, THETA, 51, 0.1)
```

```
      CALL SIMPSN(AREA2, THETA(51), (NN-51), 0.5)
      AREA1 = AREA1*DTOK
      AREA2 = AREA2*DTOK
      AREA = AREA1 + AREA2
      GO TO 4
 28   CALL SIMPSN(AREA, THETA, NN, 0.1)
      AREA = AREA*DTOK
C
C     ****************************************************************
C     COMPUTES VELOCITY AND DEPTH
C     ****************************************************************
C
 4    R(J) = RADIUS/EXP(AREA/(PI*RADIUS))
      D(J) = RADIUS - R(J)
      V(J) =(R(J)*DTOK)/(RADIUS*SL(NN))
C
      J=J+1
      NN = NN - 1
      IF(J.GT.MM) GO TO 200
      GO TO 100
 200  CONTINUE
C
C     ****************************************************************
C     BULLENS PARAMETER (R/V)(DV/DR)
C     ****************************************************************
C
      CALL DIFLA(V, MM, R, DV)
      DO 54 I = 1, MM
      A(I) = V(I)/R(I)
      B(I) = DV(I)/A(I)
 54   CONTINUE
C
      DO 57 I = 1, 574
      RH(I) = RADIUS-DH(I)
 57   CONTINUE
      CALL DIFLA(VH,574,RH,DVH)
      DO 55 I = 1, 574
      AH(I) = VH(I)/RH(I)
      BH(I) = DVH(I)/AH(I)
 55   CONTINUE
C
C     ****************************************************************
C     PRINTS OUTPUT.
C     ****************************************************************
C
      PRINT 23, DATE
 23   FORMAT (1H1///5X, 39HINPUT DISTRIBUTION AND OUTPUT STRUCTURE, 60X,
     1A8/5X,39H****************************************,60X,8H********//
     2 5X, 11HDELTA(DEGS), 3X, 18HSLOWNESS(SECS/DEG), 3X, 10HDEPTH(KMS),
     3 3X, 11HRADIUS(KMS), 3X, 16HVELOCITY(KM/SEC), 3X, 12HDV/DR(SEC-1),
     4 3X, 12H(R/V)(DV/DR)/)
      DO 24  I = 1, MM
      MMM = MM + 1 - I
      PRINT 25, DELTA(I), SL(I), D(MMM), R(MMM), V(MMM), DV(MMM), B(MMM)
 25   FORMAT (5X,F10.2,5X,F10.3,5X,F10.1,5X,F10.1,5X,F10.3,7X,F10.5,
     1 5X, F10.3)
      PUNCH 3, D(MMM), V(MMM)
 3    FORMAT (5X, 2F10.5)
 24   CONTINUE
C
C     ****************************************************************
C     GRAPH OUTPUT.
C     ****************************************************************
      CALL GRAPH
C
      CALL SECCLK(TF)
      TS = TF - TS
      PRINT227, TS
 227  FORMAT (////15X, 20HTIME TAKEN FOR JOB =, F7.3, 8H SECONDS)
C
      RETURN
      END
T        SUBTYPE,FORTRAN,LMAP,LSTRAP
      SUBROUTINE GRAPH
C
C     THIS SUBROUTINE PRODUCES GRAPHS USING A SC4060 PLOTTER.
C
C     ****************************************************************
C
      COMMON/GRFF/TITLE(20),XMAX,XMIN,YMAX,YMIN,INDX,INDY,
     1IND,IDOT,ANSTR1,IF,XLIMIT,YLIMIT,SCALX,SCALY
      COMMON DELTA(500), SL(500), D(500), V(500), B(500), DH(600),
     1  VH(600), BH(600), N
      DIMENSION XTITLE(5), ATITLE(10), BTITLE(10), ZTITLE(5), CTITLE(10)
      DATA(XTITLE(I),I=1,5)(4HDISTANCE IN DEGREES      SLOWNESS SEC/DEG)
     1,
     2(ATITLE(I),I=1,10)(80HCOMPOSITE SLOWNESS  --      DISTANCE CURVE
     3.                  )
      DATA(BTITLE(I),I=1,10)(80HBULLENS PARAMETER (R/V)(DV/DR) - DEPTH
     1     ......HERRINS 1968 CURVE                ),
```

```
     2(/TITLE(I),I=1,5)(4HDEPTH (KMS)              VELOCITY KM/SEC ),
     3(CTITLE(I),I=1,10)(80HVELOCITY - DEPTH CURVE      ...HERRIN 1968
     4CURVE                    )
      DATA AJOIN(8HJOIN     ), BLANK(8H         )
      CALL SDATE(DATE)
C
C     ***************************************************************
C                  GRAPH OF DISTANCE - SLOWNESS.
      DO 8 I=1,5
      TITLE(I)=XTITLE(I)
 8    CONTINUE
      DO 9 I=1,10
      TITLE(I+5)=ATITLE(I)
 9    CONTINUE
      TITLE(16)=DATE
      ANSTR1=AJOIN
      IF = 3
      IND=0
      IOOT = 48
      XMAX=0.
      XMIN=0.
      YMAX=0.
      YMIN=0.
      INDX=1
      INDY=1
      CALL CARGRF(DELTA,SL,N)
      CALL ENDFME
C
C     ***************************************************************
C                  GRAPH OF VELOCITY - DEPTH.
      DO 29 I = 1, 5
      TITLE(I)=ZTITLE(I)
 29   CONTINUE
      DO 27 I=1,10
      TITLE(I+5)=CTITLE(I)
 27   CONTINUE
      DO 1 I = 1, 3
      TITLE(I+8) = BLANK
 1    CONTINUE
      XMAX=0.
      XMIN=0.
      YMAX=0.
      YMIN=0.
      CALL CARGRF(D, V,N)
      CALL ENDFME
C
C     ***************************************************************
C                  GRAPH OF VELOCITY - DEPTH (LOWER MANTLE).
      XMAX = 0.
      XMIN = 0.
      YMAX = 0.
      YMIN = 0.
      DO 2 I = 1, 10
      TITLE(I+5) = CTITLE(I)
 2    CONTINUE
      IND = 1
      IOOT = 48
      NB = N - 90
      CALL CARGRF(D, V, NB)
      CALL ENDFME
      XPLOT1 = (DH(125) - XLIMIT)*SCALX + 123.
      YPLOT1 = 923. - (VH(125) - YLIMIT)*SCALY
      DO 52 I = 126, 574
      XPLOT2 = (DH(I)-XLIMIT)*SCALX + 123.
      YPLOT2 = 923. - (VH(I)-YLIMIT)*SCALY
      CALL DOTLIN(XPLOT1, YPLOT1, XPLOT2, YPLOT2)
      XPLOT1 = XPLOT2
      YPLOT1 = YPLOT2
 52   CONTINUE
      CALL ENDFME
C
C     ***************************************************************
C                  GRAPH OF BULLENS PARAMETER - DEPTH
      DO 62 I = 1, NB
      B(I) = -B(I)
      IF(B(I).GT.2.) B(I) = 2.
      IF(B(I).LT.-2.) B(I) = -2.
 62   CONTINUE
      DO 63 I = 1, 574
      BH(I) = -BH(I)
 63   CONTINUE
C
      DO 41 I = 1, 2
      TITLE(I+3) = BLANK
 41   CONTINUE
      DO 42 I = 1, 10
      TITLE(I+5) = BTITLE(I)
 42   CONTINUE
      YMAX = 0.
      YMIN = 0.
```

```
      IND = 1
      IDOT = 48
      CALL CARGRF(D, B, NB)
      XPLOT1 = (DH(130) - XLIMIT)*SCALX + 123.
      YPLOT1 = 923. - (BH(130) - YLIMIT)*SCALY
      DO 40 I = 131, 574
      XPLOT2 = (DH(I)-XLIMIT)*SCALX + 123.
      YPLOT2 = 923. - (BH(I)-YLIMIT)*SCALY
      CALL OUTLIN(XPLOT1, YPLOT1, XPLOT2, YPLOT2)
      XPLOT1 = XPLOT2
      YPLOT1 = YPLOT2
 40   CONTINUE
      CALL ENDFME
C
      CALL ADVFLM(3)
      CALL FINISH
C
      RETURN
      END
T        SUBTYPE,FORTRAN,LMAP,LSTRAP
      SUBROUTINE SIMPSN(A, Y, N, H)
C     ******************************
C
C     THIS SUBROUTINE CALCULATES THE AREA UNDER CURVES USING SIMPSONS
C     RULE WITH END CORRECTIONS FOR ANY NUMBER OF ORDINATES.
C     ALSO REQUIRED IS SUBROUTINE DIFFER.
C
C     PLEASE RETURN TO DEREK J. CORBISHLEY.
C
C     A       AREA CALCULATED UNDER CURVE.
C     Y       ARRAY CONTAINING FUNCTION VALUES.
C     N       NUMBER OF ORDINATES.
C     H       SPACING OF ORDINATES.
C
      DIMENSION Y(N), DY(500),
C
      A = 0.
      AREA = 0.
      AREA2 = 0.
      AREA3 = 0.
      AREA5 = 0.
      AREA6 = 0.
      ERR = 0.
C
      AA = FLOAT(N)/2.




      NB = N/2
      AA = 2.*AA
      BN = FLOAT(2*NB)
C
      IF(AA.NE.BN) GO TO 1
C
C      N IS EVEN,HENCE USE QUADRATURE FOR ODD NO. OF PANELS.
C

C     AREA FOR 1 PANEL  (N = 2)
C
      IF(N.NE.2) GO TO 2
      A = (Y(1) + Y(2))*H/2.
      RETURN
C
C     AREA FOR 3 PANELS  (N = 4)
C
 2    AREA3 = (3.*(Y(2)+Y(3)) + (Y(1)+Y(4)))*3.*H/8.
      A = AREA3
      IF(N.NE.4) GO TO 3
      RETURN
C
C     AREA FOR 5 PANELS  (N = 6)
C
 3    IF(N.GT.6) GO TO 12
      AREA6 = (Y(4) + Y(5)*4. + Y(6))*H/3.
      AREA5 = AREA6 + AREA3
      A = AREA5
      RETURN
C     ******************************************************************************
C     AREA FOR ZERO PANELS  (N = 1)
C
 1    IF(N.NE.1) GO TO 6
      A = 0.
      RETURN
C
C     AREA FOR 2 PANELS  (N = 3)
C
 6    AREA2 = (Y(1) + 4.*Y(2) + Y(3))*H/3.
      IF(N.NE.3) GO TO 7
      A = AREA2
      RETURN
C     ******************************************************************************
C     AREA FOR 4 OR MORE PANELS  (N.GE.5)
C
```

```
 12   AREA3 = (3.*(Y(N-2)+Y(N-1)) + (Y(N-3)+Y(N)))*3.*H/8.
      K = N - 3
      GO TO 13
 7    K = N
 13   M = (K - 1)/2
      DO 5 I = 2, M
      II = 2*I - 2
      III = 2*I - 1
      AREA = AREA + Y(III) + 2.*Y(II)
 5    CONTINUE
C
      AREA = AREA + Y(1)/2. + Y(K)/2. + 2.*Y(K-1)
      AREA = AREA*2.*H/3.
      AREA = AREA3 + AREA
C
C     CALCULATION OF ERROR CORRECTIONS.
C
      DO 8 I = 2, M
      II = 2*I - 2
      III = 2*I - 1
      ERR = ERR + Y(III) - Y(II)
 8    CONTINUE
C
      ERR = ERR + Y(1)/2. + Y(K)/2. - Y(K-1)
      ERR = ERR*4.*H/15.
C
      CALL DIFFER(Y, DY, K, H)
C
      CORR = (DY(K) - DY(1))*H*H/15.
      ERR = ERR - CORR
      AREA = AREA + ERR
C
      A = AREA
C
      RETURN
      END

T        SUBTYPE,FORTRAN,LMAP,LSTRAP
      SUBROUTINE QUAD(A, B, C, X1, X2)
C     **********************************
C
C     SOLVES A QUADRATIC EQUATION FOR REAL SOLUTIONS ONLY.
C
C     RETURN TO DEREK J. CORBISHLEY.
C
```

```
      FACT = B*B - 4.*A*C
      IF(FACT-1.)1, 2, 2
 1    PRINT 4
 4    FORMAT (/5X, 29HUNREAL SOLUTIONS TO QUADRATIC/)
      RETURN
 2    X1 = (-B + SQRT(FACT))/(2.*A)
      X2 = (-B - SQRT(FACT))/(2.*A)
C
      RETURN
      END
T        SUBTYPE,FORTRAN,LMAP,LSTRAP
      SUBROUTINE DIFLA(F,N,X,DERIV)
      DIMENSION X(N),F(N),DERIV(N)
C      DIFFERENTIATES USING LAGRANGE METHOD
C      N = NUMBER OF POINTS
C      DEIV=DIFFERENTIATED VALUE AT EACH POINT
      L=N-2
      DO 1 I=1,L
      J=I+1
      A=X(I)+X(I+1)
       B=X(I+1)+X(I+2)
      C=X(I) +X(I+2)
      D=X(I) -X(I+1)
      E=X(I+1)-X(I+2)
      G = X(I) - X(I+2)
      BB=F(I+1)*(2.0*X(J)-C)/(-D*E)
      CC=F(I+2)*(2.0*X(J)-A)/(G*E)
      AA =F(I)*(2.0*X(J)-B)/(D*G)
      DERIV(J) =AA +BB +CC
 1     CONTINUE
      I=1
      J=I
      GO TO 10
 11    I=N-2
      J =N
 10    CONTINUE
      A=X(I)+X(I+1)
       B=X(I+1)+X(I+2)
      C=X(I) +X(I+2)
      D=X(I) -X(I+1)
      E=X(I+1)-X(I+2)
      G=X(I) -X(I+2)
      AA =F(I)*(2.0*X(J)-B)/(D*G)
      BB=F(I+1)*(2.0*X(J)-C)/(-D*E)
      CC=F(I+2)*(2.0*X(J)-A)/(G*E)
```

```
      DERIV(J) =AA +PB +CC
      IF(J.EQ.1)GO TO 11
      RETURN
      END
T        SUBTYPE,FORTRAN,LMAP,LSTRAP
      SUBROUTINE DIFFER(F,FD,N,H)
C     ***************************
C
C     PLEASE RETURN TO C. BLAMEY, BLACKNEST.
C
C     F------FUNCTION VALUES.
C     FD-----DIFFERENTIATED FUNCTION.
C     N------NUMBER OF POINTS IN FUNCTION.
C     H------INTERVAL EQUIVALENT TO DT.
C
C
      DIMENSION F(N), FD(N)
C
      FD(1) = -25.*F(1)+48.*F(2)-36.*F(3)+16.*F(4)-3.*F(5)
      FD(2) = -25.*F(2)+48.*F(3)-36.*F(4)+16.*F(5)-3.*F(6)
      N2 = N - 2
      DO 10 I = 3, N2
      FD(I) = F(I-2)-8.*F(I-1) + 8.*F(I+1) - F(I+2)
 10   CONTINUE
      FD(N-1) = 25.*F(N-1)-48.*F(N-2)+36.*F(N-3)-16.*F(N-4)+3.*F(N-5)
      FD(N)   = 25.*F(N)  -48.*F(N-1)+36.*F(N-2)-16.*F(N-3)+3.*F(N-4)
      H2 = 1./(12.*H)
      DO 20 I = 1, N
      FD(I) = FD(I)*H2
 20   CONTINUE
      RETURN
      END
```

```
8         TYPE,COMPILGO,F4
T         SUBTYPE,FORTRAN,LMAP,LSTRAP
C     TRUNCATE                                        DEREK J. CORBISHLEY.
C     ********.                                      **********
C     KOLMOGOROV - SMIRNOV STATISTIC.
C     ********************************
C
C     THIS PROGRAM COMPUTES THE CUMULATIVE DISTRIBUTION AND CHECKS THE
C     KOLMOGOROV-SMIRNOV STATISTIC AT THE 95 PER CENT LEVEL.
C     (SEE MASSEY,F.J., 1951, J.STAT.SOC.AMERICA., 46, P68-78)
C
C     THE NUMBER OF VALUES SHOULD BE PREFERABLY GREATER THAN 50.
C     IF CARD 4 IS PUNCHED AND THE KOL-SMIR. STATISTIC HAS BEEN EXCEEDED
C     THEN THE DISTRIBUTION WILL BE TRUNCATED BY SD STANDARD DEVIATIONS
C     FROM THE MEDIAN. VARIANCES FROM MEDIAN AND MEAN ARE CORRECTED FOR
C     TRUNCATION.STATISTICS AND KOL.-SMIR. DISTANCE ARE THEN RECOMPUTED.
C     (OTHERWISE LEAVE CARD 4 BLANK)
C
C     OUTPUT INCLUDES GRAPHS.
C
C     INSTRUCTIONS FOR USE
C
C     1. CARD WITH
C         THE FIRST CARD IS A STANDARD 4060 CARD
C
C     2. CARD WITH
C         TITLE DESCRIBING SAMPLE
C         (PUNCH IN COLUMNS 1-80)
C
C     3. CARD WITH
C         FORMAT TO READ DATA IN.
C         (PUNCH IN COLUMNS 1-80 AND INCLUDE FORMAT II AT END IN COL.80)
C
C     4. CARDS WITH
C         SD  DATA IS TRUNCATED BY SD STANDARD DEVIATIONS.
C             PUNCH (62X, F10.5).
C
C     5. CARDS WITH
C        VALUES OF DISTRIBUTION X.THE LAST CARD MUST HAVE 1 IN COL 80.
C        FORMAT FOR PUNCHING GIVEN IN INSTRUCTION 3
C
C     ***************************************************************
C     ***************************************************************
C                  THIS SUBROUTINE READS IN THE DATA.
C
      COMMON X(6000), XC(6000), YC(6000),   YNC(6000),PIT(6000),EVENT(60
     100), N,ASD,XH(6000),YINC(6000)
      COMMON/GRFF/TITLE(20),XMAX,XMIN,YMAX,YMIN,INDX,INDY,IND,IDOT,
     1 ANSTR1,IF,XLIMIT,YLIMIT,SCALX,SCALY
      DIMENSION FMT(10)
C
      CALL SCLIBR
      CALL EDUMP
      CALL SDATE(DATE)
C     ****************
C
  100 READ 2,(TITLE(I),I=6,15)
      PRINT2,(TITLE(I),I=6,15)
      READ 2, FMT
      PRINT2, FMT
    2 FORMAT(10A8)
      READ 4,ASD
      PRINT 4, ASD
    4 FORMAT (62X, F10.5)
      I=1
   25 READ FMT, PIT(I), X(I), EVENT(I), IND
      IF(IND.EQ.1) GO TO 24
      I=I+1
      GO TO 25
   24 N=I-1
C
      CALL SECCLK(TS)
      PRINT 1, DATE
    1 FORMAT(1H1//4X,39HKOLMOGOROV-SMIRNOV TEST OF DISTRIBUTION, 72X, A8
     1, /4X,39H----------------------------------------,72X,8H--------//)
C
C
      CALL AREAD
C     **********
C
      CALL SECCLK(TF)
      TS=TF-TS
      PRINT 3,TS
    3 FORMAT(/////5X,20HTIME TAKEN FOR JOB =, F7.3, 8H SECONDS)
      GO TO 100
      END
T        SUBTYPE,FORTRAN,LMAP,LSTRAP
      SUBROUTINE AREAD
C     ****************
C
```

```
      COMMON X(6000), XC(6000), YC(6000),   YNC(6000),PIT(6000),EVENT(60
     100), N,ASD,XH(6000),YINC(6000)
      COMMON/GRFF/TITLE(20),XMAX,XMIN,YMAX,YMIN,INDX,INDY,IND,IDOT,
     1 ANSTR1, IF,XLIMIT,YLIMIT,SCALX,SCALY
      DIMENSION YN(10000), DIF(10000)
C
      PRINT 29,(TITLE(I),I=6,15)
 29   FORMAT(10A8)
      PRINT 1,N,(X(I),I=1,N)
 1    FORMAT(//4X,18HNUMBER IN SAMPLE =,I5//4X,12HDATA USED --//(4X,
     112F10.5))
C
      CALL ORDABC(N,X,PIT,EVENT)
C
      BSD = 20.
      IOUT = 1
 13   AN = N
C
C
      CALL STATIS(X,N,AN,XBAR,XMED,VARX,CVARX,SKEW,AKURT,SD,BSD,VARM,
     1 CVARM)
C     **************************************************
C
      CALL HIST(X,N,XC,YC,XH)
C     ************************
C
C
      PRINT 10
 10   FORMAT(///4X,85HM1 = SUM(X-XBAR)/N,  VARIANCE = M2,  SKEWNESS = M3
     1/M2**1.5,  KURTOSIS = (M4/M2**M2)-3.)
C
      PRINT44,XBAR,XMED,VARX,CVARX,VARM,CVARM,SD,SKEW,AKURT
 44   FORMAT(//4X,6HMEAN =,F10.5//4X,8HMEDIAN =,F10.5,//4X,10HVARIANCE =
     1,F10.5//4X,20HCORRECTED VARIANCE =,F10.5//4X,22HVARIANCE FROM MEDI
     2AN =,F10.5//4X,24HCORR. VAR. FROM MEDIAN =,F10.5//4X,20HSTANDARD D
     3EVIATION =,F10.5//4X,10HSKEWNESS =,F10.5//4X,10HKURTOSIS =,F10.5)
C
C     COMPUTES THEORETICAL DISTRIBUTION.
      PI2S=SQRT(8.*ATAN(1.)*CVARM)
      PI2S=1./PI2S
      SIG2=-2.*CVARM
      SIG2 = 1./SIG2
      SUM=0.
C
      DX = ABS(XH(N-1) - XH(1))/FLOAT(N-1)




      XH1 = XH(1) - DX
      DO22 I=1,N
      BI = I
      XC(I) = XH1 + DX*BI
      YN(I)=PI2S*EXP((XC(I)-XMED)*(XC(I)-XMED)*SIG2)
      YN(I) = YN(I)*100.*DX
      YNC(I)=YN(I)+SUM
      SUM=YNC(I)
 22   CONTINUE
C     INTERPOLATES THE CALCULATED ARRAY(XC,YNC) TO THE SAME X SPACING
C     AS THE OBSERVED ARRAY(XH,YINC).
      DO 23 I = 1, N
      CALL DIVDIF(N,XC,YNC,XH(I),YINC(I))
      DIF(I) = ABS(YC(I) - YINC(I))
 23   CONTINUE
C
C     PLOTS GRAPHS
      CALL PPLOT
C     **********
C
C     COMPUTES THE MAXIMUM KOLMOGOROV - SMIRNOV DISTANCE.
      CALL AMAX(DIF,N-1,DMAX)
C     ***********************
      DMAX=DMAX/100.
      DISKS=1.3581/SQRT(N)
      PRINT 4,DMAX,DISKS
 4    FORMAT(//5X,29HMAXIMUM KOLMOGOROV DISTANCE =,F10.3/
     1         5X,29H95 PER CENT STATISTIC       =,F10.3)
      IF(DMAX.LT.DISKS) GO TO 3
      PRINT5
 5    FORMAT(14X,30H***** STATISTIC EXCEEDED *****)
C
C     TRUNCATES DATA.
      BSD = ASD
      IF(IOUT.GT.1) GO TO 3
C
      PRINT 6, ASD
 6    FORMAT (//5X, 37HDATA HAS BEEN TRUNCATED TO A LIMIT OF, F10.2,2X,
     14HS.D./5X,22HVALUES OF X REJECTED =)
      I = 1
      ASD = ASD*SQRT(CVARM)
 12   IF(ABS(X(I)).GT.ASD) GO TO 7
      I = I + 1
      IF(I.GT.N) GO TO 11
      GO TO 12
```

```
  7     PRINT 9, X(I), PIT(I), EVENT(I)
  9     FORMAT (35X, F10.5, 6X, A8, 6X, A8)
        N = N - 1
        DO 14 J = I, N
        X(J) = X(J+1)
        PIT(J) = PIT(J+1)
        EVENT(J) = EVENT(J+1)
 14     CONTINUE
        IF(I.GT.N) GO TO 11
        GO TO 12
 11     IOUT = 2
        GO TO 13
C
  3     RETURN
        END
T           SUBTYPE,FORTRAN,LMAP,LSTRAP
        SUBROUTINE ORDER(N,A)
C       **********************
C
C       THIS SUBROUTINE ORDERS THE ARRAY A INTO ASCENDING SIZE OF A (FOR
C       N NEGATIVE) OR DECENDING  SIZE (FOR N POSITIVE).
C
        DIMENSION A(N)
C
        IF(N) 5,70,35
C
   5    N=-N
        N1=N-1
        DO 30 I=1,N1
        I1=I+1
            DO 20 J=I1,N
            IF(A(I)-A(J))20,20,10
  10        S=A(J)
            A(J)=A(I)
            A(I)=S
  20        CONTINUE
  30    CONTINUE
        RETURN
C
  35    N1=N-1
        DO 60 I=1,N1
        I1=I+1
            DO 50 J=I1,N
            IF(A(I)-A(J))40,50,50
  40        S=A(J)
            A(J)=A(I)
            A(I)=S
  50        CONTINUE
  60    CONTINUE
  70    RETURN
        END
T           SUBTYPE,FORTRAN,LMAP,LSTRAP
        SUBROUTINE ORDABC(N,A,B,C)
C       **************************
C
C       THIS SUBROUTINE ORDERS THE ARRAYS A,B,C INTO ASCENDING SIZE OF A.
C
        DIMENSION A(N), B(N), C(N)
C
        N1 = N - 1
        DO 30 I = 1, N1
        I1 = I + 1
        DO 20 J = I1, N
        IF(A(I) - A(J)) 20, 20, 10
  10    S = A(J)
        T = B(J)
        U = C(J)
        A(J) = A(I)
        B(J) = B(I)
        C(J) = C(I)
        A(I) = S
        B(I) = T
        C(I) = U
  20    CONTINUE
  30    CONTINUE
C
        RETURN
        END
T           SUBTYPE,FORTRAN,LMAP,LSTRAP
        SUBROUTINE STATIS(X,N,AN,XBAR,XMED,VARX,CVARX,SKEW,AKURT,SD,ASD,
       1 VARM,CVARM)
C       ***************************************************************
C
C       THIS SUBROUTINE CALCULATES THE FOLLOWING STATISTICS FROM THE
C       DISTRIBUTION X(1).....X(N)
C             AN   = N
C             XBAR = MEAN OF DISTRIBUTION
C             XMED = MEDIAN
C             VARX = VARIANCE
C             CVARX= VARIANCE CORRECTED FOR TRUNCATION BY ASD STANDARD
```

```
C                  DEVIATIONS.
C           VARM = VARIANCE FROM MEDIAN.
C          CVARM = CORRECTED VARIANCE FROM MEDIAN.
C           SKEW = SKEWNESS
C           AKURT= KURTOSIS
C           SD   = STANDARD DEVIATION
C                          1
C
      DIMENSION X(N)
C
      N = -N
      CALL ORDER(N,X)
      IMID = N/2
      M = IMID*2
      IF(M.EQ.N) GO TO 2
      IMID = IMID + 1
      XMED = X(IMID)
      GO TO 3
 2    XMED = (X(IMID) + X(IMID+1))/2.
 3    CONTINUE
      SUMX =0.;
      SUMX2=0.
      SUMX3=0.
      SUMX4=0.
      VARM = 0.
      DO 1 I=1,N
      SUMX = SUMX + X(I)
      X2 =X(I)*X(I)
      SUMX2 =SUMX2 +X2
      SUMX3 =SUMX3 +X2*X(I)
      SUMX4 =SUMX4 +X2*X2
      VARM = (X(I)-XMED)*(X(I)-XMED) + VARM
 1    CONTINUE
      VARM = VARM/AN
      XBAR = SUMX/AN
      A2MNT = SUMX2/AN
      VARX =A2MNT -XBAR*XBAR
      A3MNT=SUMX3/AN - 3.*XBAR*A2MNT + 2.*(XBAR**3)
      A4MNT=SUMX4/AN - 4.*XBAR*SUMX3/AN +6.*XBAR*XBAR*A2MNT-3.*(XBAR**4)
      SKEW=(A3MNT*A3MNT)/(VARX**3)
      SKEW=SQRT(SKEW)
      SKEW=SIGN(SKEW,A3MNT)
      AKURT=(A4MNT/(VARX*VARX))-3.
      CALL CORV(ASD, VARX, CVARX)
      CALL CORV(ASD,VARM,CVARM)




      SD = SQRT(CVARX)
C
      RETURN
      END
T        SUBTYPE,FORTRAN,LMAP,LSTRAP
      SUBROUTINE HIST(X, N, U, C, XH)
C     ********************************
C
C     THIS SUBROUTINE COMPUTES THE CUMULATIVE FREQUENCY.
C     X------X-ARRAY READ IN (N POINTS)
C     U------CUMULATIVE X-ARRAY.
C     C------CUMULATIVE Y-ARRAY (AS A PERCENTAGE)
C     XH-----CUMULATIVE X-ARRAY (AT U/2 SPACING)
C
      DIMENSION X(N), U(N), C(N), XH(N)
      AN = N
      F = 1.
      K = 0
      C(K) = 0.
      L = 0
      I = 2
      K = 1
      SUM = 0.
      U(1) = X(1)
      XH(1) = (X(1) + X(2))/2.
      C(1) = 100./AN
 3    IF(X(I).NE.X(I-1)) GO TO 2
      U(K) = X(I)
      XH(K) = (X(I) + X(I+1))/2.
      F = F + 1.
      C(K) = (100./AN)*F + C(K-1)
      I = I + 1
      IF(I.GT.N) GO TO 4
      GO TO 3
 2    K = K + 1
      U(K) = X(I)
      XH(K) = (X(I) + X(I+1))/2.
      F = 1.
      C(K) = (100./AN) + C(K-1)
      I = I + 1
      IF(I.GT.N) GO TO 4
      GO TO 3
 4    N = K
      RETURN
      END
```

```
T        SUBTYPE,FORTRAN,LMAP,LSTRAP
      SUBROUTINE HPLOT
C     ****************
C
C     THIS SUBROUTINE PLOTS THE OBSERVED (XH,YC) AND THEORETICAL
C     (XC,YNC) CUMULATIVE FREQUENCY DISTRIBUTIONS ON A SC4060 PLOTTER.
C     (SEE YOUNG,J.B. AND DOUGLAS,A., 1968. HMSO AWRE 041/68)
C
      COMMON X(6000), XC(6000), YC(6000),   YNC(6000),PIT(6000),EVENT(60
     100), N,ASD,XH(6000),YINC(6000)
      COMMON/GREF/TITLE(20),XMAX,XMIN,YMAX,YMIN,INDX,INDY,IND,IDOT,
     1 ANSTR1,IF,XLIMIT,YLIMIT,SCALX,SCALY
C
      DATA PCEN(8HPERCENT ),CLASS(8HCLASS LI),ALIM(8HMITS    ),BLANK(8H
     1        )
      DATA AJOIN(8HJOIN    )
C
      CALL SDATE(TITLE(16))
C
      TITLE(1)=CLASS
      TITLE(2)=ALIM
      TITLE(3)=BLANK
      TITLE(4)=PCEN
      TITLE(5)=BLANK
      XMAX=0.
      XMIN=0.
      YMAX = 0.
      YMIN=0.
      INDX = 1
      INDY = 1
      ANSTR1 = AJOIN
      IF = 3
      IND=1
      IDOT=48
C
      CALL CARGRF(XH,YC,N-1)
C
      IND=2
C
      CALL CARGRF(XC,YNC,N-1)
      CALL ENDFME
C
      RETURN
      END
T        SUBTYPE,FORTRAN,LMAP,LSTRAP
```

```
      SUBROUTINE DIVDIF(N, X, Y, XO, YO)
C     **********************************
C
C     THIS SUBROUTINE INTERPOLATES USING THIRD DIVIDED DIFFERENCES.
C     (SEE -METHODS OF MODERN PHYSICS- JEFFREYS AND JEFFREYS,1956,P261)
C     THERE IS NO RESTRICTION ON ARGUMENT OR FUNCTION SPACING. THE
C     PROGRAM REQUIRES A MINIMUM OF N=4 POINTS TO OPERATE.
C
C     N--------NUMBER OF VALUES IN INPUT.
C     X--------INPUT ARGUMENT ARRAY.
C     Y--------INPUT FUNCTION ARRAY.
C     XO-------INTERPOLATE ARGUMENT VALUE.
C     YO-------INTERPOLATED FUNCTION VALUE.
C
C     RETURN TO DEREK J. CORBISHLEY.
C
      DIMENSION X(N), Y(N)
C
      IF(N.GE.4) GO TO 12
      PRINT 13
 13   FORMAT (/10X, 36HNO INTERPOLATION AS N MUST BE .GE. 4/)
      RETURN
 12   IF(XO - X(1)) 3, 2, 3
 2    YO = Y(1)
      RETURN
C
 3    IF(XO - X(N))5, 6, 5
 6    YO = Y(N)
      RETURN
C
 5    DO 9 J = 1, N
      IF(X(J).GE.XO) GO TO 10
 9    CONTINUE
 10   I = J - 1
      IF(XO.GE.X(N))I = N-1
      IF(I.LT.1) I = 1
      K = I - 1
      IF(K.LT.1) K = 1
      IF(K.GT.(N-2)) K = N-2
      L = K
      IF(L.GT.(N-3)) L = N-3
C     ***********************************************************************
      CALL DD3(X(L), Y(L), D3)
C     ***********************************************************************
      II = I-1
```

```
      IF(II.LT.1) II = 3
      A = XO - X(II)
      B = A*D3
C     ***************************************************************
      CALL DD2(X(K), Y(K), D2)
C     ***************************************************************
      C = D2 + B
C     ***************************************************************
      CALL DD1(X(I), Y(I), D1)
C     ***************************************************************
      D = (XO - X(I))*(XO - X(I+1))
      E = D*C
      F = (XO - X(I))*D1 + Y(I)
      YO = E + F
C
      RETURN
      END
T        SUBTYPE,FORTRAN,LMAP,LSTRAP
      SUBROUTINE DD1(X, Y, F1)
C     ************************
C     THIS SUBROUTINE FORMS FIRST DIVIDED DIFFERENCES.
C
      DIMENSION X(2), Y(2)
C
      F1 = (Y(2) - Y(1))/(X(2) - X(1))
C
      RETURN
      END
T        SUBTYPE,FORTRAN,LMAP,LSTRAP
      SUBROUTINE DD2(X, Y, F2)
C     ************************
C     THIS SUBROUTINE FORMS SECOND DIVIDED DIFFERENCES.
C
      DIMENSION X(3), Y(3)
C
      CALL DD1(X(2), Y(2), A)
      CALL DD1(X(1), Y(1), B)
C
      F2 = (A - B)/(X(3) - X(1))
C
      RETURN
      END
T        SUBTYPE,FORTRAN,LMAP,LSTRAP
      SUBROUTINE DD3(X, Y, F3)
C     ************************
```

```
C     THIS SUBROUTINE FORMS THIRD DIVIDED DIFFERENCES.
C
      DIMENSION X(4), Y(4)
C
      CALL DD2(X(2), Y(2), A)
      CALL DD2(X(1), Y(1), B)
C
      F3 = (A - B)/(X(4) - X(1))
C
      RETURN
      END
T        SUBTYPE,FORTRAN,LMAP,LSTRAP
      SUBROUTINE NTRUNC(C, P)
C     ***********************
C
C     THIS SUBROUTINE CALCULATES THE AREA (PROBABILITY -P(K)) UNDER A
C     NORMAL CURVE THAT HAS BEEN TRUNCATED AT C(K).
C     C(K) IS THE VALUE SUCH THAT (K) PER CENT OF THE DISTRIBUTION LIES
C     WITHIN C(K) OF THE MEAN. P(K) WILL BE INDEPENDENT OF THE MEAN AND
C     VARIANCE OF THE POPULATION.
C     (SEE FREEDMAN BSSA VOL 56 NO.3, P677-695, JUNE 1966)
C
C
C
      PI = 4.*ATAN(1.)
      H = C/500.
      AREA = 0.
      DO 1 I = 1, 500
      Y = C*FLOAT(I)/500.
      Y2 = Y*Y
      ORD = Y2*EXP(-Y2/2.)
      AREA = AREA + 2.*ORD
1     CONTINUE
C
      Y = C
      Y2 = Y*Y
      ORD = Y2*EXP(-Y2/2.)
      AREA = AREA - ORD
C
      P = H*AREA/2.
      P = SQRT(2./PI)*P
C
      RETURN
      END
T        SUBTYPE,FORTRAN,LMAP,LSTRAP
```

```
      SUBROUTINE CORV(ASD,VARX,CVARX)
C     ********************************
C
C     THIS SUBROUTINE CORRECTS THE VARIANCE (VARX) TO ALLOW FOR
C     TRUNCATION BY -ASD- STANDARD DEVIATIONS. (SOLN. = CVARX).
C
C
      CALL NTRUNC(ASD, P)
      CVARX = VARX/P
      RETURN
      END
```

REFERENCES

ABMR (1962). Aeromagnetic Map. Australian Bureau of Mineral Resources, Tennant Creek. SE: G237-14. June 1962.

Adams, L. H. and Williamson, E. D. (1923). The Composition of the Earth's Interior. Smithsonian Rep., 241-260.

Agger, H. E. and Carpenter, E. W. (1964). A Crustal Study in the Vicinity of the Eskdalemuir Seismological Array Station. Geophys.J.Roy.Astr.Soc., 9, 69-83.

Anderson, D. L. (1964). Universal Dispersion Tables. 1. Love waves across oceans and continents on a spherical Earth. Bull.Seism.Soc.Am. 54, 681-726.

Anderson, D. L. (1967). Phase Changes in the Upper Mantle. Science, 157, 1165-1173.

Anderson, D. L. and Julian, B. R. (1969). Shear Velocities and Elastic Parameters of the Mantle. Jnl.Geophys.Res. 74, 12, 3281-3286.

Anon. AWRE (1967). Data Processing Facilities and Data Available at the UKAEA Data Analysis Centre for Seismology. Pamphlet No. 2.

Ansell, J. (1969). Personal Communication.

Bartlett, M. S. (1937). Properties of Sufficiency and Statistical Tests. Proc.Roy.Soc.Lon. Series A, 160, 268-282.

Birch, F. (1952). Elasticity and Constitution of the Earth's Interior. Jnl.Geophys.Res. 57, 2, 227-286.

Birtill, J. W. and Whiteway, F. E. (1965). The Application of Phased Arrays to the Analysis of Seismic Body Waves. Phil.Trans.A., 258, 421-493.

Blamey, C. and Gibbs, P. G. (1968). The Epicentres and Origin Times of some Large Explosions. Geophys.J. Roy.Astr.Soc. 16, 1-7.

Borcherdt, C. A. and Roller, J. C. (1967). Preliminary interpretation of a seismic refraction profile across the large aperture seismic array, Montana. Technical Letter 2, National Centre for Earthquake Research, Menlo Park, California.

Born, M. and Mayer, M. (1931). "The Theory of Solids". Hanbuch der Physik, 24, 708.

Bridgman, P. W. (1950). "Physics of High Pressures". New York.

Bugayevskiy, G. N. (1964). Travel time curve of seismic waves and structure of the mantle. Voprosy Seysmichnosti Sibiri, Akad. SSR Sibirskoye Otdeleriye, Inst. Zemnoy Kory Trudy, 18, 151-168.

Bullen, K. E. (1940). The Problem of the Earth's Density Variations. Bull.Seism.Soc.Amer. 30, 235-50.

Bullen, K. E. (1949). Compressibility-pressure hypothesis and the Earth's interior. Mon.Not.Roy.Astr.Soc., Geophys.Sup., 5, 355-368.

Bullen, K. E. (1963). "An Introduction to the Theory of Seismology". 3rd edition. C.U.P.

Byerly, P. (1942). "Seismology". Prentice-Hall.

Carder, D. S. (1964). Travel times from central Pacific nuclear explosions and inferred mantle structure. Bull.Seism.Soc.Amer. 54, 2271-2294.

Carpenter, E. W., Marshall, P. D. and Douglas, A. (1967). The Amplitude-Distance curve for Short Period Teleseismic P-waves. Geophys.J.Roy.Astr.Soc., 13, 61-70.

Chinnery, M. A. and Toksoz, M. N. (1967). P-wave Velocities in the Mantle below 700 kms. Bull.Seism.Soc.Amer., 57, 199-226.

Clark, S. P. and Ringwood, A. E. (1964). Density Distribution and Constitution of the Mantle. Rev.Geophys. 2, 35.

Cleary, J. R. (1967). Analysis of the Amplitudes of Short Period P-waves recorded by Long Range Seismic Measurement Stations in the distance range 30° to 102°. Jnl.Geophys.Res. 72, 18, 4705-4712.

Cleary, J. R., Wright, C. and Muirhead, K. J. (1968). The Effects of Local Structure upon Measurements of the Travel Time Gradient at the Warramunga Seismic Array. Geophys.Jnl.Roy.Astr.Soc. 16, 21-29.

Corbishley, D. J. (1969). Multiple Array Measurements of the P Wave Travel Time Derivative. Geophys.J.Roy. Astr.Soc., in press.

Douglas, A. (1966). A Special Purpose Least Squares Program. AWRE Report No. O-54/66.

Douglas, A. and Corbishley, D. J. (1968). Measurement of $dT/d\Delta$. Nature, 217, 1243-1244.

Doyle, H. A. and Hales, A. L. (1967). An Analysis of the Travel Times of S Waves to North American Stations in the Distance Range 28° to 82°. Bull.Seism.Soc.Amer., 57, 761-772.

Evernden, J. F. (1953). Direction of Approach of Rayleigh Waves and Related Problems (Part 1). Bull.Seism.Soc. Amer. 43, 335-374.

Fairbairn, H. W. (1943). Packing in ionic minerals. Bull.Geol.Soc.Amer., 54, 1305-1374.

Fairborn, J. W. (1967). Lateral Variations in Mantle P-wave Velocities determined from $dT/d\Delta$ Measurements at LASA. Annual Report 31st October 1967, for A.F. Office of Scientific Research, M.I.T.

Fisher, R. A. (1950). "Statistical Methods for Research Workers". 11th edition. Oliver and Boyd. 209.

Freedman, H. W. (1966). A Statistical Discussion of P_n Residuals from Explosions. Bull.Seism.Soc.Amer. 56, 677-695.

Freedman, H. W. (1968). Seismological Measurement and Measurement Error. Bull.Seism.Soc.Amer. 58, 1261-1272.

Greenfield, R. J. and Sheppard, R. M. (1969). The Moho Depth Variations under the LASA and their effect on $dT/d\Delta$ Measurements. Bull.Seism.Soc.Amer., 59, 409-420.

Herrin, E. (ed.), Arnold, E. P., Bolt, B. A., Clawson, G. E., Engdahl, E. R., Gordon, D. W., Hales, A. L., Lobdell, J. L., Nuttli, O., Romney, C., Taggart, J. and Tucker, W. (1968). Special Number - 1968 Seismological Tables for P phases. Bull.Seism.Soc.Amer., 58, 1193-1241.

HMSO (1961). "Modern Computing Methods." National Physical Laboratory. HMSO, London. 2nd edition.

Ibrahim, A. B. K. and Nuttli, O. W. (1967). Travel time Curves and Upper Mantle Structure from Long Period S Waves. Bull.Seism.Soc.Amer., 57, 5, 1063-1092.

Jeffreys, H. (1961). "Theory of Probability". 3rd edition. O.U.P.

Jacob, A.W.B. (1969). Crustal Phase Velocities Observed at the Eskdalemuir Seismic Array. Geophys.J.Roy.Astr. Soc., 18, 2, 189-198.

Johnson, L. R. (1969). Array Measurements of P Velocities in the Lower Mantle. Bull.Seism.Soc.Amer., 59, 973-1008.

Kelly, E. J. (1964). Limited Network Processing of Seismic Signals. M.I.T. Lincoln Lab. Group Report 44.

Kelly, E. J. (1969). Personal communication to R. J. Greenfield and R. M. Sheppard (1969). Bull.Seism. Soc.Amer., 59, 409-420.

Kondorskaya, N. V., Paylov, L. N., Pustovitenko, A. N. and Solov'ev, S. L. (1967). Some Results of a Study of the Longitudinal Wave Spectra from Earthquakes in the Far East. Izvestia Akad.Nauk. SSSR, Earth Physics, 1, 60-75.

Kondorskaya, N. V. and Slavina, L. B. (1969). Some Results of Investigating Travel Times of P Waves. AN SSSR. Izvestiya. Fizika Zemli, 2, 19-36.

Lilwall, R. C. and Douglas, A. (1969). Estimation of P Wave Travel Times using the Joint Epicentre Method. Geophys.J.Roy.Astr.Soc. In press.

Massey, F. J. (1951). The Kolmogorov-Smirnov Test for Goodness of Fit. Jnl.Amer.Stat.Soc. 46, 68-78.

Muirhead, K. J. (1968). "The Reduction and Analysis of Seismic Data using Digital Computers". Ph.D. Thesis. A.N.U.

Niazi, M. and Anderson, D. L. (1965). Upper Mantle Structure of Western North America from Apparent Velocities of P-waves. J.Geophys.Res. 70, 18, 4653.

Owen, D. B. (1962). Handbook of Statistical Tables, Mass. 439.

Payne, N. A. and Irons, B. (1968). Private communication to O.C. Zienkiewicz. "The Finite Element Method in Structural and Continuum Mechanics". McGraw-Hill. Page 8.

Repetti, W. C. (1928). "New Values for Some of the Discontinuities in the Earth". Dissertation, St. Louis University.

Richter, C. F. (1958). "Elementary Seismology". Freeman.

Sacks, I. S. (1966). Diffracted Wave Studies of the Earth's core 1. Amplitudes, core size, and rigidity. Jnl.Geophys.Res., 71, 1173-1193.

Sacks, I. S. (1967). Diffracted P-wave Studies of the Earth's core, 2, Lower Mantle Velocity, Core Size, Lower Mantle Structure. Jnl.Geophys.Res. 72, 10, 2589-2594.

Scheffé, H. (1964). "The Analysis of Variance". 4th edition. John Wiley and Sons.

Sheppard, R. M. (1967). Values of LASA Time Station Residuals, Velocity and Azimuth Errors. M.I.T. Lincoln Lab. Group Report, 44.

Snedecor, G. W. and Cochran, W. G. (1967). "Statistical Methods". 6th edition. Iowa State U.P.

Steinhart, J. S. and Meyer, R. P. (1961). Explosion Studies of Continental Structure. Carnegie Inst., Washington Publ. 622.

Truscott, J. R. (1964). The Eskdalemuir Seismological Station. Geophys.J.Roy.Astr.Soc., 9, 59.

Tukey, J. W. (1960). A Survey of Sampling from Contaminated Distributions, in: "Contributions to Probability and Statistics". E. Olkin et.al., Stanford U.P. 448-485.

Tukey, J. W. (1962). The Future of Data Analysis. Ann.Math.Stat. 33, 1-67.

Underwood, R. (1967). "The Seismic Network and its Applications". Ph.D. Thesis, A.N.U.

Vinnik, L. P. and Nikolayev, A. V. (1969). Microstructure of the Travel Time Curve of a Longitudinal Wave. Institute of Physics of the Earth; Moscow, Doklady Adademii Nauk SSSR, Vol. 186, No. 3, 571-574.

Vvedenskaya, A. V. and Balakina, L. M. (1959). Double refraction in the Earth's Mantle. Izvestia Akad. Nauk SSSR, Geophys.Ser. 7, 1138-1146.

Weichert, D. H. and Whitham K. (1969). Calibration of the Yellowknife Seismic Array with First Zone Explosions. In press.

Willey, G., Cleary, J. R. and Marshall, P. D. (1969). Comparison of Least Squares Analysis of Long and Short Period P Wave Amplitudes. In press.

Williams, C. A. (1950). On the Choice of the Number and Width of Classes for the Chi-square Test of Goodness of Fit. Jnl.Amer.Stat.Soc. 45, 77-86.

Worthington, M. (1969). "The Structure under the WRA Seismic Array: A Study of Rayleigh Wave near Surface Dispersion". M.Sc. Thesis. Durham University.

Young, J. B. and Douglas, A. (1968). Map, Time Series and other Plotting Routines for use with the Stromberg-Carlson 4020 Plotter. AWRE Report No. 041/68.

Young, J. B. and Gibbs, P. G. (1968). GEDESS: A Series of Computer Programs for Deriving Information at Selected Seismic Recording Sites, for Signals from known Hypocentres. AWRE Report No. O-54/68.